PREDICTIVE MODELLING OF MULTI-PERIOD GEOARCHAEOLOGICAL RESOURCES AT A RIVER CONFLUENCE

Phase 1 Report (PNUM 3357)

A. G. Brown[1], C. Carey[1], K. Challis[2], A. Howard[3] & L. Cooper[4]

[1] School of Geography, Archaeology & Earth Resources, Amory Building, Rennes Drive, University of Exeter EX4 4RJ

[2] Institute of Antiquity and Archaeology, University of Birmingham

[3] Birmingham Archaeology & HP Visual & Spatial Technology Centre

[4] University of Leicester Archaeological Services (ULAS),

June 2005

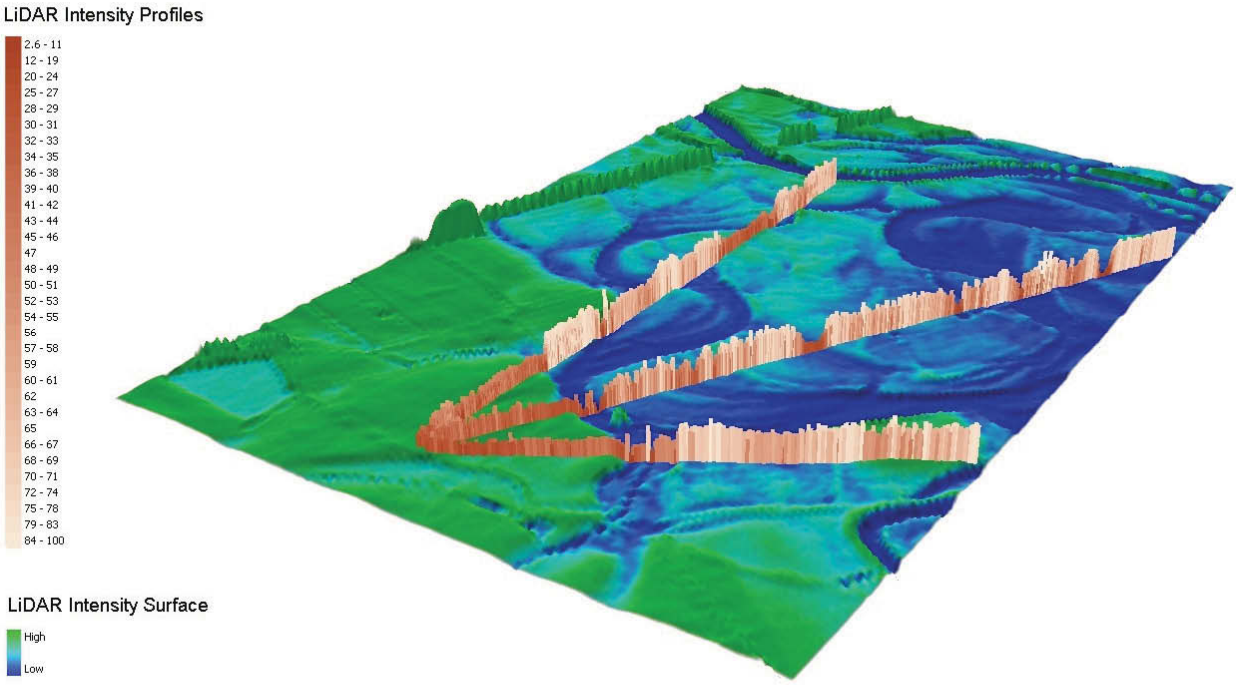

I. Executive Summary

This report describes a multi-method to characterise the archaeological resource of a complex confluence zone between to rivers in the East Midlands, UK (Trent and Soar). The aims of the project centred upon the evaluation of LiDAR, IFSAR and GPR for the semi-automated production of a chronostratigraphic model that could be related to traditional techniques of data collection such as geomorphological survey and plotting of the archaeological resource. The results showed that LiDAR last pulse return produced an accurate DTM, which defines the topographical complexity of the area. The results were found to be very comparable to geomorphological mapping. IFSAR data was found to reveal less of the subtle within terrace/unit variation identified by LiDAR but still identified the terrace sequence.

GPR transects provided technical experience in the survey of such complex alluvial terrain. GPR survey performed well on the gravel bodies including the terraces and agreed well with gouge auger surveys. GPR could resolve the edge of terraces and palaeochannels but not the internal stratigraphy or depth of the deeper and lowest palaeochannels due to a combination of radar absorbent silt and clay and a high water table. GPR survey revealed that the LiDAR intensity of return data appeared to reflect the sub-surface stratigraphy probably through variations in soil moisture. Archaeological resource evaluation showed that the pattern of finds was a result of differential erosion and deposition, visibility and intensity of survey. The high archaeological resource of the area is probably due to it being a transport node but this resource is buried in zones of the valley floor of different ages and modes of deposition.

Along with geomorphological mapping LiDAR and GPR were able to resolve the valley floor into three surfaces and a number of individual features. Using a combination of geomorphological mapping, dGPS, IFSAR, LiDAR and GPR a predictive chronostratigraphic model of the confluence zone was produced. This model will be tested in phase II by coring, sediment characterization and a dating programme.

II. Acknowledgements

This report has been written with the considerable support and help from many individuals. Technical and cartographic advice is acknowledged from S. Rouillard, H. Jones and D. Fraser. The landowners of the target area must be thanked for access and in particular Lafarge Aggregates Ltd. for both access and the provision of data.

III Contents

CHAPTER 5: THE GROUND PENETRATING RADAR SURVEYS

CHAPTER 6: DATA INTEGRATION OF REMOTE SENSED AND GROUND PENETRATING RADAR SURVEY DATA

IV LIST OF FIGURES AND TABLES

Chapter 1

Chapter 3

Chapter 4

Chapter 5

Chapter 6

Chapter 7

Chapter 8

Chapter 9

V. LIST OF TABLES

Chapter 3

Chapter 4

Chapter 9

CHAPTER 1: INTRODUCTION

This project was framed to address the core ALSF theme of developing capacity to manage aggregate extraction landscapes in the future (English Heritage 2004). In addition it addresses several other ALSF themes, namely:

- Characterising the (archaeological) resource and developing evaluation frameworks, predictive tools and mitigation strategies.
- Development [of] remote sensing and predictive techniques and mitigation strategies.
- Training and professional development: to raise awareness of issues and to improve the quality of historic environment work undertaken in response to aggregate extraction.
- Development of advanced visualisation and immersive three-dimensional models of landscape development. Although largely part of phase 2 of the project, this has the potential to address the theme of interpretation and outreach to the community of the knowledge gained from work related to aggregate extraction.

1.1 Summary of aims and objectives

The aim of this project is to predictively model the landscape of a major river confluence over a time-scale of millennia and at a spatial scale appropriate for archaeological management. The overall purpose is:

- To establish a RIGOROUS research model for the future development of predetermination designs for site evaluation.
- To assess the effectiveness of various airborne and ground based remote sensing methods in alluvial environments.
- To derive relationships between pre-extraction site survey data and likely chronostratigraphic and environmental data as part of archaeological assessment.

This research will assist regulatory bodies (i.e. County Councils) in demanding and specifying rapid evaluations of geoarchaeological potential as part of the implementation of PPG16. The novelty of the approach lies in the integration of high-resolution topographical, archaeological and geological (three-dimensional sub-surface) data within a Geographical Information System (GIS). The technical innovation will be the combination of Inteferometric Synthetic Aperture Radar (IFSAR), Airborne Laser Altimetry (LiDAR), CW Differential GPS (DGPS), Ground Penetrating Radar (GPR) and other ground based remote sensing techniques. This research will contribute to the framework for management of the archaeological resource in the Trent Valley developed through Trent Valley GeoArchaeology (Bishop *et a*l. 2002) and provide a transferable model for the geoarchaeological investigation and management of valley floor archaeology.

1.2 The study area

The study area is a block of the Trent/Soar confluence landscape approximately 2 by 4 km (Fig. 1.1). The area abuts the main area of Trent Valley GeoArchaeology (TVG) interest and is close to but not overlapping sites of continuing research by University of Leicester Archaeological Services (ULAS). The area is not zoned for aggregate extraction although the area to the west is. Extraction of these adjacent areas will allow boundary sedimentary information to be used in modelling.

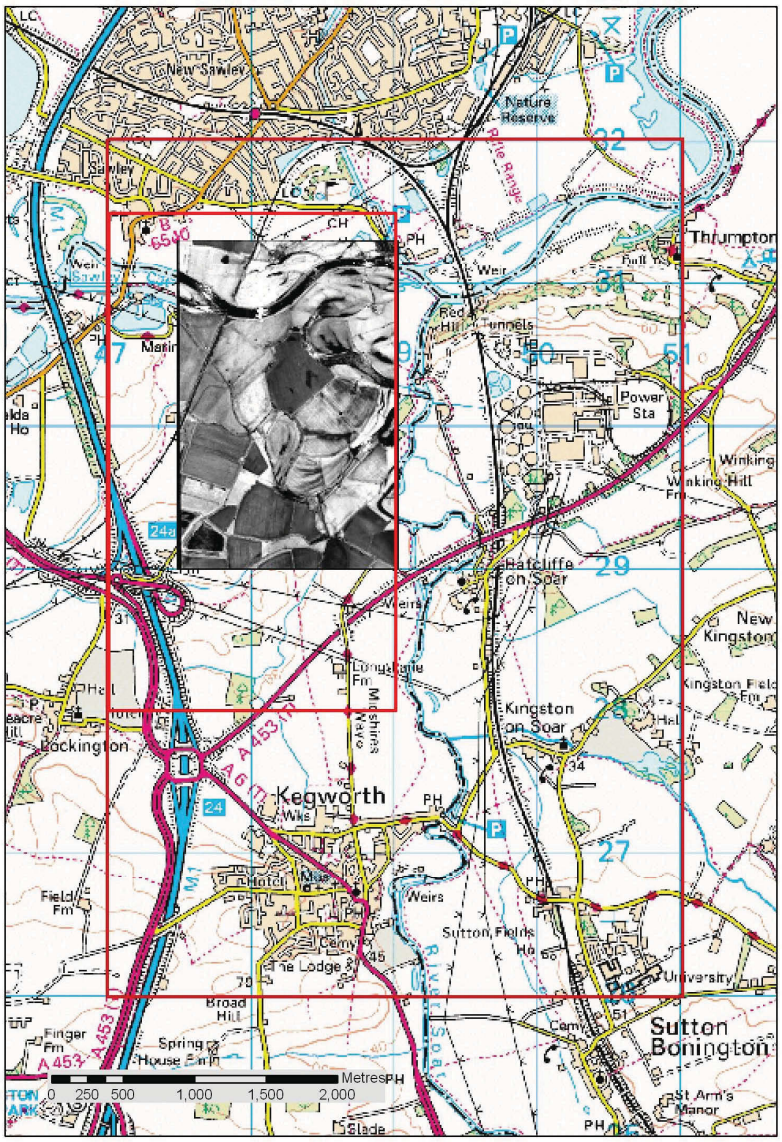

Fig 1.1: The study area over the 1:50,000 Ordnance Survey map (by permission of OS).

1.3 Project background

Recent archaeological work on the Thames and other British floodplains suggests that river confluences have been the foci of settlement and human activity since the earliest post-glacial periods. At confluences the high density of palaeochannels provides an opportunity to determine records of past environmental change. Migration of rivers channels also provides an environment with high potential for the burial and preservation *in situ* of cultural and environmental materials. Unfortunately this potential is generally only realised during the destruction of the land surface by development and subsequent 'rescue' archaeological investigation.

It is the nature of the archaeological record of floodplains that there is a direct link between the geomorphology, including the nature and distribution of channels, levees, gravel bars, terrace remnants, etc. and the distribution and nature of archaeological materials, from flint scatters to structures. Therefore there is a predictive capability in the subsurface geomorphology, stratigraphy and buried land surfaces.

1.4 Previous work

The Middle Trent is one of the archaeologically richest stretches of alluvial landscape in the UK. Finds include medieval bridges (the Hemington Bridges excavations, funded by English Heritage), a Norman milldam, fishweirs and dugout canoes (Salisbury *et al*., 1984; Cooper, 2003). The study area (a block of floodplain 8 km^2) is centred on the Lockington Marshes at the confluence of the Trent and Soar. This area is rich in cultural archaeology lying immediately east of the nationally significant prehistoric ritual landscape of the Derbyshire Trent Valley (Riley, 1987). Recent finds from a Bronze Age barrow cemetery (Hughes, 2000) strongly suggests that this prehistoric ritual landscape extends into the area. In the Romano-British period the area lies in the hinterland of a villa complex at Lockington and a small town, possibly a centre of ritual/religion at Red Hill, Ratcliffe on Soar (Elsdon, 1982). The area, although not threatened with imminent destruction, is earmarked for longer-term development. Pilot studies indicate the high buried archaeological potential of the locality (Ripper, 1997), which combined with a high density of sites suitable for palaeoenvironmental studies (Howard, 1997) provide an ideal zone for detailed modelling. Work by Trent Valley GeoArchaeology (Knight and Howard, 2004) has done much to provide a regional framework for the cultural, landscape and environmental archaeology of the Trent Valley. The present proposal provides an opportunity to build constructively on that framework through detailed consideration of a significant confluence zone, targeted fieldwork and innovative use of GIS and allied technologies.

CHAPTER 2: PROJECT AIMS AND OBJECTIVES

The project is envisaged as taking place in two phases, over two years. Phase one includes background research, remote sensing, landscape modelling, topographical and geophysical survey and will take place between May 2004 and March 2005. Phase two comprises fieldwork, geochronological and environmental modelling and will take place from April 2005. Detailed aims and objectives for phase one, and broad aims for phase two are provided below.

2.1 Phase 1: (May 2004 – March 2005) Geomorphological modelling

2.1.1 1A: GIS construction and archaeological assessment.

1A1 Design and implementation of a GIS for the study area collating and integrating data from the Ordnance Survey, Geological Survey, sites and monuments records, historic mapping and existing geoarchaeological surveys (such as that undertaken by Trent Valley GeoArchaeology).

1A2 An archaeological assessment of the landscape and cultural archaeology of the study area and its hinterland placing the study area in its regional and national setting.

2.1.2 1B: Detailed investigation and mapping of the floodplain and terrace surface.

1B1 Acquisition, examination and integration into the GIS of IFSAR elevation data (digital surface model - DSM) and orthorectified radar image (ORI) data for the study area.

1B2 Acquisition, examination and integration into the GIS of LiDAR DSM and reflected laser intensity data for the study area.

1B3 Qualitative and quantitative comparison of IFSAR and LiDAR DSM.

1B4 Qualitative examination of LiDAR reflected laser intensity and IFSAR ORI image data.

1B5 Acquisition, examination and integration into the GIS of air-photography and other remotely sensed data for the study area.

1B6 DGPS survey of the study area to calibrate IFASR and LiDAR DSM, map significant landscape features, generate survey transects of significant features and locate areas of geophysical investigation. Integration into the GIS of DGPS survey data for the study area.

2.1.3 1C: Geophysical investigation of the sub-surface sand and gravel geometry in order to identify major bedforms and channel features.

1C1 Ground penetrating radar (GPR) survey of significant landscape features within the study area.

1C2 Other geophysical survey of selected landscape features in order to allow comparison of a range of techniques (conductivity, resistivity, ERGI, etc.) with GPR.

1C3 Drilling of calibration cores from palaeochannels and intervening areas to characterize model radar reflectance and calibrate other geophysical data.

2.1.4 1D: Three dimensional deposit modelling of the study area.

1D1 Production of three-dimensional and volumetric models of the reach by combining the GPR, IFSAR, LiDAR and other data.

1D2 Production of provisional chronostratigraphic models.

2.1.5 1E: Academic Reporting, Research Seminar and Archiving.

1E1 *Internet Archaeology* paper and demonstration GIS.

1E2 Academic papers.

1E3 Archiving of GIS data.

1E4 Research seminar

2.2 Phase 2: (June 2005 – March 2006) Geochronological and environmental modelling

2.2.1 2A: Establishing a geochronology for the study area.

Cores will be taken from each palaeochannel. Each channel fill will be dated by standard radiocarbon analysis of bulk samples.

2.2.2 2B: Palaeoenvironmental reconstruction.

Multi-disciplinary palaeoecological analyses of representative samples from each palaeochannel core will be undertaken (plant macrofossils, pollen and coleoptera).

2.2.3 2C: Modelling the dynamic development of the landscape.

Computer-generated palaeoenvironmental maps will be developed illustrating channel dynamics and archaeological interaction at the confluence during selected time-periods.

CHAPTER 3: MATERIALS AND METHODS

3.1 LiDAR

Traditional remote sensing based on the rectification and geocorrection of air-photographs is limited by the ability of photographic techniques to identify significant landscape features only in appropriate conditions of land cover and lighting (Riley 1987; Wilson 1982). However, since many aspects of the geomorphology of riverine landscapes are represented by variations in the microtopography of river terrace and floodplain surfaces, surviving even in frequently cultivated areas, the ability to map this microtopography should produce an effective record of such features. LiDAR provides a means to accurately and rapidly map microtopography on a large scale.

LiDAR uses the properties of coherent laser light, coupled with precise kinematic positioning provided by a differential global positioning system (dGPS) and inertial attitude determination provided by an inertial measurement unit (IMU), to produce horizontally and vertically accurate elevation measurements. An aircraft mounted laser, most often a pulse laser working at rates in excess of 30 MHz, projects a coherent beam of light at the ground surface, the reflection of which is recorded by a sensitive receiver. Travel times for the pulse/reflection are used to calculate the distance from the laser to the reflecting object. To enable coverage of a broad swath beneath the moving aircraft is scanned by using rotating mirrors to direct the laser. The spatial resolution and scan swath width are determined by the frequency of the laser pulse and altitude of the aircraft at the time of survey. The dGPS provide detailed three-dimensional information on the location of the laser unit, while the IMU provide information on the pitch, roll and yaw of the aircraft. A complete LiDAR system comprises a scanning laser coupled with a dGPS and IMU linked through a computerised control, monitoring and recording unit. Post-survey processing of the simultaneously recorded laser, location and attitude data allows reconstruction of elevation values for the ground surface. Raw survey data in the form of a three dimensional point-cloud are projected to a local map datum, sorted, filtered and used to generate a regular grid of elevation values.

Typically the laser receiver is able to record multiple returns for a single pulse, allowing recording for example of a partial return from the top of a semi-opaque object such as a woodland canopy (usually referred to as a first-pulse (FP) return) and from the opaque ground beneath the canopy (a last-pulse (LP) return). Other information, such as the intensity (amplitude) of the reflection may also be recorded. Comparison of surfaces produced from FP and LP laser returns suggest that, at least in landscapes with moderate semi-opaque ground cover LiDAR is effective in penetrating vegetation to reveal the underlying land surface. Initial examination of laser intensity data suggests that there is a fall-off in the intensity of the reflected light that corresponds with landscape features such as palaeochannels.

Analysis of LiDAR elevation products has focused on examining the effectiveness of LiDAR elevation products for identifying significant topographical features of the terrace and floodplain, quantifying relative accuracy and absolute accuracy of LiDAR elevation products compared to elevation values recorded by field survey using dGPS, and analysis of the impact of varying resolutions of LiDAR elevation data on the DSM metrics and the ability to identify significant landscape detail.

3.2 IFSAR

Airborne radar uses radio waves to measure the distance between an aircraft mounted senor and the ground surface. Interferometry relies on picking up the returned radar signal using antennas at two different locations. Each antenna collects data independently, although the information they receive is

almost identical, with little separation (parallax) between the two radar images. Instead the phase difference between the signals received by each of the two antennas is used as a basis for calculation changes in elevation. The results are enhanced by using processing techniques during data collection to generate a synthetic aperture of much greater size than the physical antenna used and so enhance resolution (Intermap 2003). Combining the principals of Synthetic Aperture Radar with Interferometry, Interferometric Synthetic Aperture Radar (IFSAR) is capable of producing both a radar image of the ground surface and calculating elevation changes to enable production of a digital surface model (DSM).

Intermap has undertaken IFSAR surveys of the entire of the UK. The results of the surveys are available as a commercial product in the form of 5m spatial resolution DSM with a vertical accuracy of between 0.5 and 1.0m and a 1.25m spatial resolution radar image. Analysis of the IFSAR products focused on investigating to what extent they were able to provide useful geoarchaeological information. The IFSAR DSM was imported into ArcGIS for visualisation and comparison with LiDAR and GPS derived elevation values. Elevation and derived slope frequency histograms were generated as well as basic DSM statistics

3.3 Aerial photography

Airborne remote sensing techniques have traditionally been employed to great effect in mapping the geomorphology and cultural archaeology of alluviated landscapes. Archaeologists have largely focused their attention on the comprehensive mapping of cropmarks and other features of the archaeological landscape revealed from the air (Riley 1980; Whimster 1989), and large areas of England have been comprehensively mapped as part of the National Mapping Programme undertaken by English Heritage (Bewley 2003). Aerial photographs have also been employed in mapping geomorphology in riverine landscapes, for example in extensive studies of the valleys of the rivers Trent (Baker 2003; Garton and Malone 1998) and Thames (Lambrick 1992; Robinson and Lambrick 1994) and in the alluvial landscapes of the Cambridgeshire and Lincolnshire Fens (Hall 1992; Hayes and Lane 1992). Such mapping of fluvial geomorphology provides a context for past cultural landscapes and assists in identifying topographical features of high archaeological potential (for example relict river channels) and isolating areas of past river erosion where little in the way of archaeological material might be expected to survive (cf Brown 1997). The systematic reconnaissance, mapping and classification of alluviated landscapes in this way has played a significant role in the strategic management of the geoarchaeological resource in the face of growing threats from aggregate extraction, housing and other development pressures (Bishop 2003). Within the present study examination of aerial photography focused on the mapping of significant landscape features, principally as a control (based on conventional techniques) for comparison to the various airborne and ground based remote sensing techniques tested.

The present study has focused on mapping landscape and geomorphological detail evident on vertical photographs. A cover search of all relevant photographs at the National Monuments Record collection (ref AP70673; appendix 1, the cover search results are annotated to indicate which photographs were viewed and reasons for selection or rejection) identified 83 oblique and 275 vertical photographs of the study area and its environs. In addition, a number of further photographs were identified and examined in the collections of Leicestershire County Council and Cambridge University.

All available photographs were viewed and selected prints digitised by scanning at 300dpi using an Epson Photoperfect 3780 desktop scanner for incorporation into the project Geographical Information System (GIS) developed using ESRI's ArcGIS 9. Air photographs were rectified and georeferenced to real world coordinates using the Georeferencing extension of ArcGIS 9 by matching significant landscape

features with those seen on the Ordnance Survey mapping. Once rectified and georeferenced topographical features of the terrace and floodplain surface were digitised directly from the air-photographs within ArcGIS to produce GIS data comprising a set of polygons and polylines with attached attributes.

Transcription of features seen on air-photographs focused on elements of the natural landscape. No attempt was made to produce crop and soil mark mapping from oblique aerial photographs, or from those vertical photographs on which such evidence was to be seen, which work has already been comprehensively undertaken by others (see below). However the extent of both earthwork and crop/soilmark ridge and furrow was mapped (Figure 6) as this broadly reflects the different geomorphological units identified across the study area.

3.4 Materials and methods Ground Penetrating Radar

3.4.1 The Ground Penetrating Radar (GPR) and application in alluvial environments

Ground penetrating radar surveys use pulses of Electromagnetic (EM) radio waves directed down into the soil profile from a transmitting antenna, in order to investigate subterranean features. When discontinuities are encountered some of these radio waves are reflected back towards the surface, whilst other waves travel further down into the soil profile until they meet other discontinuities. At the surface a receiving antenna measures the reflected waves. By measuring the time taken between emission of the radar pulse and reception back at the antenna it is possible to measure the depth of a discontinuity in the soil profile. Within a floodplain context the boundaries between different geomorphological units will be seen as discontinuities, due to their different physical properties, e.g. clay and gravel.

Data is collected in GPR survey as single transects, through pulling the GPR over the ground and collecting data either continuously or at set intervals. These GPR transects are calibrated for changes in surface topography. The transects can be viewed singly to give a vertical profile of the section. Alternatively, several spatially referenced transects can be welded together to produce a solid cube. This cube can be sliced at set intervals producing plan views of the subsurface environment.

The process of estimating the depth of discontinuities within the soil profile is complicated by different dielectric constants found within different units. The electrical properties of a sedimentary unit effect the time taken for the radar pulse to travel through that unit. The dielectric permattivity is a property of an electrical insulating material (dielectric) equal to the ratio of the capacitance of a capacitor filled with the given material to the capacitance of the identical capacitor filled with air. The specific capacitance of a vacuum is Eo = 8.85×10^{-12} Farads per metre. The relative dielectric constant (Er) for air is 1 and is approximately 81 for fresh water (Radan User Manual Definition 2004, GSSI, 128).

Within an alluvial context the relative dielectric permittivity (RDP) of different sediment units is critical; which is the ability of a sediment to absorb, reflect and be permeated by, the radar pulse. If there is a significant change in RDP between two different geomorphological units, such as clay and gravel, then strong reflections will result at the interface of the two units. The GPR pulse will be dissipated by materials of high conductivity. Therefore, sediments with high clay and water contents cause rapid attenuation of the GPR signal and are often impenetrable to higher frequency antennas, such as a 200MHz antenna. Jol and Bristow (2003) revise GPR applications and practices for mapping sediments. One of their conclusions is that GPR is most effective in electrically resistive materials such as sand, gravel, peat and limestone but decreases in data quality are seen in highly conductive materials such as

silt, clay and calcretes. Key factors that affect the RDP of an unconsolidated material can be listed as (mainly from Ekes and Friele 2003, 90):

- Pore size
- Sediment type
- Stratification
- Grain size
- Water content

It should be emphasised that although GPR survey can be used to identify and to some degree characterise sediment architecture, the mechanisms that affect the radar wave reflections are imprecisely understood. The reflection from an unconsolidated material will be a function of its water content below saturation levels; the water content itself being a function of the sediment properties (Van Dam *et al.* 2003, 257 – 273). If GPR survey is carried out over saturated sediments penetration will be limited.

In order to correctly calibrate the electric depth model created by the GPR it is important that the dielectric properties of the soil profile can be accurately estimated. This in practice is extremely difficult, as within alluvial environments any GPR transect is likely to cross a series of different geomorphological units, each having a different RDP. Therefore, a compromise has to be reached in the dielectric constant that is used. Within this project the dielectric constant of the soil was estimated through comparison with gouge core transects, which is a common method of calibration (for example see Bridge *at al.* 1998).

The gouge core transects allowed the depth of the alluvium overlying the terrace and modern floodplain gravels to be accurately measured across a whole GPR transect. The dielectric constant was then set, which identified the interface between the alluvium and the gravels at the same depth recorded by the gouge core transect. This represents a compromise on setting the dielectric constant as the calibration is taking place within an alluvium unit, not combining the average of the alluvium and gravel units. However, the gravels are impenetrable without powered coring equipment and thus the described compromise was reached through using gouge core data.

The identification of radar terminations is the basis for constructing a relative chronology for a sequence of sediment units (Bristow *et al*. 2005, 316*).* Interfaces between different geomorphological units, e.g. a silty clay unit overlying a gravel unit, represent terminal events in either deposition or erosion processes and the start of subsequent processes. Although the ages of these sediment units cannot be ascertained without absolute dating methods, relative sequences can be constructed through studying the form of the interfaces seen. This has specific importance in geoarchaeological studies of alluvial environments where erosion and deposition by channels will have both destroyed and preserved the archaeological resource.

The heterogeneity of alluvial deposits allows discontinuities to be mapped and stratigraphies to be created. This property causes special considerations for GPR survey of alluvial environments. River floodplains are heterogeneous in both X, Y and Z dimensions. Upper terraces may have gravels close to the surface, with a thin covering of alluvium, whilst modern floodplains may have a considerable degree of alluvial deposition on gravels or bedrock. Palaeochannels may have high water contents, high clay contents, with organic rich pockets. Gravel architecture can vary radically between clast to matrix supported.

For GPR survey this can be problematic, in respect of data collection and real time amplification of signal. Consider two very different units that are surveyed within the same area, such as a gravel terrace and a palaeochannel with a fill of high clay content. The gravels in the terrace will have low absorption but high reflectance properties. Conversely, the palaeochannel will have low reflectance but high

absorption properties, causing rapid attenuation of signal. In such cases, which are frequently encountered in alluvial environments, the different geomorphological units require a different amplification of signal. The amplification of the radar pulse is controlled through a gain applied to the signal. The level the GPR gain (amplification) is set at will be a compromise between obtaining good penetration in a series of different sediments and collecting clipped data, where the amplification of the signal has been too great and the minimum and maximum values are not realised. When considering alluvial stratigraphy it is often the contrast between different sediment units that is most important. Therefore, relative change and difference is as important for data collection within heterogeneous environments as absolute values.

3.4.2 GPR survey aims

The primary aim of the project is to produce a three dimensional model of the study area through combining the data resources of LiDAR, differential GPS survey, IFSAR and GPR, which can be used to create a chronostratigraphic model of the survey area and relate this to the archaeological resource (see chapter 9). In order to achieve this aim a series of GPR surveys were undertaken, to collect data on the subsurface stratigraphy of the floodplain. The subsurface stratigraphy can be used to:

a) Classify different geomorphological units.
b) Produce relative chronologies of different geomorphological units.
c) Use factors a) and b) as a guide to the potential palaeoecological and geoarchaeological resources of different sedimentary units.

In order to achieve this overall aim it was necessary to undertake GPR survey in a variety of locations within the study area. The following objectives were set for the GPR survey:

A. Development of a GPR field methodology to map large scale. geomorphological units within river floodplains.
B. Three-dimensional GPR survey of at least one area of terrace 2.
C. Three-dimensional GPR survey of at least one area of terrace 1.
D. Three-dimensional GPR survey of at least one area of the modern floodplain.
E. Integration of these data sets with the LiDAR.

In addition to these aims the GPR surveys experimented with a series of data collection parameters, in order to develop optimal survey parameters for floodplain investigation. Experimentation was made with linear and grid plan methods of data capture, different transect intervals and antenna frequencies.

3.4.3 GPR transect and grid plan data capture

When developing a field strategy, the aims and objectives of the data collection need to be considered and offset against the type and volume of data required. When considering using a GPR survey to assess floodplain stratigraphy there are a series of key issues relating to data capture. Primarily, are two-dimensional transects sufficient for data collection or is three-dimensional grid plan survey required?

A two dimensional transect will give a section view of the sediment stratigraphy. Different sediment units are identifiable as areas of different reflectance and absorbance. The spatial dimensions of any geomorphological features are not identified, although it is often possible to obtain these through other

means, e.g. field based mapping. A data grid will allow a model to be produced in three dimensions. Variation can be seen between and within different sediment units on both XY and Z axes. The extent of some individual features can also be mapped (e.g. terrace islands).

Within a three-dimensional grid plan survey other issues need to be addressed relating to field methodology. Primarily, the transect spacing will determine the level of data resolution within a survey and the degree of interpolation between data points. Secondly, the size of the survey grids combined with the transect spacing will influence the data resolution and subsequent interpretation. The difference in data capture between transects and grids also has implications for the amount of time spent 'in the field', with grid surveys taking considerably longer in staking out, data collection and data processing/interpretation.

3.4.4 Choice of survey areas

Areas were selected for GPR survey that had good LiDAR results and showed geomorphological variation, i.e. palaeochannels, gravels bars, etc. However, the presence of some arable crops meant that it was not possible to survey in some fields. Also ploughed fields, when combined with heavy rainfall, meant that other fields were unavailable for survey (fieldwork was conducted in November 2004, January and February 2005). Thus the GPR fieldwork was a compromise between areas of interest and areas of access.

3.4.5 Transect spacing

The GPR investigations were undertaken on a geomorphological scale, characterising major geomorphological units in both spatial and temporal dimensions. To this end the surveys needed to cover large areas, whilst maintaining a good level of data resolution within the survey area. In order to develop the field methodology, transect intervals of 1m, 5m, 10m and 20m were experimented with. A minimum of fifteen transects were collected per grid survey, with the ideal standard being twenty transects or greater per survey area.

3.4.6 Grid sizes

The grid sizes varied, dependant on the aims of each survey, the transect interval and the size of the field being surveyed. Table 3.1 gives the sizes of each survey, whilst the location of each survey is shown in Figure 3.1. The selection of a survey area is subjective and all surveys aimed to collect a representative sample of the features being studied.

3.4.7 GPR configuration

Two antenna frequencies were employed in the project, being 400MHz and 200MHz. The system employed was a GSSI SIR3000 unit, collecting data using both a hand held trigger on time-based collection and also with a survey wheel (Fig. 3.2). The SIR 3000 has only one fixed antenna so CMP (common mid point analysis) was not applicable and coring transects were used for data calibration. Data was collected using 512 samples/scan, with 16 bits per sample at 64 scans per second. Field filters were

set at three times the antenna frequency for the IIR vertical high pass (600MHz) and one quarter of the antenna frequency for the IIR low pass (50MHz).

Calibration of the signal amplification was made on terrace gravels, which were expected to have the highest reflectance values within the survey area. Experimentation was made to find noisy areas (such as gravels close to the surface) for calibration. The signal amplification, controlled by the number of gain points used, varied between individual transects and grid plan surveys. On individual transects 5 gain points were used to maximise penetration, although data clipping sometimes occurred when using such high gain settings. In contrast the grid plan surveys used lower gain settings, to prevent data clipping. However, this reduced the effective GPR penetration. Between 2 and 4 gain points were used on the grid surveys, varying on a survey by survey basis.

Survey name	**Size**	**Transect spacing**	**Antenna frequency (MHz)**	**Core data**
MFT1	225m	N/a	200	Gouge core 10m intervals
MFG1	125m x 225m	5m, 10m and 20m	200	Gouge core 10m intervals
MFG2	40m x 25m	1m	400	Gouge core 10m intervals
T1T1	395m length	N/a	200	Gouge core 10m intervals
T1QT	69m length	N/a	200	No but section drawn
T1T2	100m length	N/a	200	Yes gouge core
T1G1	155m x 100m	5m	200	Yes gouge core
T1G2	155m x 35m	5m	200	No
T1G3	125m x 240m	5m	200	No
T2T1	335m	N/a	200	Yes gouge core transect 10m intervals
T2G1	95m x 170m	5m	200	No

Tab 3.1: The GPR surveys.

Fig 3.2: The GPR survey about to start on the modern floodplain, using a 200MHz antenna.

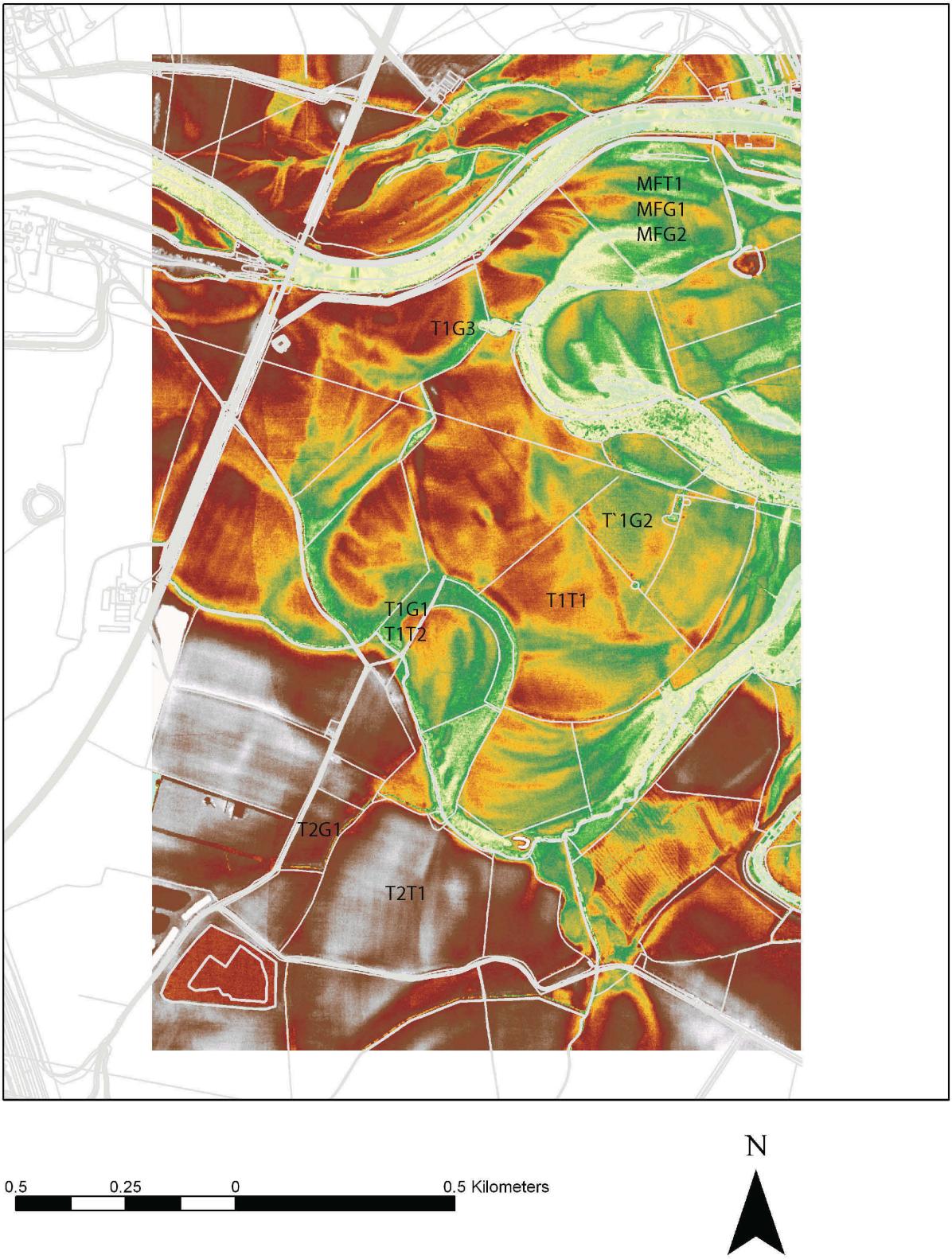

Fig 3.1: The GPR survey areas within the overall study area.

3.4.8 Field survey

All survey areas were staked out using differential GPS survey. Some of the GPR transects were collected through time based collection whereby, markers where set out at 5m intervals, with a hand held trigger being used to mark each survey point. Most transects were collected using a survey wheel, with markers were placed at 50m intervals and using with ranging rods for straight alignment. The location of all transects was recorded with the differential GPS, as where key features such as field junctions for external reference. Topographic data for GPR surface normalisation was collected at 5m intervals using the differential GPS in some surveys but in others using the last pulse DTM values from the LiDAR data.

3.4.9 GPR processing

The processing of the data followed a prescribed route, developed through experimentation with GPR data collected on alluvial deposits. Data processing is subjective. The aim of the processing steps undertaken in this project was to set the correct time zero, correct for hyperbola reflections via migration, remove background noise and increase/decrease gains to provide good contrast in the data. This is a simple processing sequence that can bring out good quality results in alluvial data sets.

For each set of survey data time zero was set through the first positive peak seen within GPR section. Migrations were undertaken through a variable velocity migration. A series of hyperboles were selected in the GPR diagram, coming from a variety of depths and sediment units. A graph was made of the relative velocity curve, taking into account the size of the parabolas combined with the depth of the parabolas, allowing changes in the velocity of the radar pulse through the profile to be calibrated. Normally several different graphs were experimented with in each survey until a satisfactory result was obtained.

Background removal filters were used to ‘clean’ the data, along with some application of vertical high pass and vertical low pass filters. Deconvolution filters were generally not used. Deconvalution filters have the ability to remove ‘ringing’, multiple reflectors caused through wave diffraction in low absorption/high reflectance environments. However, deconvolution also has the ability to remove real data, which is interpreted as the effect of multiple reflections, such as some of the reflections seen within the gravel units. In general areas of ringing were seen in the palaeochannel fills that had high water tables and high clay contents. In such cases the data was removed from the display, as the ringing appeared as data below the actual depth of penetration.

3.5 Transect coring

In order to aid interpretation of the GPR and LiDAR data and provide separate stratigraphic data, gouge core transects were undertaken on some GPR transects. Gouge core sampling was undertaken at 10m intervals along specific GPR transects. The gouge core had a 2cm diameter. The depth of each unit was recorded with a description of its composition before impenetrable gravel was encountered. In addition to the gouge sampling, a section of exposed quarry was recorded with a GPR transect being conducted along the top of the section. The quarry section allowed the comparison of a GPR transect against a drawn and photographed section. The drawn section sampled at 2.5m intervals. This provided a second means of GPR depth calibration.

3.6 Geomorphological mapping

A geomorphological map was constructed of the study area through using field based mapping and recording onto 1:10, 000 maps.

3.7 Data archive and query

ArcGIS provided the primary database for the project. ArcGIS is a Geographical Information System (GIS), which is used for the storage and exploration of data, linking together aspects of geomorphology and archaeology, in spatial and chronological dimensions. The investigation of an area of cultural landscape requires the collection of data from a range of sources involving both field based and desk based research. These strands of information are then placed together within a GIS, allowing relationships between variables to be visualised and explored.

A GIS is a spatially referenced database. Each variable can have a large number of attributes (categories) stored with it, giving a description of that variable. Data can be stored either as point data (e.g. an archaeological site), line data (e.g. a river) or as a vector (e.g. an area of river terrace). These data can then displayed and queried as a series of layers.

The following data were entered into the ArcGIS database:

I) Geomorphological maps, which were adapted through on screen digitisation
II) Geology maps supplied through the BGS
III) LiDAR intensity, DSM and DTM models
IV) IFSAR DSM and DTM models
V) Co-ordinates of the fieldwork survey areas
VI) Depth sliced GPR data
VII) 1:10000 OS maps
VIII) Digitised SMR data
IX) Bore hole locations
X) Rectified aerial photographs of the study area

3.8 Integration of Remote sensed and ground based prospection methods

ArcGIS provided the primary means of integrating the various data sources, particularly the GPR depth slices with the remote sensed LiDAR data. ArcScene was also employed to allow the layering of GPR and LiDAR data in a quasi-3D environment, permitting direct visual comparison between the data types.

CHAPTER 4: RESULTS FROM REMOTE SENSED DATA

4.1 Floodplain and Terrace Geomorphology

Two hundred and twenty six photographs from 25 separate sorties were examined as part of the study. Detailed analysis of air-photographs was restricted to those displaying clearly defined geomorphological detail, evident as crop or soilmarks, earthworks or through differential flooding. Modern landscape features, such as hedge lines, suggestive of for example relict river channels, were excluded from consideration as it was felt that these features could not be taken as definitive evidence of geomorphological features without field examination, which was to be undertaken separately; the aim of this aspect of the study being exclusively to examine the efficacy of remote techniques.

Using these criteria, clearly defined geomorphological detail was confined to only five of the 25 NMR listed sorties examined and to a set of Fairey Survey air-photographs held by Leicestershire County Council (Tab. 4.1). Evidence from these photographs (but excluding the 1945 sortie used by TVG2002) was digitised within ArcGIS to generate mapping, principally of palaeochannels (Fig. 4.5). The results of this mapping, using photographs from five sorties, may be compared with that carried out by TVG2002, (Fig. 4.1) using photographs from only two sorties (principally RAF photographs from 1946 [RAF/106G/UK/734/3099] and Aerofilms photographs from the 1970s [Aerofilms 7145 9-768]).

There appears to be agreement between the two independent studies on general disposition of all major palaeochannels, including those significant relict channels marking the boundary between terrace 1 (the Holmepierrepont Terrace) and terrace 2 (the Hemington, or floodplain terrace) and channel belts within the Hemington terrace, mapped as alluvium by the BGS.

Finer details of channel form vary between each study, probably in part as a result of the vagaries of interpretation of different workers. Significant extra detail of channels within the floodplain alluvium was revealed by photographs showing groundwater flooding in December 1954 (Fig. 4.2). Further significant detail of terraces 1 and 2 is provided on the exceptional Fairey Survey photographs of June 1976 (Fig. 4.4). The impact of the unusually dry summer conditions is evident both in the degree to which subtle detail of the geomorphology of terrace 1 and 2 is revealed and also by the very clear cropmarks of the Lockington later prehistoric settlement complex and Romano-British villa on terrace 2. Much of this detail is impossible to capture through crude digitising of channel outlines, and reference to the geocorrected photographs is required to gain full appreciation of the complex geomorphology.

Photo Ref	Year	Geo Unit	Comment
RAF/106G/UK/734	1945	T2, FP	Paleochannels revealed by flooded depressions, and earthworks (See Baker 2003).
RAF CPE UK 1865	1946	T2, FP	Palaeochannels revealed by groundwater flooding (fig. 2)
RAF 542 97	1954	T1, T2, FP	Terrace units defined by extensive overbank flooding of Trent and Soar (fig. 3)
MAL/78023	1978	T1, T2, FP	Some cm/sm evidence of geomorph
Fairey Surveys 1861	1976	T1, T2	Extensive cm/sm evidence of palaeochannels and terrace details
OS/67011	1978	T1, T2, FP	Some cm/sm evidence of geomorph

Tab 4.1: Summary of vertical sorties containing good evidence of fluvial geomorphology within the study area.

4.2 Cultural Archaeology

No systematic attempt was made to transcribe cultural archaeological details from vertical aerial photographs, nor were oblique photographs examined for such. However, evidence for the ridge and furrow remains of medieval ploughing, surviving as relict earthworks and also revealed as cropmarks and soilmarks was transcribed (Fig. 4.6). In general evidence for ridge and furrow is confined to terrace 1 (the Hemimgton terrace) and absent from terrace 2 (Holmepierrpont) and the floodplain. This probably reflect the marginal nature of the land of the Hemington terrace in the Post-Medieval period, where land use, largely of long term pasture and meadow, led to the survival of ridge and furrow otherwise eradicated by continued ploughing on the higher land of the Holmepierrepont Terrace. In contrast, the floodplain was probably never ploughed. A fragment of ridge and furrow close to the present course of the Trent may reflect an isolated relict of terrace 1. The boundaries of individual furlongs of ridge and furrow conform closely to those of geomorphological units, as do those of enclosure field boundaries – probably as the relict channels marking most unit boundaries have remained significant, seasonally flooded, landscape features.

4.3 Flooding on the River Trent

The December 1954 photographs record a significant episode of over bank flooding effecting both the Rivers Trent and Soar (Fig. 4.3). The extent of the flood waters recorded by the photographs has been used in conjunction with LiDAR elevation data to produce a visualisation of the extent of flooded and not flooded areas. This clearly defines the impact of flooding on different geomorphological units (Fig. 4.7), and a pseudo three dimensional map of the 1954 flood, based entirely in the LiDAR elevation data (Fig. 4.8) shows for example that the central portions of the Hemington terrace remain largely unaffected by flood waters.

Comparison of the photographic evidence with LiDAR intensity values (Fig. 4.9) shows areas flooded in 1954 generally display lower intensity values, while a number of higher terrace remnants within the

Hemington terrace have higher intensity values, although a substantial part of the centre of the terrace has low values. High intensity values appear to be linked to areas which on geomorphological grounds might be interpreted as bar or splay features. This may suggest that intensity is in some way linked to substrate.

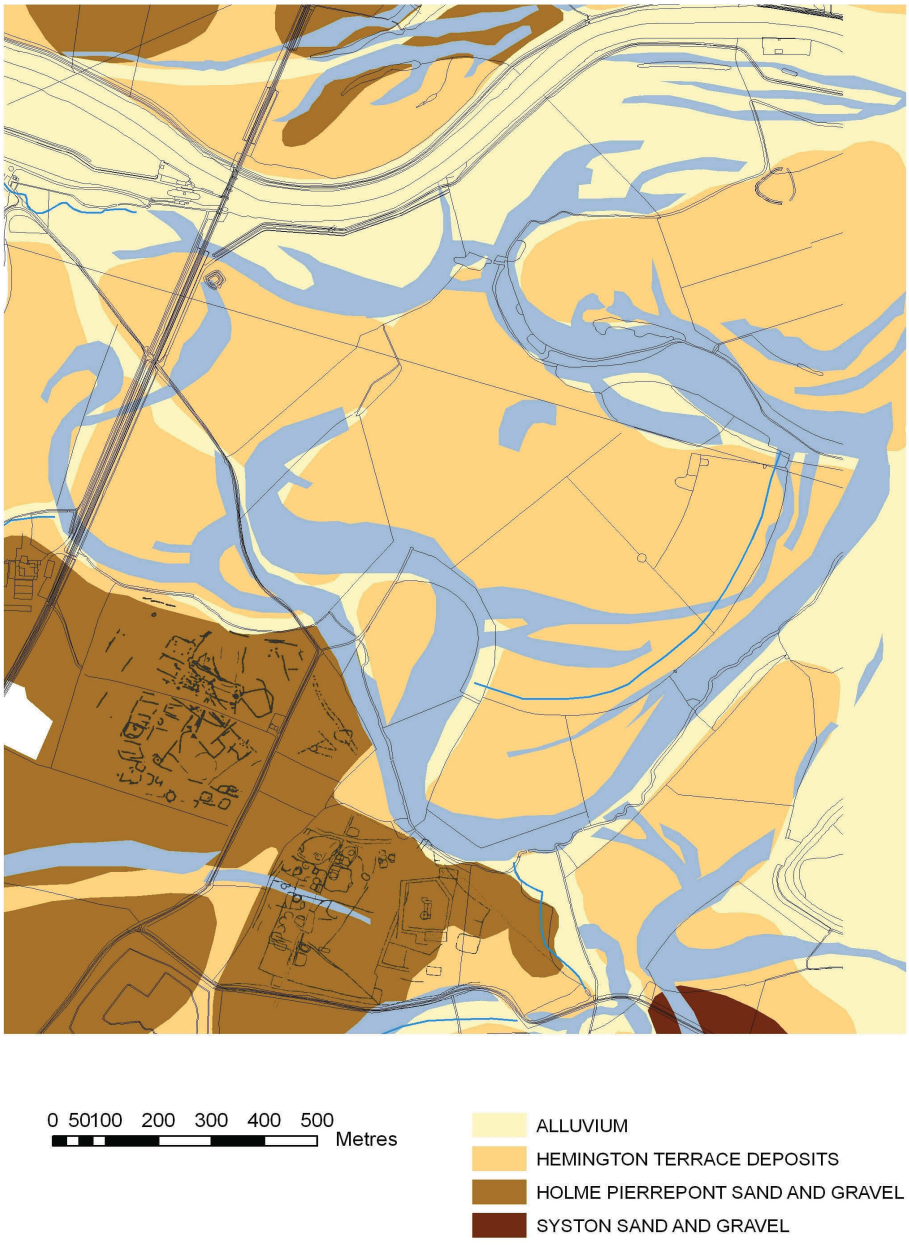

Fig 4.1: Map showing the drift geology of the study area (as recorded by the Geological Survey) with superimposed palaeochannels mapped by TVG2002 (Baker 2003) and cropmark and geophysical survey evidence for later prehistoric and Romano-British activity on the Holme Pierrpont terrace..

Fig 4.2: Geocorrected vertical air-photographs of the north-east corner of the study area taken on 2nd December 1946 (RAF CPE UK 1865 6137) showing groundwater flooding highlighting palaeochannels on the Hemington (floodplain) Terrace and floodplain.

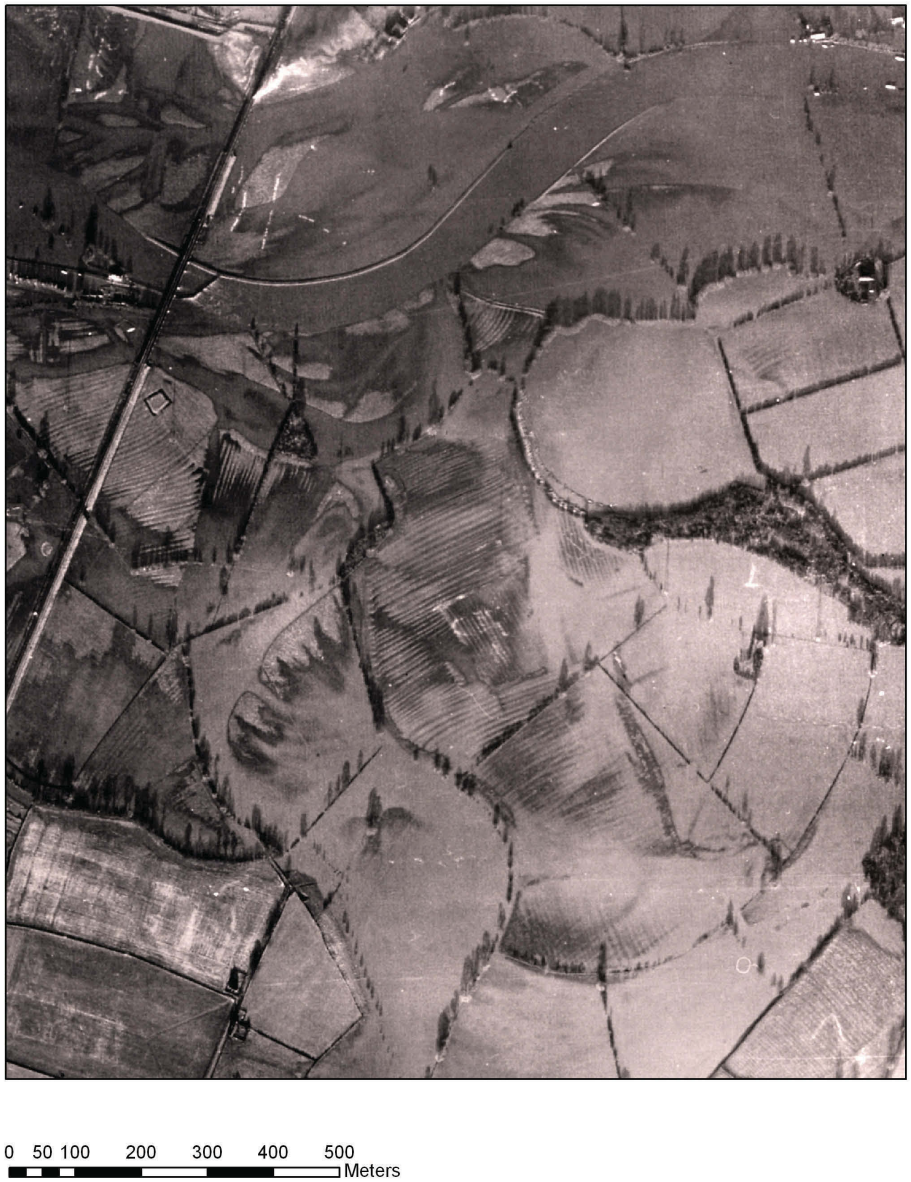

Fig 4.3: Geocorrected vertical aerial photograph mosaic of the study area taken on15th December1954 (RAF 542 97 0048 and 0049) showing extensive over bank flooding of the Rivers Trent and Soar.

Fig 4.4: Geocorrected vertical aerial photograph of the study area taken on 28th June 1976 (Fairey Surveys 1861 7615) showing extensive and well developed crop and soil mark evidence for fluvial features within the Holmepierrepont and Hemington Terraces and palaeochannels between the terrace units. The cropmarks of the Lockington villa complex are also clearly evident.

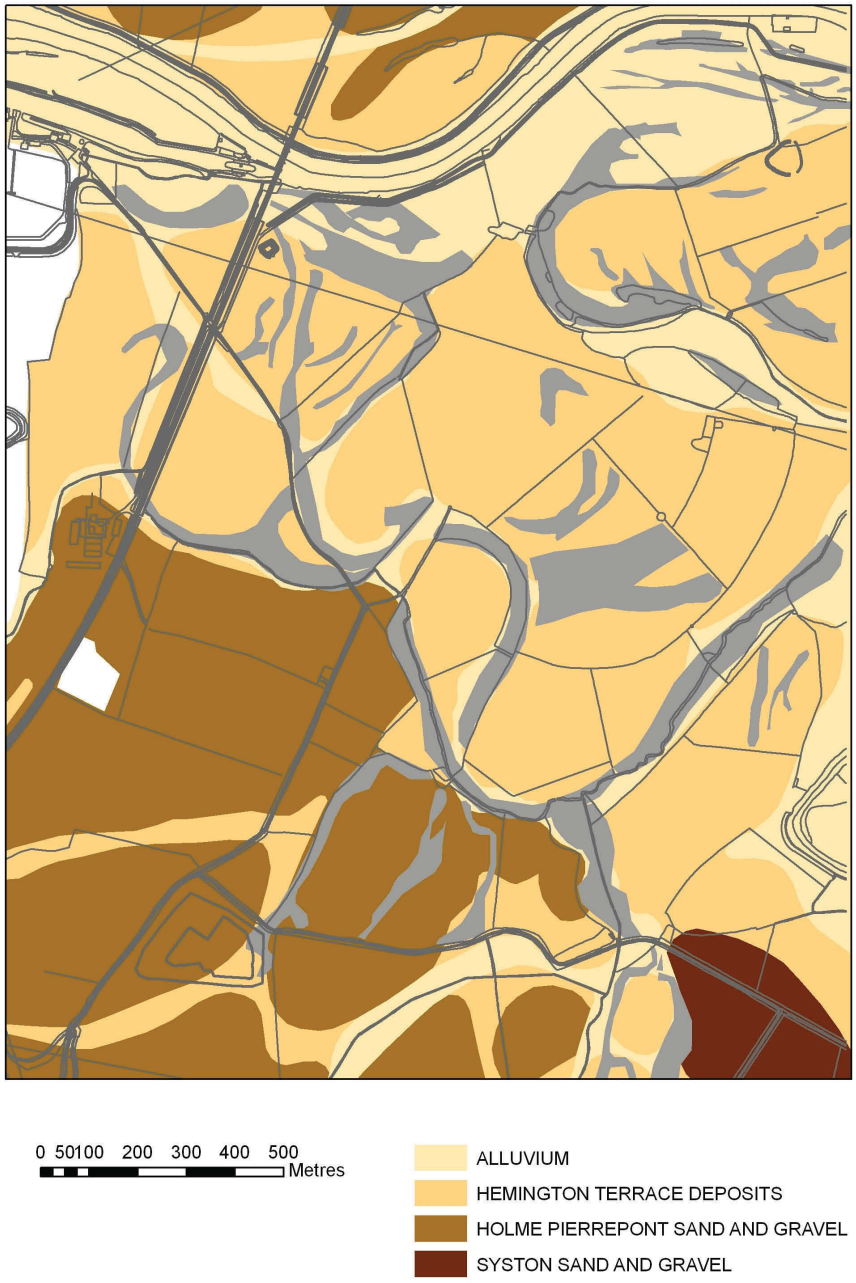

Fig 4.5: Map summarising the fluvial geomorphological features across the study area transcribed from air-photographs as part of the study. This may be compared with the work of TVG 2002 (fig.1) and with LiDAR evidence (Figs. 4.10-4.12).

Fig 4.6: Map summarising cultural archaeological remains transcribed from air-photographs of the study area with in addition the Warren Lane later prehistoric settlement complex revealed largely by geophysical survey.

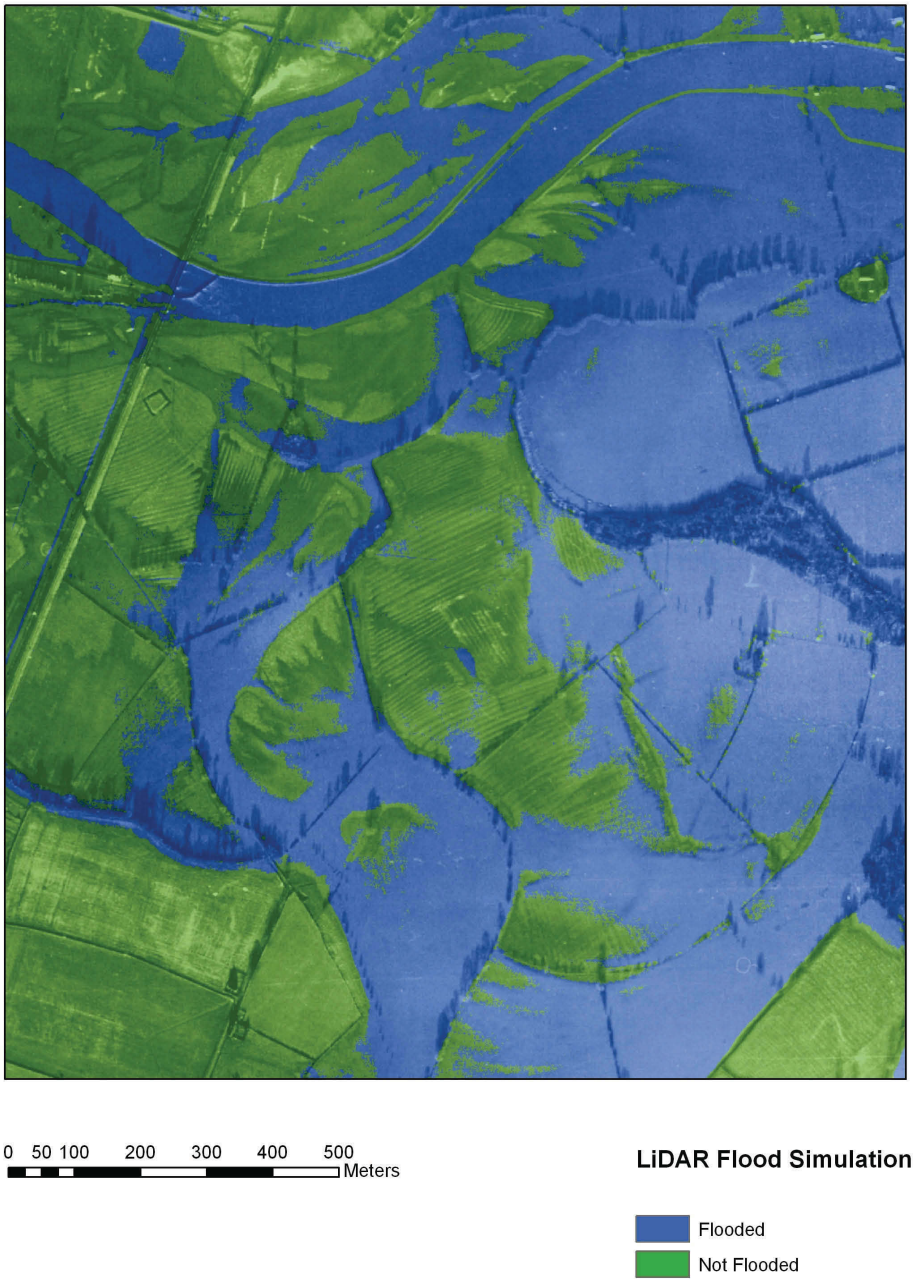

Fig 4.7: December 1954 vertical aerial photograph of the study with the Rivers Trent and Soar in flood, showing the extent of flooding (extracted by analysis of elevation values on the LiDAR DSM highlighted in blue).

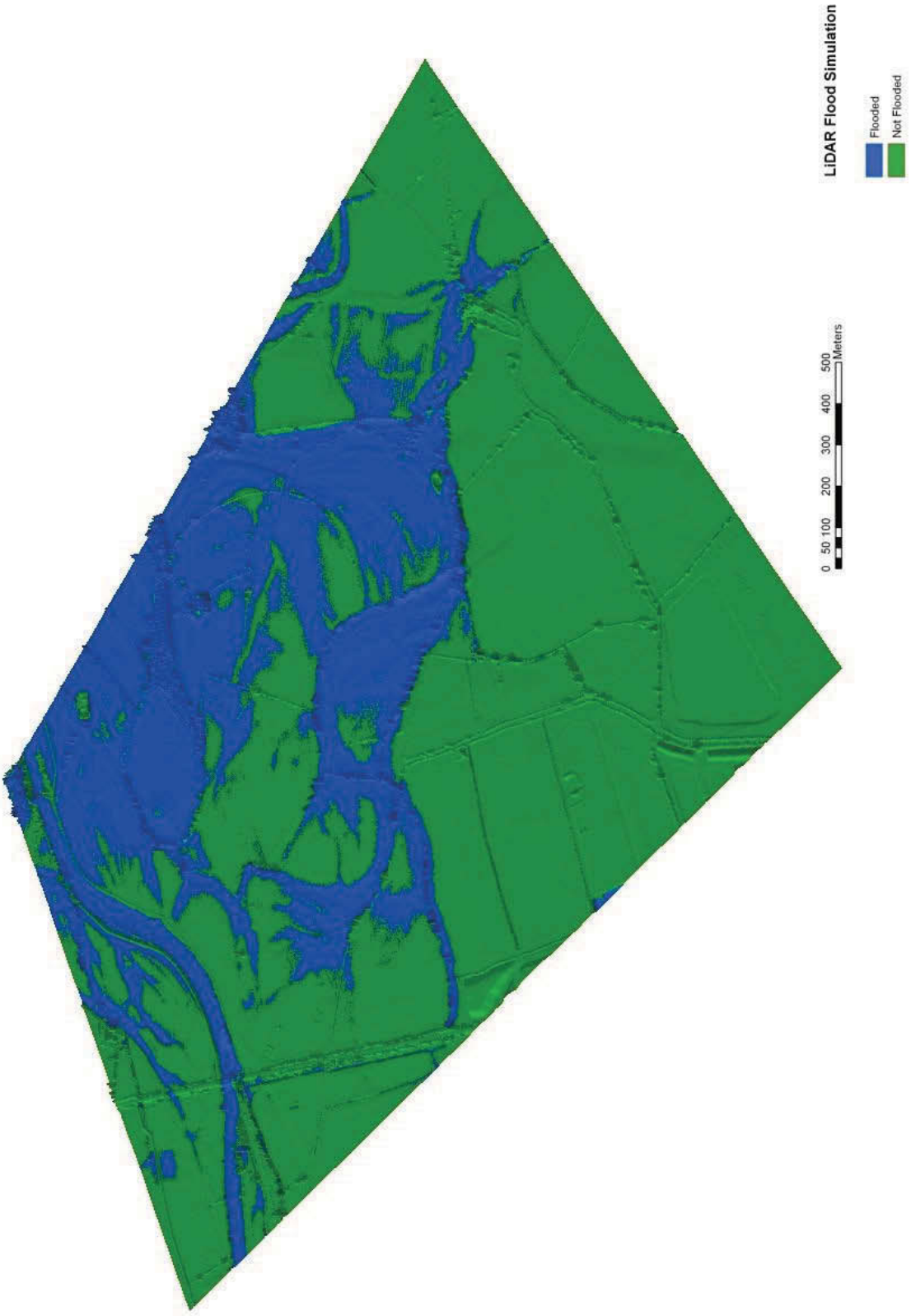

Fig 4.8: Pseudo 3D view of a LiDAR derived simulation of the extent of flooding of the study area on 15th December 1954.

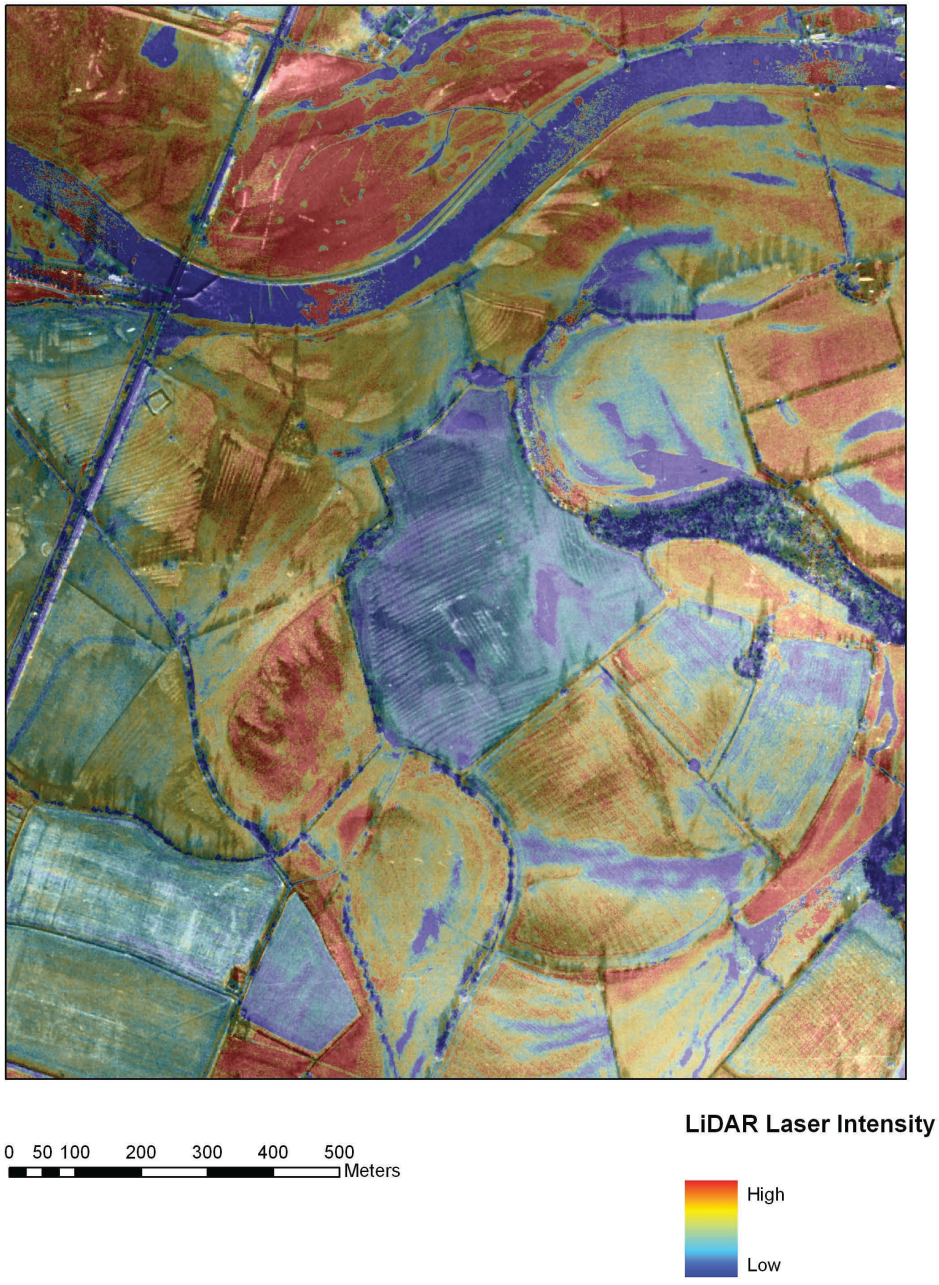

Fig 4.9: The December 1954 aerial photograph of the study area with LiDAR laser intensity data superimposed.

4.4 LiDAR Digital Surface Models

Analysis of LiDAR elevation products has focused on examining the effectiveness of LiDAR elevation products for identifying significant topographical features of the terrace and floodplain, quantifying relative accuracy and absolute accuracy of LiDAR elevation products compared to elevation values recorded by field survey using dGPS, and analysis of the impact of varying resolutions of LiDAR elevation data on the DSM metrics and the ability to identify significant landscape detail.

4.4.1 LiDAR Digital Surface Models and Geoarchaeological Mapping

Data for this project were acquired by Infoterra using an Airborne Laser Terrain Mapper (ALTM) the Optech ALTM 2033 LiDAR, collecting 1 point/m^2 (Optech 2003). The survey light was carried out as a single sortie in February 2003. The Infoterra survey provides access to point-cloud data (Fig. 4.10) as well as grid arrays of FP and LP and laser intensity data (Figs. 4.11-4.13). Initial processing of the point-cloud data was undertaken by Steve Wilkes; point cloud data were used to generate DSM by surfacing in ERDAS Imagine using a rubber sheeting algorithm to produce a regular grid.

The raw LiDAR data were processed to WGS84 projection, with ellipsoidal elevation values, transformed to British National Grid with orthographic elevation values conforming to Ordnance Datum, and a regular grid with elevation values at grid nodes, generated from the point-could. Analysis of the LiDAR data was undertaken in ArcGIS 9 after importing and conversion to ArcGIS Grid format. Basic analysis comprised a visual comparison of LiDAR FP, LP and intensity data with air-photographic and other evidence.

4.4.2 L iDAR DSM results

The utility of LiDAR elevation data for mapping floodplain and terrace geoarchaeology is immediately and spectacularly evident across the study area. The general disposition of the terrace units and the principal palaeochannels identified from air-photographs are clearly visible on the FP DSM (Fig. 4.11). However, some channels are partially obscured by vegetation, in particular the dense belt of scrubby woodland towards the northeastern edge of the study area. In contrast, the LP DSM (Fig. 4.12), from which laser returns from vegetation are excluded, clearly displays the detail of all palaeochannels without the obscuring effects of vegetation cover. This is most clearly demonstrated in a profile view through the FP and LP LiDAR data or this palaeochannels (Fig. 4.13). The ability of LiDAR to penetrate vegetation has proven particularly useful in this context.

LiDAR intensity data (Fig. 4.14) also records some palaeochannels as variations in the intensity of the reflected laser pulse. In general palaeochannels are indicated by a low level of reflections of the laser pulse; this is further discussed later. Closer comparison of extracts from the LP DSM and intensity values with aerial photographic evidence reveals the extent to which LiDAR is able to reveal geomorphological features not captured by conventional photography and also some limitations of LiDAR.

Figure 4.15 shows the modern floodplain close to the River Trent in the northeast corner of the study area. Palaeochannels and other floodplain features evident as water filled depressions in the aerial photography are clearly delineated by the LiDAR LP DSM. In addition, a number of other subtle

features, including curvilinear ridges, possibly ridge and swale, are evident on the LiDAR image, but not the aerial photograph. The LiDAR intensity data provides a further view of this area of floodplain. In general, areas of low laser reflection (darker on the image) coincide with the water filled depressions on the air photograph (although these features were not water filled at the time of the LiDAR flight as there is no evidence of characteristic reflections from water). Comparison of intensity data and air photographic evidence suggest that these depressions, with moist fills (confirmed by field inspection) are responsible for low levels of laser reflection. Not all of the topographical features evident on the DSM are seen as low intensity features on the intensity data, perhaps indicating that some depressions, although topographically clearly defined, do not have fills significantly wetter that the surrounding floodplain.

Figure 4.16 shows a part of the Hemington terrace close to the centre of the study area. Air photographic, LP DSM and intensity data all reveal a similar pattern of ridge and swale topography in the southern part of the area. The well-defined palaeochannels to the north of this are also clearly evident in both the FP DSM and intensity data, although less clear in the air photograph. However, the air-photographic evidence reveals a number of other channels as cropmarks, crossing this terrace unit that are not evident in the LiDAR data, as well as a cropmark sub-rectangular D shaped enclosure. Interestingly a roughly northwest to southeast aligned linear ridge, indicating the slight earthwork traces of a former medieval plough headland, are well defined by the LP DSM, but are not evident in the intensity data or on the air photograph. Clearly there is no simple relationship between what type of feature and in what circumstances features are revealed by LiDAR. Close comparison of the complimentary evidence of LiDAR with air photography seems necessary to generate a full picture of the geoarchaeology of the study area.

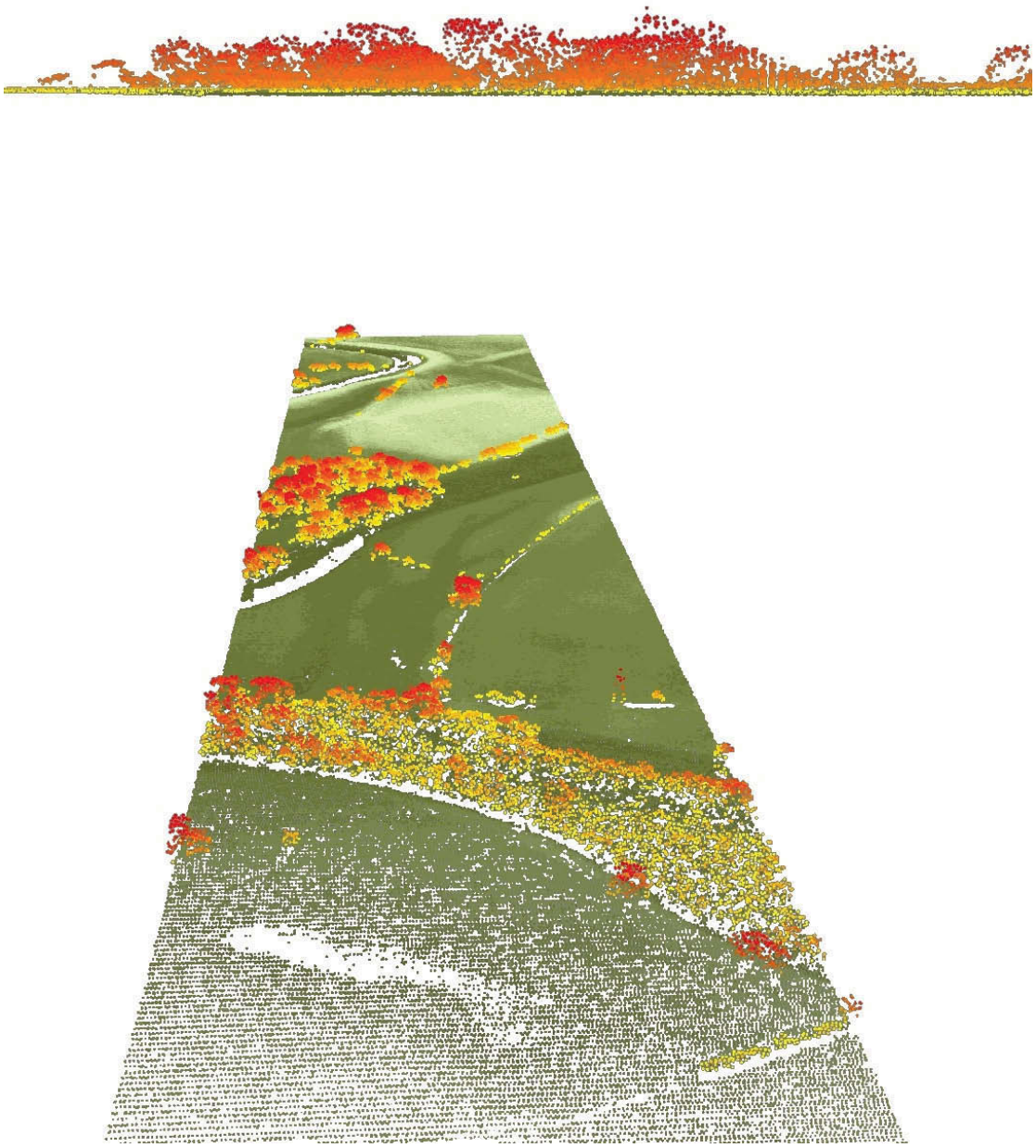

Fig 4.10: Two views of point cloud LiDAR elevation data for a part of the study area. Top a cross section through the point could and bottom an oblique view of the point cloud, both showing first pulse points (primarily vegetation) coloured red/orange and last pulse points (ground surface) coloured green.

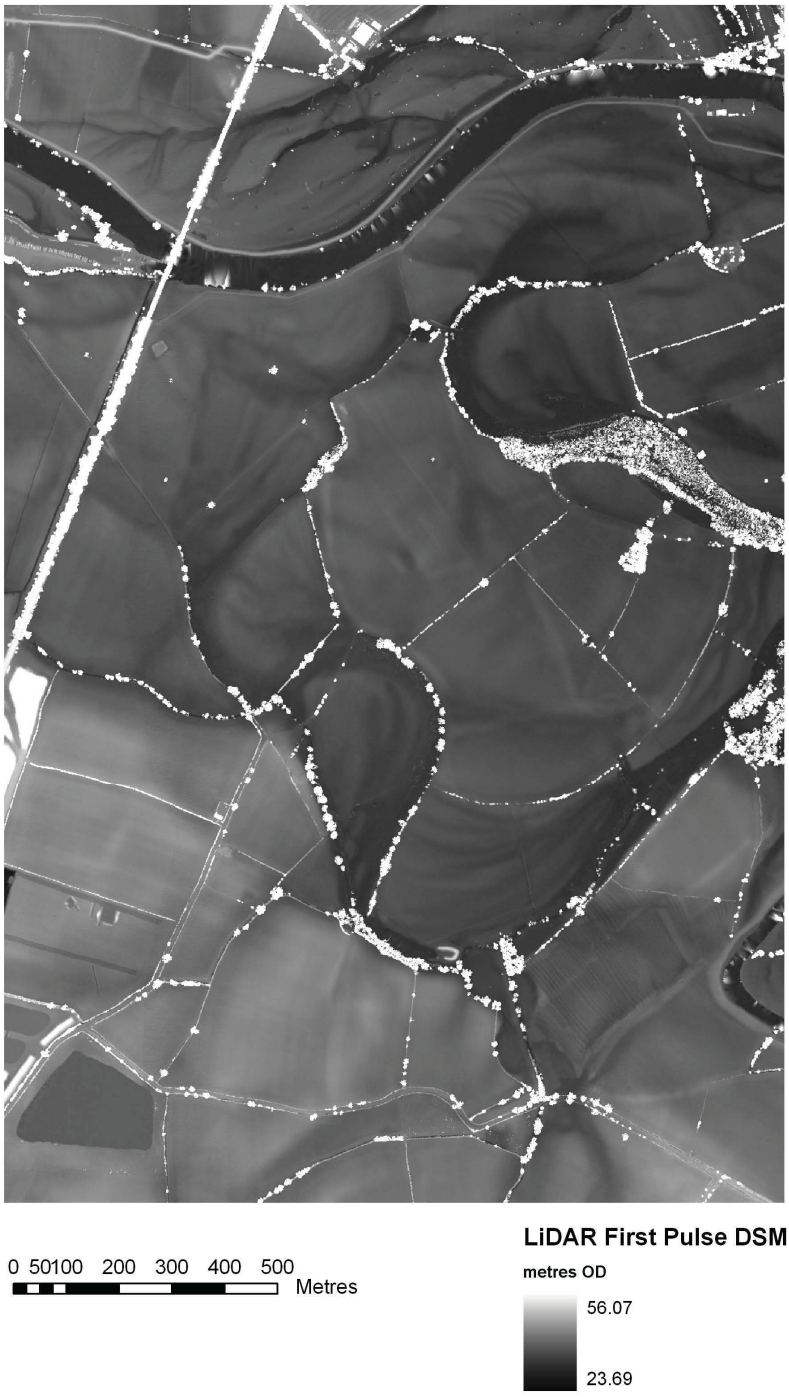

Fig 4.11: LiDAR fist pulse digital surface model of the study area.

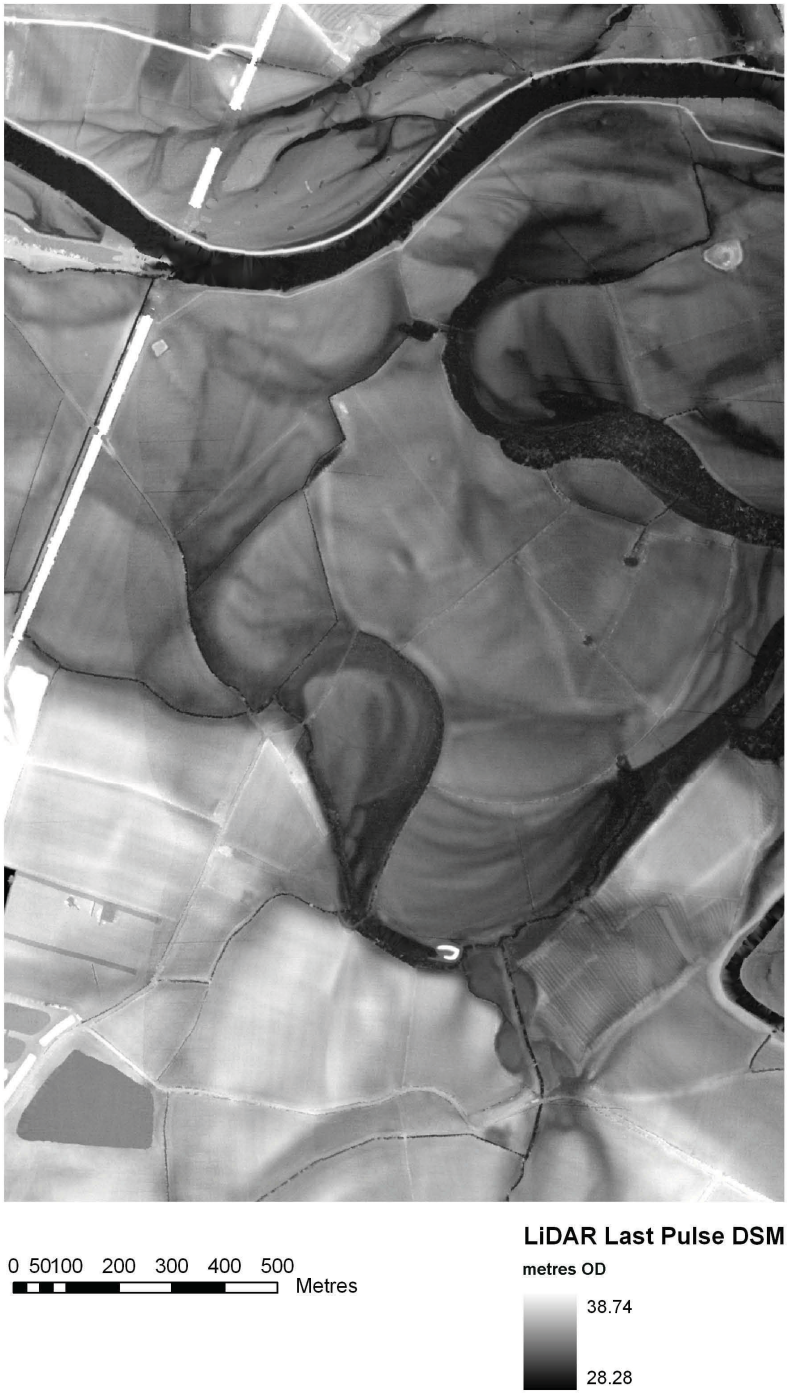

Fig 4.12: LiDAR last pulse ground digital surface model of the study area.

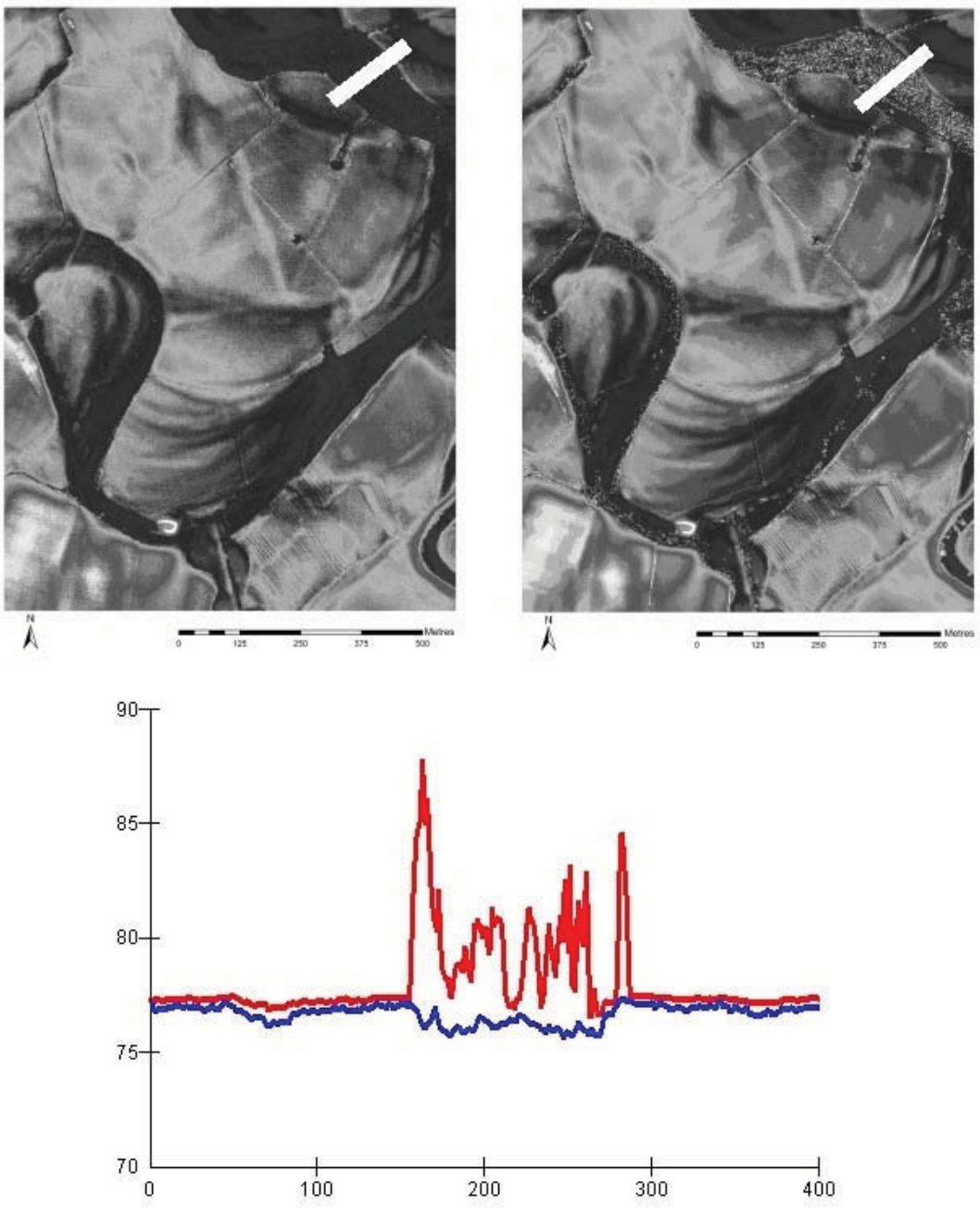

Fig 4.13: Last Pulse Ground (Left) and First Pulse (Right) LiDAR DSM of the study area with below profiles through the two DSM illustrating the facility of the LPG DSM to show the ground surface of palaeochannels beneath vegetation cover. Profile location shown by broad white line.

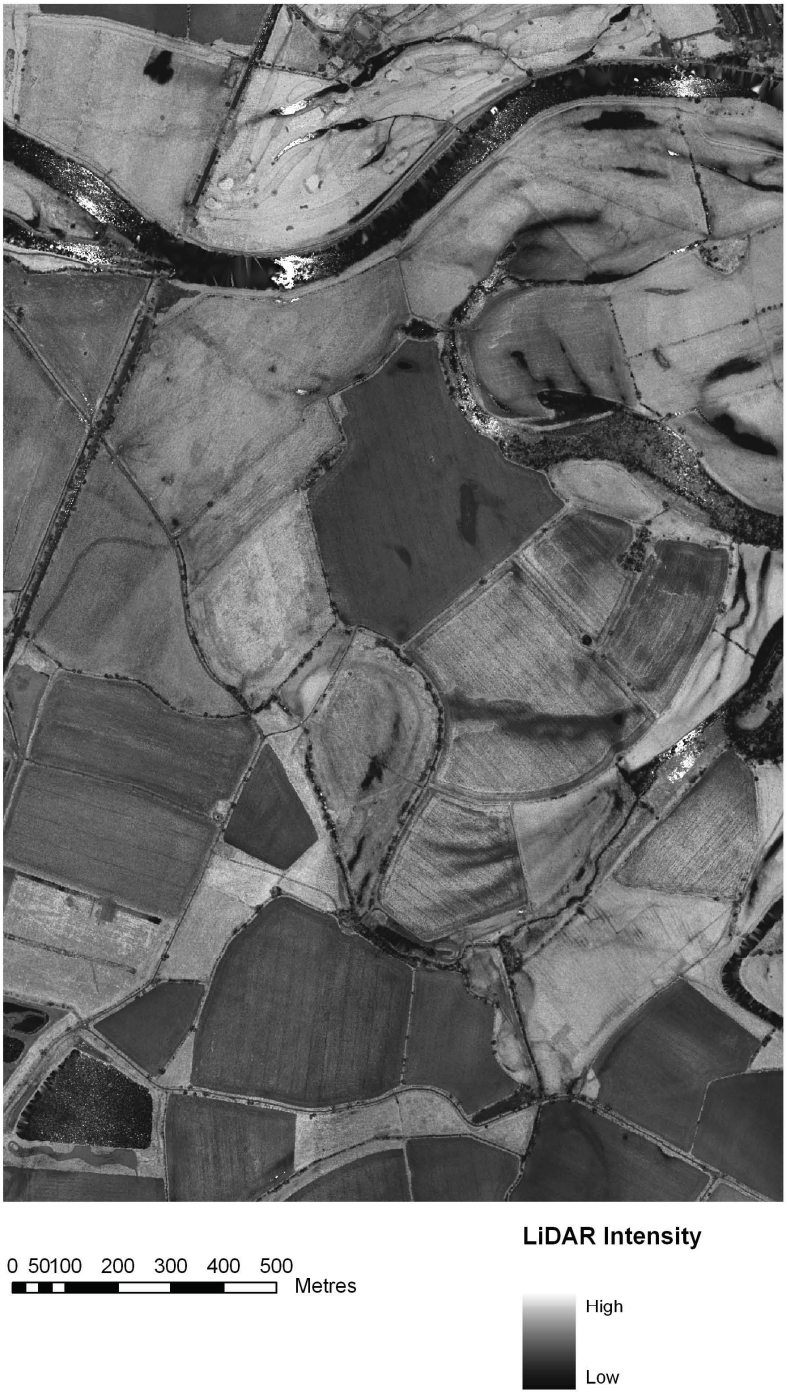

Fig 4.14: LiDAR laser intensity data for the study area.

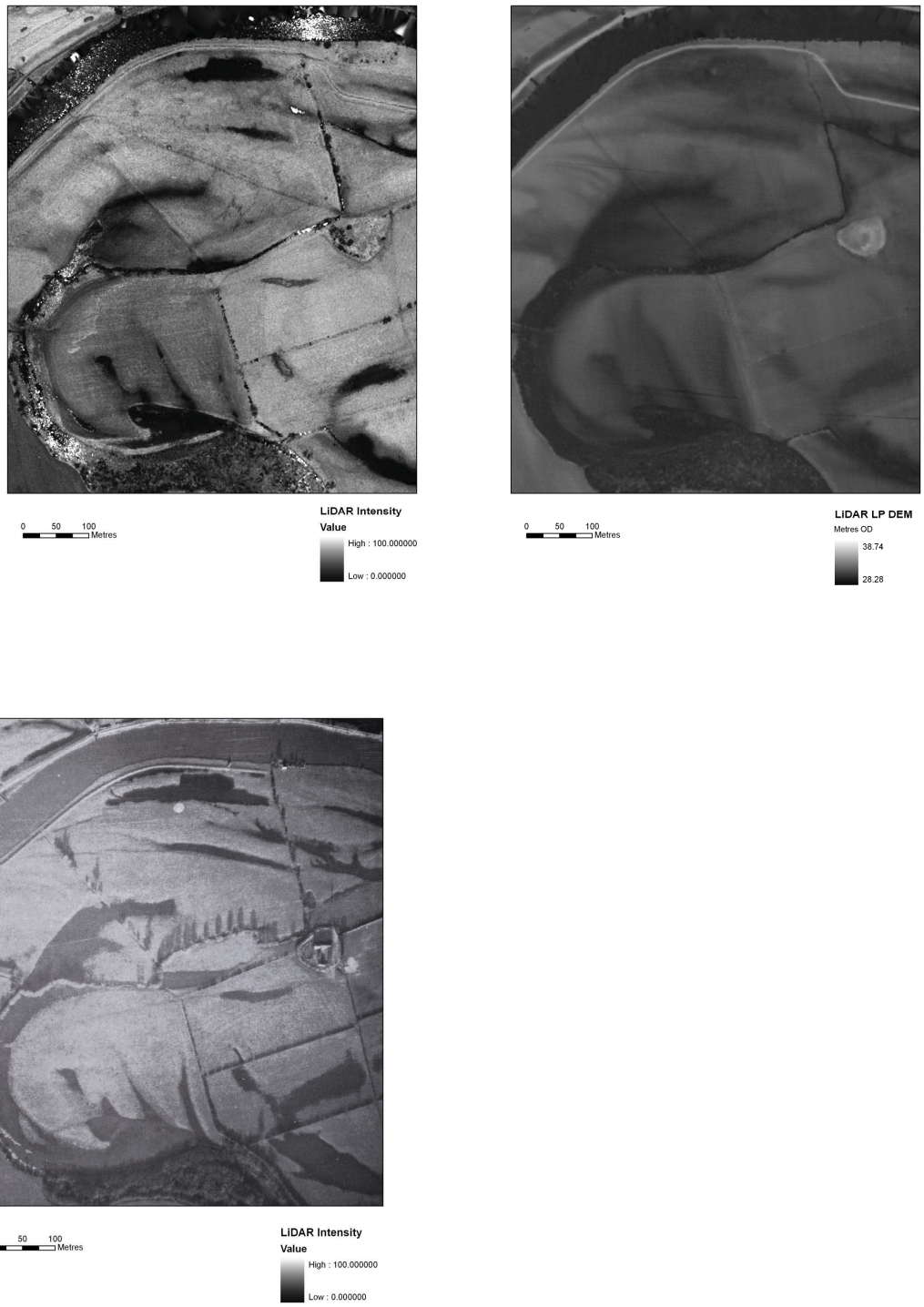

Fig 4.15: Comparison of (A) LiDAR laser intensity (B) LiDAR DSM and (C) air photographic evidence for palaeochannels within the floodplain and Hemington Terrace.

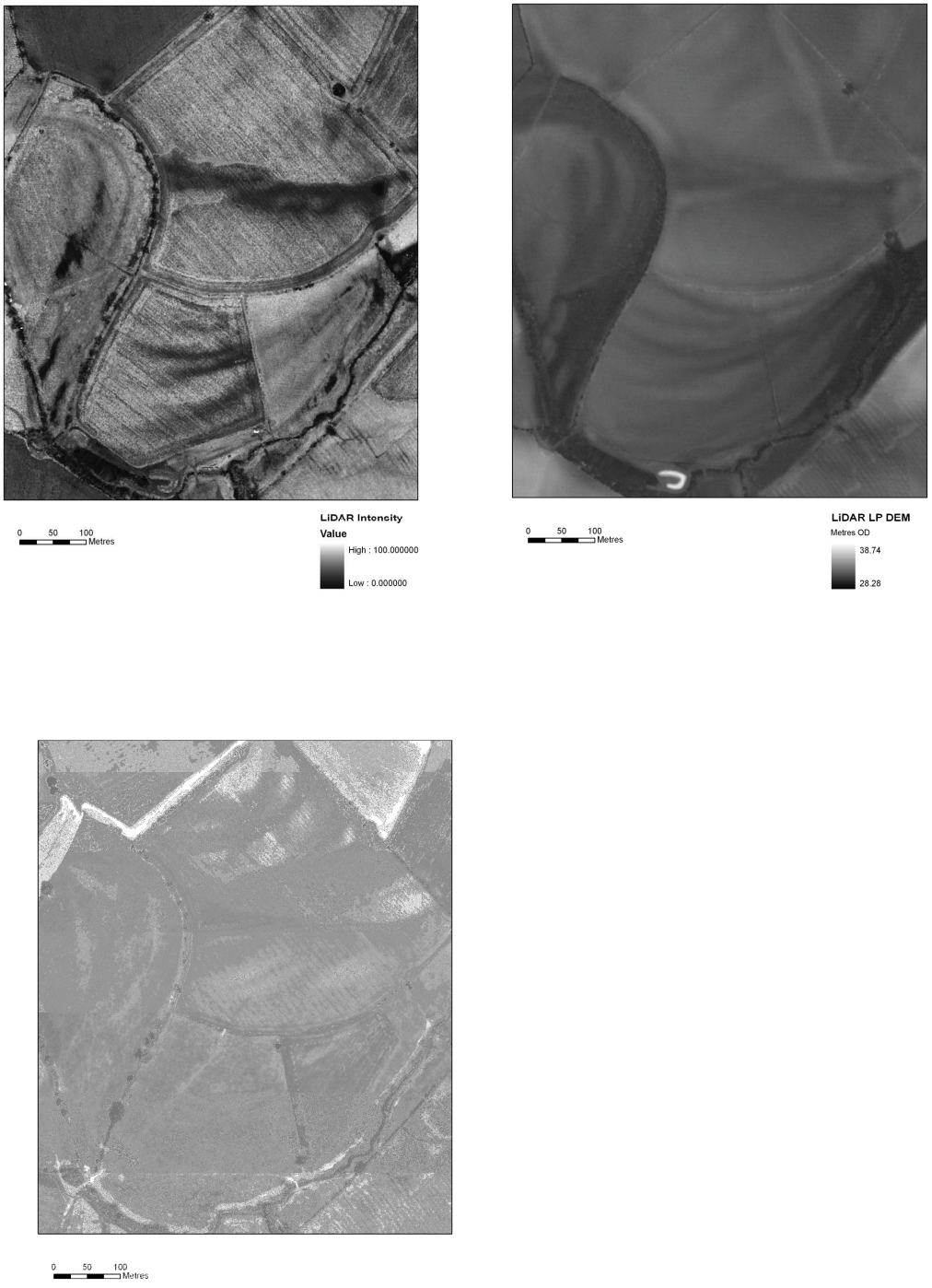

Fig 4.16: Comparison of (A) LiDAR laser intensity (B) LiDAR DSM and (C) air-photographic evidence for palaeochannels within the Hemington Terrace.

4.5 LiDAR DSM Spatial Resolution

LiDAR data was examined to determine its absolute accuracy, ability to resolve topographical features on the floodplain and terrace, and the impact of variations in spatial resolution of the elevation values on these factors. Absolute accuracy of the LiDAR elevation data was tested by comparing LiDAR LP ground elevation values, with elevation values recorded in the field using carrier phase differential GPS. Six transects across channel features were surveyed using a Leica system RD500 Real Time Kinematic Carrier Phase Differential Global Positioning System, taking elevation reading at the ground surface at approximately 0.5m intervals (Fig. 4.17: 1-6). Survey data were corrected to OSGB36 projection and orthographic elevation values conforming to Ordnance Datum using Leica Ski Pro software. The resulting elevation vales were imported into ArcGIS and their two dimensional co-ordinates used to extract elevation values from the LiDAR data at corresponding locations.

In order to test the impact of a reduction in grid resolution, the 1m LP grid was resampled to a 2m (equivalent to the resolution of the Environment Agency's standard LiDAR product) 5m and 10m grid spacing. Resampling was accomplished by extracting values from the LiDAR LP DSM at appropriate intervals. Values for the resampled grids were extracted directly from the LP DSM without averaging or otherwise calculating trends between resampled points and using these extracted values to generate a new grid at reduced resolution.

The 2m, 5m and 10m grids were compared visually to the original 1m resolution data (Figs. 4.24 – 4.28) and grid elevation and slope histograms (Figs. 4.29 and 4.30) and grid statistics for each generated (Tab. 4.2). In addition, elevation values for 1m FP and LP, 1m intensity, 2m, 5m and 10m resampled grids and 10m IFSAR elevation products were extracted for each of the six GPS survey transects used to evaluate the accuracy of the 1m DSM and a further six transects (Fig. 4.17; 6-12). Profiles generated from these extracted elevation values are shown (Fig. 4.22 – 4.23).

4.5.1 Absolute Accuracy of the LiDAR DSM

Calculations of the absolute accuracy of the LiDAR DSM compared to a GPS surveyed transect proved problematic. Comparison of LiDAR and GPS derived elevation vales showed a difference in reported elevation values of between 11.68 and 12.18m (mean 11.85m). Further investigation showed that the OD values recorded by the GPS are considerably below those expected for the area surveyed. Examination of X and Y coordinate data from the GPS survey showed close coincidence of the surveyed data with map, LiDAR and air-photographic evidence. It seems likely that there is a problem with the Z co-ordinate component of the GPS survey, probably caused by the collection of insufficient differential correction data from the fixed base station (in general significantly greater data is required to produce accurate Z co-ordinated compared to X and Y). This difficulty rendered measurements of absolute accuracy of the LiDAR elevation products impossible with the data collected and analysis has therefore been limited to assessment of relative accuracy of LiDAR and GPS (i.e. how well does LiDAR record the subtleties of topography actually evident on the ground).

4.5.2 Relative Accuracy and Resolving Ability of the LiDAR DSM

Visual comparison of the terrain detail captured by the 1m LiDAR LP DSM and that recorded by field survey using GPS may be made by comparing the profiles (Figs. 4.18 – 4.20). Profiles were recorded to represent a variety of terrain types including ridge and swale (P1; Fig. 4.18), palaeochannels (P2-5; Figs. 4.18 – 4.20) and terrace edge (P6; Fig. 4.20).

Ridge and Swale

The roughly parallel sinuous corrugations of ridge and swale, developed through successive southward channel migration, are clearly evident in the LiDAR intensity image on the line of profile 1 (Fig. 4.17 and 4.18). The surveyed ridges, captured by the GPS survey, are faithfully represented in the LiDAR 1m LP DSM as changes in elevation of about the correct magnitude (0.1-0.2m). High frequency variations in the LiDAR profile are likely to be the result of residual vegetation effects; in general both the detail and scale of the ridge and swale are captured by the LiDAR DSM.

Palaeochannel

Four profiles across a broad sinuous palaeochannel (up to 0.5m deep) within the Hemington terrace deposits were recorded. The channel is clearly evident on the LiDAR intensity image and forms a marked topographical feature on the ground, which is recorded by four GPS surveyed orthogonal profiles. Once again there is god agreement in both detail and scale between the LiDAR LPG DSM and the GPS profiles. All of the LiDAR profiles exhibit some high frequency noise, this particularly affects profiles 2 and 4, and is less evident on profile 5. Interestingly, the slight mid channel feature crossed by profiles 4 and 5 and evident as an area of higher intensity laser return on Fig. 4.17, is only weakly visible as a topographical feature on both the GPS and LiDAR data, but is far more clearly represented as a variation in intensity, particularly on profile 5 (Fig. 4.20).

Terrace Edge

The western edge of the Hemington terrace, where it has an erosive contact with a substantial sinuous palaeochannels of the Trent, forms a well defined topographical feature about 0.8m high. The terrace edge as surveyed in the field is faithfully captured by the LiDAR LPG DSM (P6; Fig. 4.20), although with some variation in the profile of the terrace surface evident.

4.6 Resolving Ability of the Resampled DSM

Resampled LiDAR DSM at 2m, 5m and 10m spatial resolution were also queried for comparison with the GPS field survey and 1m LPG DSM (Figs. 4.18 – 4.20). The effects of reduction in spatial resolution have a minimum affect at 2m resolution, although the definition of low amplitude features such as ridge and swale is reduced and the clarity with which the edges of more substantial features can be discerned is degraded. Nevertheless, for the majority of purposes the 2m spatial resolution data is suitable for the identification of features of floodplain and terrace topography, even if compromised in their accurate delineation. The general visual impression of the 2m DSM (Fig. 4.25) is good, and there appears to be little or no loss in resolution compared to the 1m data, even though only 25% of the original data remains (c 800k values as compared to 3.3million for the 1m DSM).

Casual visual inspection of the entire DSM when reduced to 5m (Figure 25) and 10m (Fig. 4.26) spatial resolution might also suggest that much of the detail captured at 1m resolution remains. This is incorrect. Examination of the profiles at 5m and 10m resolution shows that, beyond a general variation in elevation, none of the detail captures at 1m resolution survives and these low resolution DSM are completely unable to capture the form or edges of topographical features.

The effects of degradation in DSM resolution on the ability to identify and record archaeological features is shown (Figs. 4.27 and 4.28). Ridge and furrow clearly delineated at 1m resolution (Fig. 4.27), remain quite clearly defined at 2m resolution, are evident at 5m grid spacing but at 10m resolution are not recognisable. Likewise, the earthworks of the Bull Ring (Fig. 4.28) a small sub-square embanked

enclosure on the western edge of the study area, are clearly seen at 1m and 2m resolution, fading at 5m and not recognisable at 10m resolution.

Examination of DSM elevation histograms reveals something of the nature of the impact of reduction in grid resolution on the data. In each case, from 1m to 10m, the overall elevation histograms (Figs. 4.29 and 4.30) remain largely unaltered in shape as the reduction in data quantity does not drastically effect the spatial distribution of elevation values. The spatial distribution is the main contributor to these data. However, examination of frequency histograms for derived slope from each DSM does clearly highlight the main impact of reducing grid resolution: that is a decreasing ability to resolve fine variations in slope as both the range of slope values and the variation within the range decreases (Tab. 4.2) with decreasing resolution.

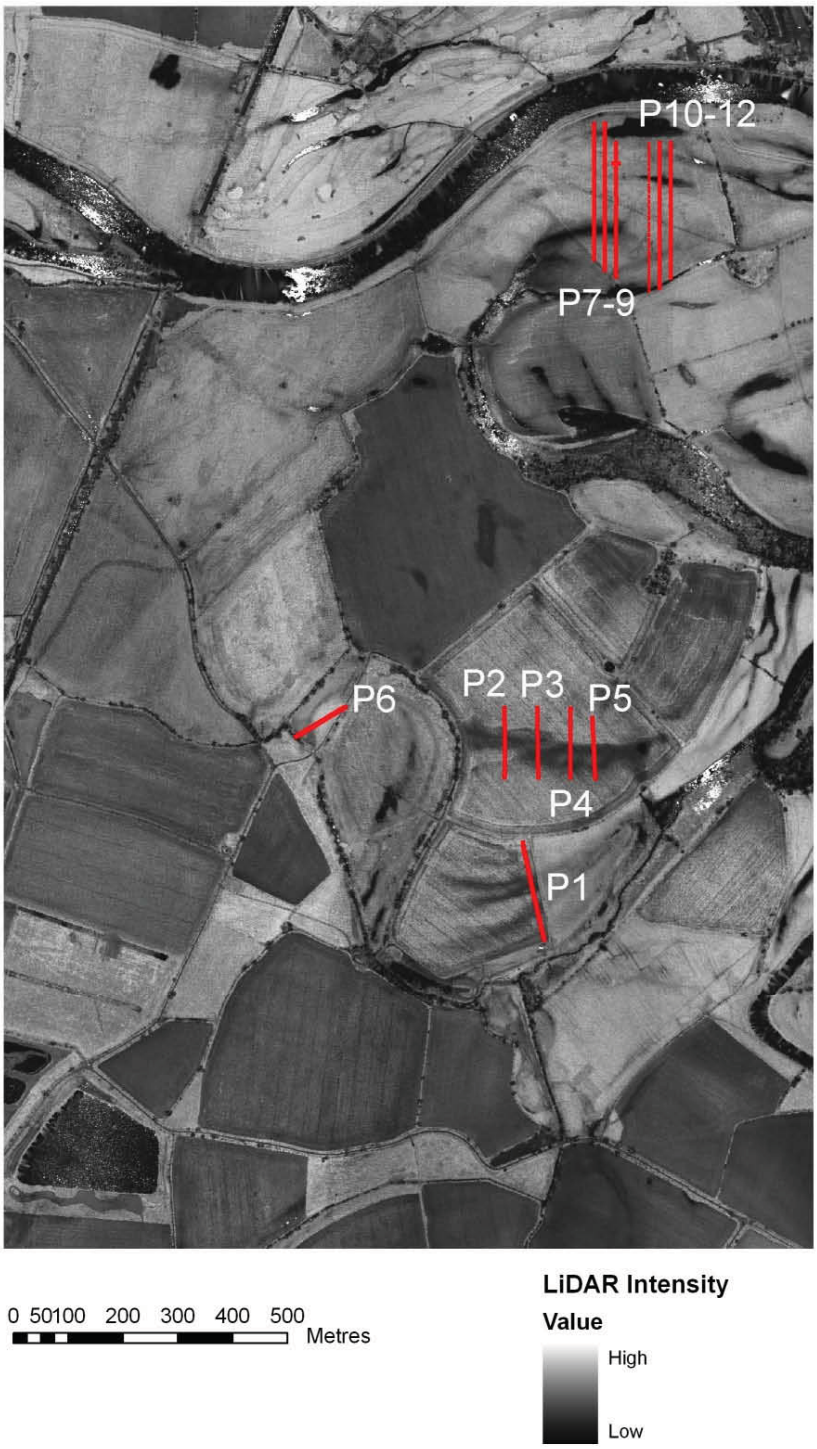

Fig 4.17: LiDAR laser intensity data for the study area with red lines indicating the location and extent of the 12 study transects.

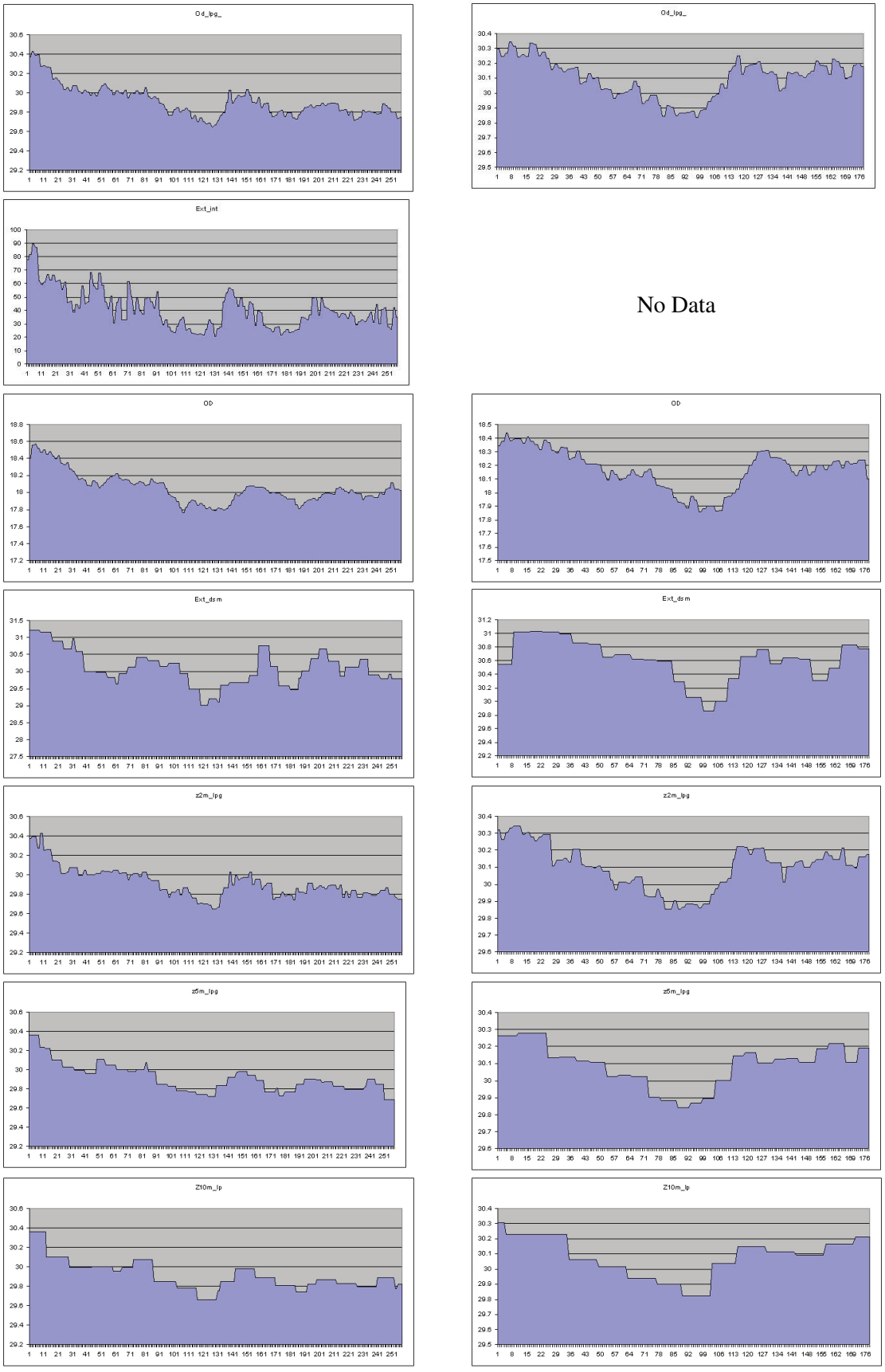

Profile 1 (T1 – ridge and swale) Profile 2 (T1 - palaeochannel)

Fig 4.18: Profiles 1 and 2 showing from top to bottom, RTK GPS elevation values, LiDAR LP DSM, LiDAR Intensity, IFSAR DSM, simulated 2m, 5m and 10m LiDAR DSM.

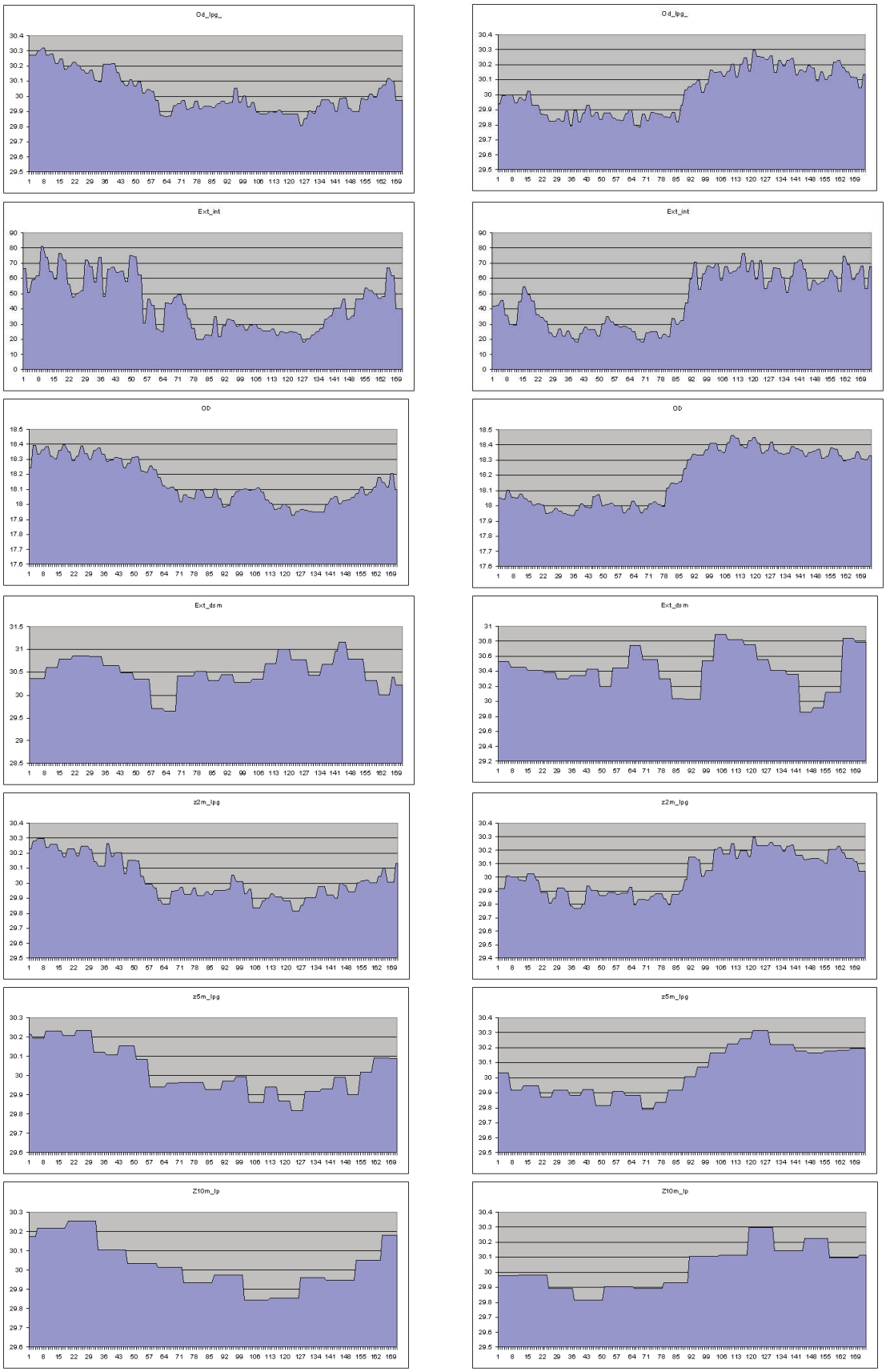

Profile 3 (T1- palaeochannel) Profile 4 (T1- palaeochannel)

Fig 4.19: Profiles 3 and 4 showing from top to bottom, RTK GPS elevation values, LiDAR LP DSM, LiDAR Intensity, IFSAR DSM, simulated 2m, 5m and 10m LiDAR DSM.

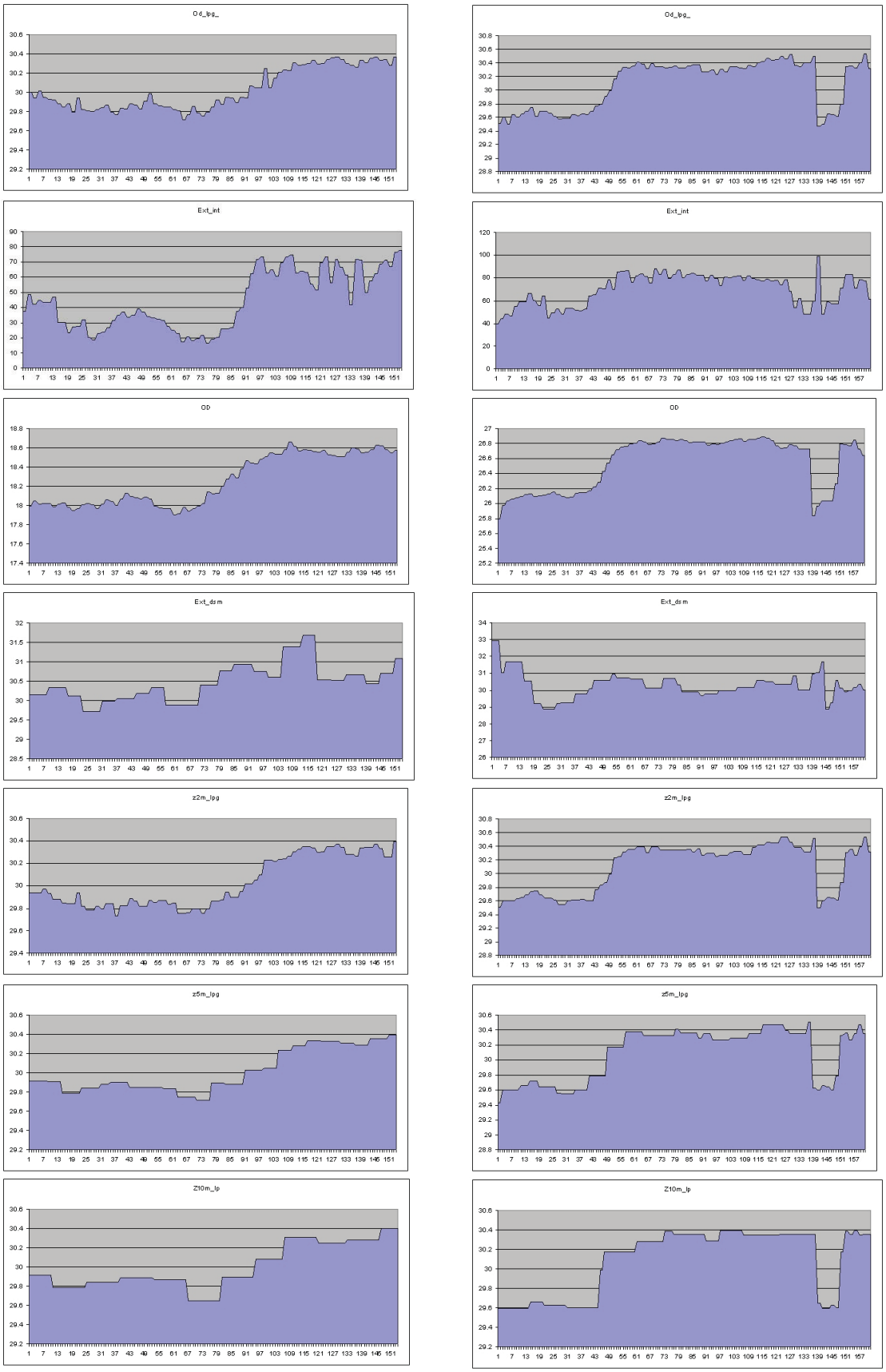

Profile 5 (T1- palaeochannel)

Profile 6 (T1 – terrace edge)

Fig 4.20: Profiles 5 and 6 showing from top to bottom, RTK GPS elevation values, LiDAR LP DSM, LiDAR Intensity, IFSAR DSM, simulated 2m, 5m and 10m LiDAR DSM.

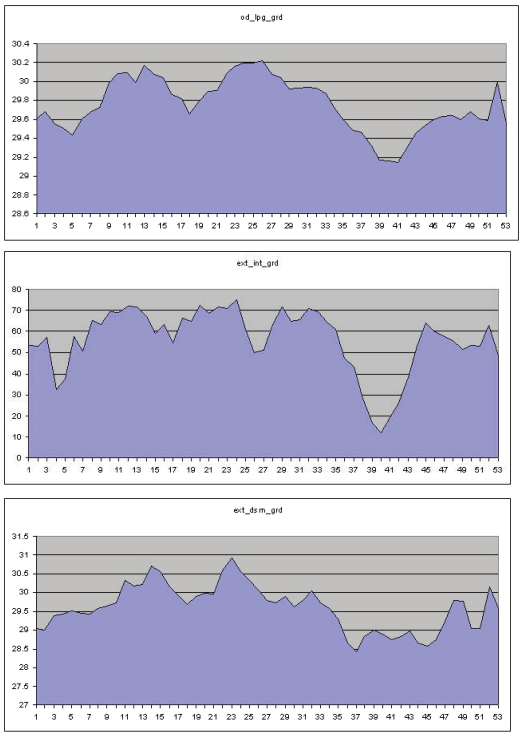

Profile 7 (MFP - palaeochannel)

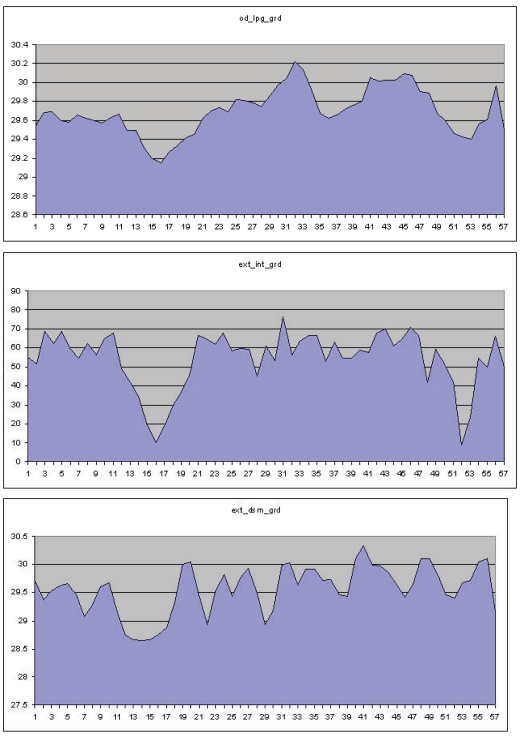

Profile 8 (MFP - palaeochannel)

Fig 4.21: Profiles 7 and 8 showing from top to bottom LiDAR LP DSM, LiDAR intensity and IFSAR DSM.

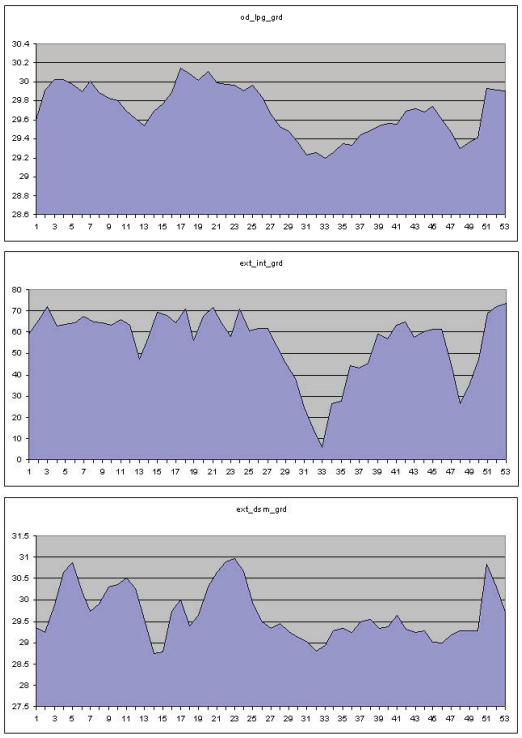

Profile 9 (MFP - palaeochannel)

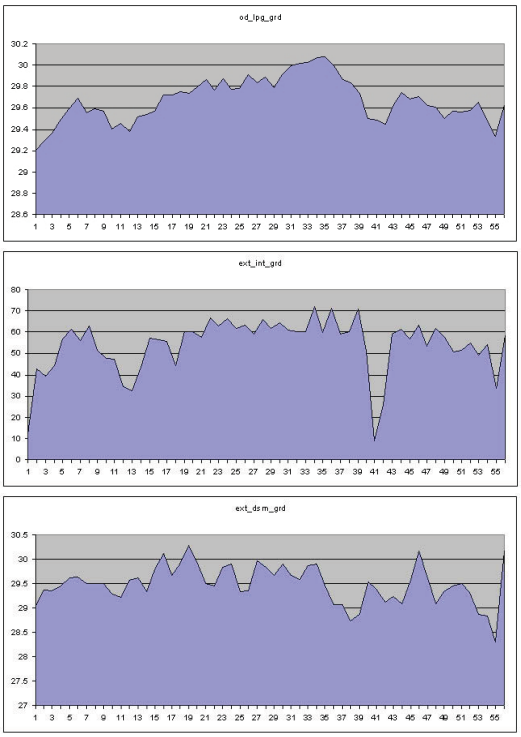

Profile 10 (MFP - palaeochannel)

Fig 4.22: Profiles 9 and 10 showing from top to bottom LiDAR LP DSM, LiDAR intensity and IFSAR DSM.

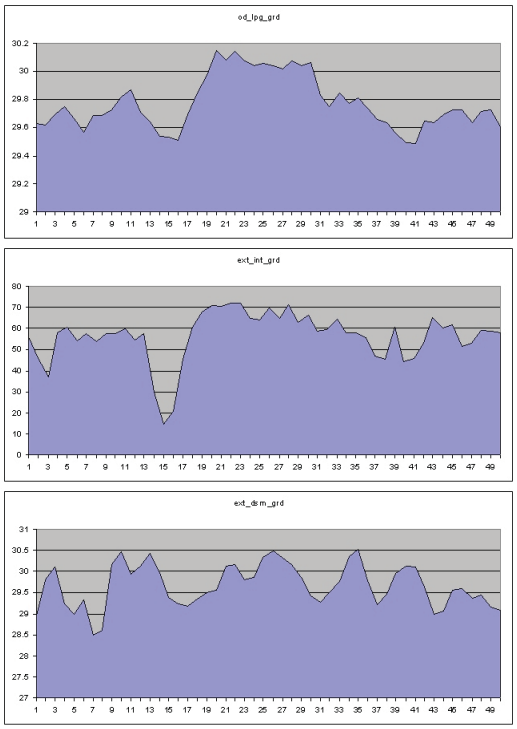

Profile 11 (MFP - palaeochannel)

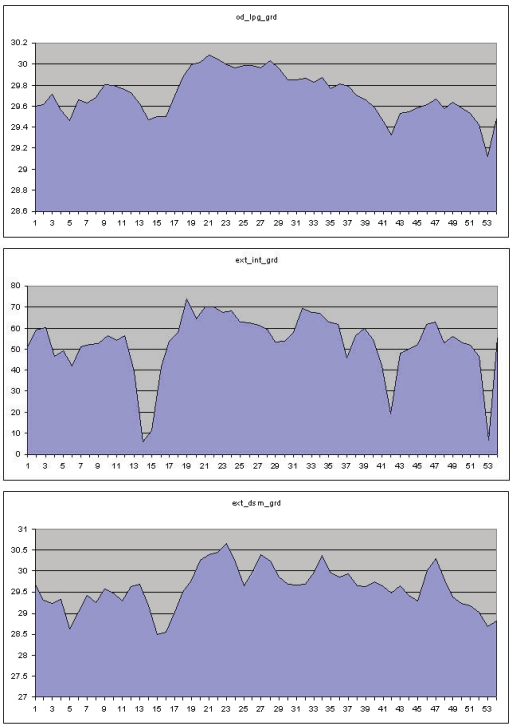

Profile 12 (MFP - palaeochannel)

Fig 4.23: Profiles 11 and 12 showing from top to bottom LiDAR LP DSM, LiDAR intensity and IFSAR DSM.

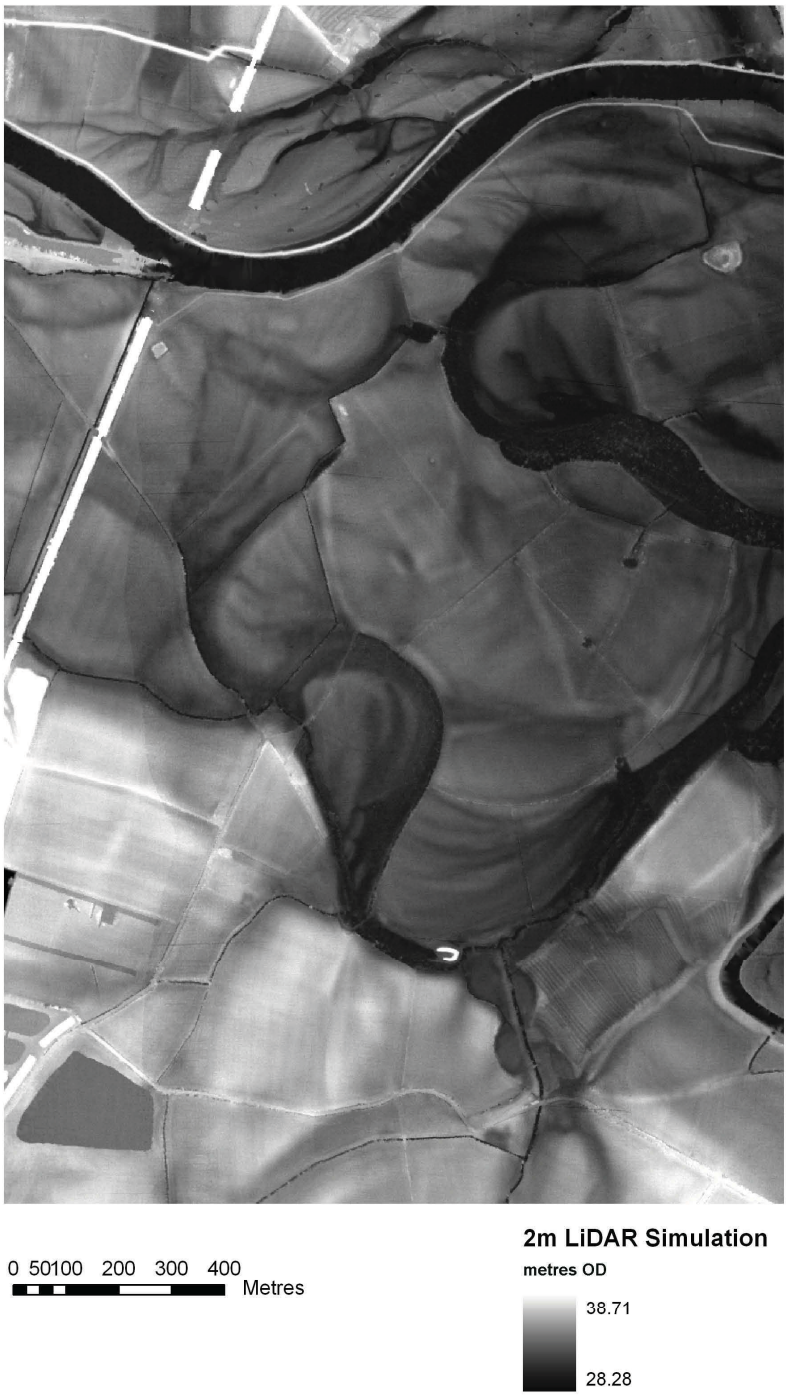

Fig 4.24: Simulated 2m LiDAR Last pulse ground digital surface model.

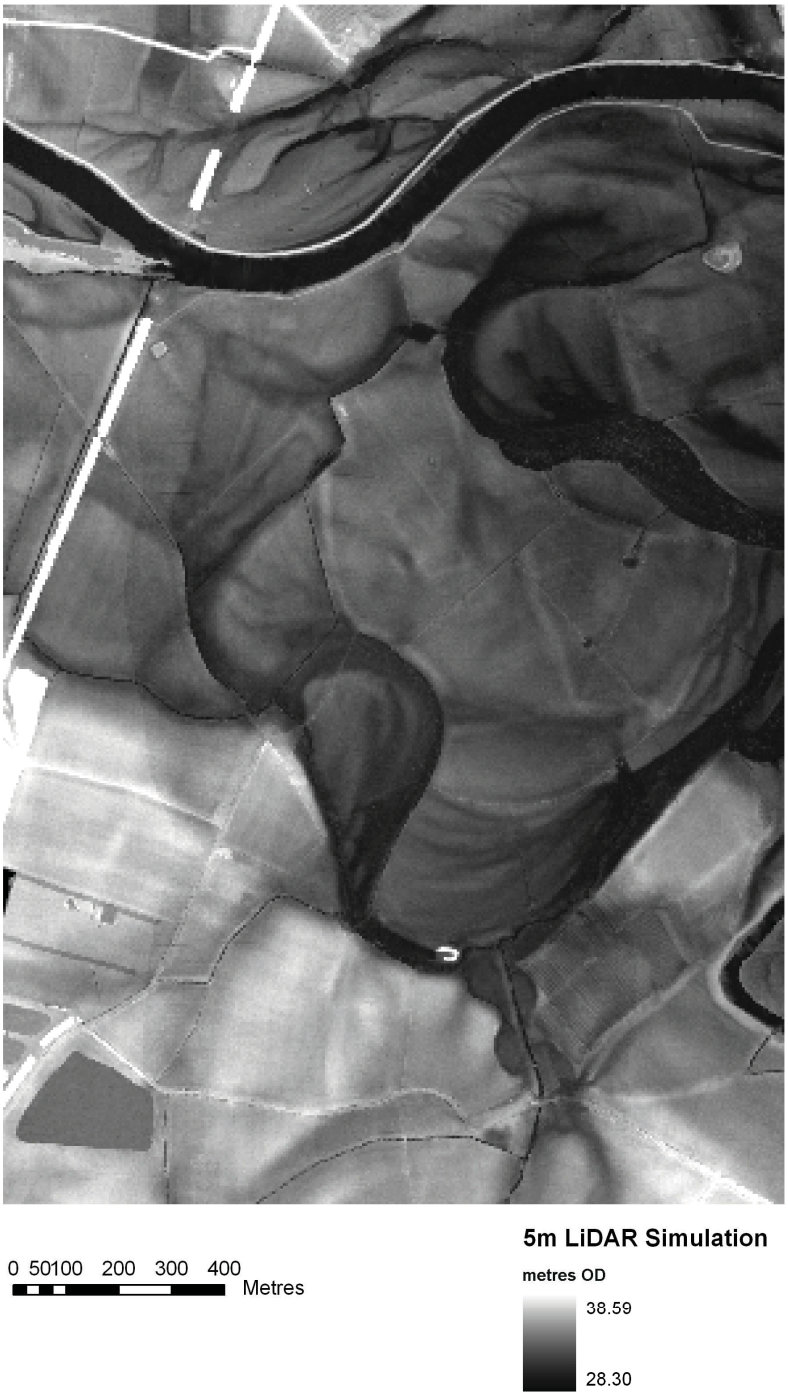

Fig 4.25: Simulated 5m LiDAR Last pulse ground digital surface model.

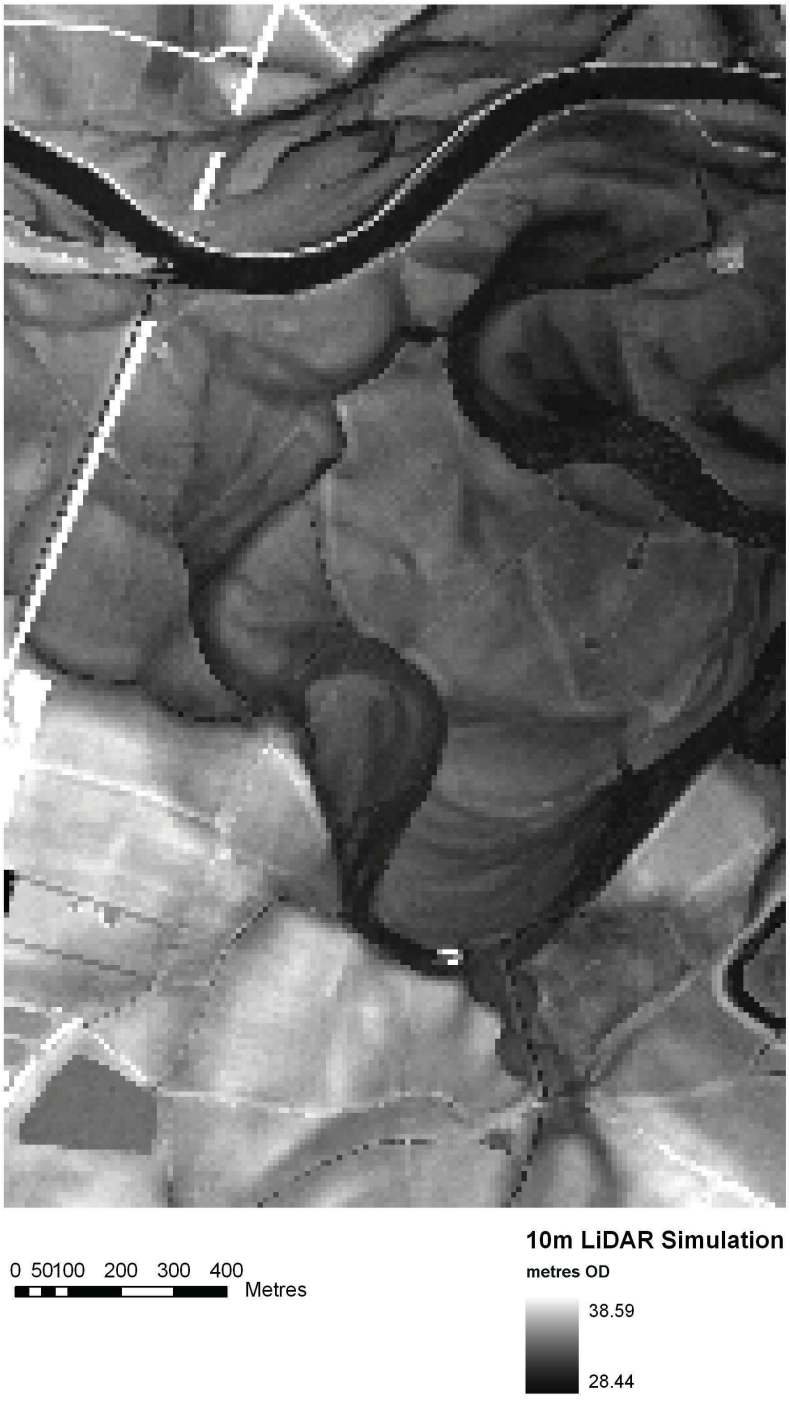

Fig 4.26: Simulated 10m LiDAR Last pulse ground digital surface model.

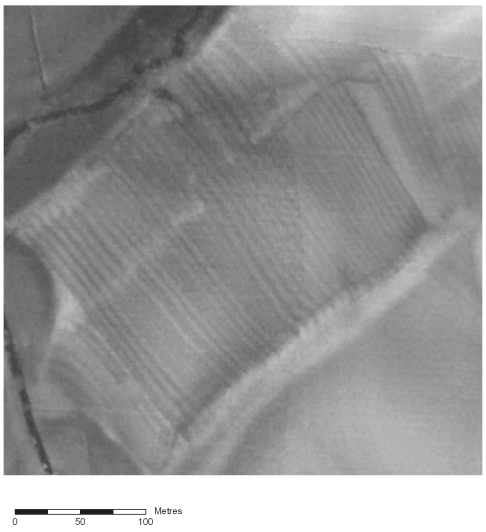

1m

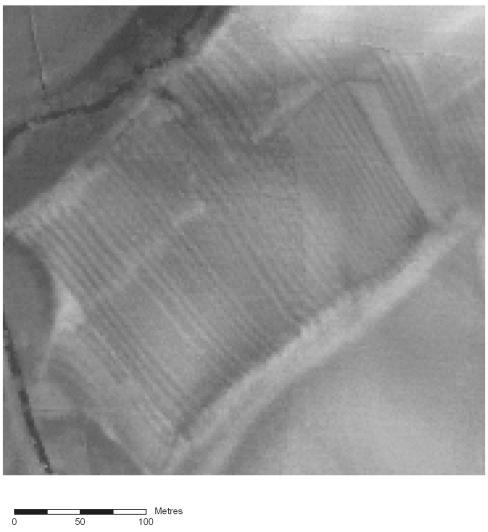

2m

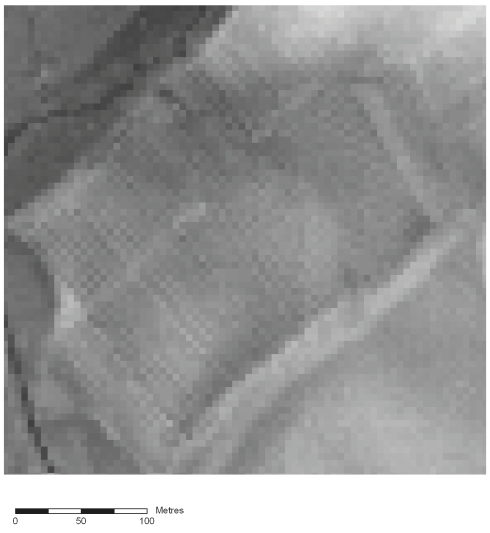

5m

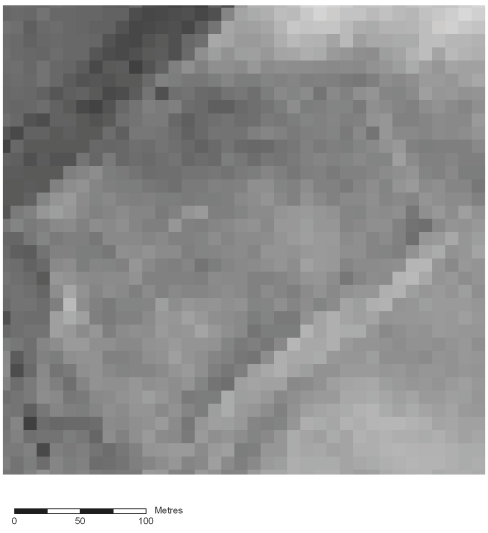

10m

Fig 4.27: LiDAR DSM of an area of earthwork ridge and furrow in the southeast corner of the study area showing the impact of variations in spatial resolution.

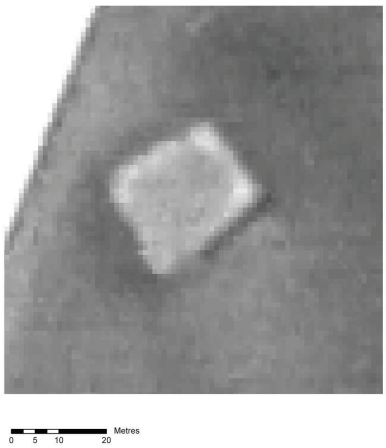

1m

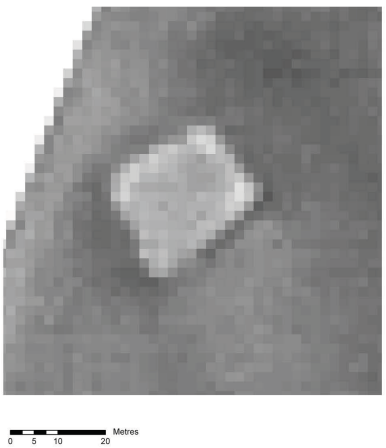

2m

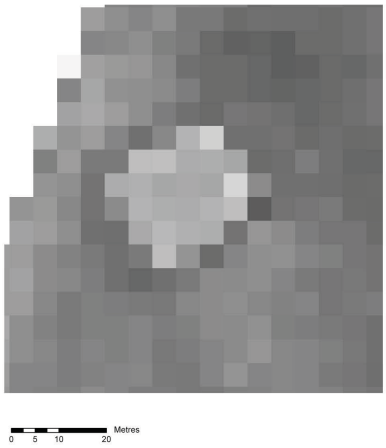

5m

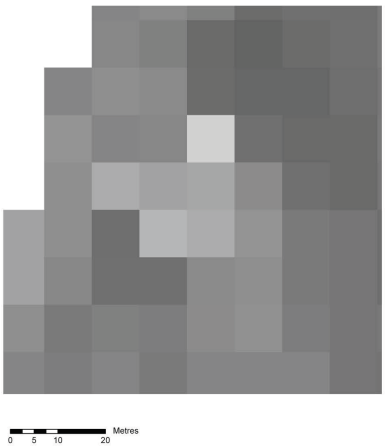

10m

Fig 4.28: LiDAR DSM of the earthworks of the Bull Ring in the northwest corner of the study area showing the impact of variations in spatial resolution.

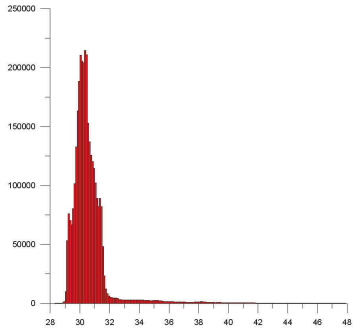

LiDAR 1m First Pulse DSM

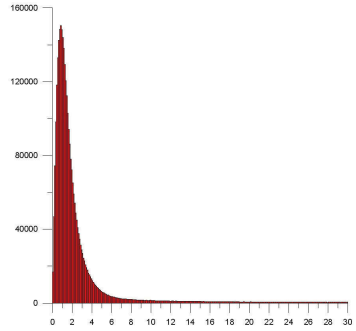

LiDAR 1m First Pulse Slope

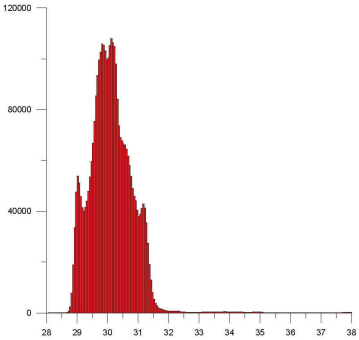

LiDAR 1m Last Pulse DSM

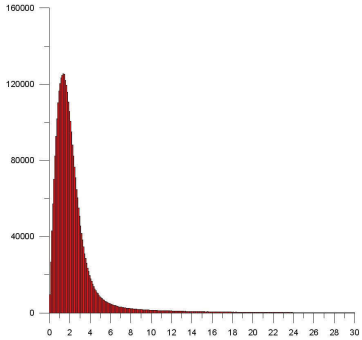

LiDAR 1m Last Pulse Slope

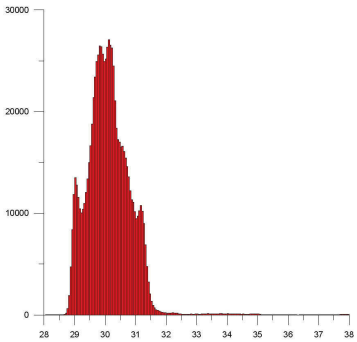

LiDAR 2m Last Pulse DSM

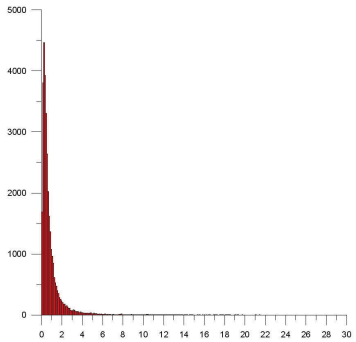

LiDAR 2m Last Pulse Slope

Fig 4.29: Elevation (left) and slope (right) histograms for LiDAR 1mFP, 1mLP and 2m DSM data for the entire study area.

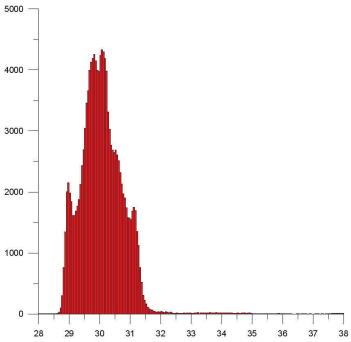

LiDAR 5m Last Pulse DSM

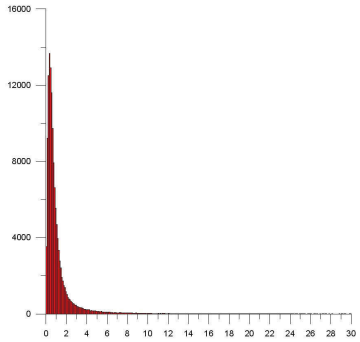

LiDAR 5m Last Pulse Slope

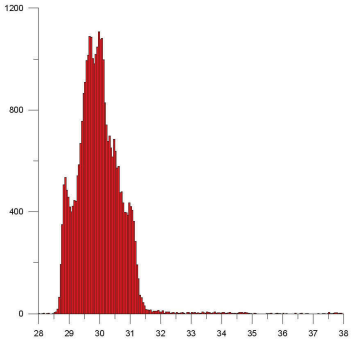

LiDAR 10m Last Pulse DSM

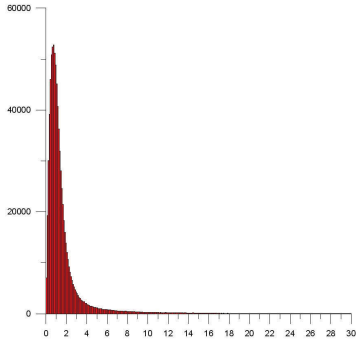

LiDAR 10m Last Pulse Slope

Fig 4.30: Elevation (left) and slope (right) histograms for LiDAR 5m, and 10m DSM data for the entire study area.

DSM 1m FPA			DSM 1m LPG		DSM 2m LPG	
Number of values	3355744	Number of values	Number of values	3355744	Number of values	839504
Minimum	23.69	Minimum	Minimum	28.29	Minimum	28.29
Maximum	56.07	Maximum	Maximum	38.74	Maximum	38.71
Range	32.38	Range	Range	10.45	Range	10.42
Mean	30.621	Mean	Mean	30.388	Mean	30.388
Standard deviation	1.4704	Standard deviation	Standard deviation	0.75695	Standard deviation	0.75738
Skew	4.784	Skew	Skew	2.276	Skew	2.279

DSM 5m LPG		DSM 10m LPG	
Number of values	134680	Number of values	33744
Minimum	28.31	Minimum	28.44
Maximum	38.6	Maximum	38.6
Range	10.29	Range	10.16
Mean	30.39	Mean	30.393
Standard deviation	0.75916	Standard deiation	0.76173
Skew	2.285	Skew	2.292

Slope 1m FPA			Slope 1m LPG		Slope 2m LPG	
Number of values	3355744	Number of values	Number of values	3355744	Number of values	839504
Minimum	0	Minimum	Minimum	0	Minimum	0
Maximum	84.58	Maximum	Maximum	67.22	Maximum	51.26
Range	84.58	Range	Range	67.22	Range	51.26
Mean	5.5135	Mean	Mean	2.583	Mean	1.792
Standard deviation	13.059	Standard deviation	Standard deviation	3.376	Standard deviation	2.9405
Skew	3.694	Skew	Skew	5.444	Skew	5.96

Slope 5m LPG		Slope 10m LPG	
Number of values	134680	Number of values	33744
Minimum	0	Minimum	0
Maximum	32.91	Maximum	21.42
Range	32.91	Range	21.42
Mean	1.2137	Mean	0.88408
Standard deviation	2.1507	Standard deviation	1.4057
Skew	6.229	Skew	5.929

Tab 4.2: Statistics for the various LiDAR DSM and derived slope values.

4.7 LiDAR Laser Intensity

LiDAR intensity data provides an indication of the intensity or amplitude of the reflection of the laser pulse from the ground surface. Many factors can affect the reflected laser intensity. Initial casual examination of LiDAR intensity data for the study areas suggests that there is a reduction in the intensity of the reflected light that corresponds with landscape features such as palaeochannels (Figs. 4.14, 4.15 and 4.31). Variations in the reflectivity of various earth surface materials to laser light of differing wavelength are quite well documented (for example see Wehr and Lohr, 1999: 74) and damp soil conditions are known to reduce reflectivity. It is possible that the increased soil moisture associated with palaeochannels and perhaps other associated variations in soil and vegetation properties, are responsible for the reduced reflectivity of the laser pulse. The present study has aimed to examine several aspects of LiDAR intensity data through visual comparison of intensity values with other ground and airborne remotely sensed data and though field measurement of volumetric soil moisture at selected sample locations.

4.8 Laser Intensity and Cropmark Formation

The analysis of LiDAR intensity data was undertaken largely within ArcGIS and ArcScene. Visual comparison of extracts from the intensity data with aerial photographic evidence and cropmark plots focused on examination of whether any aspects of the cultural archaeology, visible as crop or soilmarks on conventional aerial photographs, were evident in the intensity data. An extract from the June 1976 vertical photograph of the study area (Fairey Surveys 1861 7615) with excellent cropmark formation was geocorrected to accurately fit the LiDAR intensity image using ArcGIS. Published plots for the cropmarks for the Lockington villa and later prehistoric settlement complex (Ripper & Butler 1999) were scanned and similarly georeferenced to the LiDAR intensity data.

These data were visually compared within ArcGIS, using the GIS to produce accurately co-registered images showing in each instance; the air-photograph, colour-shaded intensity data, air-photograph and intensity data merged and the cropmark plot. In addition, the air-photographic and intensity data were similarly compared with the results of geophysical survey of the Warren Lane complex (Ripper & Butler 1999) and previously unplotted cropmarks on the Hemington terrace. LiDAR intensity readings were extracted for the elevation profiles examined in section 3.3. Visual examination of these intensity profiles (Figs. 4.18 – 4.23) assisted in understanding how intensity values vary in relation to elevation and topographical features.

4.8.1 LiDAR Intensity and Cropmark Formation

In general there appears to be a good degree of correlation between areas of higher LiDAR intensity and areas of cropmark formation, although no convincing cases of anthropogenic features evident as cropmarks could be seen in the LiDAR data. Figure 4.32 shows the Lockington villa and prehistoric settlement complex, located on the Holme Pierrepont sand and gravel (terrace 2) at the southern edge of the study area. As well as well defined cropmarks, the air photograph shows clear variations in the character of the soil and subsoil, represented by broad darker banks probably indicating deeper and/or clayey/silty subsoil. Cropmark formation is poor or non-existent on these darker bands and is largely confined to the areas of paler subsoil.

LiDAR intensity data reflects these broad subsoil divisions. The darker/silty subsoil correlates with darker bands on the air photograph, seen as areas of low LiDAR intensity and paler areas as high intensity. Merging the intensity and air-photographic images clearly shows that the low LiDAR intensity, coloured blue on Figure 4.32, coincides with the dark subsoil bands seen on the air-photograph.

Closer examination of the cropmark and intensity data (Figs 4.33 and 4.34) show that although there is a detailed correlation between subsoil effects on crop growth (seen on the air photos) and LiDAR intensity value, no actual cropmark features are evident in the intensity data. However, crop tramlines and the presence of a footpath (seen in Fig. 4.33 as a low intensity band crossing the villa site from north-west to south-east) indicate that the spatial resolution of the intensity data should be sufficiently fine to capture cropmark features. It is possible that at the time of the LiDAR survey flight ground conditions were not favourable to cropmark formation (which requires dry soil conditions inducing moisture stress in crops and allowing contrasts in available soil moisture and nutrients over buried archaeological features to affect crop growth). Similar factors area likely to affect LiDAR intensity readings, since soil moisture is thought to be the main contributor to variations in reflected laser intensity. Put simply, if conditions were not favourable to the formation of cropmarks (the survey flight was made during February 2003 which was relatively dry, with only 20.2mm rain reported by the nearest weather station at Sutton Bonington, as opposed to a monthly average on 50mm – data from Met Office) they may also have not favoured detection of anthropogenic features using LiDAR.

Figure 4.35 shows a further comparison of cropmark and intensity data, in this instance the cropmarks are those of a small sub-square D shaped enclosure, partly obscured by palaeochannels formation, within the Hemington terrace deposits at SK484300. The cropmark and channels are clearly defined on the air-photography. LiDAR intensity data shows some slight variations in intensity value that hints at the pattern of palaeochannels evident on the air-photograph, but is otherwise unhelpful.

Together, this evidence suggest that LiDAR intensity data is of limited use in detecting buried anthropogenic features as it does not function outside of the parameters (dry conditions, crops experiencing moisture stress) in which such features may anyway be detected by cropmarks. It would nonetheless be useful to examine LiDAR intensity data acquired at a time of good cropmark formation to investigate the possibility that intensity readings may reveal features or levels of detail not visible as cropmarks alone.

Finally, Figure 4.36 shows a comparison of air-photography, LiDAR intensity and geophysical (magnetometer) survey results for the Warren Lane later prehistoric settlement complex located on the Holme Pierrepont Sand and Gravel. Variations in LiDAR intensity in this image to some extent reflect subsoil character as revealed by the air-photograph, but appear largely to be a product of the different crops present in the two fields imaged. Both LiDAR and air-photography fail to reveal the wealth of sub-surface anthropogenic features identified by the magnetometer survey. These cautionary results highlight the need to pursue complimentary remote sensing campaigns in environments as complex and geomorphologically heterogeneous as a river confluence zone.

4.9 LiDAR Intensity and Topography

Figures 4.18 – 4.23 provide LiDAR intensity profiles for the 12 elevation profiles examined as part of the investigation of LiDAR DSM resolution. It can be seen that intensity levels vary closely in relation to elevation such that low elevation features correspond to areas of low intensity ands vice versa. In general variations in LiDAR intensity are likely to reflect soil and subsoil characteristic of the lower elevation areas, rather than be a direct reflection of elevation. The majority of the lower elevation features indicate

geomorphological features such as ridge and swale (Fig. 4.18) and palaeochannels (Figs. 4.19, 4.22 – 4.23). Areas of palaeochannels provide a particularly strong coincidence of variation in intensity and elevation and in some cases intensity variation exaggerate the effects of relatively slight variations in elevation (for example Figs. 4.21 and 4.22). It seems likely that intensity levels are largely affected by the increase in soil moisture prevalent in palaeochannels compared to the surrounding landscape.

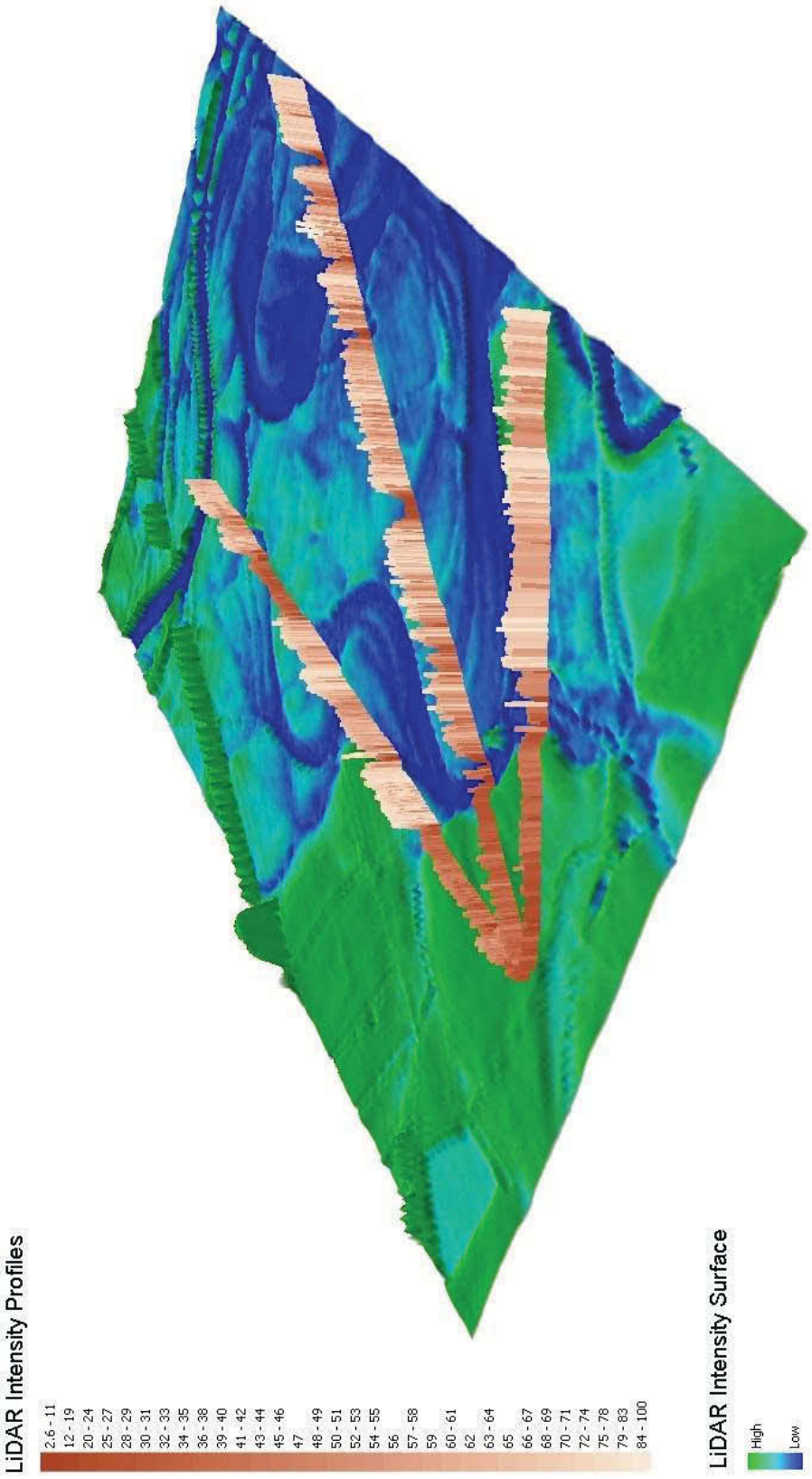

Fig 4.31: Pseudo 3D view of the LiDAR LP DSM of the study area colour shaded to reflect variations in laser intensity. The extruded profiles show variations in intensity data along each profile line as variations in height of the profile and colour shading of the profile bar.

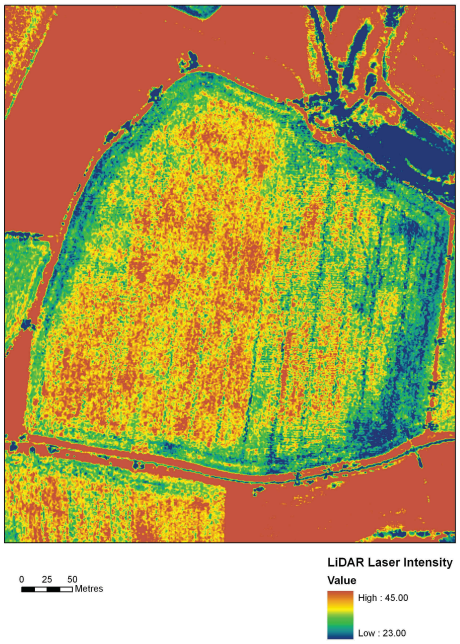

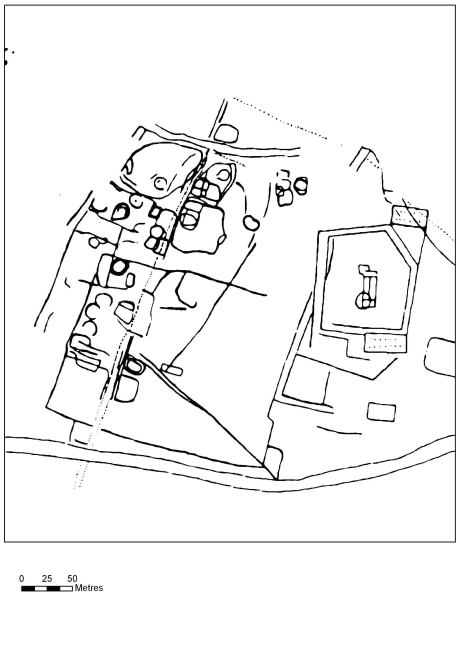

Fig 4.32: Comparison of (A) cropmark evidence on air photography, (B) LiDAR intensity, (C) intensity and cropmark evidence merged and (D) cropmark plot, for the later prehistoric settlement complex and Romano-British villa at Lockington.

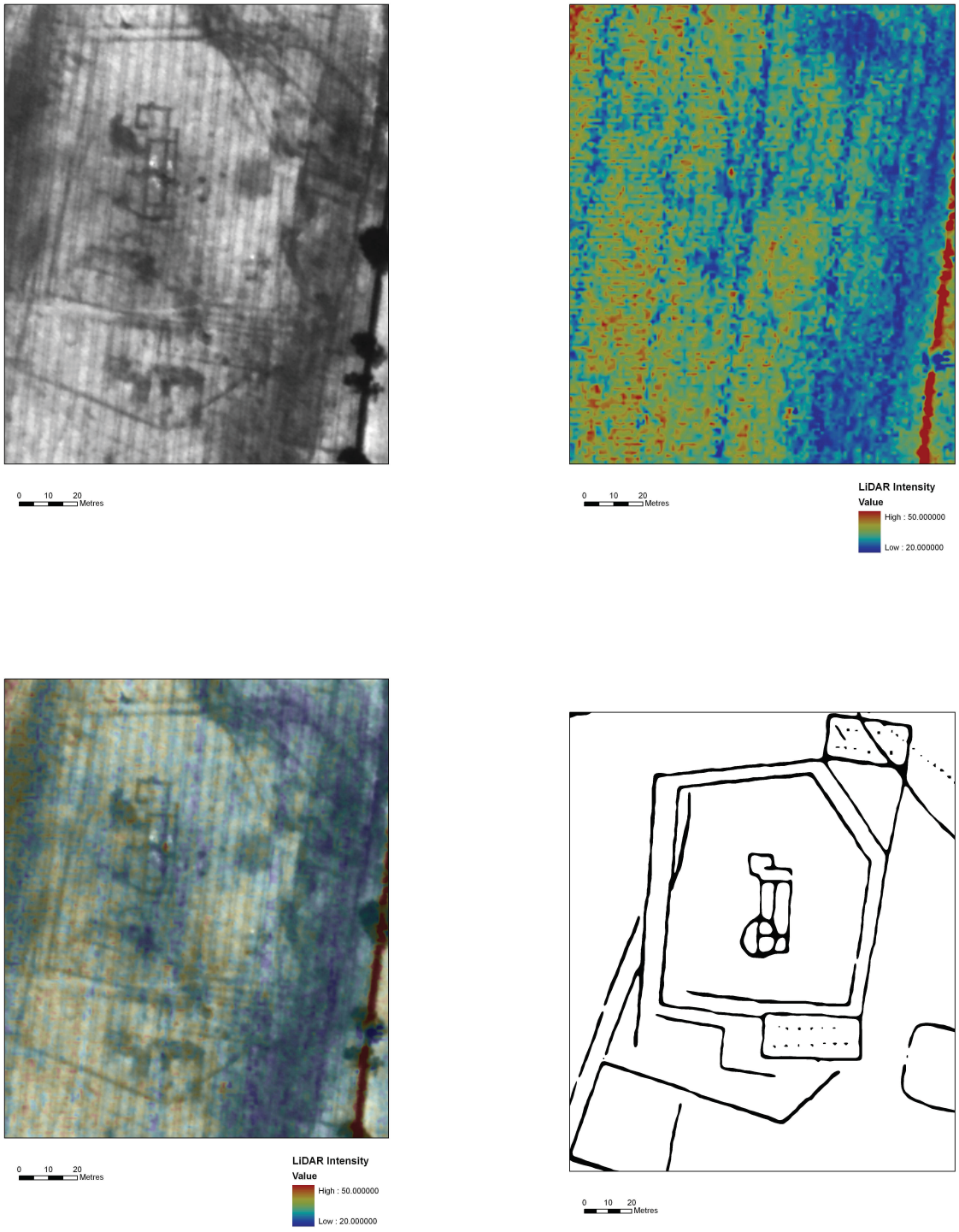

Fig 4.33: Comparison of (A) cropmark evidence on air photography, (B) LiDAR intensity, (C) intensity and cropmark evident merged and (D) cropmark plot, for the Lockington villa.

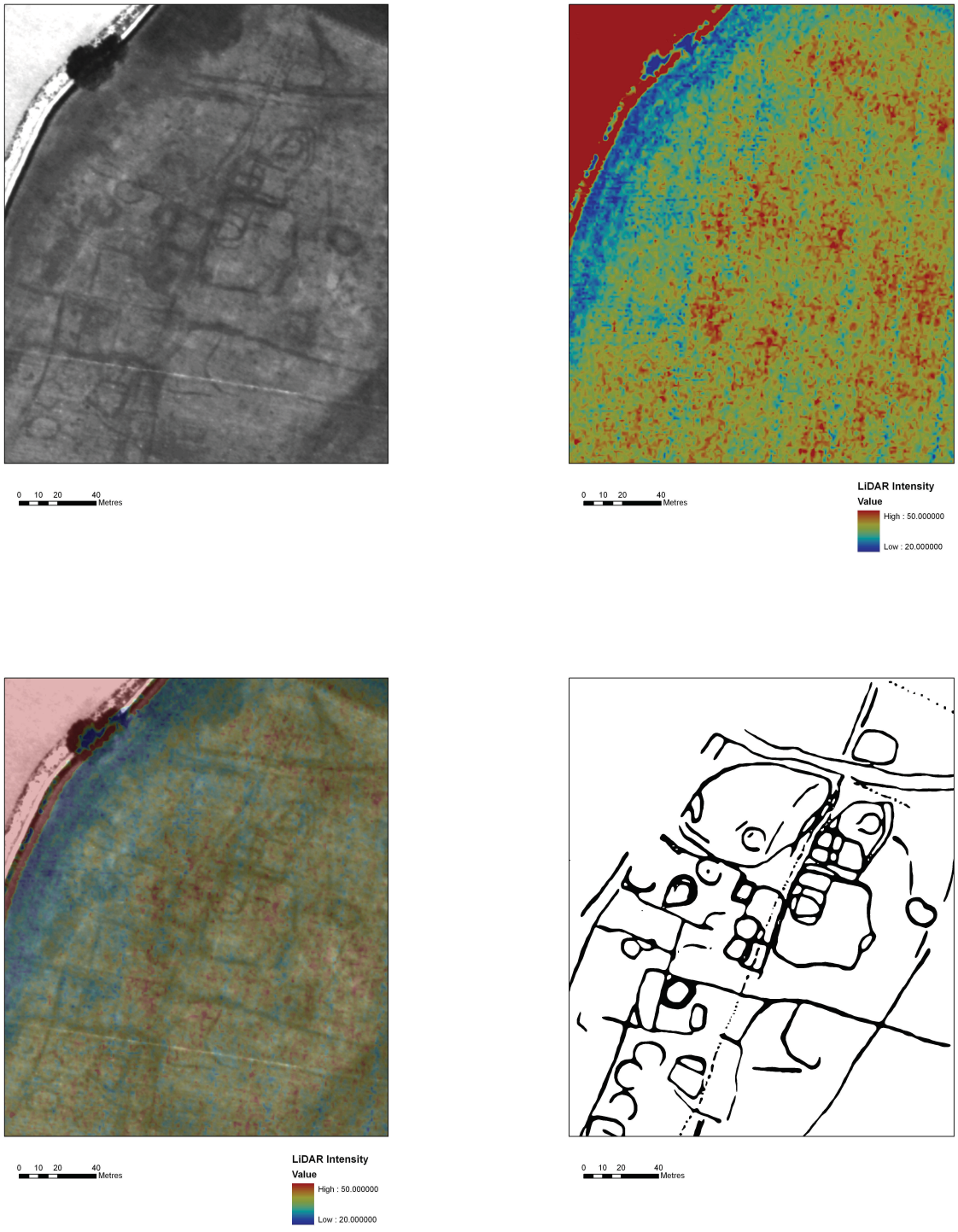

Fig 4.34: Comparison of (A) cropmark evidence on air photography, (B) LiDAR intensity, (C) intensity and cropmark evident merged and (D) cropmark plot, for the later prehistoric settlement complex at Lockington.

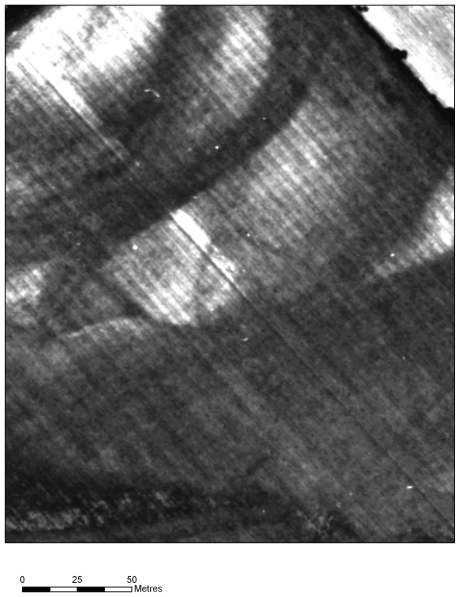

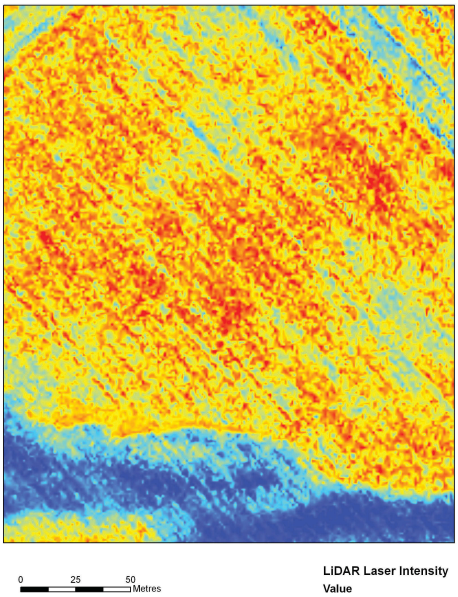

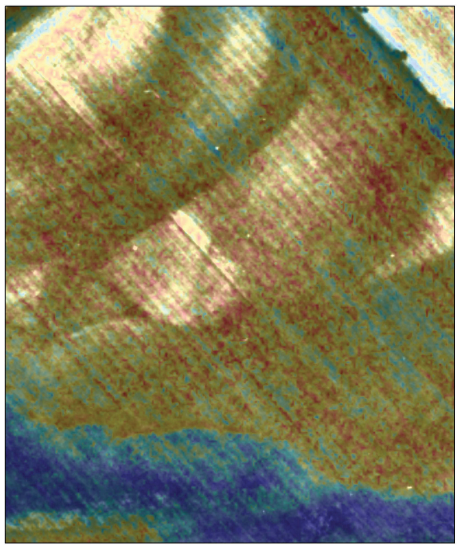

Fig 4.35: Comparison of (A) cropmark evidence on air photography, (B) LiDAR intensity, (C) intensity and cropmark evident merged and (D) cropmark plot, for the small sub-square D shaped enclosure at SK484300

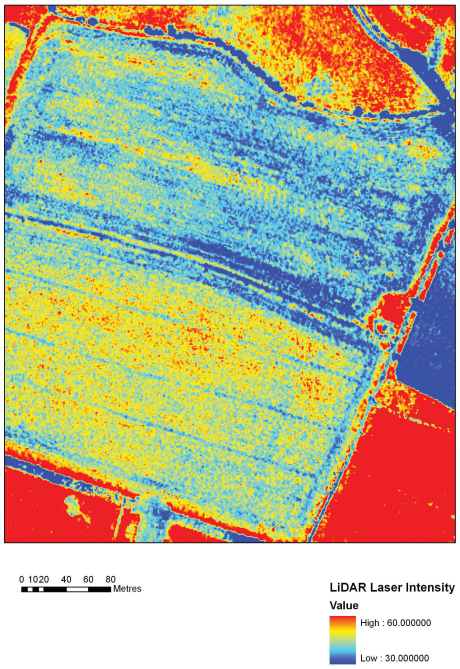

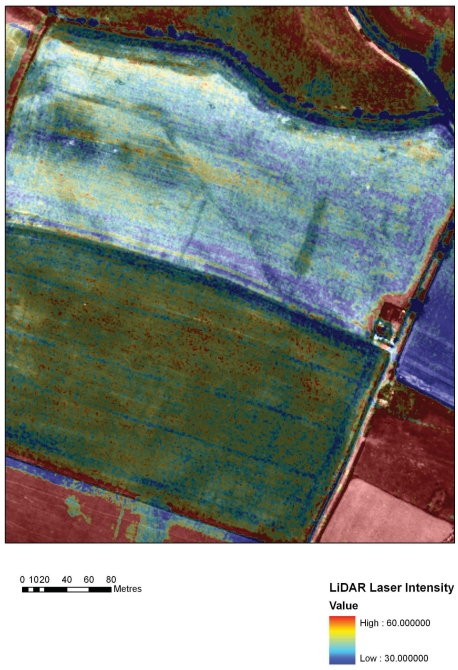

Fig 4.36: Comparison of (A) cropmark evidence on air photography, (B) LiDAR intensity, (C) intensity and cropmark evident merged and (D) geophysical survey plot, for the later prehistoric settlement complex at Warren Lane.

4.10 Soil Moisture and Laser Intensity

This component of the analysis of LiDAR intensity data aimed to test the hypotheses that intensity values vary in relation to soil moisture. Soil moisture measurements were taken at significant locations within each of the geomorphological zones identified within the study area (i.e. modern floodplain, Holme Pierrepont Sand and Gravel and Hemington Sand and Gravel). Moisture readings were taken using a Delta T Devices PR2 profile probe attached to a ML2x ThetaProbe and HH2 soil moisture meter. The ThetaProbe measures *in-situ* volumetric soil moisture content to within 1%, removing the need to recover samples for laboratory and analysis. In conjunction with the PR2 profile probe the equipment is able to obtain moisture readings at different depths within a vertical soil profile (up to six sensors in the 100cm probe).

Moisture readings were taken at topsoil and subsoil depth (c 10cm and c 50cm) as it proved impossible to auger suitable holes for insertion of the profile probe to its full depth in the deposits across the study area. The project design envisaged recording soil moisture at the same locations at seasonal intervals, to determine average soil moisture for each location. In the event equipment supply difficulties prevented this, and a single set of moisture readings were collected in April 2005 at 35 sample points spread across the three major geomorphological zones within the study area (Fig. 4.37).

The location of each soil moisture reading was recorded using GPS, and location and moisture data combined and imported into ArcGIS 9. Using the GIS, LiDAR intensity values were extracted for each soil moisture sample location and these and the moisture values were combined using Microsoft Excel. Data for each geomorphological unit were then examined separately to test the relationship between LIDAR intensity and soil moisture

All data were standardised (by subtracting the mean and dividing by the standard deviation) and the standardised values used to produce scatter plots for each geomorphological zone (Fig. 4.38) as well as a graph showing variations in volumetric topsoil and subsoil moisture and LiDAR intensity within and across each geomorphological unit (Fig. 4.39). Basic correlation coefficients were calculated to describe the relationships between topsoil moisture, subsoil moisture and LiDAR intensity within each geomorphological zone. In addition, variations in soil moisture and intensity were represented graphically as bar graphs superimposed on the LiDAR intensity image within ArcGIS (Fig. 4.40).

There appears to be a strong negative correlation between LiDAR intensity and soil moisture. The variations appear consistent within geomorphological and across geomorphological zones, although moisture and intensity values between zones vary too widely for meaningful comparison. For example, areas of low soil moisture on the higher gravels of terrace 2, while exhibiting a relatively low LiDAR intensity compared to terrace 1 and the modern floodplain (possibly because of vegetation differences) nonetheless display a consistent inverse relationship to soil moisture levels within the unit. Likewise, on the modern floodplain, where LiDAR intensity levels are significantly higher than on terrace 2, variations in intensity are still reflected by corresponding inverse variations in soil moisture.

The correlation coefficients for each geomorphological zone are tabulated below (Tab. 4.3).

MF (alluvium)	Topsoil Moisture and LiDAR Intensity = -0.741
	Subsoil Moisture and LiDAR Intensity = -0.541
T1 (Hemington)	Topsoil Moisture and LiDAR Intensity = -0.926

Subsoil Moisture and LiDAR Intensity = -0.589

T2 (Holme Pierrepont) Topsoil Moisture and LiDAR Intensity = -0.815
Subsoil Moisture and LiDAR Intensity = -0.219

Tab 4.3: Tabulated coefficients of correlation between volumetric moisture of topsoil, subsoil and LiDAR Intensity for each geomorphological zone.

In each case there is a strong inverse relationship between topsoil moisture levels and LiDAR intensity and a less pronounced inverse relationship between subsoil moisture and intensity. The geographically determined nature of these variations is effectively illustrated (Fig. 4.39), where examination of the bar graphs shows that, whatever the absolute levels of soil moisture and intensity, variations are linked to geomorphological features. For example within terrace 1, soil moisture increases where measured within a palaeochannels and LiDAR intensity shows a corresponding decrease. Given the limited data gathered to date it is not possible to demonstrate statistically sound relationships between soil moisture and intensity. Nevertheless, the results to date show promise and suggest that further work gathering more soil moisture data at different seasons, and to examine the effect of variations in soil moisture at depth, may yield significant results.

Sample No	Topsoil Moisture %	Subsoil Moisture %	LiDAR Intensity	Topsoil Standardised	Subsoil Standardised	Intensity Standardised
12	16.90	27.20	42.329830	-2.270541	-0.519756	-0.637927
13	28.20	30.40	28.613565	-1.332487	-0.256589	-1.407291
14	26.60	31.60	30.947359	-1.465309	-0.157901	-1.276386
15	25.10	21.90	35.837856	-1.589829	-0.955628	-1.002071
16	26.70	18.00	36.932568	-1.457007	-1.276363	-0.940667
17	29.50	27.80	30.221449	-1.224569	-0.470412	-1.317103
18	25.80	18.20	28.560318	-1.531719	-1.259915	-1.410278
19	28.50	32.70	31.434139	-1.307583	-0.067437	-1.249081
20	33.50	27.50	45.617989	-0.892515	-0.495084	-0.453489
21	40.00	26.50	25.966194	-0.352926	-0.577324	-1.555786
22	34.90	20.10	57.494923	-0.776296	-1.103660	0.212705
23	47.50	45.80	84.856277	0.269676	1.009906	1.747442
24	48.30	41.00	81.069893	0.336086	0.615154	1.535059
26	47.10	25.30	74.904305	0.236470	-0.676012	1.189222
27	43.70	40.20	83.392311	-0.045776	0.549363	1.665326
28	50.00	45.60	85.998024	0.477210	0.993458	1.811484
29	50.60	43.20	75.255852	0.527018	0.796082	1.208941
30	60.50	50.40	50.312374	1.348852	1.388210	-0.190174
31	60.70	58.10	56.597992	1.365455	2.021457	0.162395
32	60.20	54.60	47.744099	1.323948	1.733617	-0.334233
33	53.70	40.60	54.018414	0.784360	0.582259	0.017703
34	50.90	45.40	54.869591	0.551922	0.977010	0.065446
35	52.70	45.20	30.498705	0.701346	0.960562	-1.301551
36	56.20	42.60	52.512970	0.991894	0.746738	-0.066740
37	53.20	22.50	53.989609	0.742853	-0.906284	0.016087
38	47.80	36.50	65.945023	0.294580	0.245075	0.686683
39	49.90	7.60	59.758495	0.468908	-2.131658	0.339672
40	49.40	32.40	67.582253	0.427401	-0.092109	0.778518
41	50.20	43.40	64.621849	0.493812	0.812530	0.612464
42	49.20	24.90	64.307289	0.410799	-0.708908	0.594820
43	47.10	38.50	61.494431	0.236470	0.409555	0.437043
44	45.80	27.70	67.691284	0.128552	-0.478636	0.784633
45	45.10	18.80	51.081062	0.070443	-1.210571	-0.147058
46	48.30	14.80	61.208416	0.336086	-1.539531	0.421000
47	65.00	46.20	35.931637	1.722414	1.042802	-0.996810

Tab 4.4: Tabulated volumetric soil moisture and corresponding LiDAR intensity data also showing standardised values.

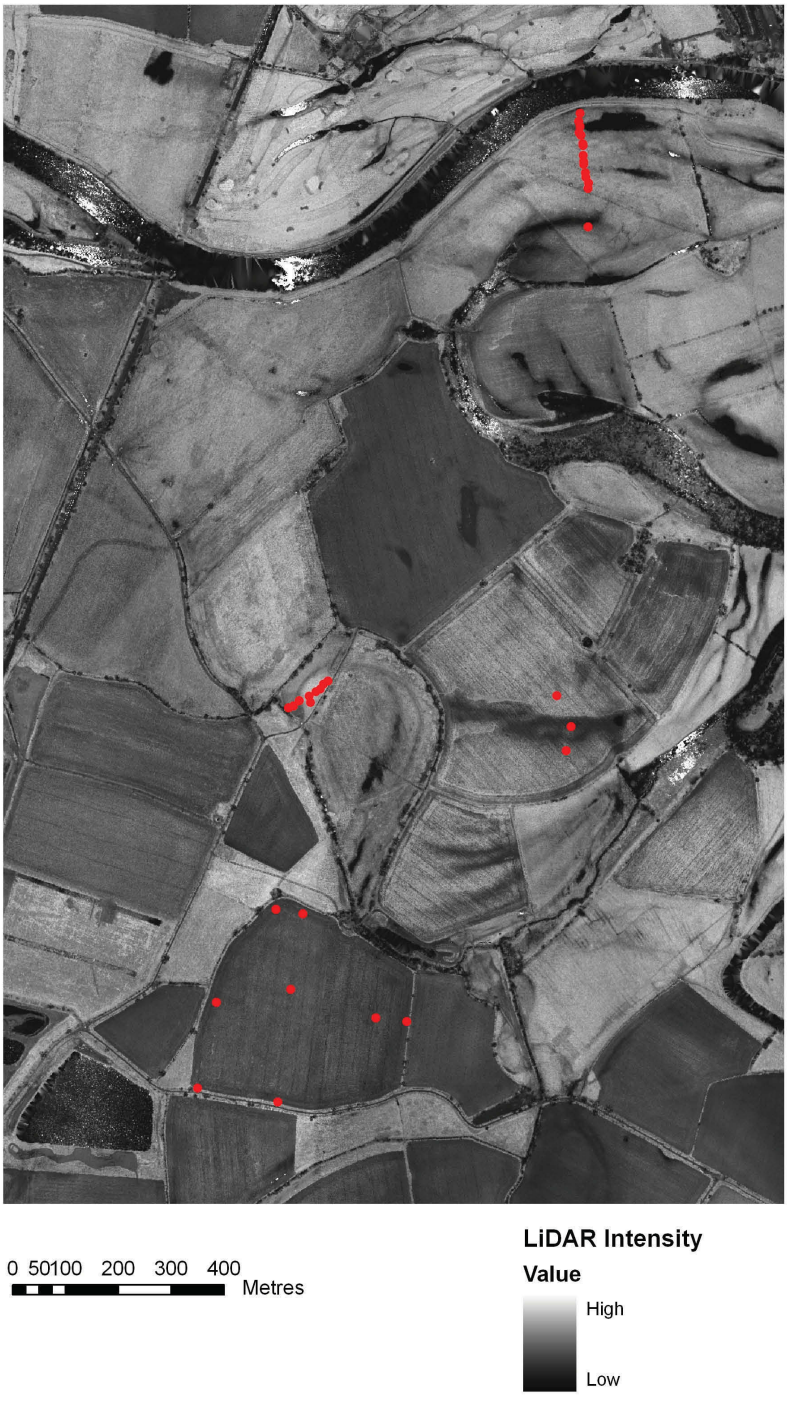

Fig 4.37: LiDAR intensity data for the study area with the locations of *in-situ* volumetric soil moisture readings shown in red.

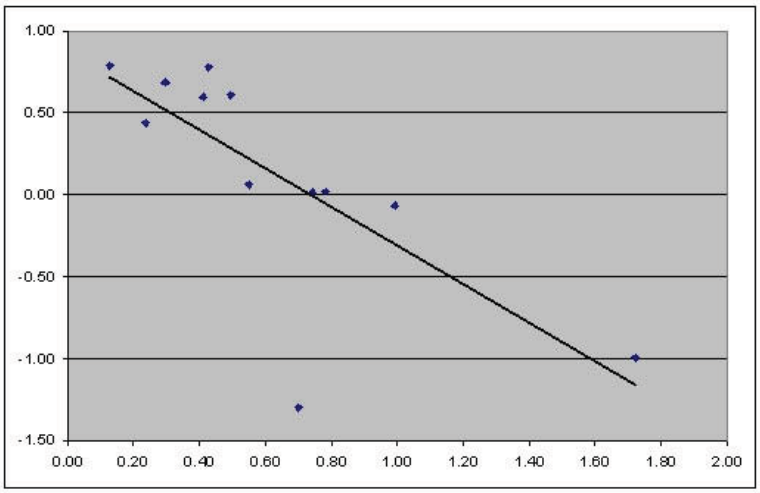

Modern Floodplain

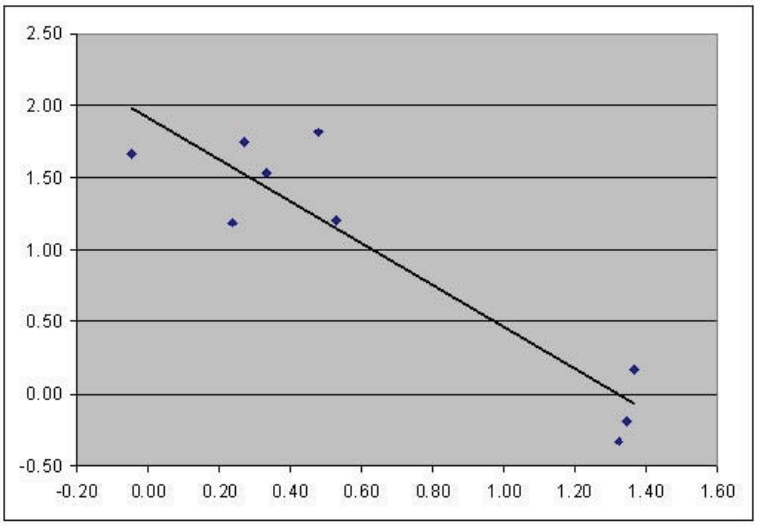

Terrace 1 (Hemington)

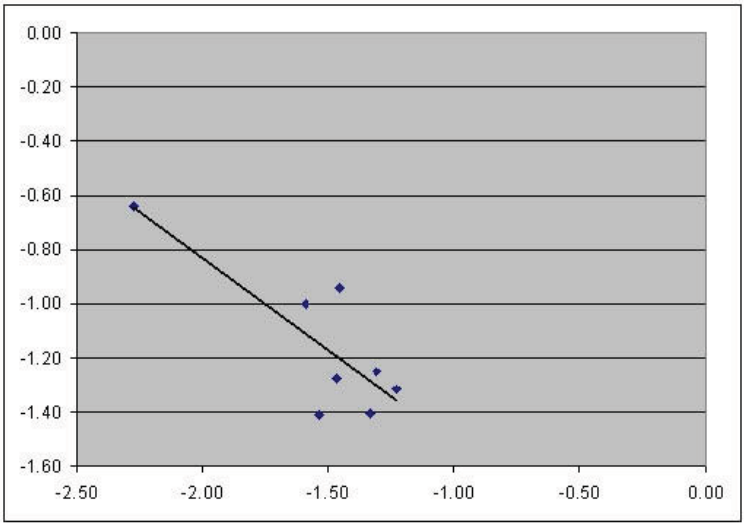

Terrace 2 (Holme Pierrepont)

Fig 4.38: Scatter plots with fitted trend lines showing the relationship between topsoil moisture and LiDAR intensity in each geomorphological zone. In each graph x axis is soil moisture y axis is LiDAR intensity. Units are standard deviation.

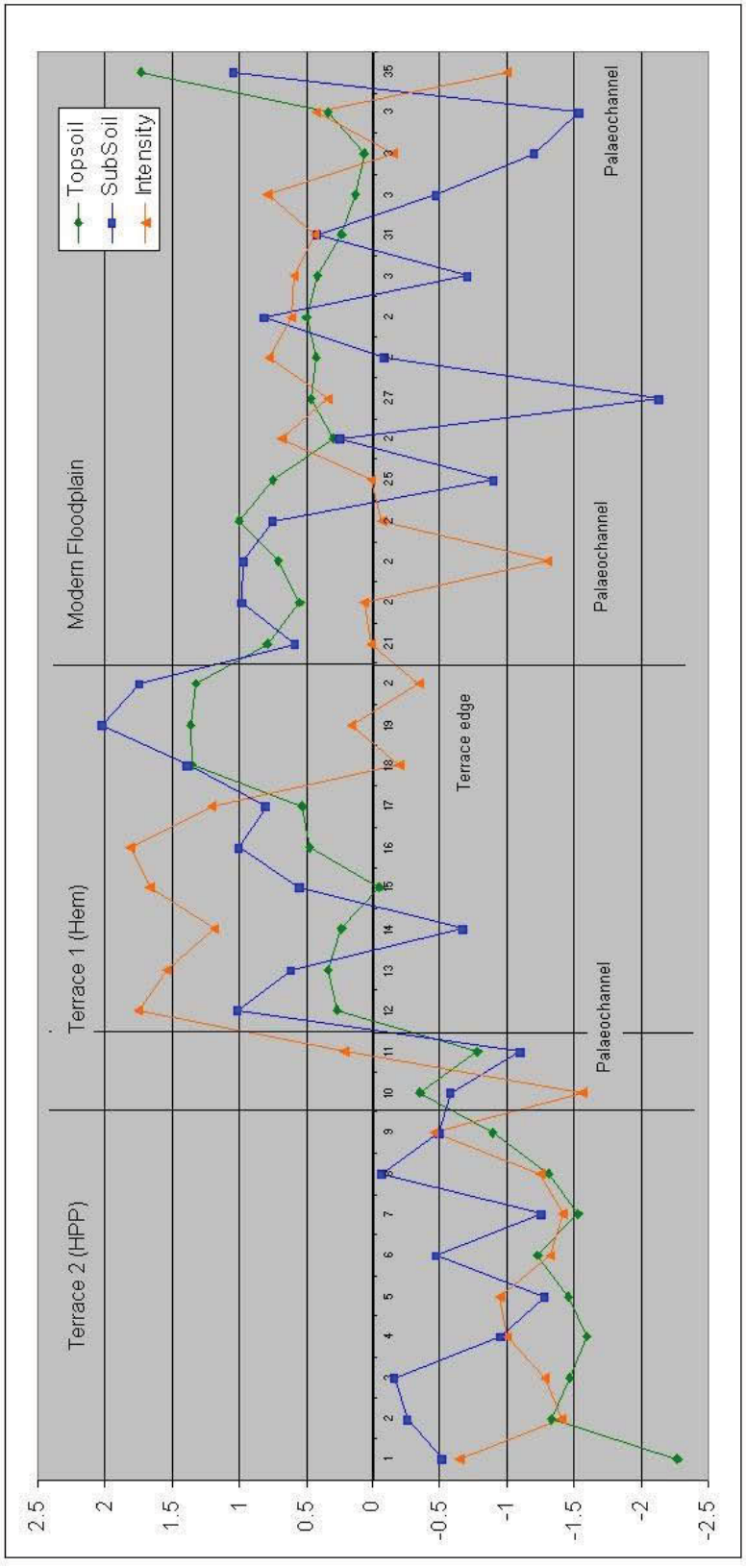

Fig 4.39: Line graph showing standardised variations in volumetric soil moisture in the topsoil (green), subsoil (blue) and LiDAR laser intensity (orange) at ach sample location, vertical bars indicate the boundaries between geomorphological units, annotations indicate geomorphological features. Graph axes are in units of standard deviation.

Terrace 2 (Holme Pierrepont)

Terrace 1 (Hemington)

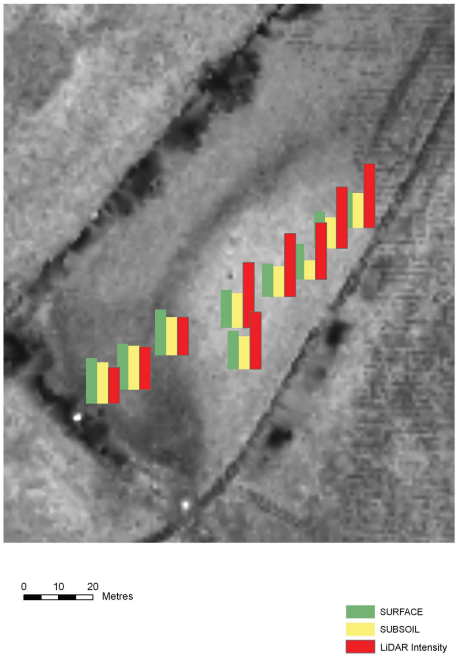

Terrace 1 (Hemington)

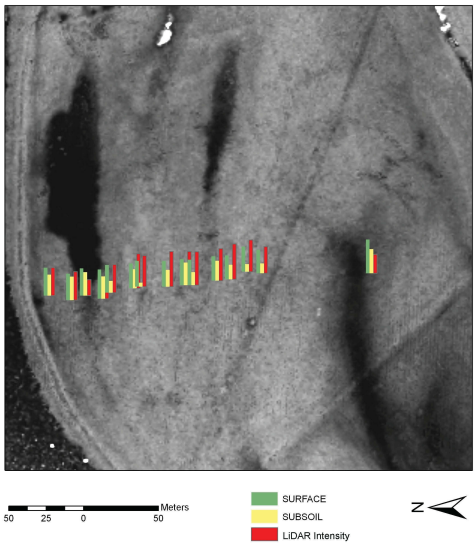

Modern floodplain

Fig 4.40: Maps showing LiDAR intensity with superimposed bar charts showing volumetric soil moisture readings at the surface (green) at subsoil level (yellow) and corresponding LiDAR intensity value at sample locations 1-4.

4.11 Inteferometric Synthetic Aperture Radar

Airborne radar uses radio waves to measure the distance between an aircraft mounted senor and the ground surface. Interferometry relies on picking up the returned radar signal using antennas at two different locations. Each antenna collects data independently, although the information they receive is almost identical, with little separation (parallax) between the two radar images. Instead the phase difference between the signals received by each of the two antennas is used as a basis for calculation changes in elevation. The results are enhanced by using processing techniques during data collection to generate a synthetic aperture of much greater size than the physical antenna used and so enhance resolution (Intermap 2003). Combining the principals of Synthetic Aperture Radar with Interferometry, Interferometric Synthetic Aperture Radar (IFSAR) is capable of producing both a radar image of the ground surface and calculating elevation changes to enable production of a digital surface model (DSM).

Intermap has undertaken IFSAR surveys of the entire of the UK. The results of the surveys are available as a commercial product in the form of 5m spatial resolution DSM with a vertical accuracy of between 0.5 and 1.0m and a 1.25m spatial resolution radar image. Analysis of the IFSAR products focused on investigating to what extent they were able to provide useful geoarchaeological information. The IFSAR DSM was imported into ArcGIS for visualisation and comparison with LiDAR and GPS derived elevation values. Elevation and derived slope frequency histograms were generated as well as basic DSM statistics (Fig. 4.43, Tab. 4.5). Profiles across the IFSAR DSM were generated at each location used to assess LIDAR DSM accuracy and resolution (Fig. 4.17) to allow direct comparison of the resolving ability of the IFSAR DSM compared to LiDAR. Finally, a crude approximation of the variation in elevation values reported by the IFSAR DSM as compared to LIDAR was produced by subtracting elevation values for the LiDAR first pulse DSM from those for the IFSAR DSM (Fig. 4.44).

4.11.1 IFSAR DSM

In general the IFSAR DSM is successful in distinguishing the broad geomorphological units of the study area, in particular the elevation changes between the Holme Pierrepont (T2) and Hemington (T1) terraces and the modern floodplain (Fig. 4.41). Profiles across the study area (Fig. 47) show that the broad changes in elevation that distinguish these units are recorded by the IFSAR DSM. However, IFSAR provides a relatively poor record of the subtle microtopographic features that are the basis of mapping and understanding floodplain and terrace geomorphology. While it is possible to distinguish a number of the palaeochannels evident on LiDAR and air photographic imagery in the IFSAR DSM, these are not represented with anywhere near the clarity seen in the LiDAR data. Close comparison of profiles through the IFSAR DSM at key geomorphological features (Figs. 4.18 – 4.23) show that the 10m resolution of the IFSAR data, though able to distinguish features is not able to adequately represent their form, thus ridge and swale is rendered as a series of crude stepped ridges (Fig. 4.18, P1) and palaeochannels profiles are similarly crudely represented (see especially Fig. 4.18, P2 and Figure P3 and 4). Some features, such as the terrace edge in Fig. 4.20, P6) are not represented at all, and in areas of low relief, especially the modern floodplain, results are wholly unreliable (Figs. 4.21 – 4.23).

Finally, comparison of the elevation values reported by the IFSAR and LiDAR FP DSM show some variations between the two products (Figs. 4.42 and 4.44). The majority of variations are in areas of vegetation cover and a probably a product of the differing technologies ability of represent and penetrate vegetation, as well as variations in the actual vegetation canopy at the times of the two survey flights.

4.11.2 IFSAR ORI

Radar imagery responds largely to changes in the texture of the land surface and so records different land surface properties to both conventional aerial photography and LiDAR laser intensity information. ORI data was compared with other sources of information about the ground surface in the study area to test its utility in identifying significant floodplain features. The IFSAR ORI provides a fair overall representation of the study area (Fig. 4.45), but fails comprehensively to detect the significant geomorphological features. Close comparison of extracts from the ORI with air photo and LiDAR data (Fig. 4.46, compare with Figs. 4.15, 4.16 and 4.32) indicate that although some crude variations in texture, corresponding to subsoil variations and geomorphological features, are evident, the resolution and reliability of the ORI for detecting such features is poor. The IFSAR ORI does not contribute significantly to the geoarchaeological investigation of the study area and its further investigation cannot be recommended.

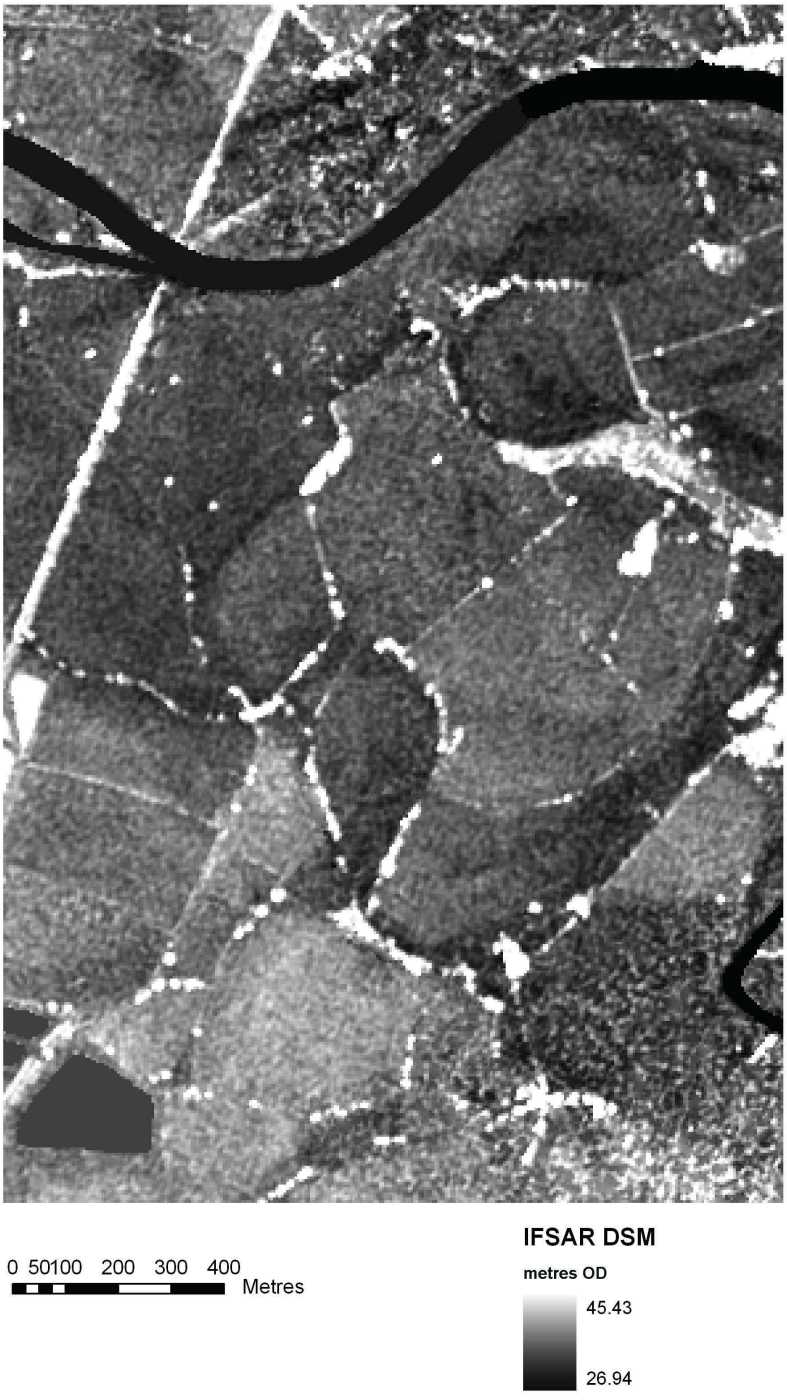

Fig 4.41: IFSAR (Radar) 10m digital surface model of the study area.

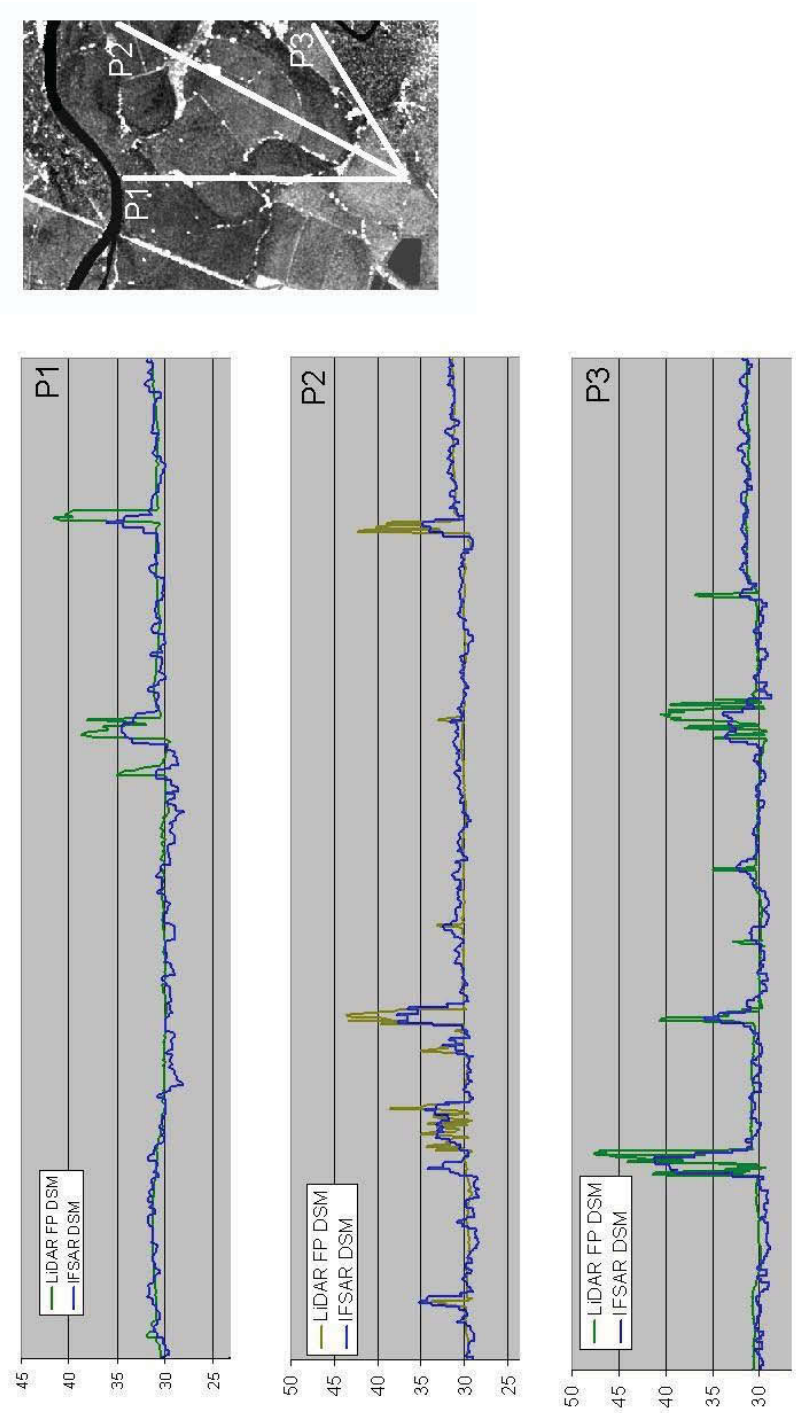

Fig 4.42: Profiles through the LiDAR and IFSAR DSM of the study area showing the elevation of the major geomorphological units.

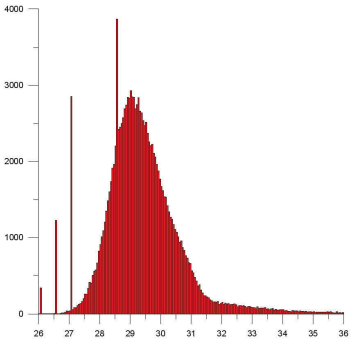

IFSAR 10m DSM

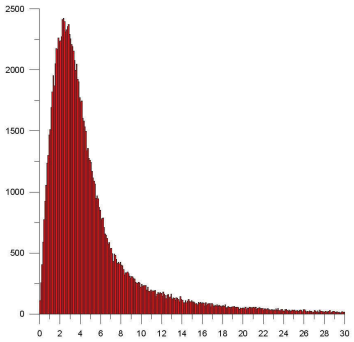

IFSAR 10m Slope

Fig 4.43: Left elevation and right slope for IFSAR DSM data for the entire study area.

DSM IFSAR	
Number of values	133930
Minimum	26.94
Maximum	45.44
Range	18.5
Mean	30.357
Standard deviation	1.3921
Skew	2.029

Slope IFSAR	
Number of values	133930
Minimum	0
Maximum	57.36
Range	57.36
Mean	5.0564
Standard deviation	5.2662
Skew	2.844

Tab 4.5: Statistics for the IFSAR DSM and derived slope values.

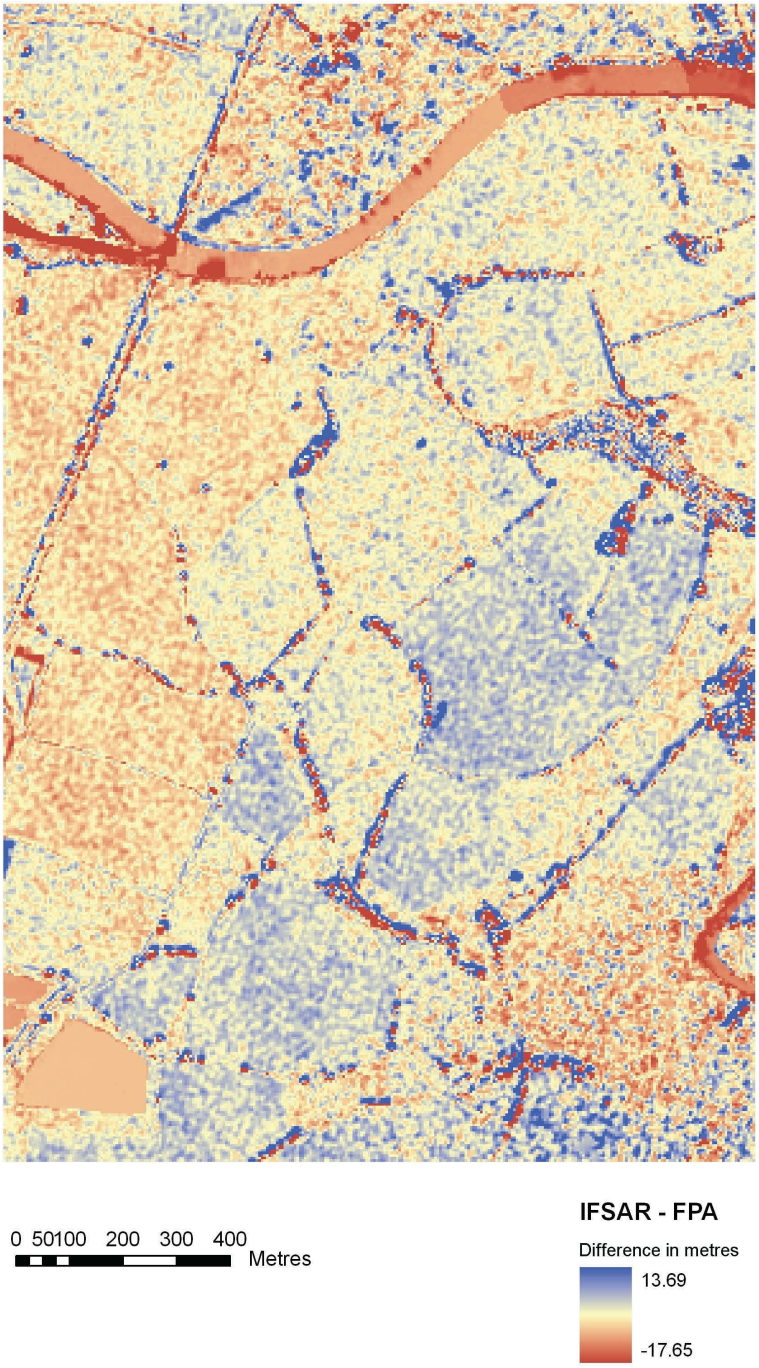

Fig 4.44: Difference between elevation values recorded by the IFSAR (Radar) 10m digital surface model of the study area and the LiDAR first pulse surface model.

Fig 4.45: IFSAR (Radar) Orthorectified Radar Image (ORI) of the study area.

Modern Floodplain (compare fig. 15)

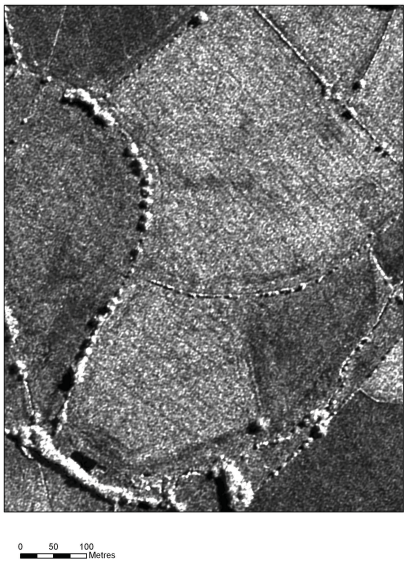

Terrace 1 (compare fig.16)

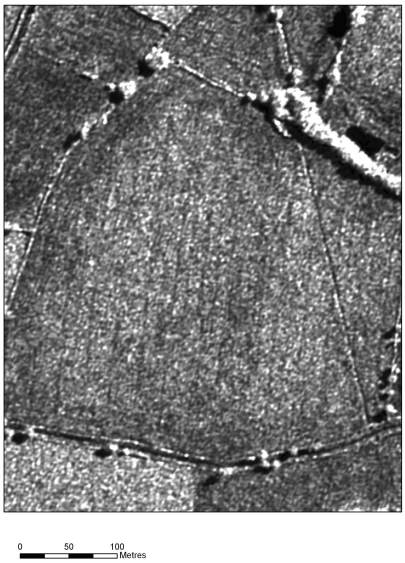

Terrace 2 (Lockington villa: compare fig. 32)

Fig 4.46: IFSAR ORI of selected parts of the study area.

CHAPTER 5: THE GROUND PENETRATING RADAR SURVEYS

5.1 The GPR surveys on the modern floodplain

The GPR surveys on the modern floodplain consisted of one GPR gouge core survey (MFT1) and two grid surveys (MFG1 and MFG2). The survey areas were selected after consulting the LiDAR images, targeting a series of palaeochannels and gravel deposits. The surveys on the modern floodplain were also used to investigate the data resolution of using three different sample intervals for the geomorphological investigation of alluvial landscapes.

5.1.1 Modern floodplain transect 1

The location of the modern floodplain transect 1 (MFT1) investigated three palaeochannels with associated gravels deposits, shown through the LiDAR last pulse DTM (Fig. 5.1). The transect used a 200MHz antenna. The modern floodplain presented a difficult environment for GPR survey caused by radically sediment types, i.e. palaeochannels and gravels units, combined with a high soil water content. The gouge core transect calibrated the dielectric constant at 30. The transect was processed through migrating the data with a variable velocity model, accounting for the differences in the electrical properties of the units surveyed. Further processing of the transect used a horizontal high pass filter at 80 scans length, a vertical high pass filter of 100MHz and vertical low pass filter of 600MHz. The GPR reflection values had a minimum of –120 and a maximum of 128.

Three palaeochannels are evident within the GPR section (MFC1, MFC2 and MFC3), shown against the interpretation of the GPR section and the gouge core data (Fig. 5.2). There are also a series of interpreted gravel deposits, units MF1, MF3, MF4, MF5 and MF6. These gravel units are not homogeneous and variation is seen in their structure. For example MF3 and MF4 are large gravel deposits with a series of strongly reflecting layers, whilst MF6 is a much smaller unit, which has a lower number of higher reflecting layers. The strongly reflecting layers shows a sequence of units with different electrical properties.

The identification of structure within the palaeochannels is limited, a product of the nature of their fills. The unit MF2 is visible located within the palaeochannel MFC1. From the gouge core transect it is known that MF2 is below the depth that gravel deposits were encountered. However, the identification of MF2 as a gravel/sand deposit is subjective, a product of the rapid attenuation of GPR signal in the palaeochannel above MF2. This inhibited effective GPR penetration. The structure of the palaeochannel deposits was not realised and the gouge core transect showed the palaeochannels to have a fill composed of red brown clay combined with a high water content. Palaeochannels MFC2 and MFC3 both have variation in their fill revealed through the gouge core transect, which is not identifiable in the GPR section. When considering the high water content of the soils on the lower floodplain the GPR penetration was good, achieving a depth of just over 2m under the gravel units. Penetration was less within the palaeochannels, generally under 1m.

Support for the GPR interpretation comes from the gouge core transect, which correlates well with the GPR section. From the GPR interpretation a stratigraphic sequence is suggested where the gravels units MF3 and MF4 are the earliest features in the transect. The channels MFC1, MFC2 and MFC3 are later

and erosive into the earlier gravel units. MF2 is associated with palaeochannel MFC1 and thus post dates units MF3 and MF4.

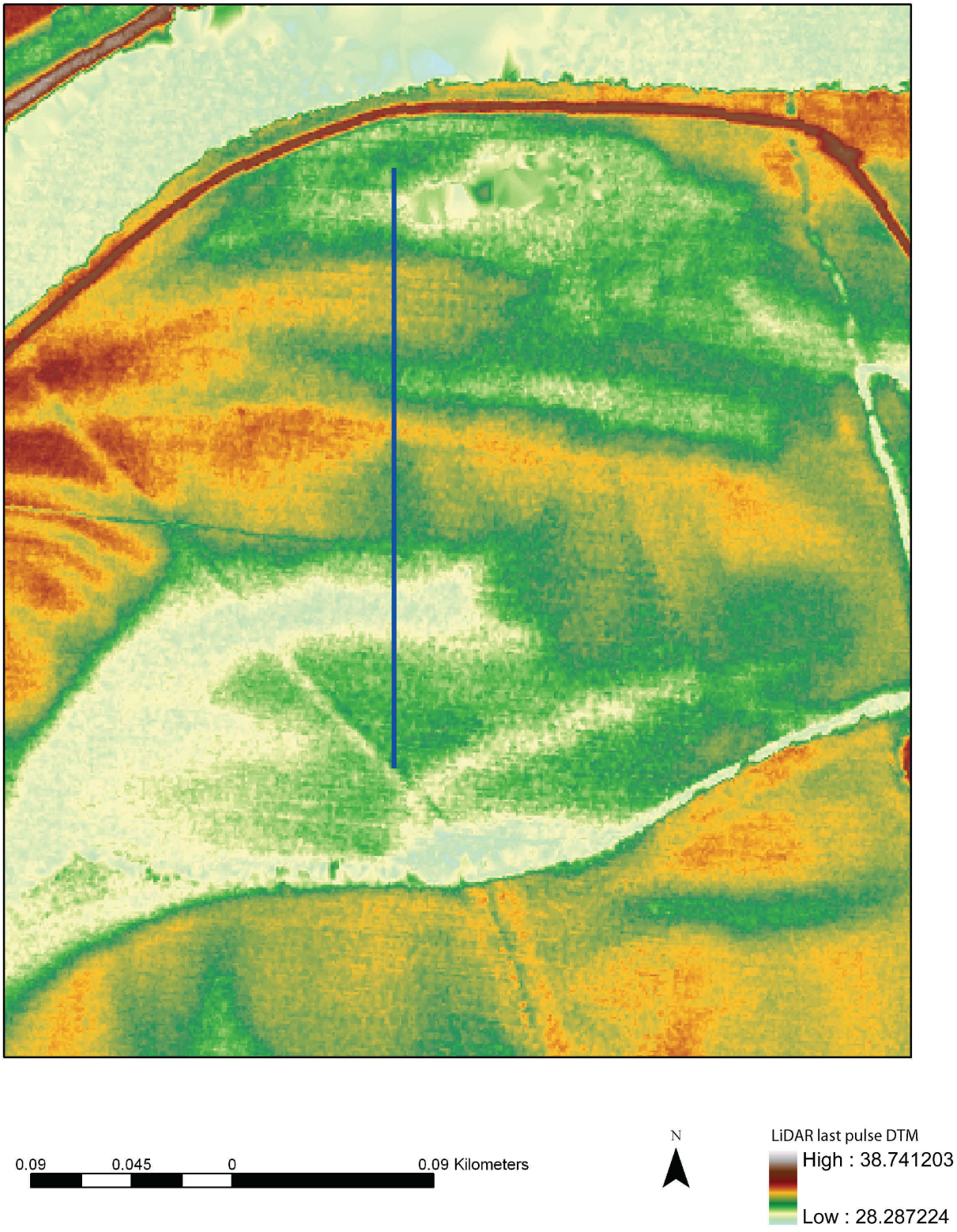

Fig 5.1: The location of the MFT1 transect on the modern floodplain.

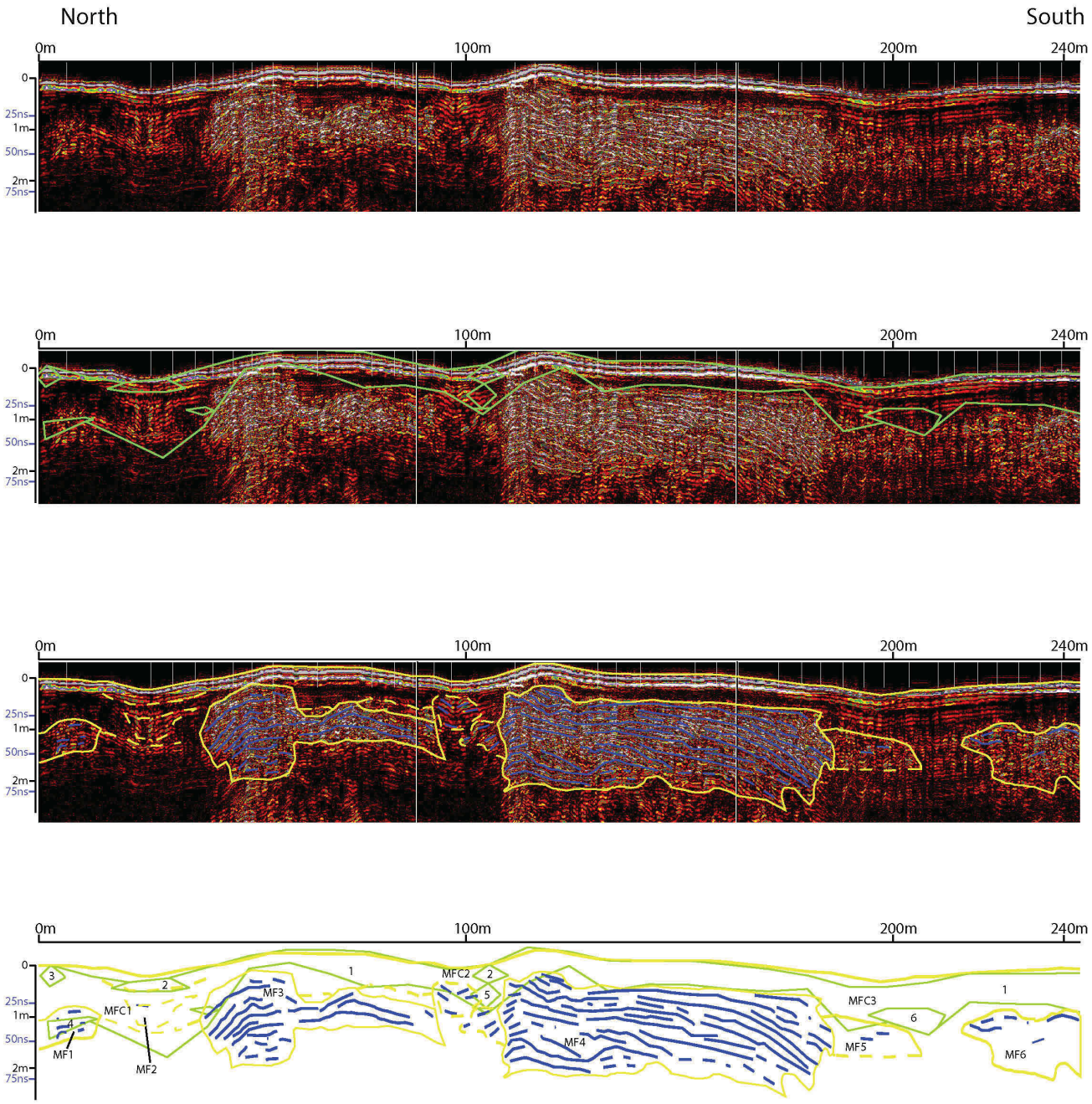

Fig 5.2: The MFT1 transect, shown with the gouge core transect and also with an interpretation of the data. The transect clearly shows the structure of the gravels but penetration in the palaeochannels is poor.

5.1.2 Modern floodplain grid 1 survey (MFG1)

The MFG1 survey covered an area of the modern floodplain, using a 200MHz antenna with a 5m transect interval collecting 25 transects of data. The dielectric constant of the soil was set through using the MFT1 transect calibration at 30. The GPR reflectance values had a minimum of –120 and a maximum of 128. Data was sampled at 0.5m intervals, using a 0.3m depth slice. The depth slices are shown with the LiDAR last pulse DTM at 70% transparency. This grid survey was also used to experiment with the use of different transect intervals being 5m, 10m and 20m. The presentation of the results will describe the 5m transect intervals. Then a comparison will be given between the different transect intervals.

Within the survey area MFT1 transect identified three palaeochannels (MFC1, MFC2 and MFC3), which are also visible through the LiDAR intensity (Fig. 5.3). These channels are evident in the LiDAR last pulse DTM, as are several elevated areas (Fig. 5.4), which correspond to MF3 and MF4 and MF6 identified on the transect survey MFT1. During the MFG1 survey palaeochannel MFC1 was only partially surveyed due to standing water within the channel truncating transects and will be largely ignored in the following discussion.

The 0.85m – 1.15m depth slice is below the alluvium overlying the gravels units and also the GPR near field zone. The two channels MFC2 and MFC3 are visible as areas of lower reflectance/higher absorbance, indicating higher clay/water contents within the channels (Fig. 5.5). The units MF3 and MF4 are shown to be continuous strong reflecting/weakly absorbing units. Unit MF6 is also visible. Like on the MFT1 transect this unit is shown to be different to the palaeochannel fills but a weaker reflecting unit than either MF3 or MF4.

The 1.35m – 1.65m time slice shows feature MF3 to be just visible, defining a shallower deposit of gravels than MF4 (Fig. 5.6). The 1.85m – 2.15m time slice shows MF4 as an area of stronger reflectance (Fig. 5.7). The gravel unit MF3 is no longer definable but some scattered higher reflectance values are visible. Penetration was not achieved deeper than the 1.85m – 2.15m depth slice, due to high water contents. The palaeochannel fills caused rapid attenuation of the radar signal. Thus definition of their form at depths over 1m is highly subjective.

The comparison between the different sample intervals can be visually assessed through comparing the sample intervals at different time slices. On each survey only the visible features are identified, as a method of interpreting the loss of feature resolution through using different sample intervals. At the 0.85m - 1.15m depth slice (Fig. 5.8) the channels MFC2 and MFC3, the gravel deposits MF3, MF4 and MF6 are visible on the 5m transect interval survey. On the equivalent 10m transect interval depth slice the gravel deposits MF3 and MF4 and the palaeochannels MFC2 and MFC3 are recognisable but are not as well defined as on the 5m interval survey. MF6 is not identifiable as a discrete feature. On the equivalent 20m transect interval survey depth slice the data resolution has decreased considerably. The channels MFC2 and MFC3 are still identifiable but they have poor definition. The gravel deposits MF3 and MF4 are still apparent, although less well defined.

A second comparison of the three sample intervals is made at the depth slice of 1.35m – 1.65m (Fig. 5.9). On the 5m transect interval survey the gravel deposit MF4 is evident, with MF3 less pronounced at this depth. The two channels MFC2 and MFC3 are both identifiable as areas of high absorbance. On the 10m transect survey the gravel deposit MF4 is still visible. The channel MFC2 is still visible but its definition has been reduced. The palaeochannel MFC3 is no longer identifiable but an area of high absorbance/low reflectance is seen. Interestingly the gravel deposit MF3 is visible as a much larger feature than on the 5m transect interval. This is a product of interpolation of fewer data points over a larger area. Some of these data points have high reflectance values, exerting more influence on the

interpolation process in the 10m data set. On the 20m transect survey the only definable feature is the gravel deposit MF4. General areas of high absorbance low reflectance are seen over MFC2 and MFC3 but they are poorly defined. The results from the comparison of the different depth slices from the different transect interval surveys confirms that smaller transect intervals give a correspondingly better level of feature identification on alluvial deposits. It is suggested that the 5m transect interval is routinely employed for GPR survey of floodplain structure in geoarchaeological investigations.

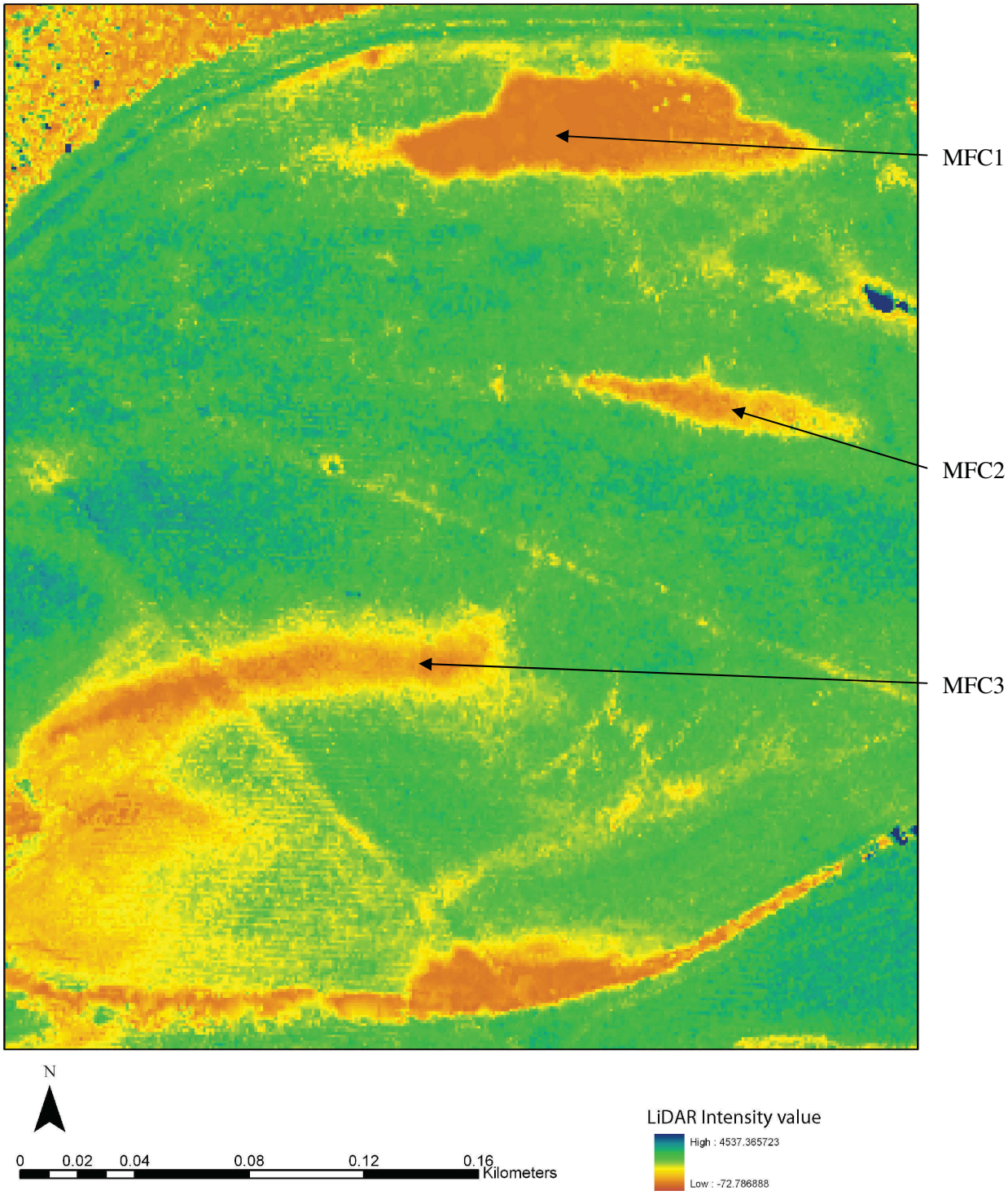

Fig 5.3: The LiDAR intensity plot over the MFG1 survey area, highlighting palaeochannels MFC1, MFC2 and MFC3.

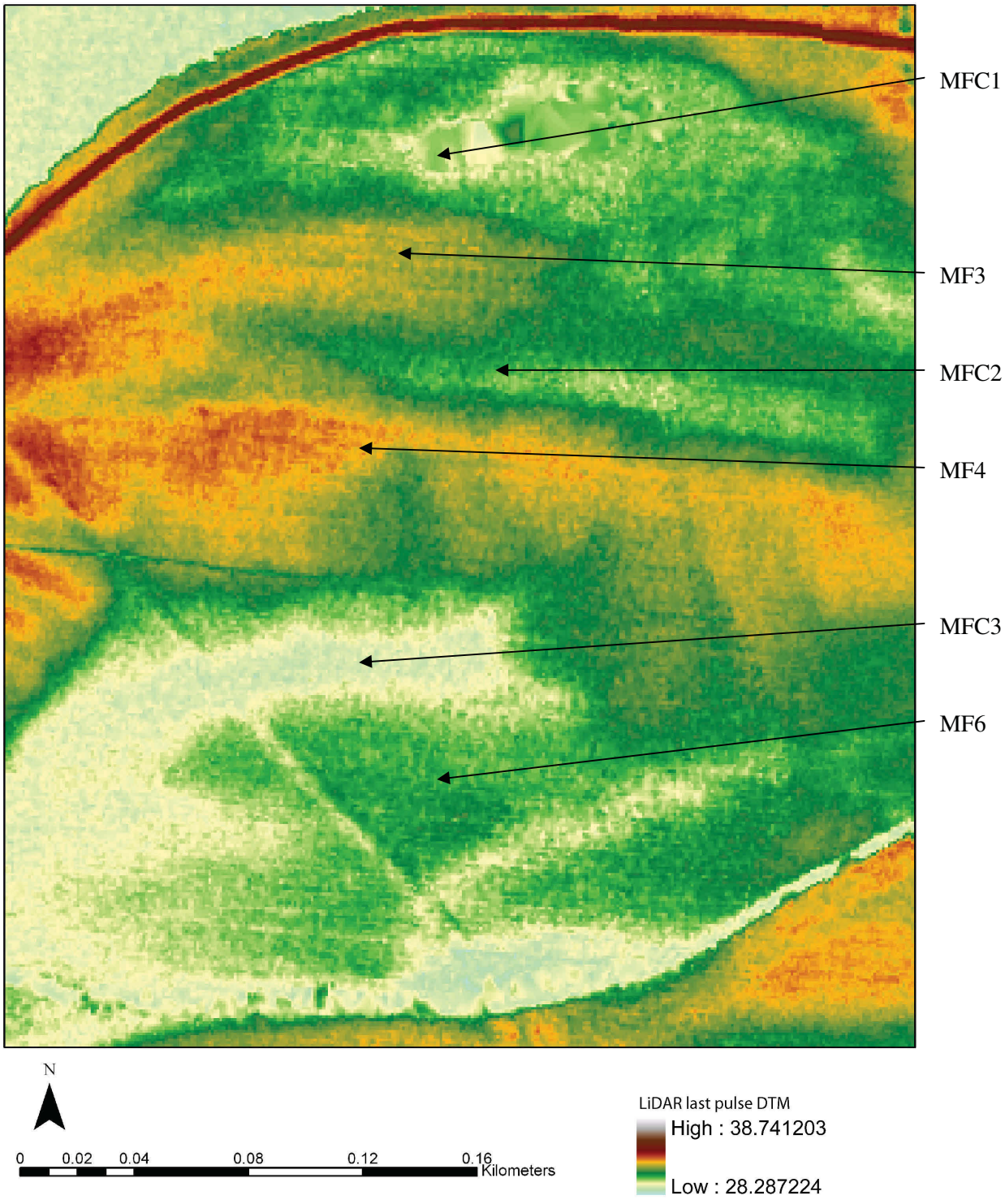

Fig 5.4: The LiDAR last pulse DTM showing the surface topographic features within the MFG1 survey area. These features were shown in cross section through survey MFT1.

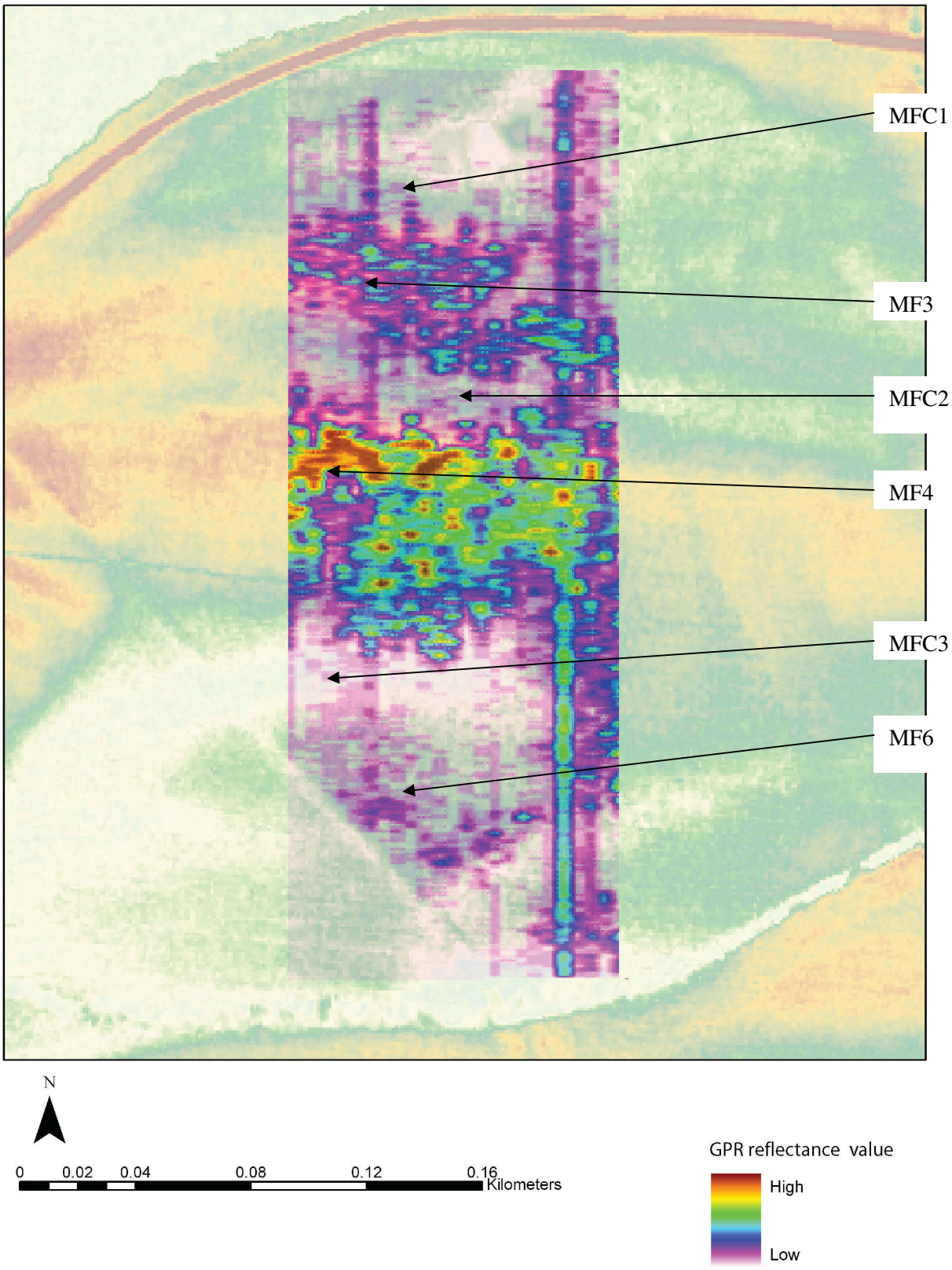

Fig 5.5: The T1G1 survey 0.85m – 1.15m depth slice. The gravel units MF3 and MF4 are clearly visible, as are the palaeochannels MFC2 and MFC3. MF6 is apparent but is a weaker reflecting unit then either MF3 or MF4.

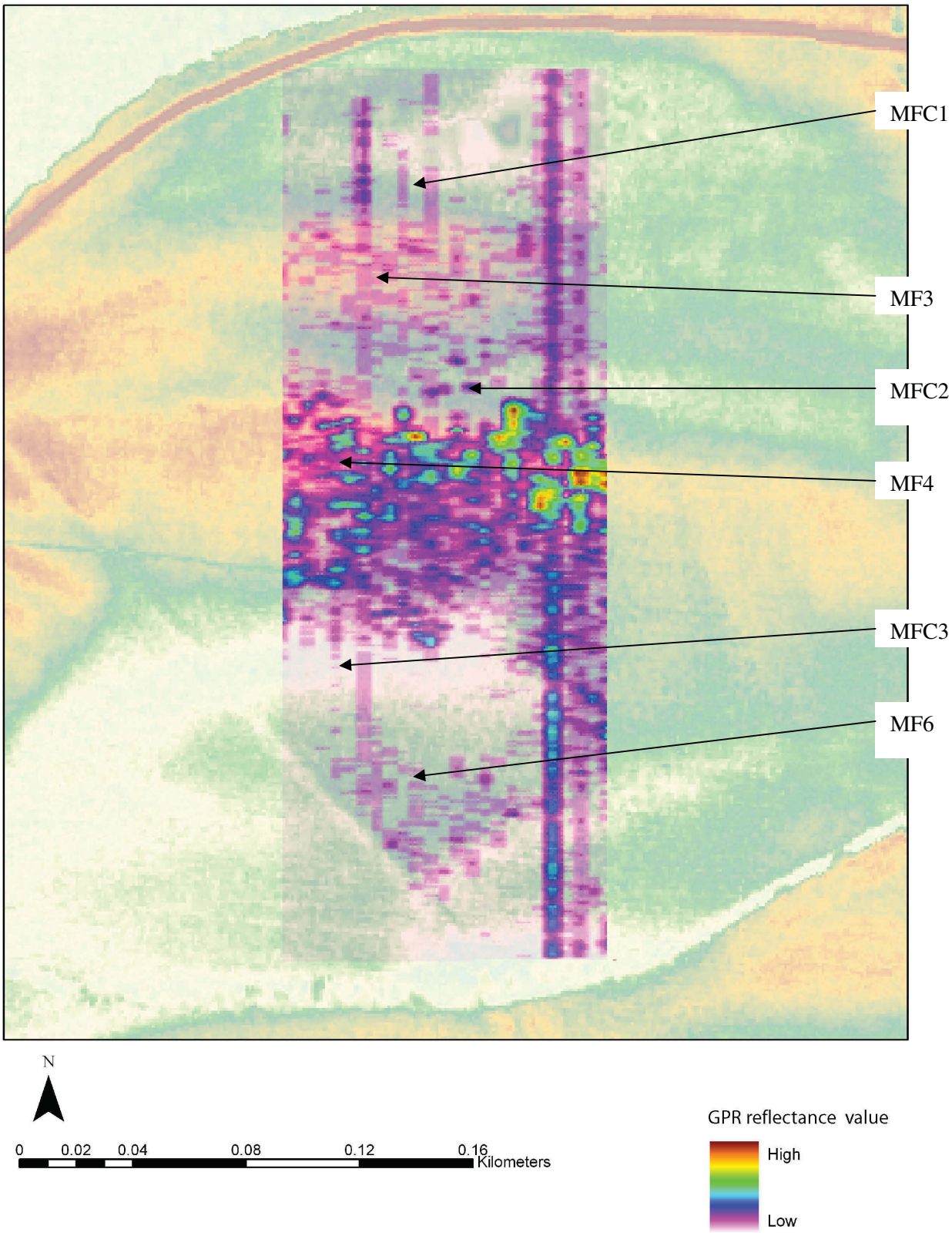

Fig 5.6: The MFG1 survey, 0.35m – 1.45m depth slice. MF3 is again the dominant feature, with the palaeochannels MFC2 and MFC3 evident. MF3 is much reduced at this depth less obvious at this depth, showing that it is a shallower and smaller feature than MF4.

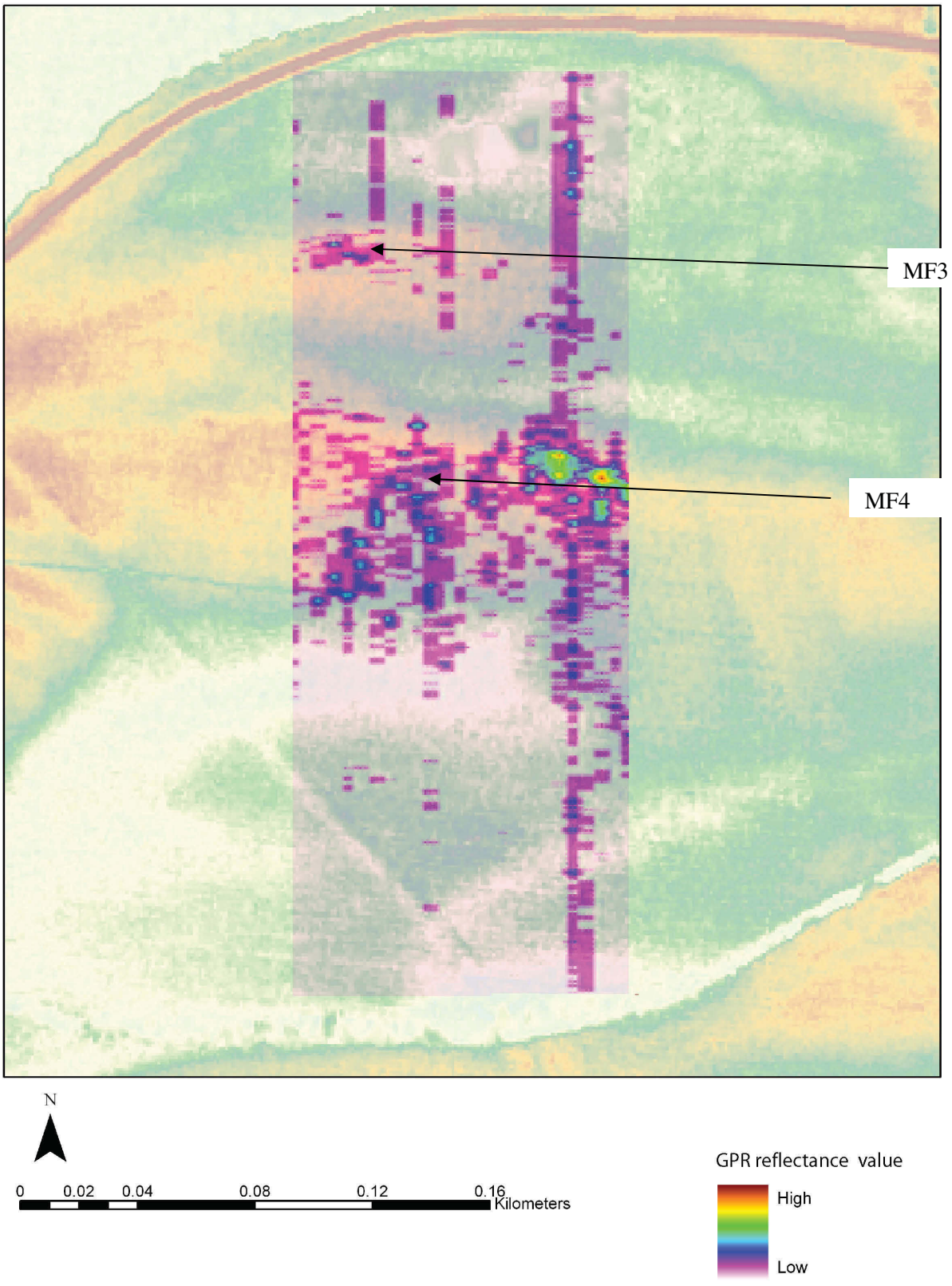

Fig 5.7: The MFG1 survey, at the 1.85m – 2.15m depth slice. The only really interpretable feature at this depth is the lowest levels of MF4.

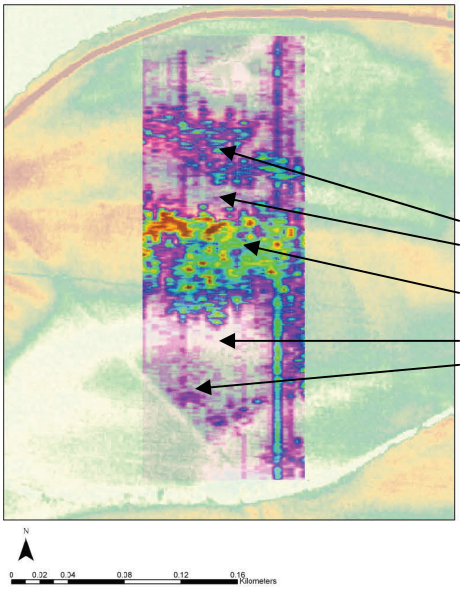

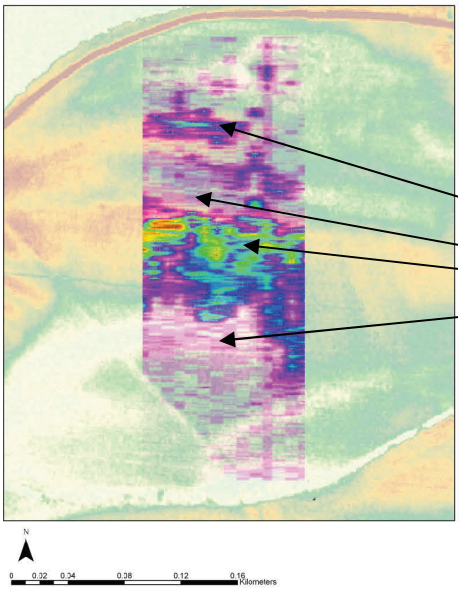

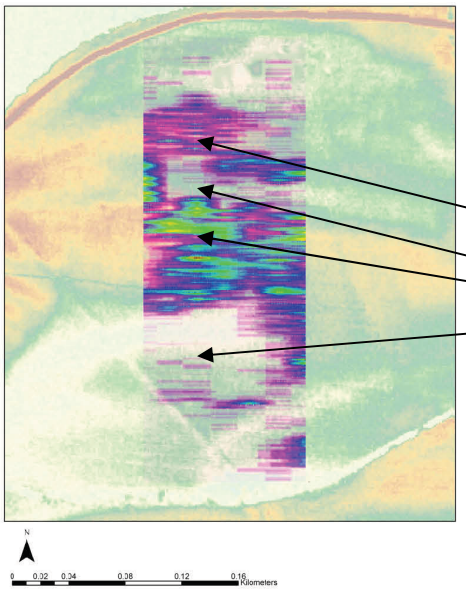

Fig 5.8: A comparison of the effect of different transect intervals on data quality using the MFG1 survey 0.85m – 1.15m depth slice. It is clear that as the transect interval increases there is a corresponding loss in data. By the 20m transect interval the features have become very poorly defined.

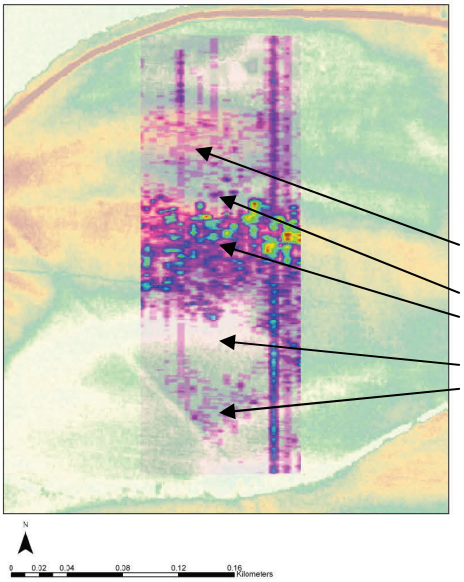

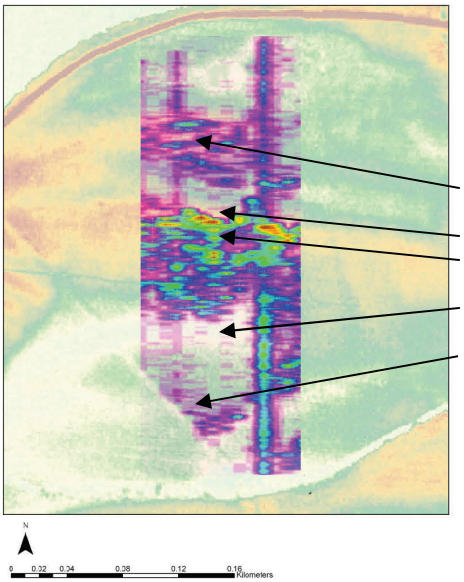

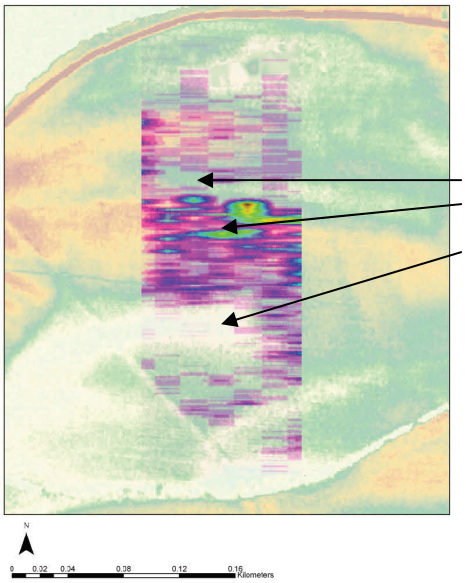

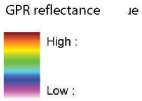

Fig 5.9: A comparison of the effect of different transect intervals on data quality using the MFG1 survey 1.35m – 1.65m depth slice. It is clear that as the transect size increases there is a corresponding loss in data.

5.1.3 Modern floodplain grid 2 high resolution survey (MFG2)

A second survey was conducted on the modern floodplain using a 400MHz antenna to survey over part of the palaeochannel MFC1 leading onto the gravel bar MF3 (Fig. 5.10). The survey used a 1m transect interval collecting 25 transects of data. The data was analysed through a variable velocity migration. The data was sliced at 0.25m intervals, using a depth slice of 0.1m. The images are shown with the LiDAR intensity plot at 70% transparency. The dielectric constant was set through reference to the gouge core transect. The reflectance values ranged from a minimum of –20 to a maximum of +80.

The LiDAR last pulse DTM shows the palaeochannel MFC1 and the area of slightly higher topography, which is the gravel deposit MF3 (Fig. 5.11). The 0.2m – 0.3m depth slice shows the edge of the palaeochannel MFC1 and the start of the gravel deposit MF3. The 0.45m – 0.55m depth slice shows the edge of MF3 clearly, and the channel MFC1 (Fig. 5.12). There is also variation evident between MF3 and MFC1, with MF7 and MF8 also visible. These are interpreted as a product of variation in sediment structure, related to the depositional environment, although further definition is not possible. At the 0.70m – 0.80m depth slice the features MF3, MF7, MF8 and MFC1 are still recognisable (Fig. 5.13). Deeper penetration was not achieved. Penetration into, and definition within, the palaeochannel was limited with the 400MHz antenna. Little new information was gained on the structure of these sediments using the higher resolution survey and higher frequency antenna.

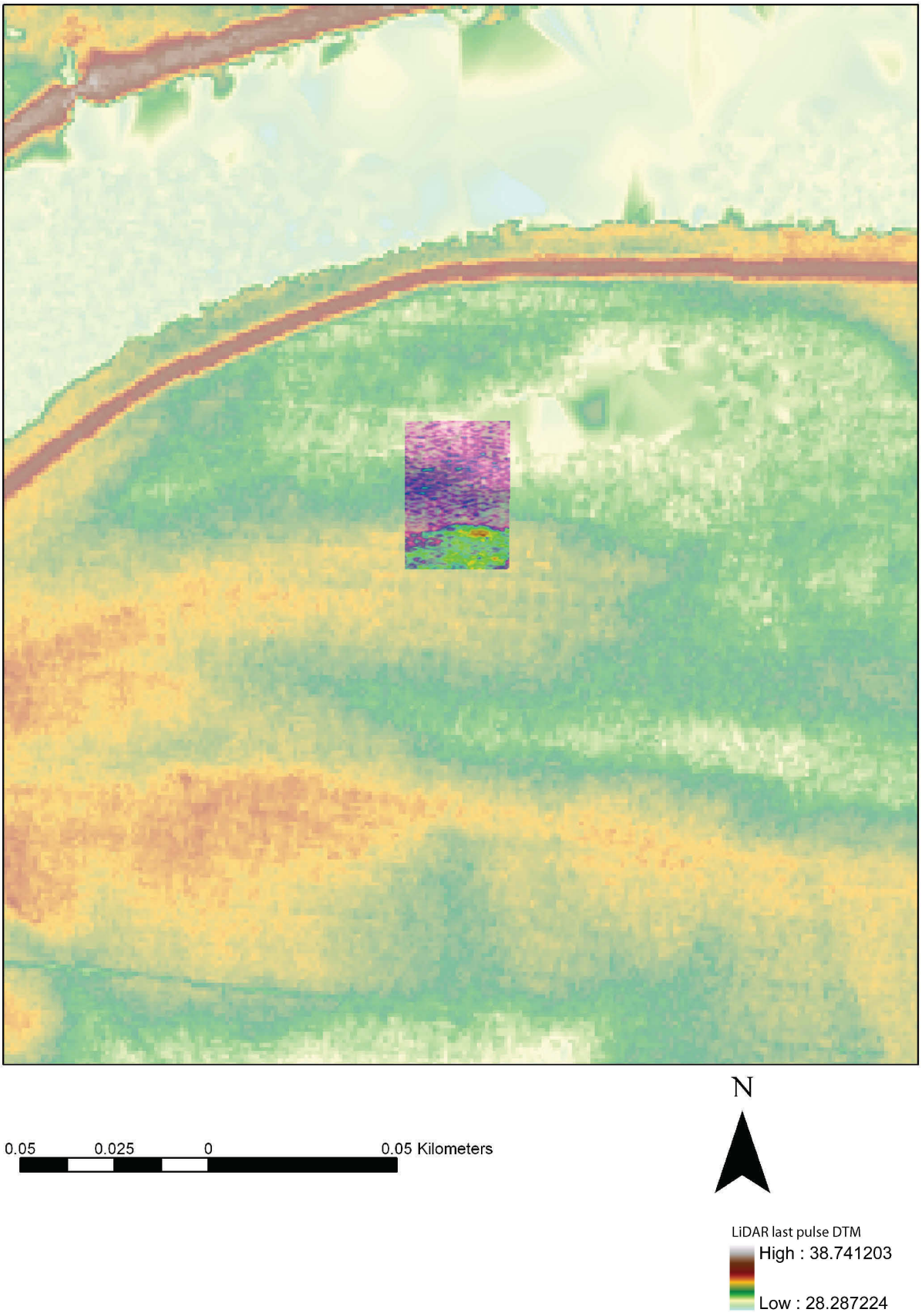

Fig 5.10: The location of the MFG2 survey, shown on the LiDAR last pulse DTM.

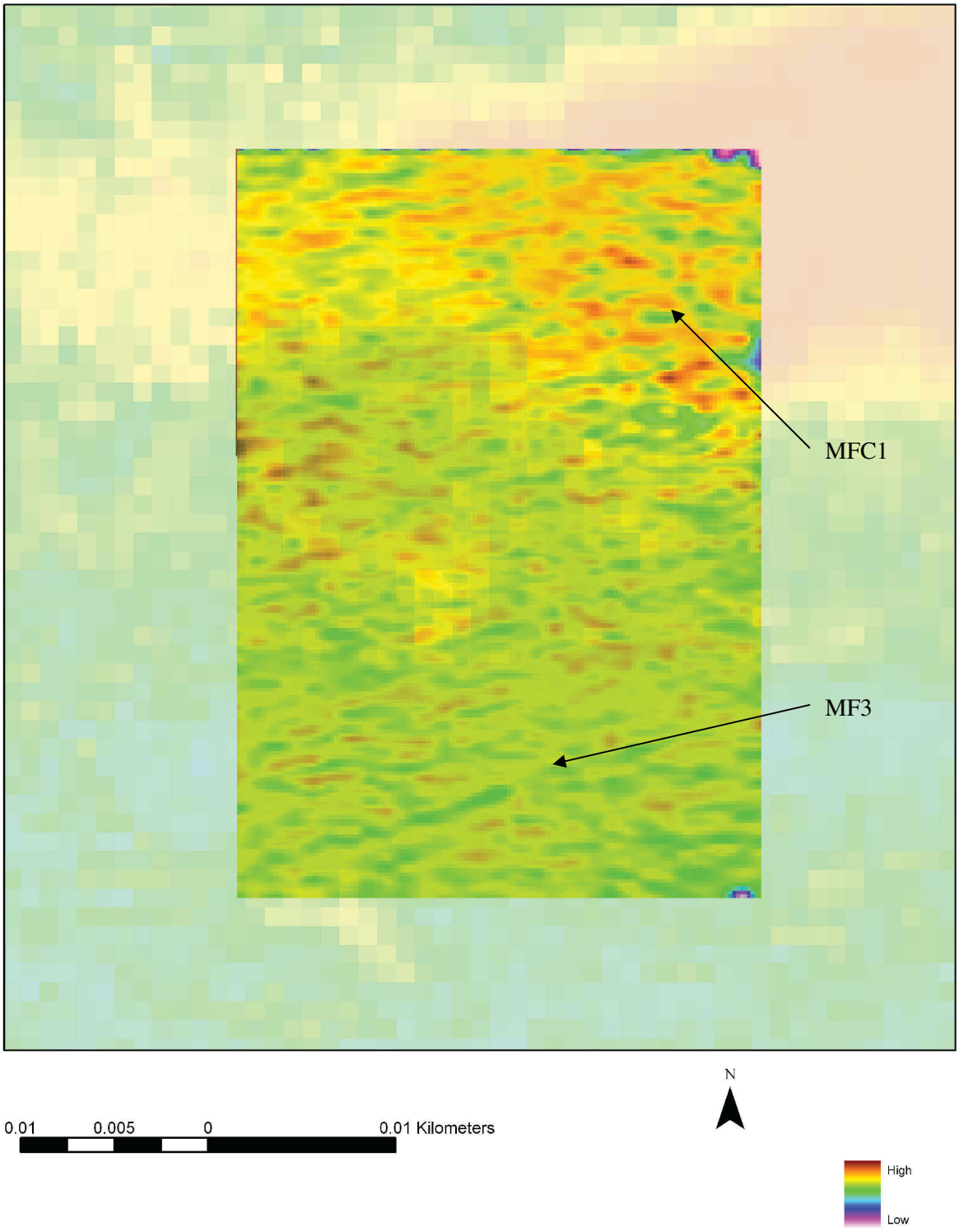

Fig 5.11: The MFG2 survey 0.2m – 0.3m depth slice. MF3 and MFC1 are just visible in this image, although there is interference due the time slice being located within the GPR near field zone.

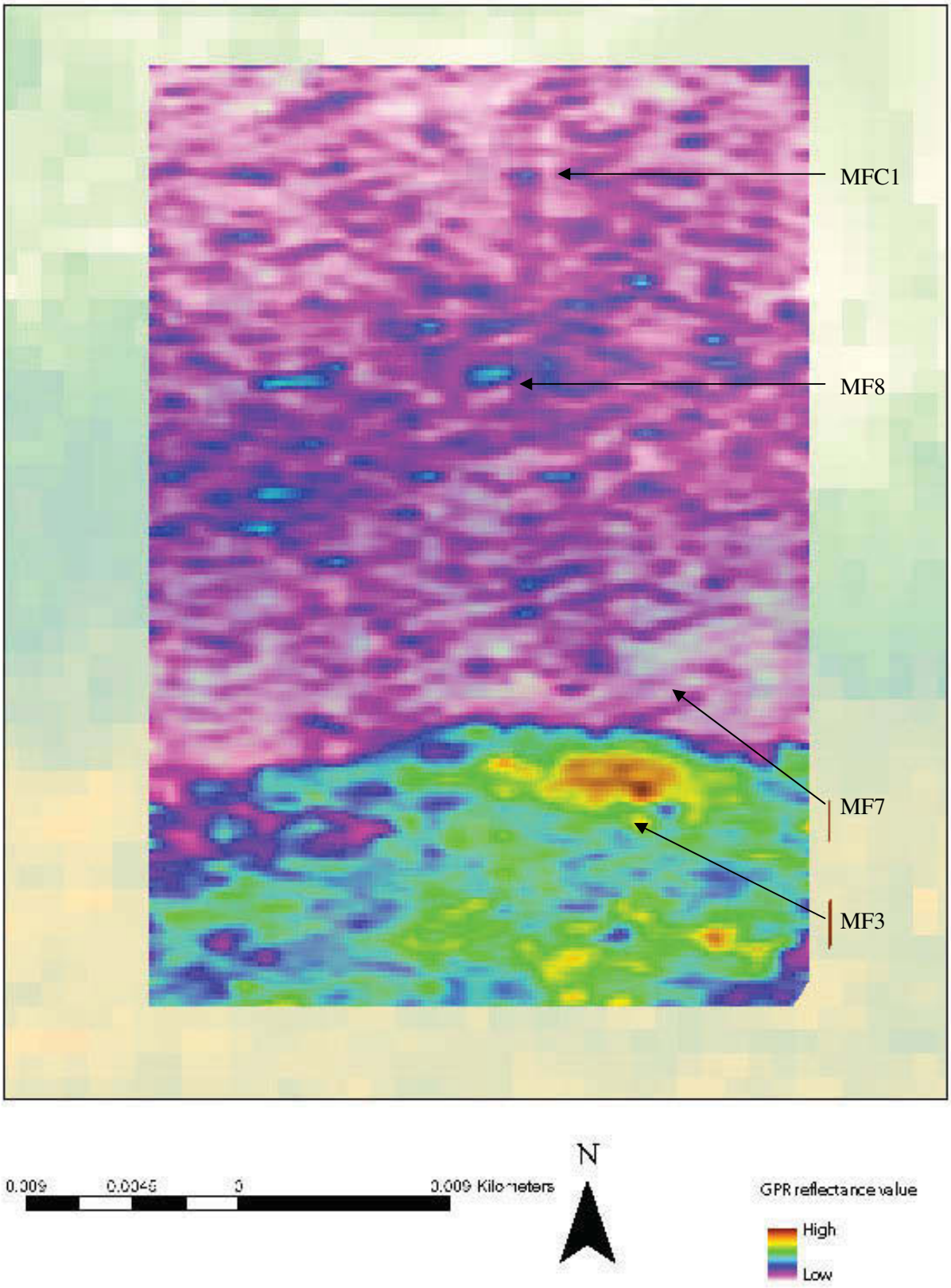

Fig 5.12: The MFG2 survey, 0.45m – 0.55m depth slice. The features of MF3, MFC1, MF7 and MF8 visible.

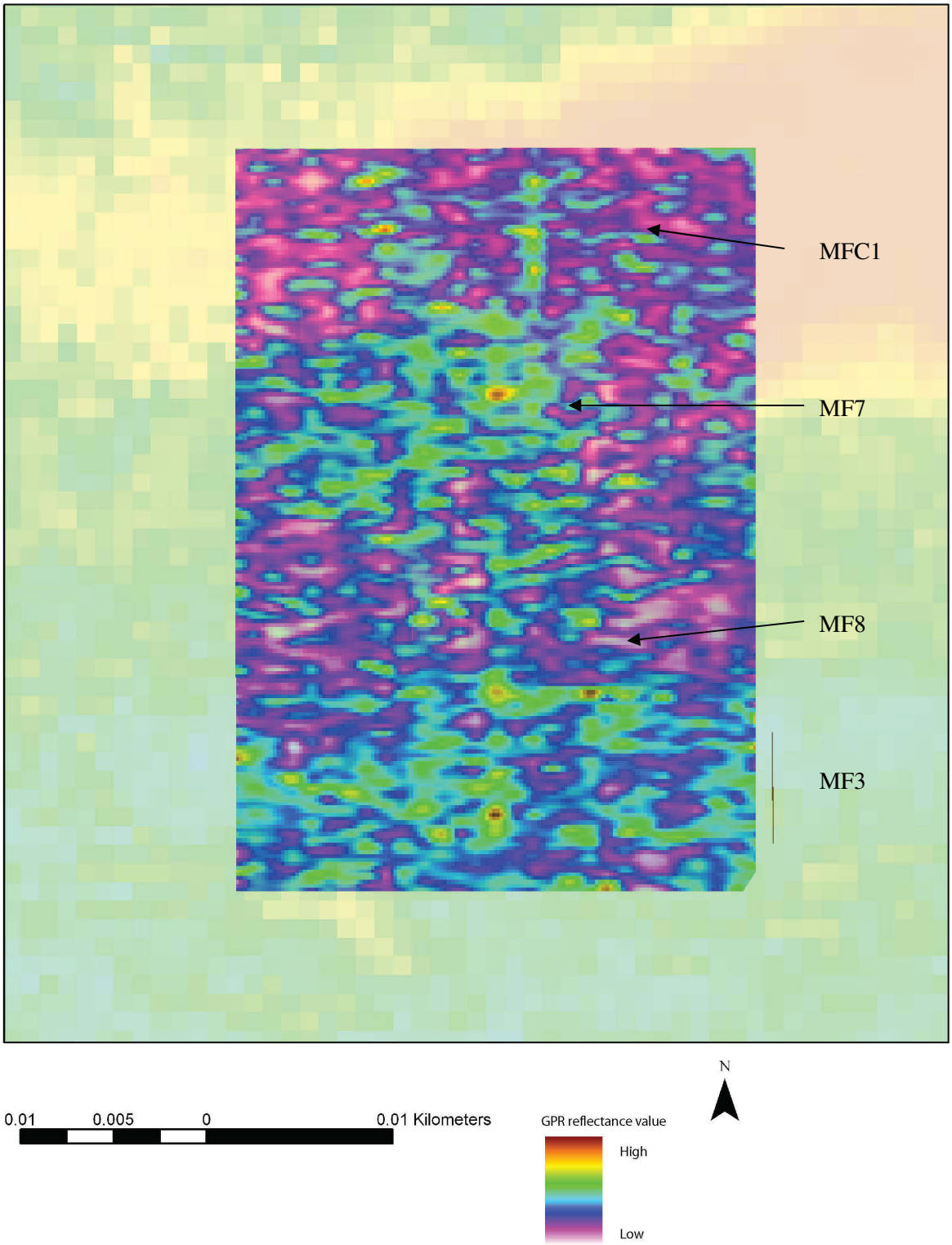

Fig 5.13: The MFG2 survey at the 0.7m – 0.8m depth slice. MFC1, MF7, MF8 and MF3 are still identifiable at this depth, although the depth of penetration has almost been reached.

5.1.4 Summary of the GPR results from the modern floodplain

From the results of the three surveys undertaken on the modern floodplain the following summary can be given of the application of GPR survey on this modern floodplain:

- The depth of alluvium varies considerably on the modern floodplain, from shallow on the gravel deposits to much thicker deposits within the palaeochannels.
- A considerable depth of gravel exists on the lower floodplain, in places extending to over 2m and deeper (the contact with bedrock was not seen).
- The dielectric constant for the modern floodplain had to be relatively set high due to high resistance to the transmission of the radar pulse.
- This resistance is interpreted as a product of the high water content of the sediments on the modern floodplain.
- The gouge core transect provided the depth calibration on the modern floodplain. There is good agreement between the GPR and gouge core data.
- The MFT1 and MFG1 surveys clearly identified a series of geomorphological units, interpreted as palaeochannels and gravel deposits.
- From the MFT1 and MFG1 surveys a basic alluvial stratigraphy is suggested, whereby the three palaeochannels MFC1, MFC2 and MFC3 post date the gravel deposits MF3 and MF4, and have eroded into this deposit.
- Penetration into the palaeochannels on the MFT1 and MFG1 surveys was shallow. This is interpreted as a product of high water table and high clay contents within the palaeochannels.
- The features identified by the LiDAR intensity and last pulse DTM have their corresponding stratigraphy shown through the GPR surveys.
- The MFG1 survey allowed three transect intervals to be compared in their usefulness for mapping floodplain stratigraphy. The results strongly suggested that a 5m transect interval with the 200MHz antenna produced the best results.
- The MFG2 survey allowed greater detail to be seen in the top 0.8m of the modern floodplain sediments.
- The MFG2 survey could not identify features below 0.8m, due to the higher frequency antenna being used.
- The MFG2 survey failed to reveal significant further structure within the channel fill, due to rapid signal attenuation.

5.2 The GPR surveys on terrace 1

The GPR surveys on terrace 1 consisted of a three grid surveys and three transect surveys. The areas for the surveys were selected after consulting the LiDAR images and targeted a series of terrace deposits with associated palaeochannels.

5.2.1 Terrace 1 transect 1 (T1T1)

The terrace 1 transect 1 (T1T1) survey was 395m long, running in a north/south direction, targeting two areas of terrace 1 intersected by a large palaeochannel (Fig. 5.14). The transect employed a 200MHz antenna, using high gain settings for maximum penetration. This has caused some data to be clipped with the minimum and maximum values not being realised over particularly strong reflectors, such as when gravels were very close to the surface. Through calibration with the gouge core transect the dielectric constant was set at 19. The data was analysed through using a variable velocity migration.

The transect has clear structure (Fig. 5.15). The interpretation of the data clearly defines the major geomorphological units being alluvium, gravels and palaeochannels. The gravels underlying the alluvium have a heterogeneous structure. The interpretation of the data identifies two types of unit within the gravels, being stronger reflecting (T1A) and weaker reflecting (T1B) units. The weaker reflecting units (T1B1 – T1B6) may represent Devensian deposits, generally lying beneath more recent Holocene gravels (T1A1 – T1A6). Alternatively both gravel units T1A and T1B could be have been deposited in the Holocene and the difference between the two units is a product of gravel/sand ratios. The GPR pulse does not penetrate to the base of the gravels at the junction with bedrock. A unit is seen at the base of the profile on the northern end of the transect (T1D). This is not interpreted as bedrock, as it deemed too shallow at only 3m from the ground surface. This junction could represent a sand or silt dominated deposit under the gravel, which the radar does not penetrate through.

The transect has four definite palaeochannels identified, being T1C1, T1C2, T1C3 and T1C5, and one more speculative palaeochannel T1C4. The four palaeochannels T1C1, T1C2, T1C3 and T1C5 are also evident through aerial photography (Fig. 5.16). The palaeochannel T1C1 is a shallow channel with the basal gravels being encountered at circa 1m from the ground surface. Palaeochannel T1C2 is also relatively shallow with a depth of circa 1.8m at its deepest but with areas of channel fill containing gravel. Likewise, palaeochannel T1C3 has a depth of 2.1m at its deepest point, with areas of gravel fill. On the south side of palaeochannel T1C3 the channel shows a greater level of incision into the terrace suggesting a higher energy erosive flow. The north side of the channel shows some evidence of depositional layers due to a lower energy flow. It is possible that T1C2 and T1C3 are two more recent palaeochannels following the course of the older palaeochannel T1C4. However, the depth T1C4 is deep at 3m and the channel form is a suggested interpretation. At this depth the radar signal has become weak and difficult to interpret.

The largest of the palaeochannels is T1C5, both in width and depth. The coring of the transect revealed a depth to gravels of 2.83m. The GPR pulse did not penetrate to the base of the palaeochannel. Dipping reflecting bands are seen on either side of the T1C5 but definition of any structure in the channel is not possible. These dipping reflecting bands represent either clay and/or sand units overlying the gravels at the edges of the channel T1C5. The level of alluvium overlying the basal gravels close to T1C5 is much deeper than on other sections of the transect. A D shaped enclosure is highlighted on Fig. 5.15, which has been partially covered by alluvium. This has importance in understanding the geoarchaeological potential of terrace 1 and is discussed in chapters 8 and 9.

The coring of T1C5 showed the fill to be a thick brown sandy clay silt, underlain by thick grey sandy clay and banded coarse medium sand. The structure of these units has proved too dense for radar penetration. The water table was also recorded in T1C5 when encountered. The area of the higher water table within the channel relates to a corresponding loss in data quality on the radar trace. Although the GPR did not to reveal the shape and structure of the channel due to the nature of its sediment fill, this is suggestive of a water logged anaerobic environment, which implies a high palaeoenvironmental potential.

The stratigraphic relationships of this transect can be summarised. The T1A deposits postdate the T1B deposits. The palaeochannels T1C1, T1C2, T1C3, T1C4 and T1C5 all post date the T1A and T1B gravel deposits, due to their incision and erosion into these units. Palaeochannels T1C1, T1C2 and T1C3 all post date the palaeochannel, through virtue of their position above T1C4. The chronological relationship between T1C4 and T1C5 is not definable though this GPR transect.

The correlation between the T1T1 interpretation and the gouge core transect is excellent, showing the relationship of the cored data to the interpreted T1T1 data. The depth at which the surface of the gravels was encountered is consistent with the depth profiling of the GPR section. The gouge core transect provided data on the depth and nature of the palaeochannel fill T1C5, when the GPR transect did not provide adequate penetration. In contrast palaeochannels T1C1 – T1C4 had excellent structure revealed through the GPR transect, especially on the nature of their gravel fills. However, the integration of the gouge core and GPR data provided the most information on the nature of the floodplain sediments.

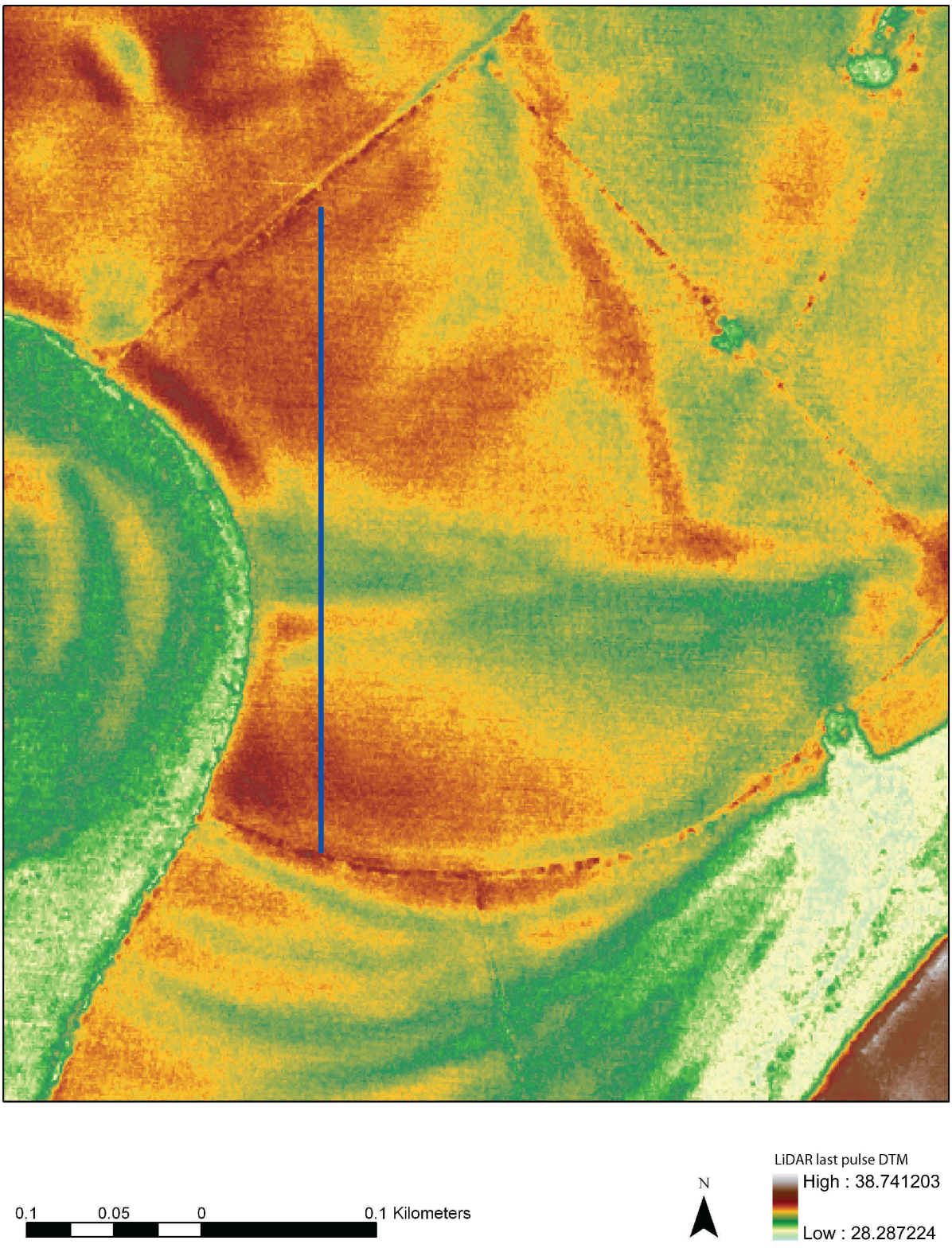

Fig 5.14: The location of the T1T1 survey on terrace 1.

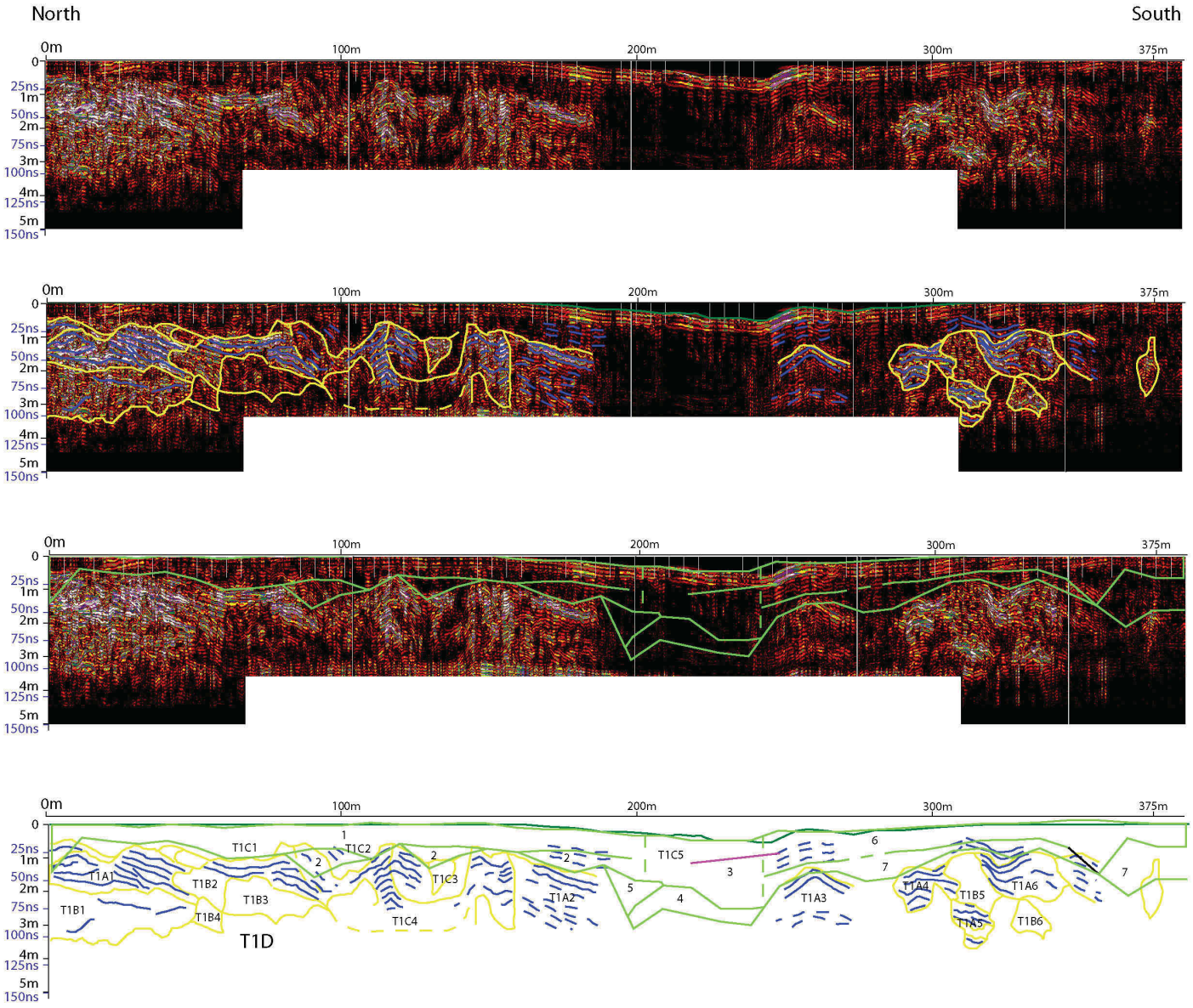

Key

Stratigraphic units from coring (numbers)
1 - Silt with red sand
2 - Coarse sand
3 - Thick brown sandy clay silt
4 - Thick grey sandy clay
5 - Banded coarse medium sand
6 - Clay and fine sand
7 - Free sand
8 - Gravel (impenetrable to thin gouge core)

Stratigraphic units from GPR interpretation (letters):
T1A(number) - gravel unit, higher reflection
T1B(number) - gravel unit, lower reflection
T1C(number) - palaeochannel
T1D - different sedimentary unit

Core transect

Boundary
Water table

GPR interpretation

Strong reflecting layer
Sedimentary boundary
Suggested reflecting layer
Suggested sedimentary boundary

Fig 5.15: The T1T1 transect, shown with interpretation and corresponding gouge core data. Penetration into the palaeochannel was poor, whilst the structure revealed in the deposits surrounding T1C5 is excellent.

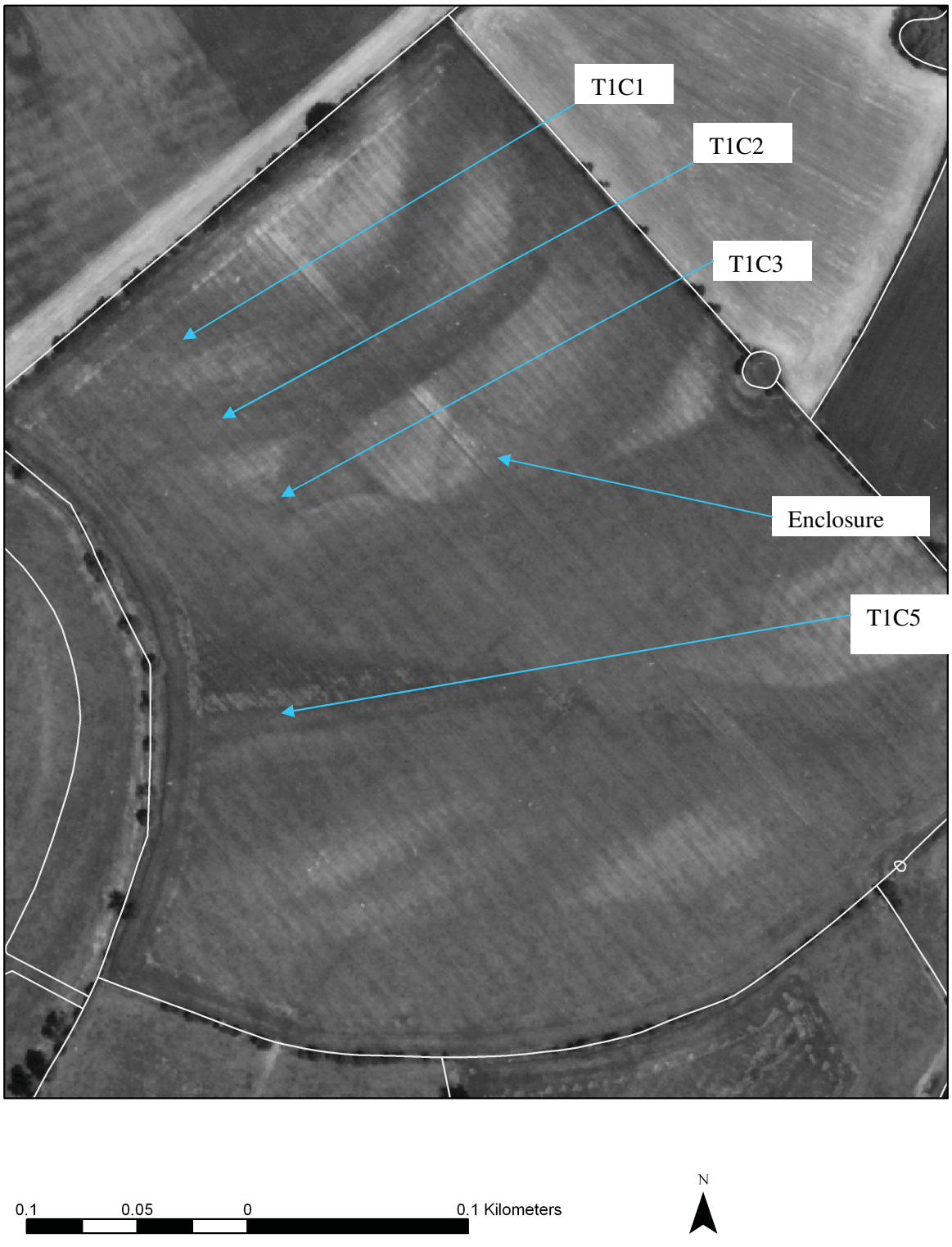

Fig 5.16: A rectified aerial photograph showing the T1T1 survey area. The channels T1C1, T1C2, T1C3 and T1C5 are highlighted, as is a D shaped enclosure that has been partially buried by alluvium deposited from T1C5.

5.2.2 Terrace 1 quarry transect T1QT

The terrace 1 quarry transect (T1QT) survey was just under 70m long, running in a southeast/northwest direction (Fig. 5.17). The T1Q1 survey ran along the edge of a Lafarge quarry at Sawley, allowing a visual comparison between a GPR transect and a recorded section. The transect employed a 200MHz antenna. The section along the transect recorded sediment stratigraphy at 2.5m intervals. The dielectric constant was set through the consulting the section drawing and also the T1T1 calibration and was set at 20.

The transect has clear structure, with the GPR interpretation compared to the section drawing (Fig. 5.18). The alluvium is clearly recognisable as QT1. Units QT4, QT5 and QT6 are interpreted as a series of layers lying on top of the basal gravels. These are high reflecting units, which with calibration from the section drawing proved to be clay and sand deposits. Below units QT5, QT5 and QT6 is gravel. There is little structure within the gravels shown on the GPR trace. The clay units (QT4, QT5 and QT6) have proved to be almost impenetrable for the GPR signal. The base of the gravel deposit is not seen. In general the correlation between the section and the GPR interpretation is good, although the section drawing reveals finer detail in the clay and sand deposits overlying the gravels. However, there is some variation between the location of the basal gravels identified by the GPR transect and the drawn section. Most notably the GPR trace does not identify unit 5 from the section. This unit has a high clay content and GPR penetration into this unit was extremely limited.

The GPR interpretation can also be compared to photographic recording of the section (Fig. 5.19). On the photograph the sediment units of QT1, QT2, QT5 and QT7 are labelled and are visually evident. QT1 proved to be a heterogeneous unit, with smaller 'pockets' of different matrix being encountered such as QT2. The quarrying has revealed substantial organic deposits that appear to have been located within the gravels (Fig. 5.20), although by the time of inspection the trees were '*ex-situ*', so their exact context is not known. On inspection these trees revealed no evidence of anthropogenic activities in the form of tool marks.

The photograph combined with the GPR interpretation and section highlights a key point about this area of terrace 1. A substantial covering of alluvium overlies the gravels, varying from between 1.5m to just over 2.5m when including the clay unit 5. This is in contrast to the T1T1 transect which generally had a much shallower level of alluvium overlying the gravels, although again in the T1T1 transect variation in alluvium depth was seen. The investigation of the gravel deposits in the quarry produced no evidence for bipartite gravel units, suggesting that the weaker reflecting units on transect T1T1 are not Devensian but Holocene gravels.

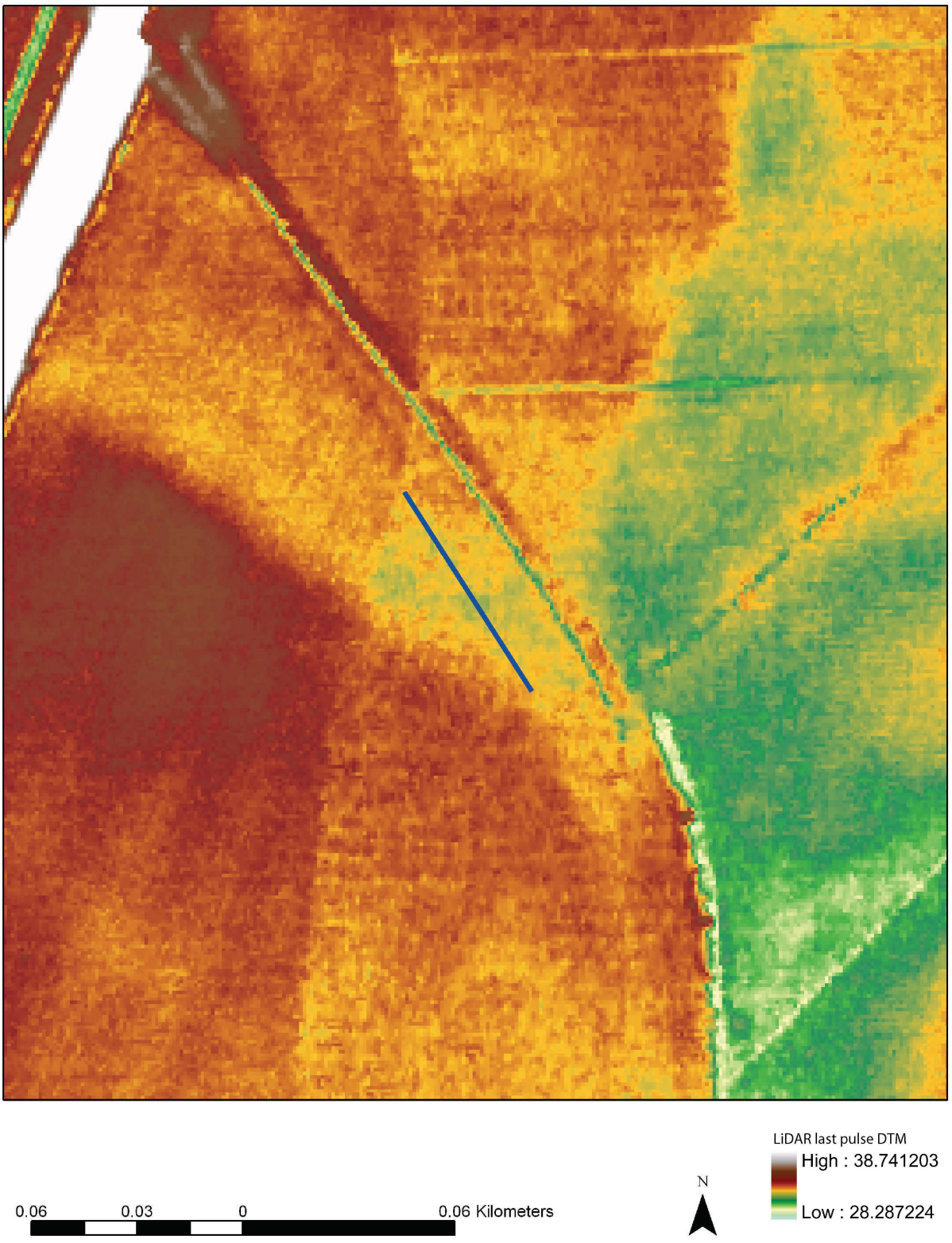

Fig 5.17: The location of the T1QT survey. The field that T1QT was surveyed in is now an active quarry, with the transect creating a section along the quarry edge.

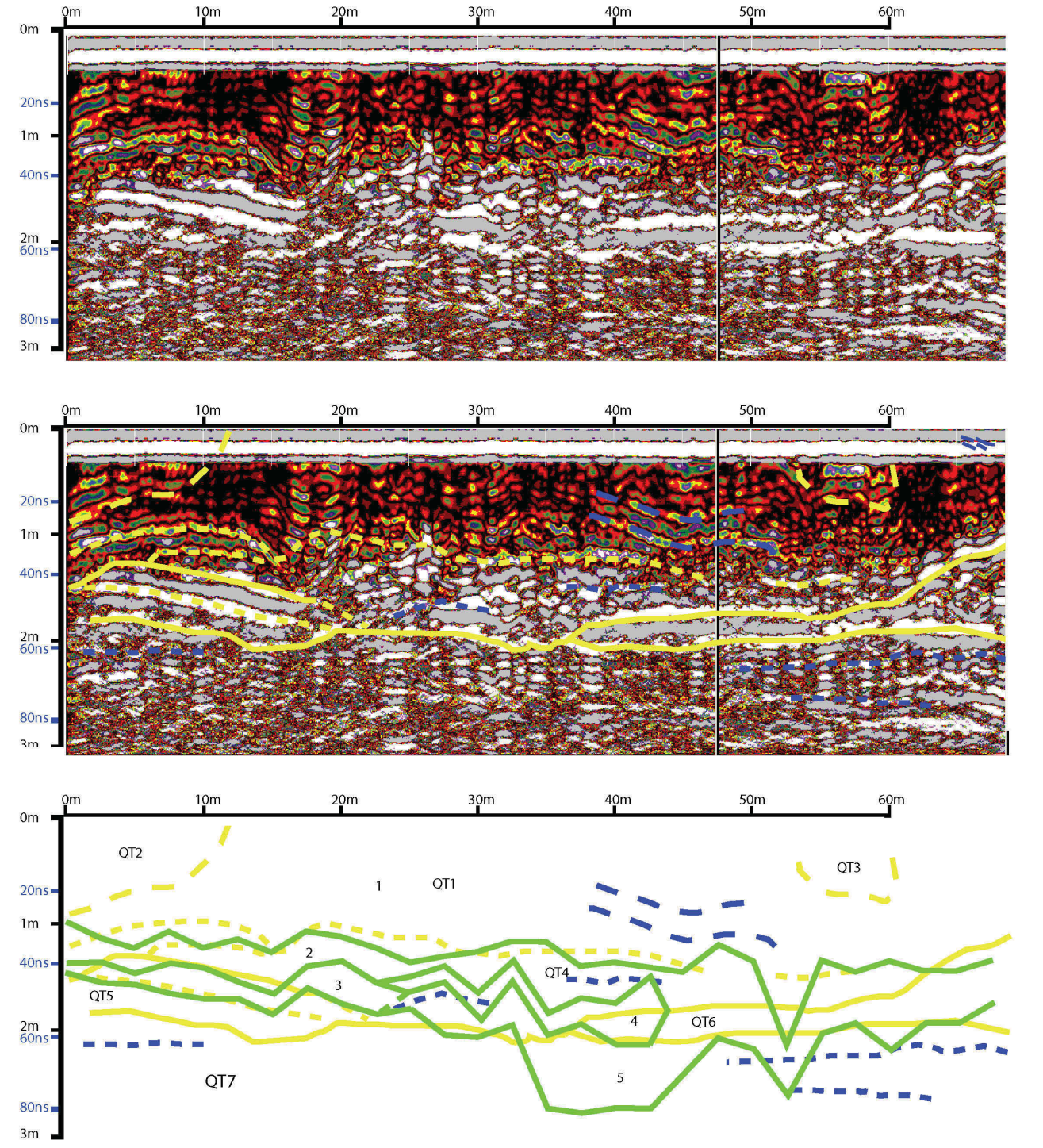

Fig 5.18: The T1QT survey, shown with interpretation and against the section drawing.

Fig 5.19: A photograph of the start of the T1QT transect, showing the main units from the GPR interpretation.

Fig 5.20: Within the gravel unit on terrace 1 were substantial organic remains, such as these three oak trees. The trees showed no evidence of anthropogenic activity, such as tool marks.

5.2.3 Terrace 1 grid 1 and terrace 1 transect 2 (T1G1 and T1T2)

The T1T2 and T1G1 surveys on terrace 1 used a 200MMHz antenna. The T1T2 survey was a single transect with gouge core data. The T1G1 survey used a 5m transect interval collecting 20 transects of data. Each GPR depth slice has a thickness of 0.2m, sliced at 0.5m intervals. The dielectric constant was set at 19 through calibration with the gouge core data. The GPR reflectance values ranged from –4 to +100. On each GPR depth slice the LiDAR intensity plot is shown as 70% transparent overlay. This area of terrace 1 has been eroded into by a palaeochannel, as shown by the LiDAR last pulse DTM, also used to show the position of T1T2 (Fig. 5.21). The LiDAR intensity shows this area of terrace 1 (T1H1) as having a different value to the palaeochannel labelled T1C6 (Fig. 5.22). A flood map produced by merging a picture of the Trent/Soar confluence in flood in 1954 combined with the LiDAR last Pulse DTM model shows that this area of terrace 1 was at the very extreme of recent major flood events (Fig. 5.23).

The transect shows the gravel deposits T1H2, with a lack of penetration into the palaeochannel T1C6 (Fig. 5.24). The unit T1H2 has a series of reflecting layers, indicating a heterogeneous structure. The GPR section defines a substantial covering of alluvium over the terrace gravels, reaching 1.5m at its maximum depth similar to the level seen in the T1QT transect. The depth to the gravel is confirmed by the gouge core transect. A palaeochannel is obvious as T1C6, but the difference between the gouge core data and the GPR transect over T1C6 is substantial, indicating rapid attenuation of the GPR signal within T1C6. The GPR interpretation also identifies T1H1 within T1C1. The composition of this unit is uncertain. GPR penetration was poor within T1C6 and T1H1 lies below the suspected depth of maximum penetration. Therefore, T1H1 is a suggested anomaly that requires further investigation to resolve its nature.

The T1G1 produced a series of depths slices that added further data to the model put forward through the interpretation of T1T2. The 0.9m – 1.1m depth slice shows T1C6 with two distinct areas of higher reflectance, with terrace 1 being visible as an area of lower reflection (Fig. 5.25). At this depth the gravels on terrace 1 are not visible, being below the alluvium. The T1T2 transect revealed a unit (T1H1) within the palaeochannel, which could be reason for the high reflectance values seen in the T1C6 at this depth slice. However, the composition of T1H2 is not known and this is a speculative interpretation.

At the 1.4m – 1.6m depth slice the gravel unit T1H2 starts to become evident on the terrace, with clear differentiation from T1C6 and also at the 1.9m – 2.1m depth slice (Fig. 5.26 and Fig. 5.27). At 2.4m - 2.6m the gravel unit T1H2 is clearly defined (Fig. 5.28). The areas of higher reflectance within T1C6 at the 2.4m – 2.6m depth slice are not interpreted as basal gravels due to their depth at between 2.4m and 2.6m. This was below the depth of penetration within T1C6. The T1T2 survey revealed that sand/gravel depth within this channel was only at 1m and 1.3m below the ground and these reflections are not interpreted as gravels. Significant penetration deeper than 2.6m was not achieved.

From the T1T2 survey and the T1G1 survey combined with the LiDAR results it is clear that the T1C6 channel has eroded into T1H2 and thus post dates the gravels in this terrace. The depth of alluvium overlying the T1H2 gravel unit is substantial and is a product of sediment deposition from large channel flooding events. This level of alluvium overlying the gravels on terrace 1 is similar to the T1QT but different to the T1T1 survey. This again highlights that there is significant differences in alluvial deposition across terrace 1, having important consequences for the archaeological resource.

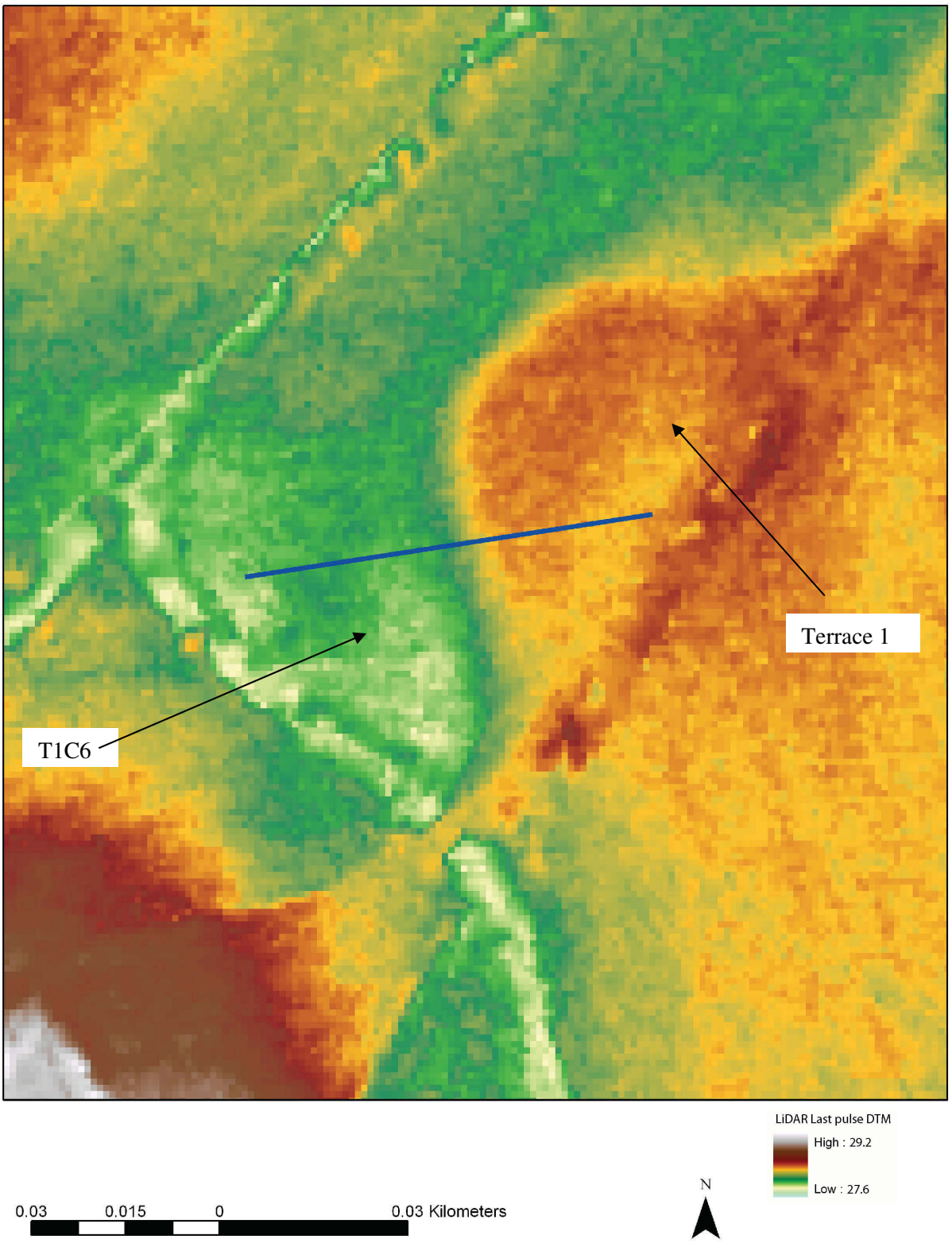

Fig 5.21: The LiDAR last pulse DTM, showing terrace 1 and the palaeochannel T1C6. The location of T1T1 is also shown.

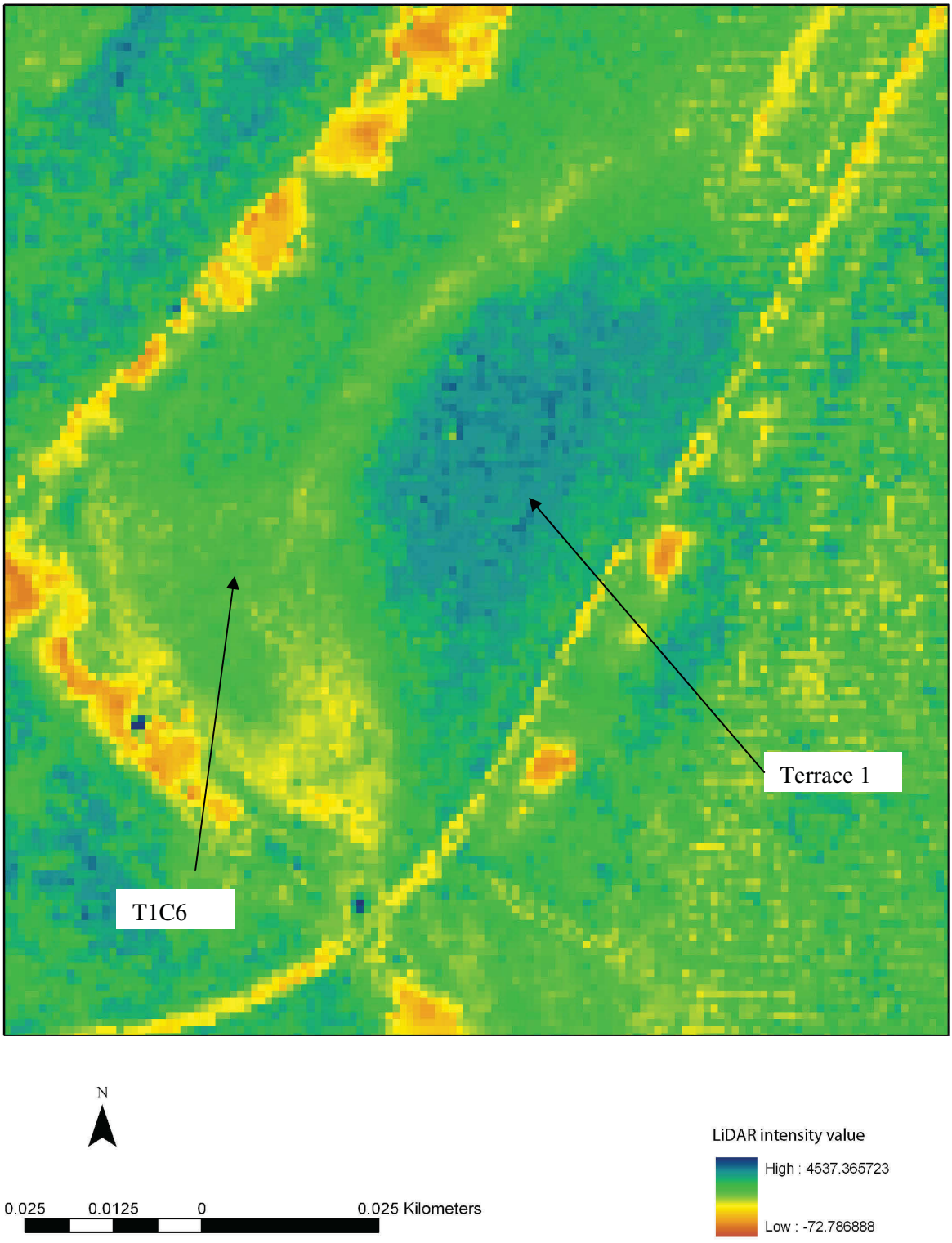

Fig 5.22: The LiDAR intensity plot, also showing a difference between terrace 1 and T1C6.

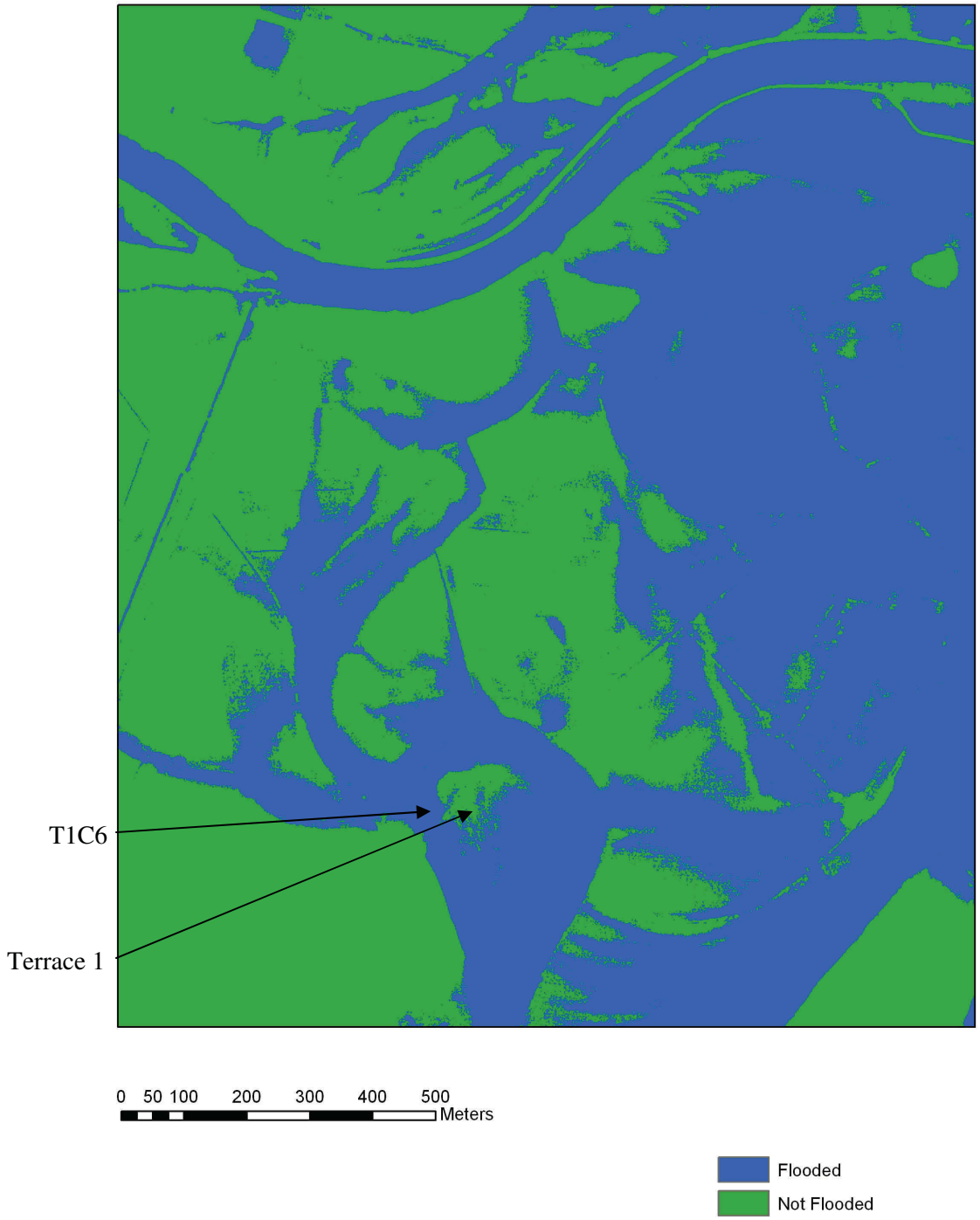

Fig 5.23: A flood map produced through combining an aerial photograph of the 1954 flood with the LiDAR last pulse DTM. Terrace 1 is shown as not flooded by the channel T1C6, although it is at the very edge of the flood boundary.

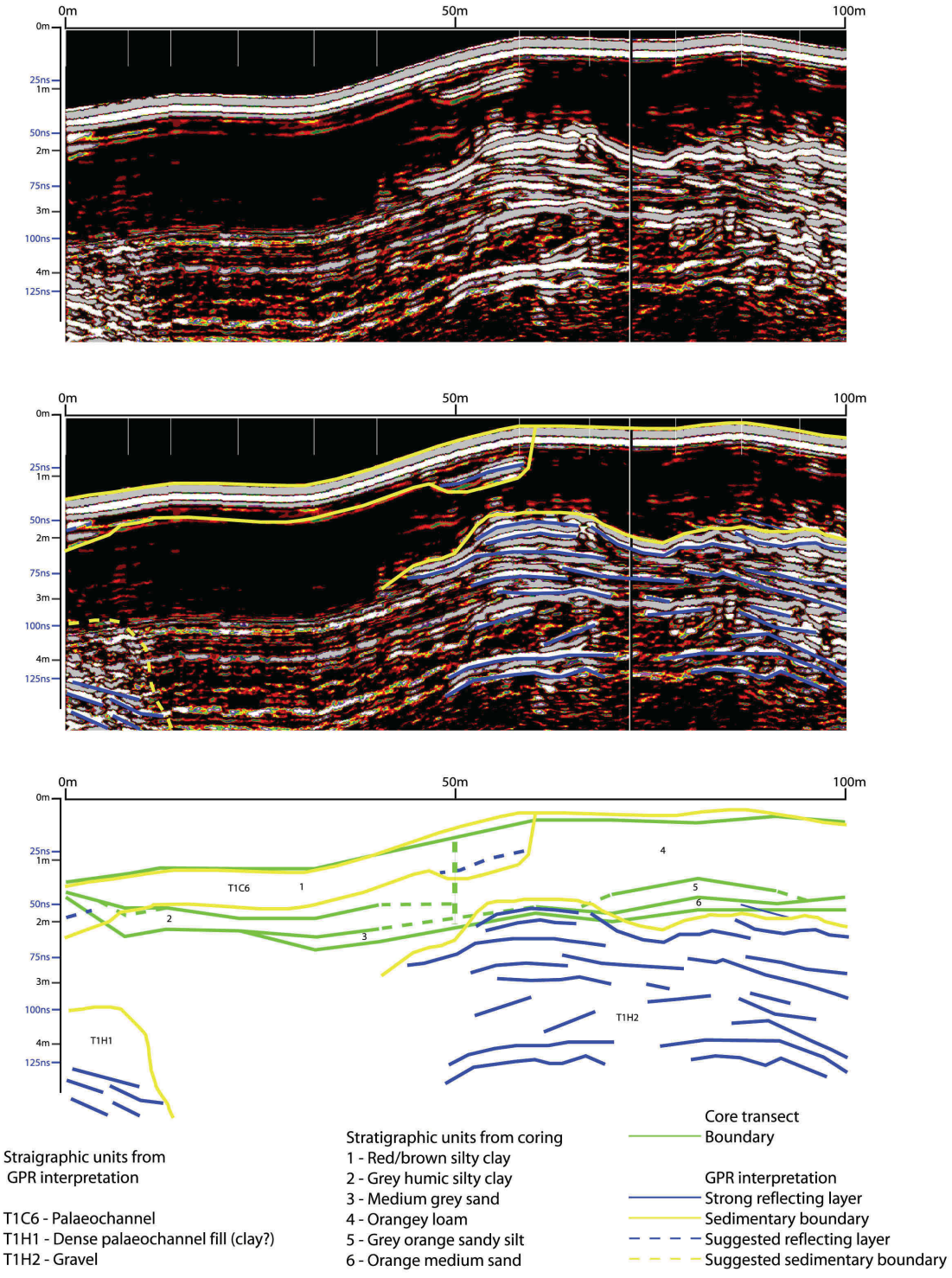

Fig 5.24: The T1T2 transect survey, shown with an interpretation and against gouge core data.

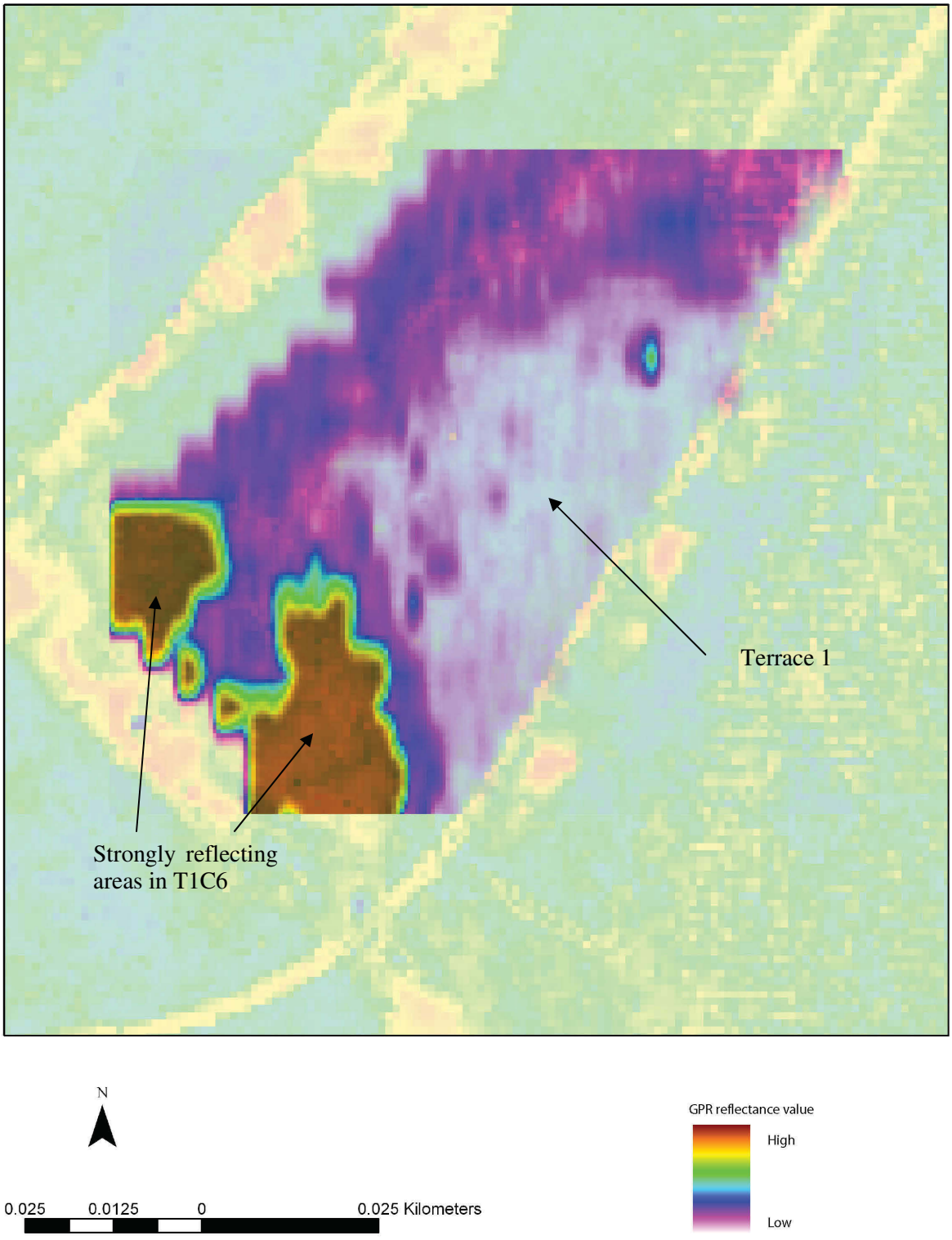

Fig 5.25: The T1G1 survey, 0.9m – 1.1m depth slice. The area of terrace 1 is still as a low reflecting unit, due to it the gravels still being under alluvium at this depth. Two strongly reflecting features are evident in T1C6.

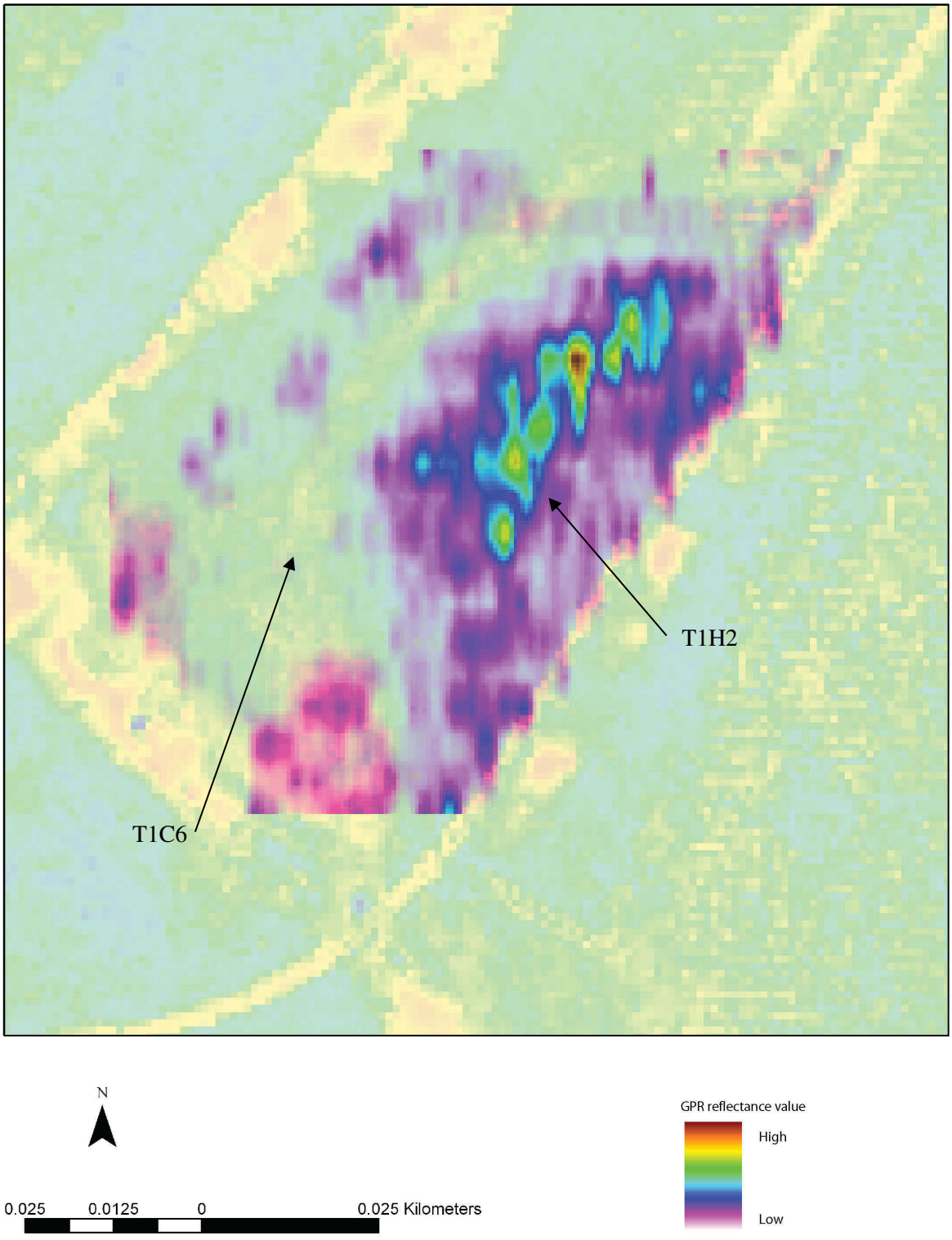

Fig 5.26: The T1G1 survey, 1.4m – 1.6m depth slice. The gravels under the alluvium on terrace 1 are becoming visible (gravel unit labelled T1H2). T1C6 is evident as a feature but it this is due to lack of penetration at shallower depths.

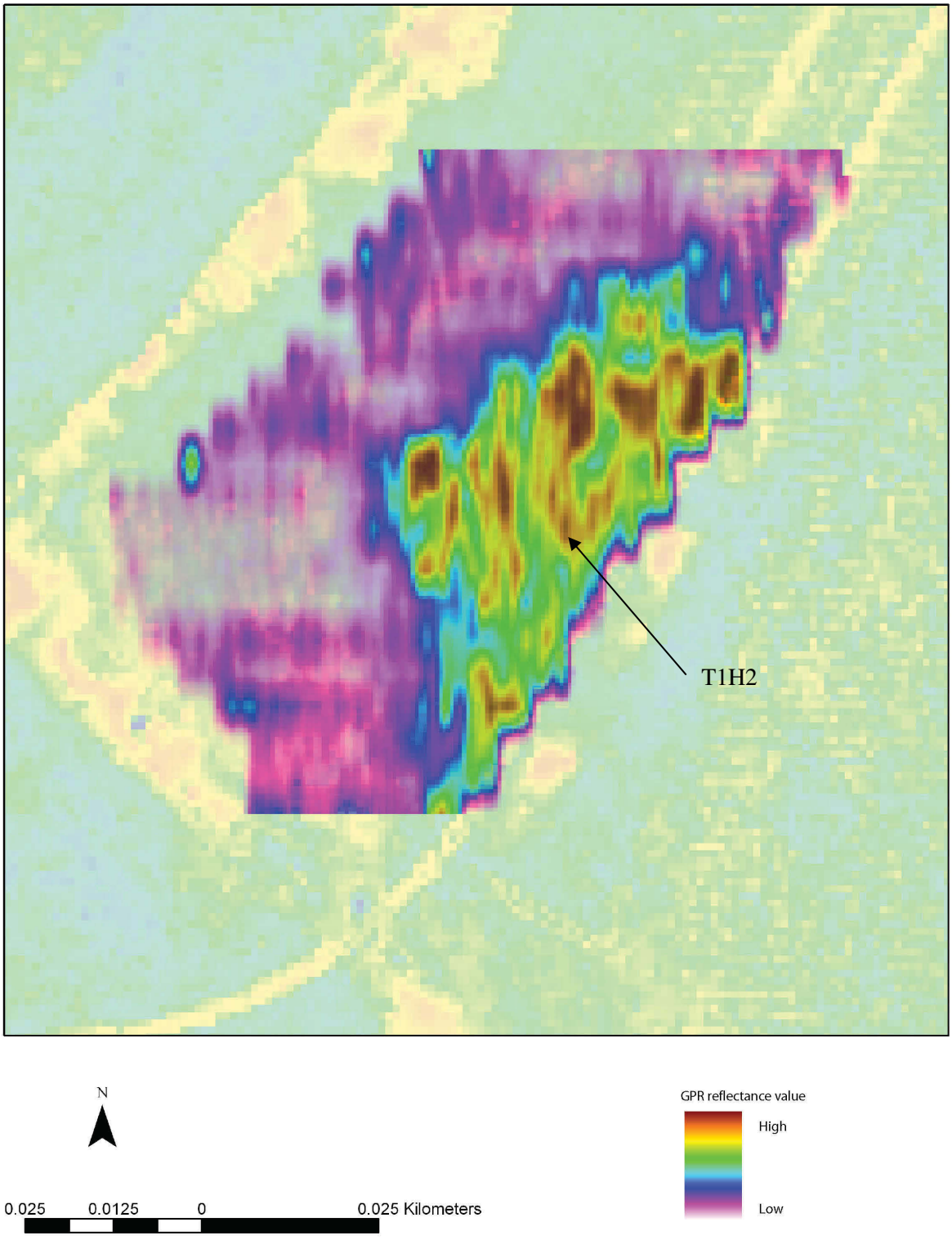

Fig 5.27: The T1G1 survey, 1.9m – 21.m depth slice, with the gravel unit T1H2 clearly visible.

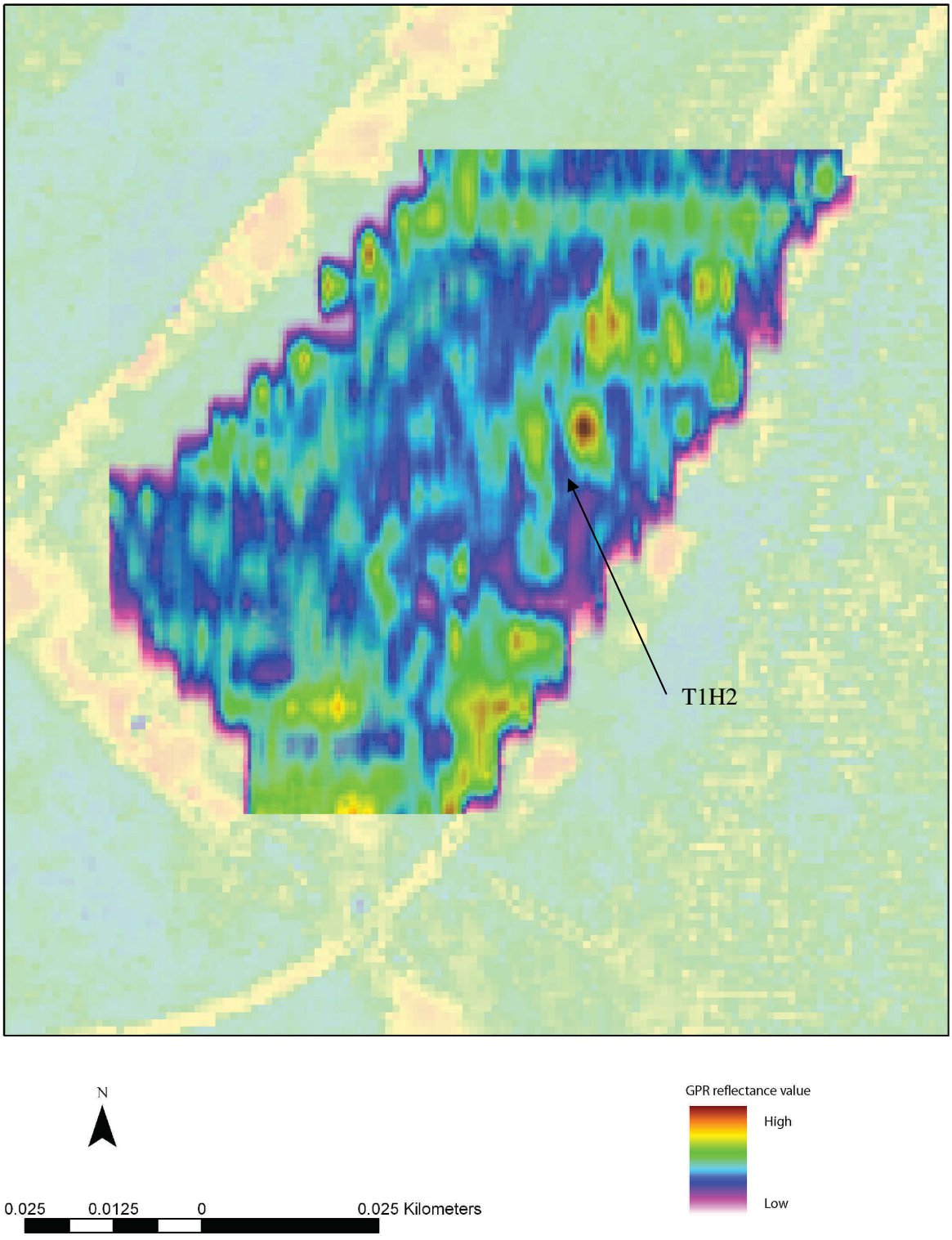

Fig 5.28: The T1G1 survey, 2.4m – 2.6m depth slice. The maximum depth of penetration is being reached but T1H2 is still identifiable.

5.2.4 Terrace 1 Grid 2 survey (T1G2)

The T1G2 used a 5m transect interval and collected a small grid of only 8 transects. The data was processed through using a variable velocity migration. No comparative gouge core transect was undertaken within this survey area. The dielectric constant was set at 19, through the calibration made on T1T1 in the adjacent field. The GPR reflectance values ranges from –56 to +128. The T1G2 survey area had no major topographical variation as shown through the LiDAR last pulse DTM (Fig. 5.29). The LiDAR intensity plot of the T1G2 survey area did reveal variation within terrace 1, not apparent through the DTM model (Fig. 5.30). The variation in intensity values is interpreted as relating to variation in sediment water content. The T1G2 survey results are shown within the LiDAR intensity plot at 70% transparency. The depth slices are 0.2m thick, sliced at 0.5m intervals.

The 0.4m – 0.6m depth slice shows a subtle variation across the survey area, with a slight difference in reflection values between the south and north of the survey area (Fig. 5.31). The 0.9m – 1.1m depth slice reveals clear variation within the T1G2 survey area (Fig. 5.32). Two areas of strongly reflecting gravels are seen (T1H3 and T1H4). Interspersed between these two areas of gravel is an area of lower reflectance/higher absorbance, interpreted as a palaeochannel (T1C7). The depth of alluvium overlying the gavel unit T1H4 is less than 0.9m, due to its visibility at this depth. The gravel units T1H3 and T1H4 and T1C7 palaeochannel are visible in the 1.4m – 1.6m depth slice (Fig. 5.33). The 1.9m – 2.1m depth slice still shows the gravel unit T1H4 but the gravel unit T1H3 is no longer apparent (Fig. 5.34). The palaeochannel T1C7 is still visible. This general pattern of palaeochannel T1C7 and gravel unit T1H4 is seen in the 2.4m – 2.6m and 2.9m – 3.1m time slices (Fig. 5.35 and 5.36). Further penetration is not seen below this depth, with the base of the gravels not being encountered.

A three-dimensional model created in Radan shows the structure of the GPR survey clearly (Fig. 5.37). The gravel unit T1H4 is shown with incision from the avolsed channel (T1C7), with a clear erosional bounding surface. T1H3 is interpreted as a gravel unit within the palaeochannel T1C7, either a gravel bar or remnant terrace. This interpretation is interesting as the channel T1C7 was not evident through the DTM model but variation was visible within the LiDAR intensity data. The GPR penetration in T1C7 is shallow, at circa 1m depth. This is interpreted as a product of high water and clay content. T1C7 could be targeted for dating and palaeoenvironmental samples, due to high water content and potential anaerobic conditions, allowing good anaerobic preservation. From the three-dimensional model a chronology of these main units can be suggested. The oldest unit is the area of terrace 1 T1H4, which has been eroded into by the palaeochannel T1C7. T1H3 is interpreted as being formed through the palaeochannel T1C7 and is thus contemporary with an active stage of the T1C7.

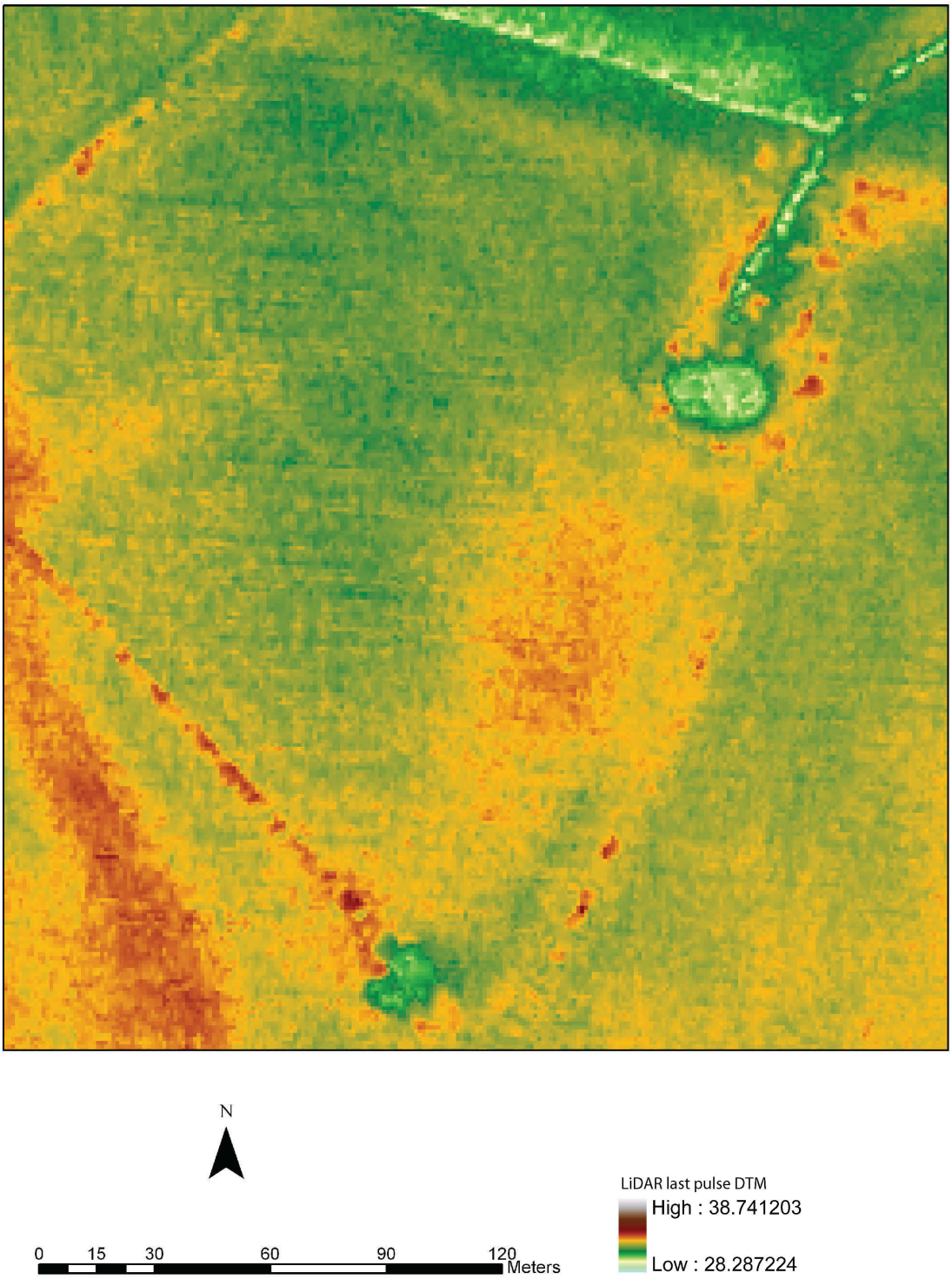

Fig 5.29: The LiDAR last pulse DTM of the T1G2 survey area. There is no significant topographic variation evident, which can be related to a change in geomorphology.

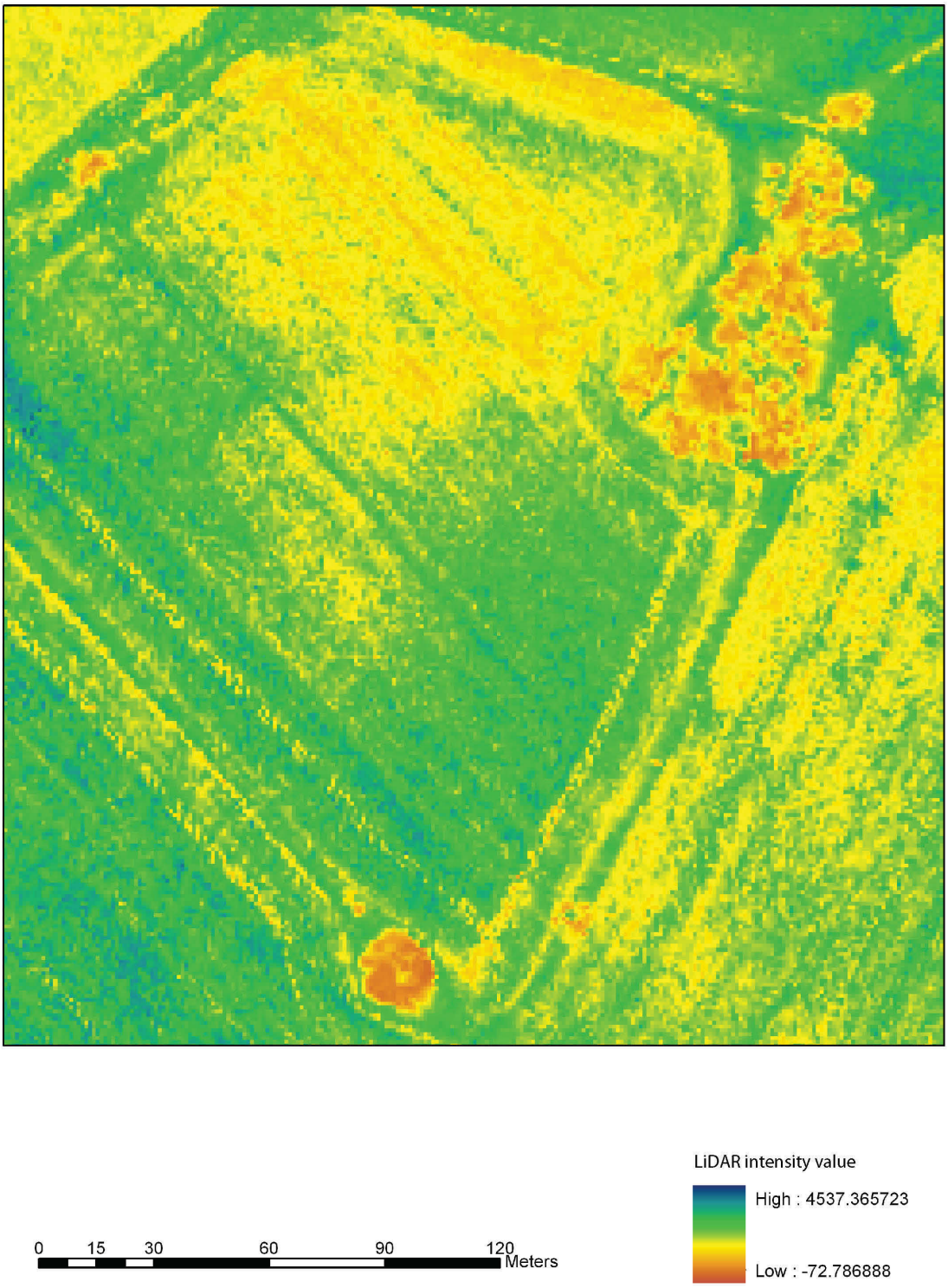

Fig 5.30: The LiDAR intensity over the T1G2 survey area. An area of lower intensity values are visible to the north of the survey area, whilst higher values are seen to the south.

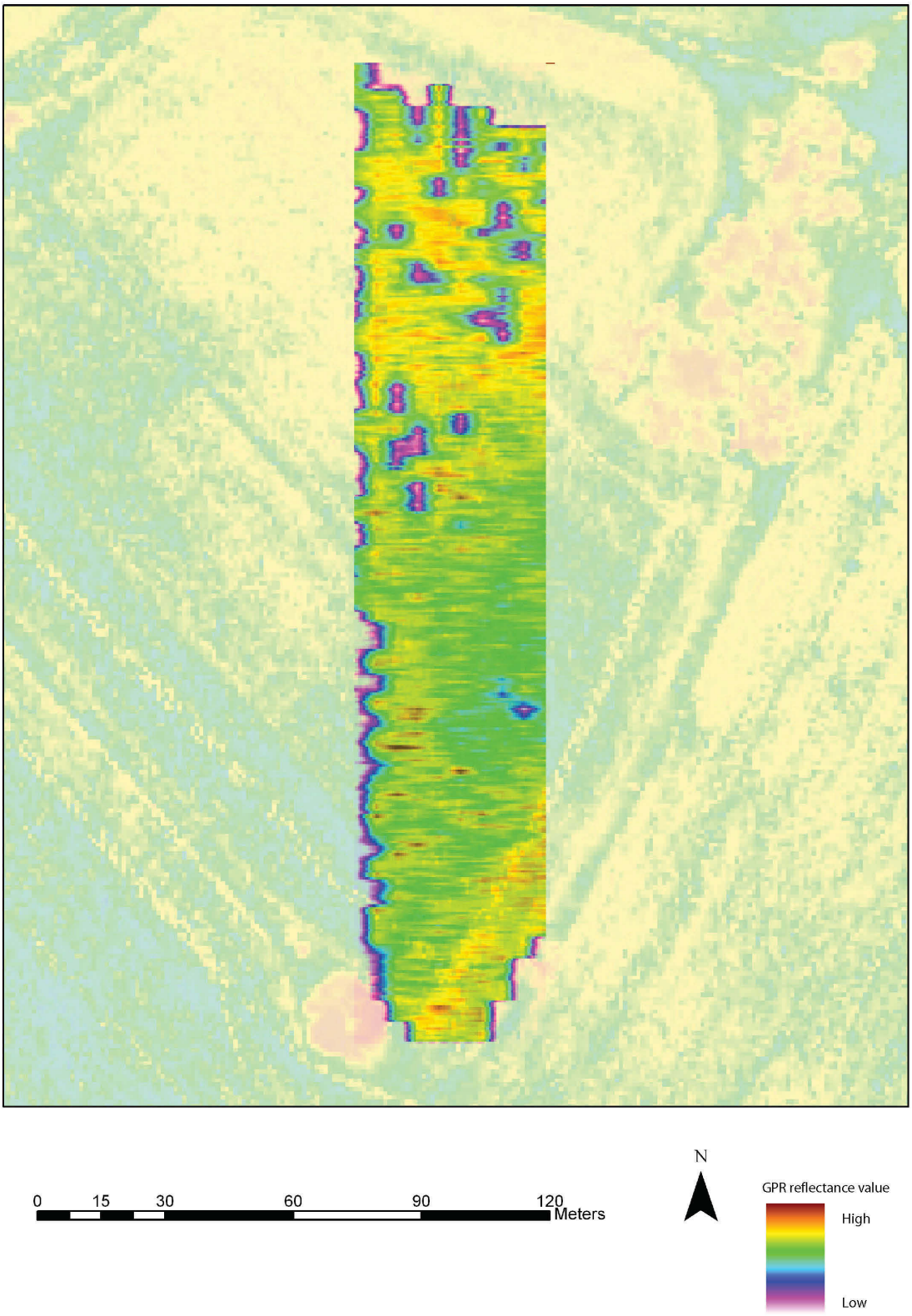

Fig 5.31: The T1G2 survey, 0.4m – 0.6m depth slice. Although this depth slice is still within the GPR near field zone, there is a slight change in reflectance between the north and south areas of the survey.

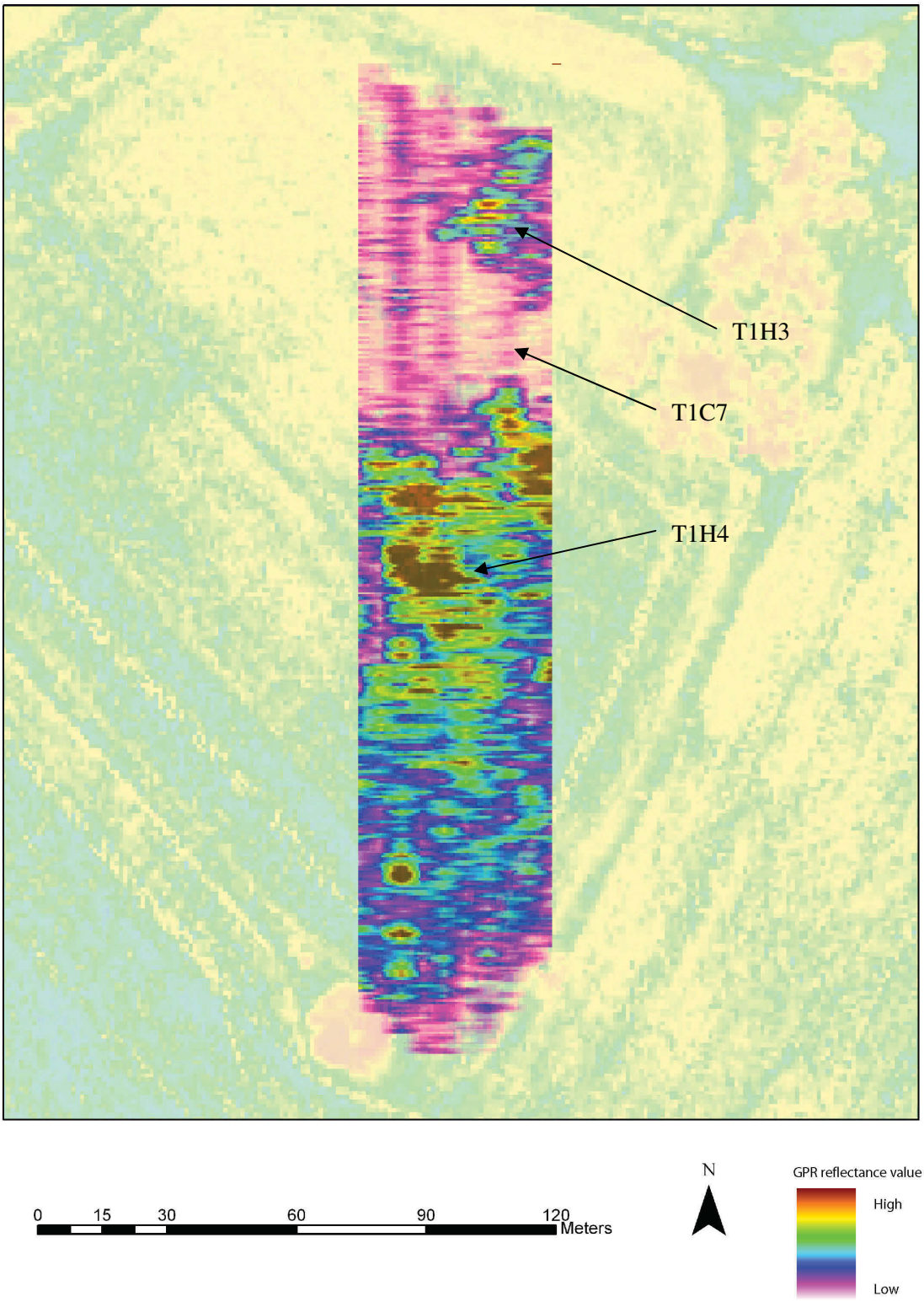

Fig 5.32: The T1G2 survey, at the 0.9m – 1.1m depth slice. At this depth slice a series of features are clearly visible being the terrace gravels T1H4, a palaeochannel T1C7 and another area of gravels T1H3.

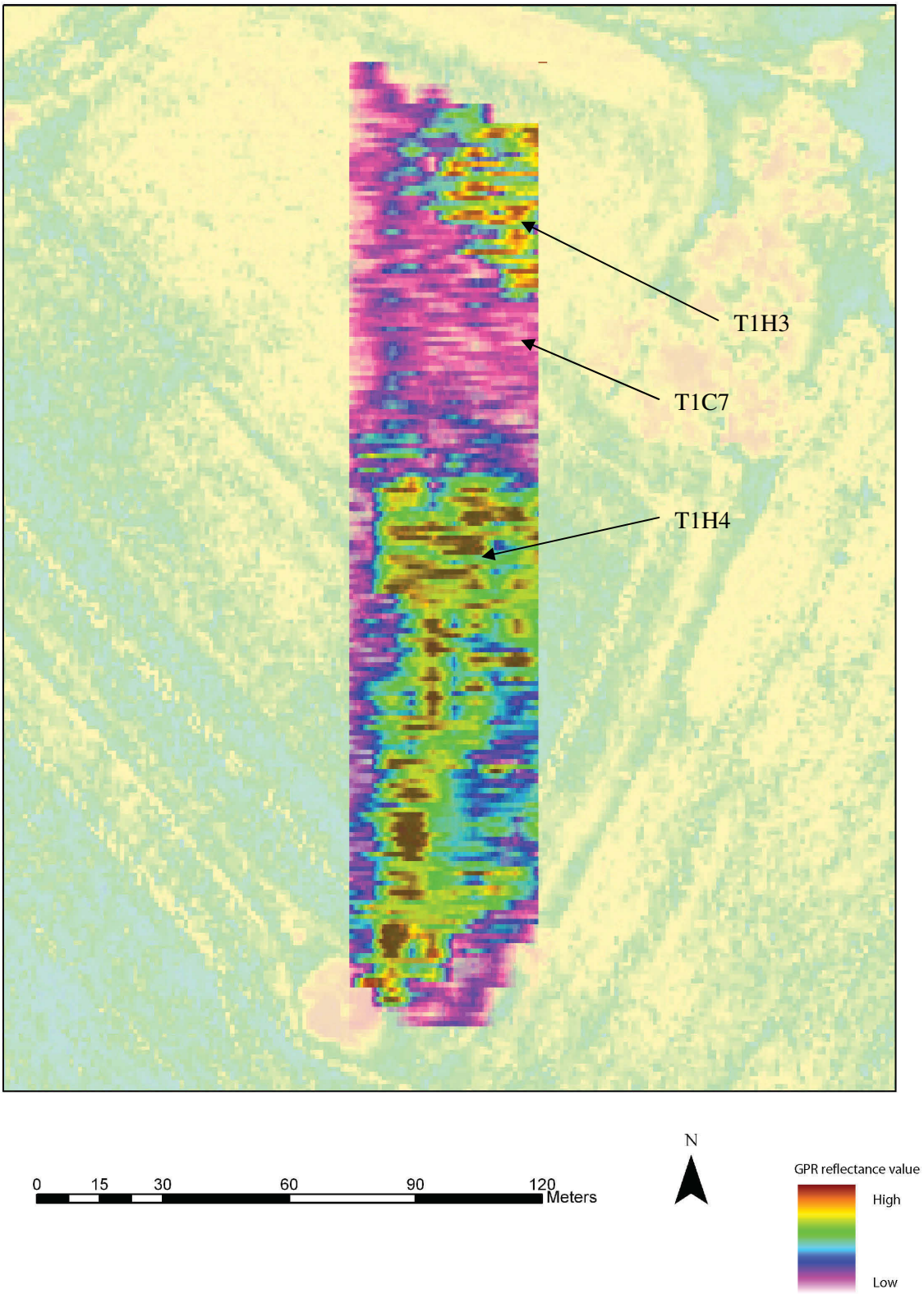

Fig 5.33: The T1G2 survey, 1.4m – 1.6m depth slice. The features T1H3, T1H4 and T1C7 are still evident.

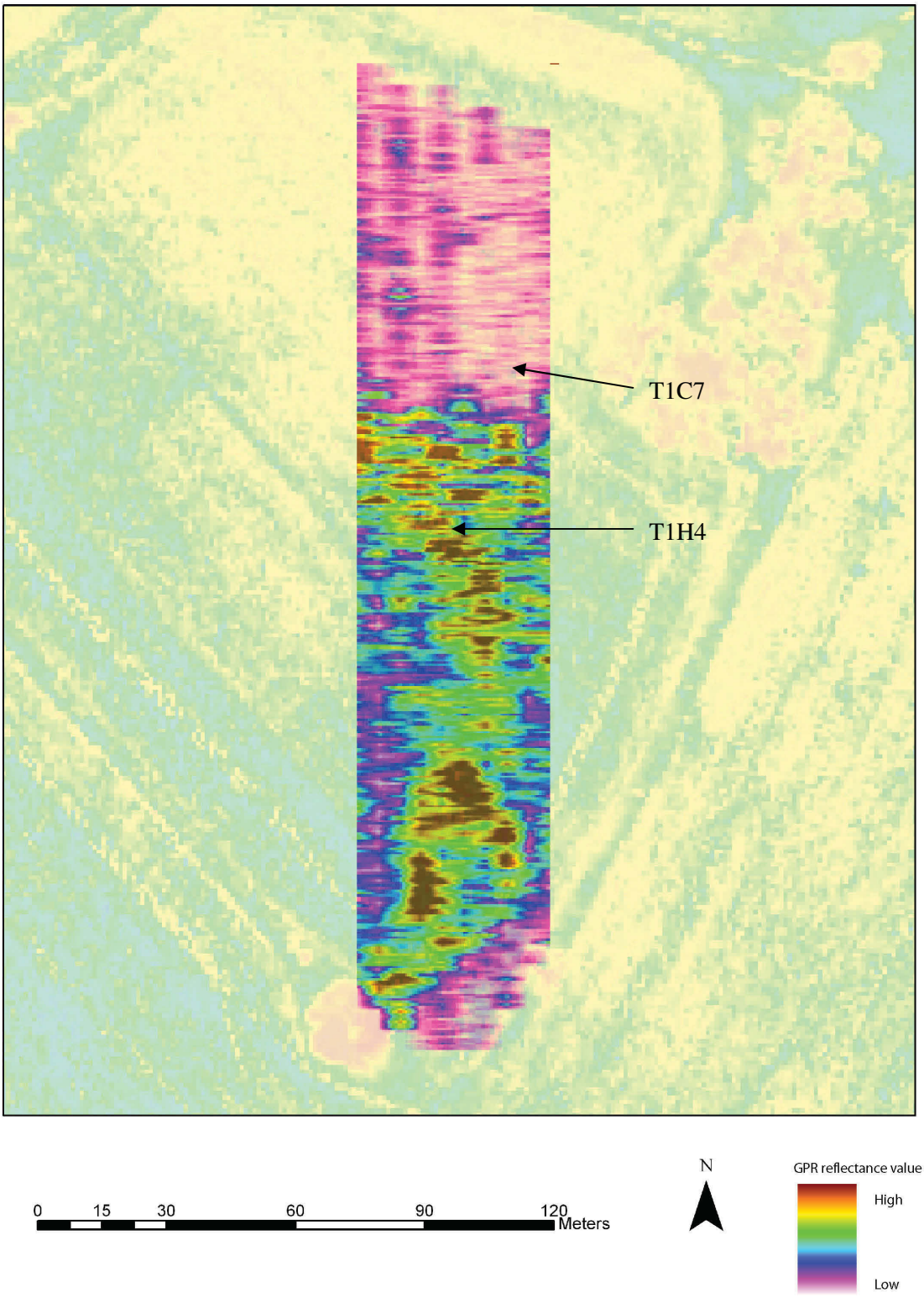

Fig 5.34: The T1G2 survey, 1.9m – 2.1m depth slice. The gravel unit T1H3 is not evident at this depth.

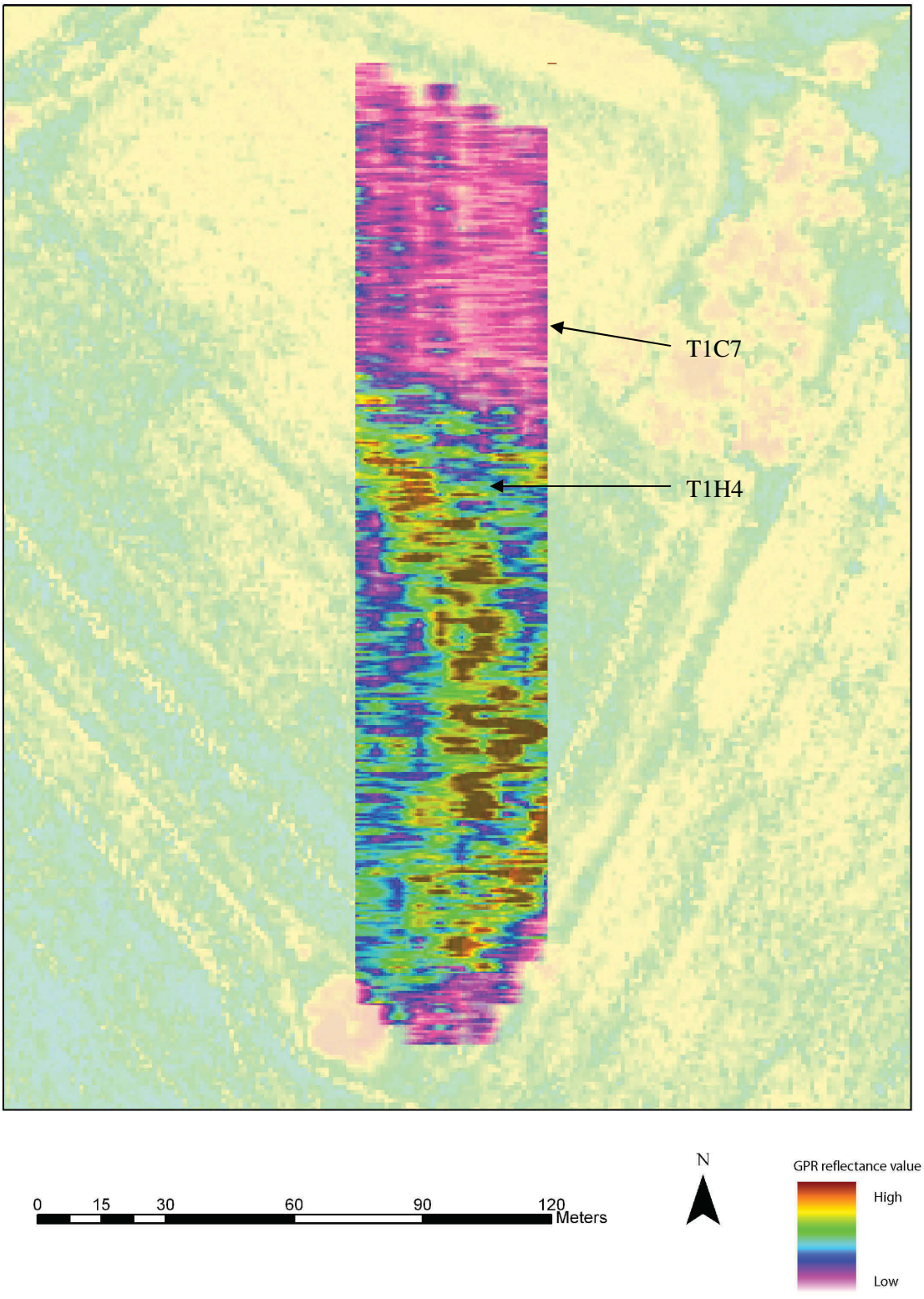

Fig 5.35: The T1G2 survey, 2.4m – 2.6m depth slice. The gravel unit T1H4 and the palaeochannel T1C7 are evident.

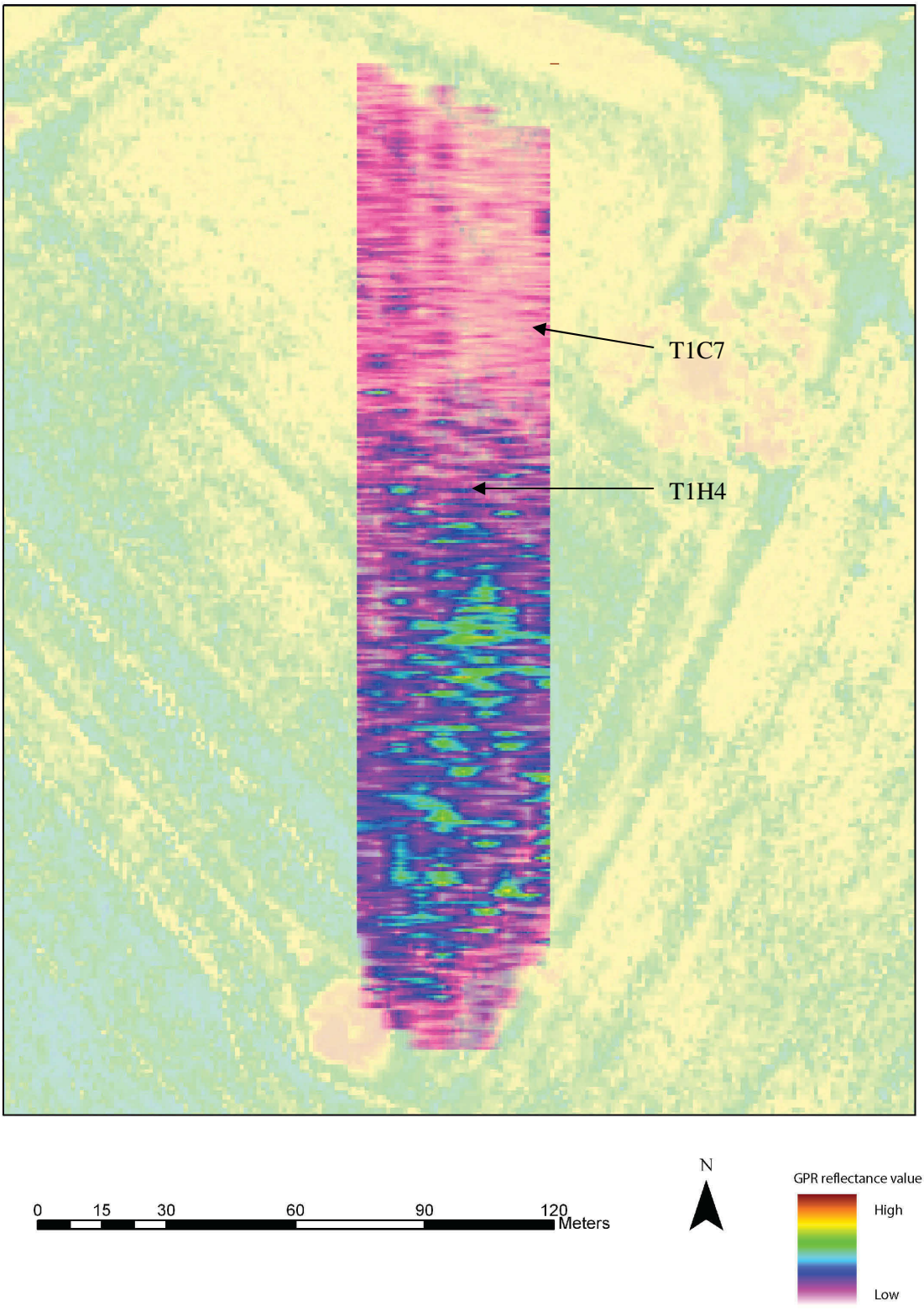

Fig 5.36: The T1G2 survey, 2.9m – 3.1m depth slice. Again the gravel unit T1H4 and the palaeochannel T1C7 are evident.

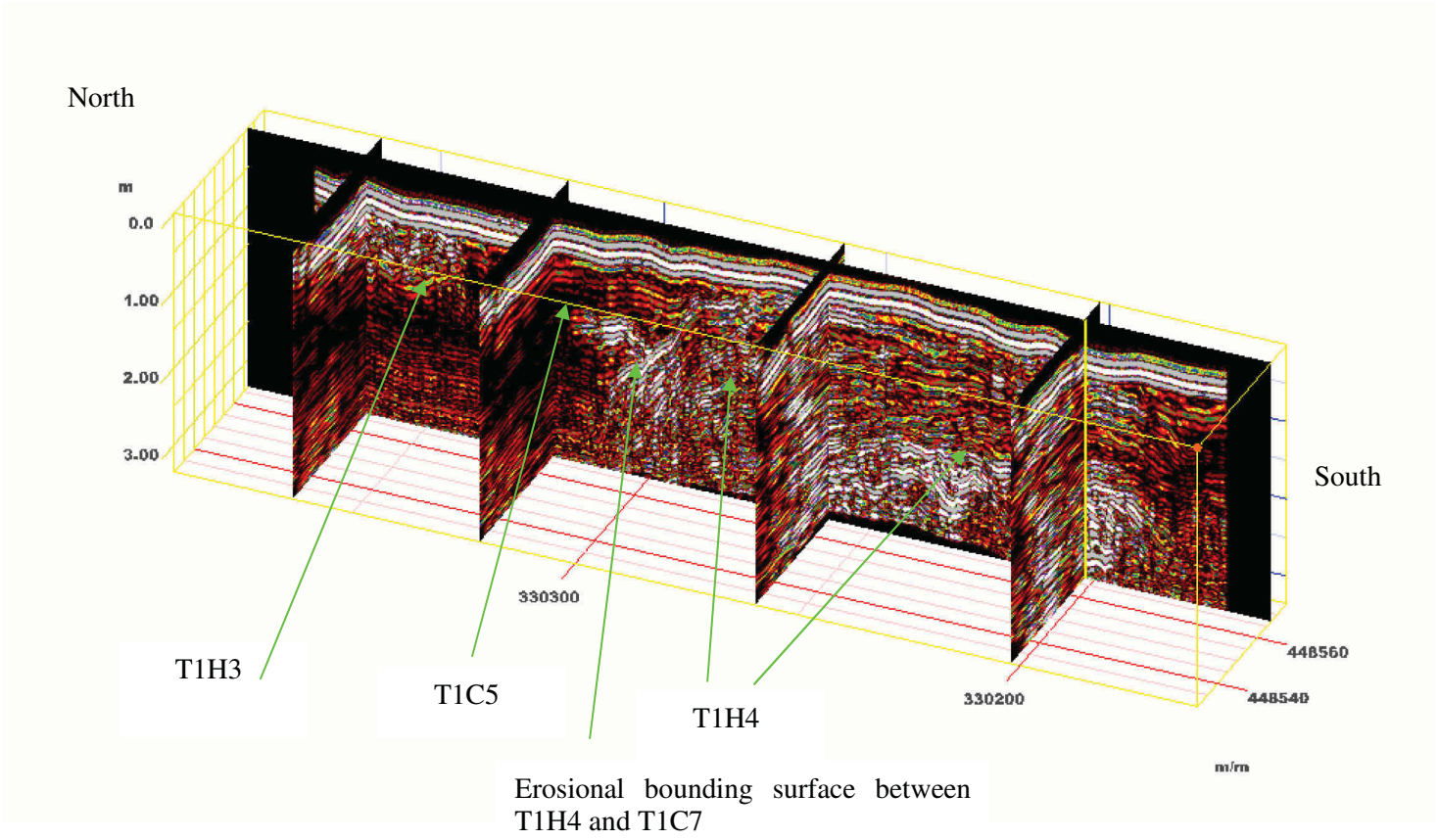

Fig 5.37: A pseudo 3D section produced through Radan, showing the relationships of T1H4, T1H3 and T1C7. There is a clear erosional bounding surface between T1H4 and T1C7. T1H3 appears to be a relatively shallow feature within T1C7.

5.2.5 T1 G3 survey

The T1G3 survey used a 5m transect spacing with a 200MHz antenna, collecting twenty transects of data. Data was processed through using a variable velocity migration. No comparative gouge core transect was undertaken within this survey area, so the calibration was made through the T1T1 transect, with the dielectric constant set at 19. The GPR reflectance values vary from –48 to +128. The LiDAR last pulse DTM clearly identifies terrace 1 that has been eroded into by the palaeochannel T1C8 (Fig. 5.38). The LiDAR intensity shows a change in intensity between the palaeochannel T1C6 and terrace 1 (Fig. 5.39).

The 0.4m – 0.6m depth slice clearly shows a difference in reflectance between the palaeochannel and the terrace that it has incised into (Fig. 5.40). At this time slice the palaeochannel shows up as an area of lower reflectance and higher absorption when compared to the terrace. The high reflection values from T1H6 shows the gravels have been encountered, meaning the alluvium on top of the gravels on this area of terrace is thin at circa 50cm or less. The 0.9m – 1.1m depth slice shows the same pattern as the 0.5m depth slice, with T1C8 clearly differentiated from terrace 1 (Fig. 5.41). However, at this depth slice the pattern of reflectance is opposite to the 0.4m – 0.6m time slice. At the 0.9m – 1.1m depth T1C8 is still visible as an area of high reflectance/low absorption, whilst the T1H6 unit is visible as an area of lower reflectance and high absorption. The change in reflectance properties of the sediments at this depth is interpreted as being a product of the water table in the palaeochannel. The water table has been encountered, effectively stopping deeper penetration and causing a high level of reflectance, relative to terrace 1. The terrace gravels do show some higher area of reflectance, interpreted as gravel.

The 1.4m – 1.6m time slice shows some differentiation between T1H6 and T1C8. Effective penetration into the T1C8 is not seen at this depth and general noise is encountered within the palaeochannel (Fig. 5.42). At this depth another feature is evident within the T1H6 gravel unit, labelled T1H6a. This is interpreted as either a section of palaeochannel within the terrace or an area of different sediments within the gravels, e.g. a sand bar. This is the maximum depth of penetration, with the gravel/bedrock boundary not being encountered. The GPR interpretation agrees with the LiDAR interpretation that channel T1C8 is later than the gravel unit T1H6, having partially eroded into it.

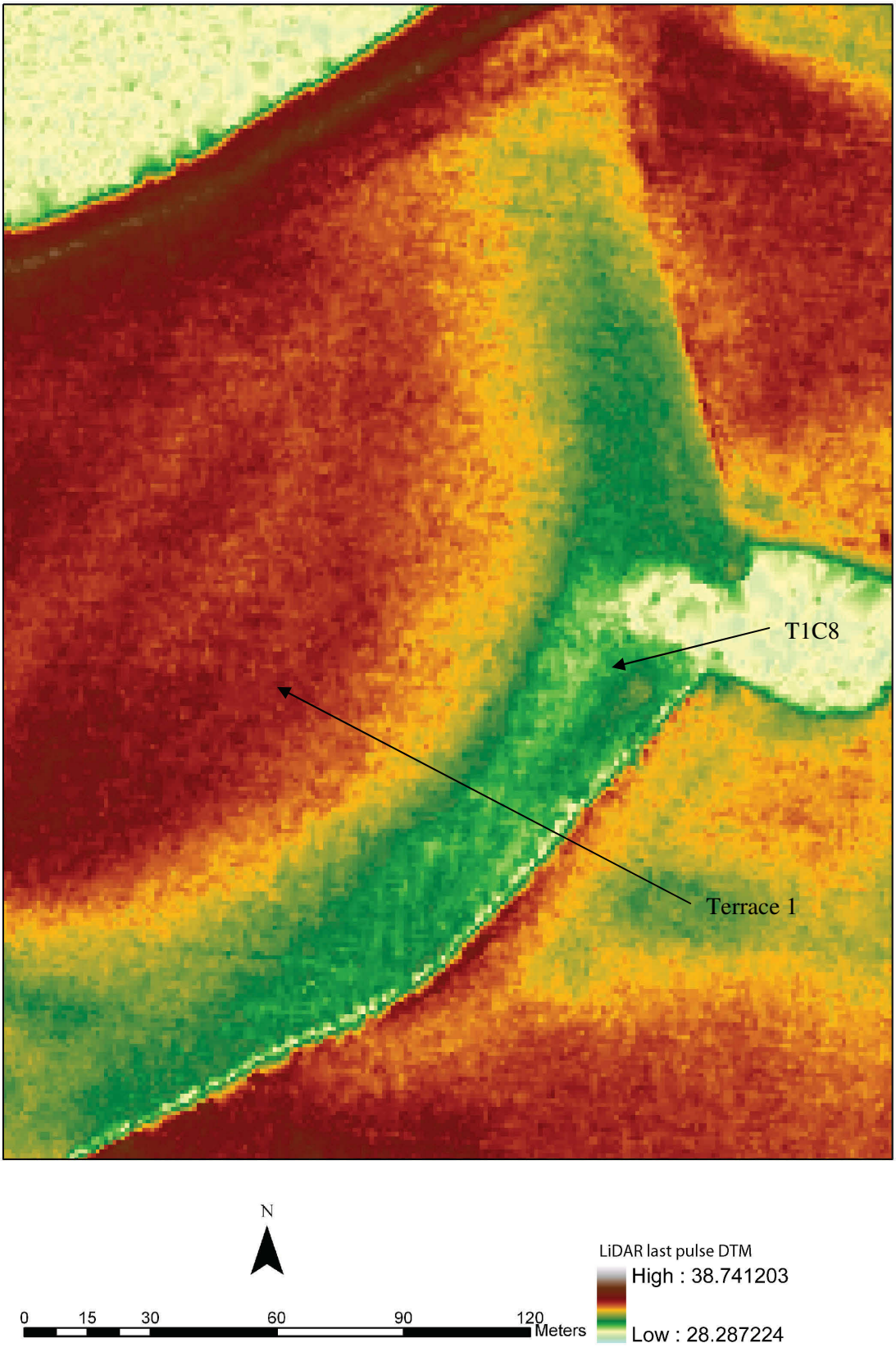

Fig 5.38: The LiDAR last pulse DTM over the T1G3 survey area. Palaeochannel T1C8 and terrace 1 are the dominant features.

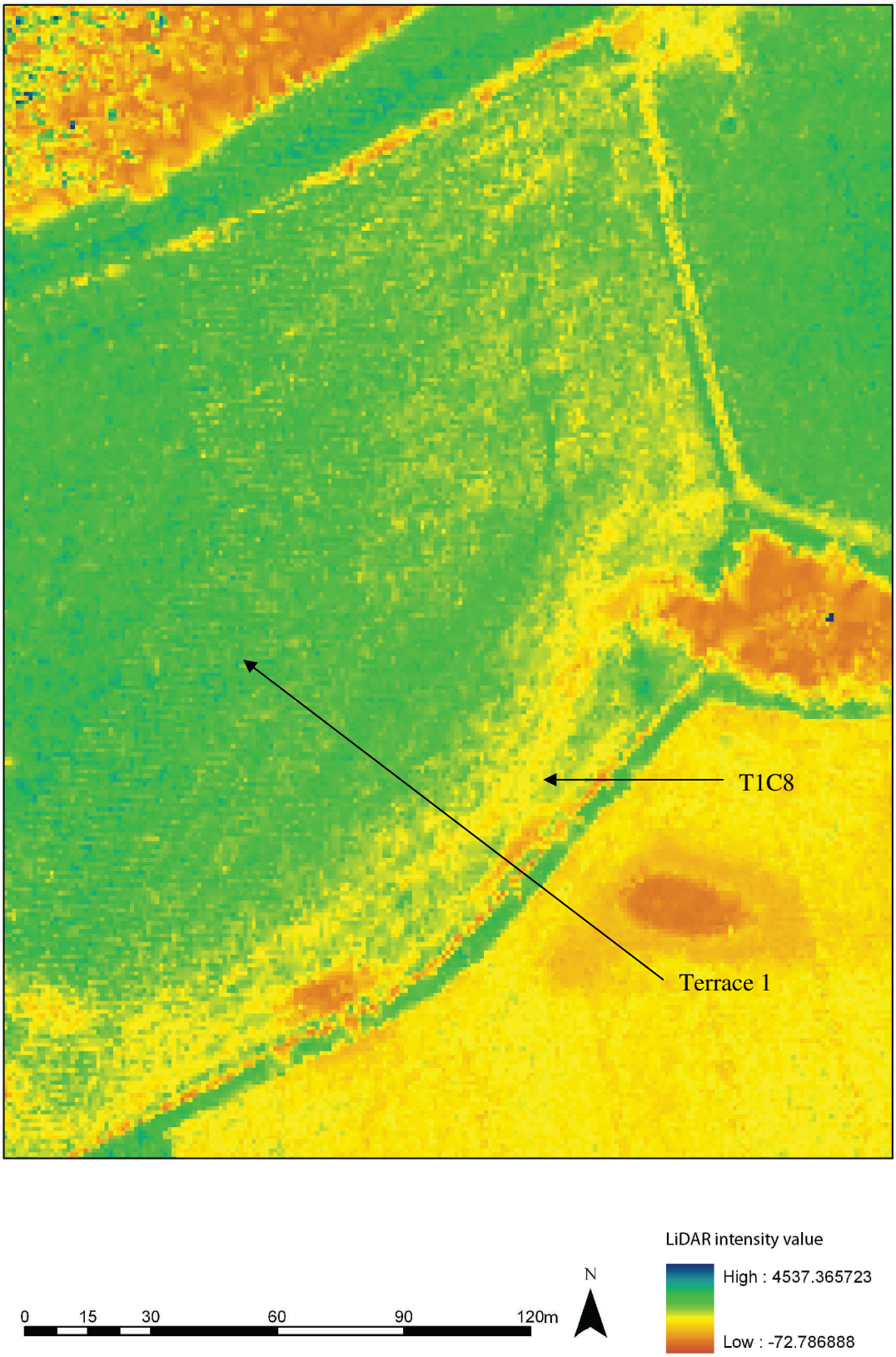

Fig 5.39: The LiDAR intensity plot over the T1G3 survey area. T1C8 and terrace 1 are again visible, although not as obvious as through the DTM.

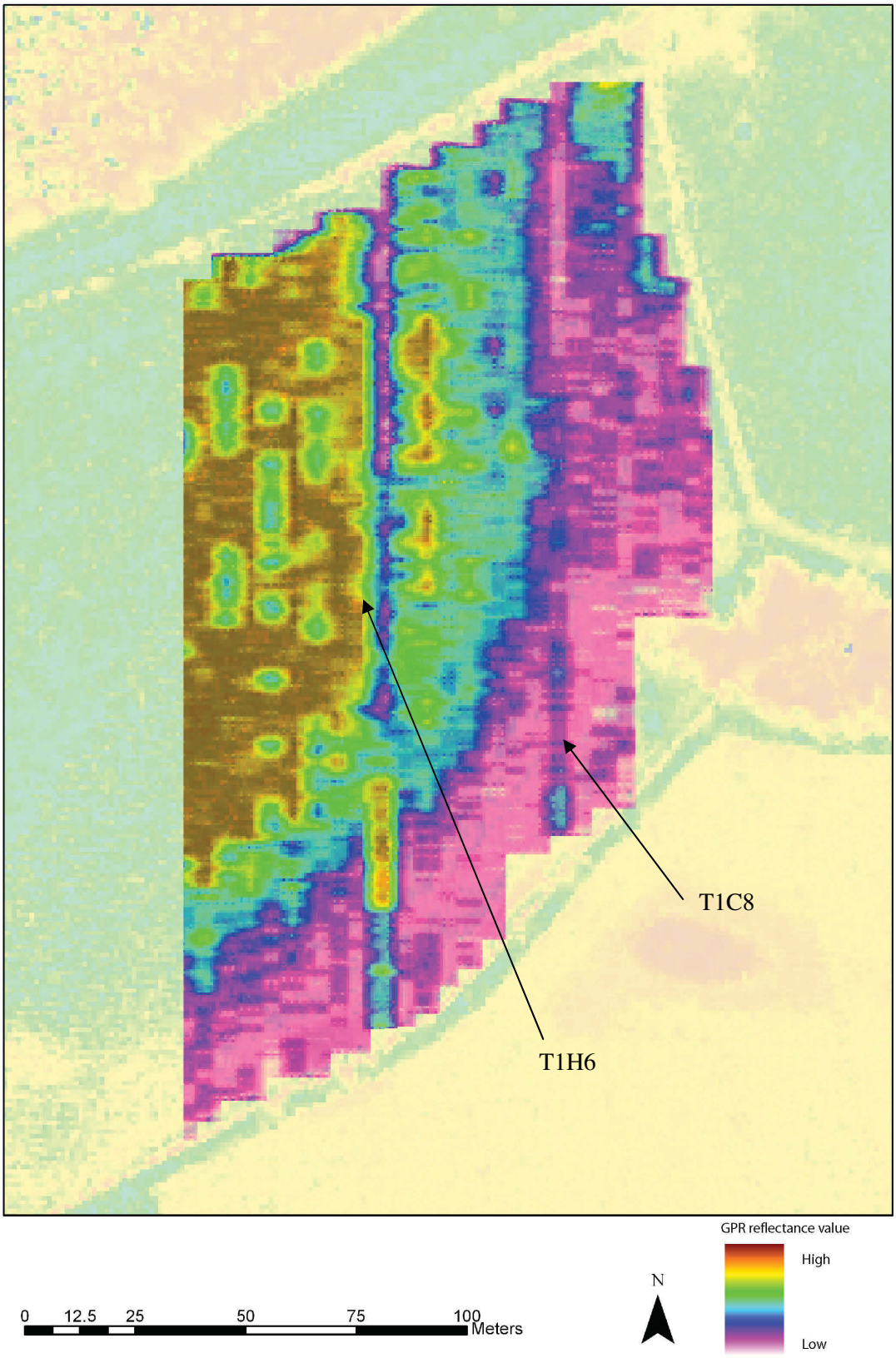

Fig 5.40: The T1G3 survey, 0.4m – 0.6m depth slice. The palaeochannel T1C8 is visible as an area of low reflectance whilst the gravel unit T1H6 is visible on terrace 1.

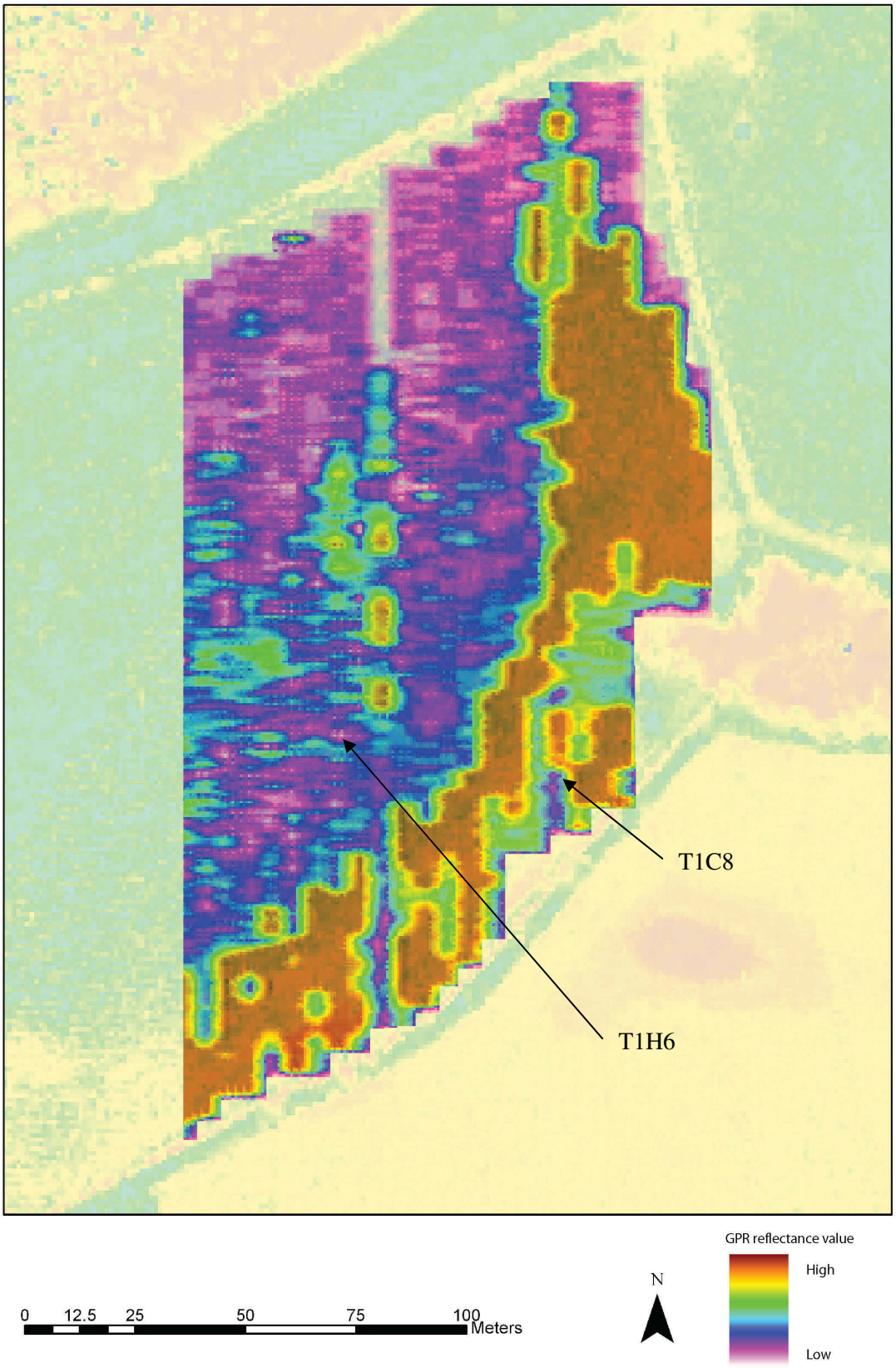

Fig 5.41: The T1G3 survey 0.9m – 1.1m depth slice. At this depth the palaeochannel channel is showing high reflectance values and could be related to its high water table.

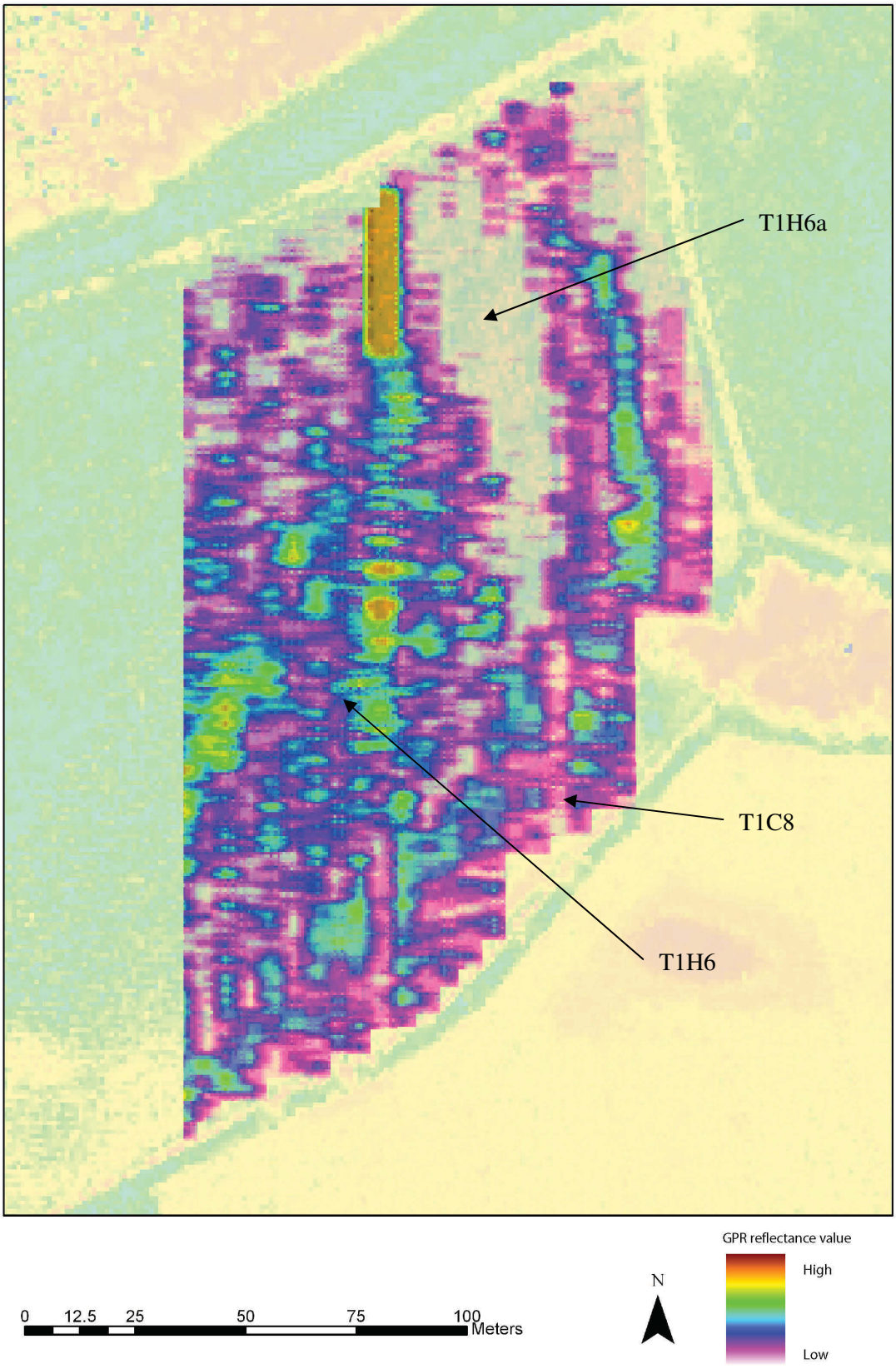

Fig 5.42: The T1G3 survey, 1.4m – 1.6m depth slice. The limit of penetration is being reached, with the palaeochannel just discernable from the gravel unit T1C6.

5.2.6 Summary of the GPR surveys on the middle unit

Three transect surveys and three grid surveys were undertaken on terrace 1. Terrace 1 defines the relationship between the Devensian terrace 2 and the modern floodplain. Terrace 1 is interesting due to the relationship of areas of the terrace 1 with palaeochannels that have undergone avolsion events. The GPR surveys have revealed much information on the stratigraphic organisation of terrace 1 and associated palaeochannels. The key points of the terrace 1 GPR surveys can be summarised as:

Terrace 1 transect 1:

- There was a good correlation between the GPR and gouge core transect.
- The alluvium overlying the terrace 1 gravels is quite shallow at circa 40cm – 50cm, although variation in depth is evident.
- Four definite and one other possible palaeochannel were identified along the transect.
- The terrace 1 gravels have a heterogeneous structure, with a number of sub units being identifiable.
- The gravel sub units maybe the difference between earlier Pleistocene and later Holocene gravels.
- Alternatively all the gravels in the transect may have been produced in the Holocene, the difference in units merely relating to differences in the depositional environment.
- Channel T1C5 was a deep channel with a clay fill ascertained through the gouge core transect, indicating a high palaeoenvironmental and geoarchaeological potential.
- GPR penetration into T1C5 was shallow.
- T1C5 has deposited alluvium onto areas of terrace 1, potentially burying archaeology.

Terrace 1 quarry transect

- A considerable depth of alluvium was seen on the terrace 1 gravels, between 1.5m and 2.5m.
- A series of clay layers lay above the terrace gravels, stopping GPR penetration into the gravels.
- Some of these clay layers produced a high GPR reflection response.
- Correlation between the GPR interpretation and the recorded section was generally good, although some variation was seen between the contact of the alluvium with the gravels.
- Organic deposits were evident in the quarry, most notably three large oak trees.
- Inspection of the gravels within the quarry did not reveal any evidence for bipartite grave units, suggesting that this area of terrace 1 contains only Holocene gravel deposits.

Terrace 1 transect 2 and terrace 1 grid 1:

- The relationship between the gouge core and GPR data was good.
- The 0m – 0.2m depth slice shows that the near field zone has a similar reflectance pattern to the LiDAR intensity data, which is interpreted as a function of water content, between the terrace and channel.
- The terrace gravels start to protrude at the 1.4m – 1.6m time slice and are visible at the 1.9m – 2.1m time slice.
- The level of alluvium on terrace 1 was deep, reaching a depth of 1.4m to sand.

- Some areas of the palaeochannel T1C6 have very high reflectance levels, which may relate to gravel deposits within the channel.
- The definition of the palaeochannel T1C6 was poor due to the fill of the channel being a silty clay that reduced GPR penetration.

Terrace 1 grid 2:

- The LiDAR last pulse DTM revealed no significant topographic variation in the survey area.
- The LiDAR intensity plot clearly identified a difference in sedimentary units in the survey area, interpreted as a product of different soil moisture contents.
- A palaeochannel containing a gravel bar that had cut into terrace has been interpreted from the GPR data.
- The alluvium covering the terrace 1 gravels was relatively shallow, clearly visible by the 0.9m – 1.1m depth slice. An interpreted alluvium depth of 0.6m is suggested.
- The GPR penetration into the palaeochannel was shallow, suggesting a high water content and/or high clay content.
- Due to the interpreted conditions within the palaeochannel T1C7 channel it is suggested the channel is cored for palaeoenvironmental samples.

Terrace 1 grid 3:

- The survey identified a palaeochannel that had eroded into a section of terrace 1.
- The gravels identified on terrace 1 were heterogeneous in their structure.
- The alluvium on this area of terrace 1 gravels was shallow at 0.5m or less.
- Penetration into the palaeochannel T1C8 was shallow suggesting a waterlogged/clay filled channel.
- It is suggested that the palaeochannel is cored for palaoenvironmental samples.

The terrace 1 unit can be seen to be heterogeneous in its composition, a product of the dynamic confluence environment. Several areas of terrace 1 have high levels of alluvium overlying gravels, demonstrated by the T1G1 survey and the T1QT survey. Other areas have relatively shallow alluvium overlying the terrace 1 gravels such as on the T1T1 survey. It is clear that some of the palaeochannels that have eroded into terrace 1 have also deposited significant quantities of alluvium onto the terrace, potentially burying archaeological sites, such as the enclosure identified on the T1T1 survey. Understanding the heterogeneous composition of terrace 1 is important in developing the chronostratigraphic model and for identifying areas of archaeological potential within the survey area.

5.3 The GPR surveys on terrace 2

The GPR investigations on terrace 2 consisted of one transect survey and one grid survey.

5.3.1 Terrace 2 transect 1 (T2T1)

The T2T1 transect ran for 335m from east to west (Fig. 5.43), using a 200MHz antenna. Data processing used a variable migration model. A gouge core transect ran along the GPR transect, sampling at a 10m interval. The LiDAR last pulse DTM does not identify any significant topographic variation within the survey area. Aerial photography of terrace 2 reveals a wealth of archaeological monuments and also a section palaeochannel, T2C1 (Fig. 5.44). Calibration of the GPR transect was made through using data from the gouge core transect and the dielectric constant was set at 24.

The T2T1 transect interpretation classifies the alluvium overlying the terrace 2 gravels (Fig. 5.45). The gravels of terrace 2 are apparent as a strongly reflecting unit (T2B1). Some limited variation is seen in the gravel structure and three sub units are labelled as T2D1, T2D2, T1D3 and T1D4. The transect does not identify any palaeochannels such as T2C1, identified through aerial photography. The transect does show topographic variation between 175m – 230m and this may relate to an older palaeochannel. The deposits identified as unit 3 on the gouge core transect may represent the base of a palaeochannel fill but they are shallow and are considered to have a low palaeoenvironmental potential. The contact with the bedrock is seen at circa 4m below ground surface. Overall the GPR interpretation and the gouge core data provide a good correlation. The level of alluvium overlying the gravels deposits on terrace 2 is shallow, generally between 30cm – 40cm.

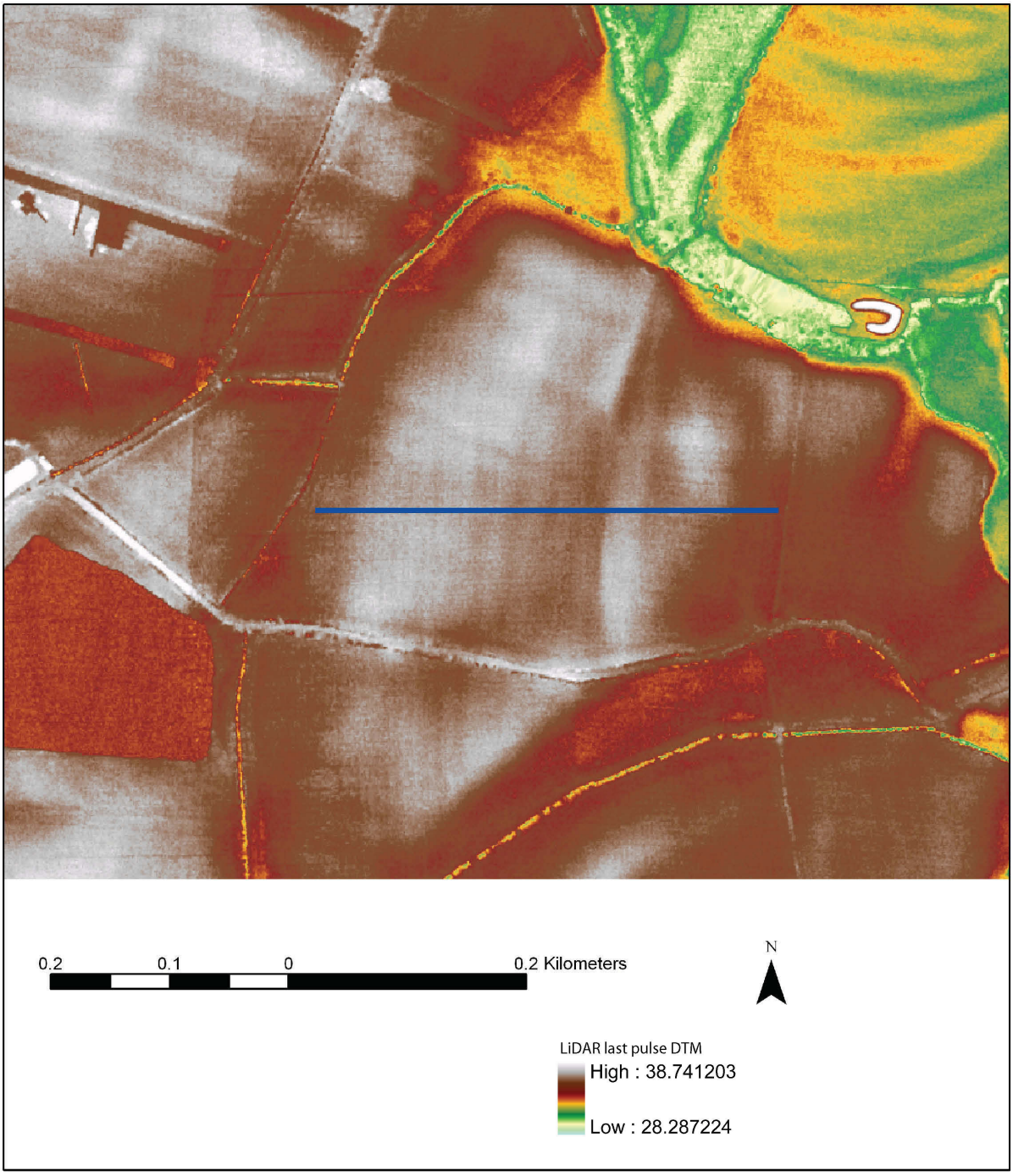

Fig **5.43:** The location of the T2T1 transect, shown on the LiDAR last pulse DTM. There is no major topographic variation seen in the survey area.

Fig 5.44: A rectified aerial photograph of the T2T1 survey area, showing a possible palaeochannel, T2C1.

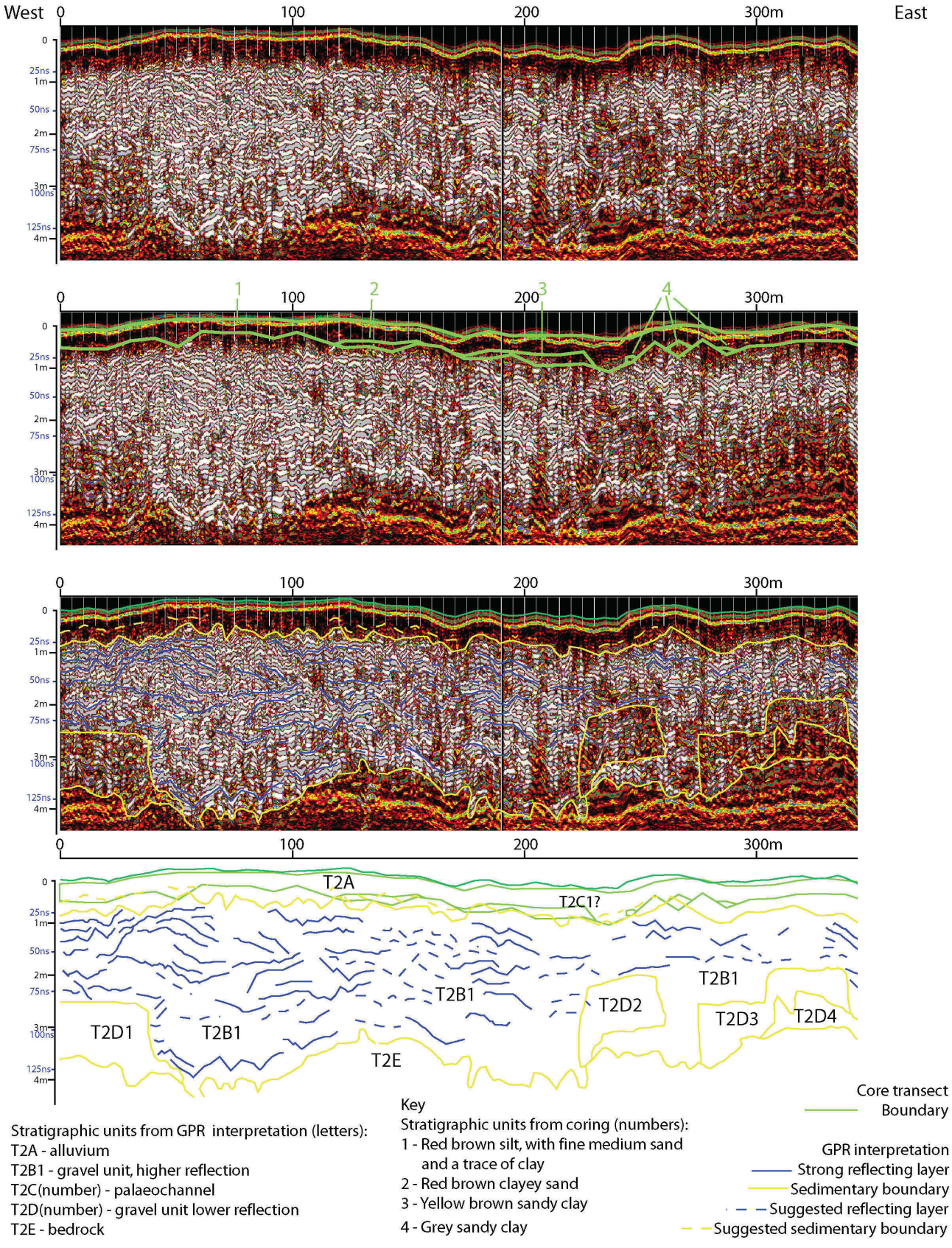

Fig 5.45: The T2T1 GPR transect shown with interpretation and against the gouge core transect.

5.3.2 Terrace 2 grid 1 survey (T2G1)

This survey utilised a 200MHz antenna collecting twenty transects of data using a 5m transect interval. No coring work was undertaken within this field but the same dielectric constant is applied from the T2T1 calibration in the adjacent field. The GPR reflectance values ranged from –112 to +128. The data was processed through a variable velocity migration. The T2T1 survey is depth sliced at 0.5m intervals using a 0.2m depth slice, shown with the LiDAR intensity at 70% transparency. The LiDAR last pulse DTM identifies this area as terrace 2 but reveals little topographic variation within the field (Fig. 5.46). The LiDAR intensity values depict some subtle variation between the northern and southern end of the survey area (Fig. 5.47).

The time slicing of the GPR survey adds further evidence to the interpretation of the LiDAR intensity results. The 0.4m – 0.6m time slice gives a high reflectance value across most of the survey area being at the edge of the gravel alluvium interface (Fig. 5.48). The 0.9m – 1.1m time slice displays more marked variation within the survey area, with lower reflectance/higher absorbance values at the southern end of the survey (T2A1) and high reflectance lower absorbance values at the northern end (T2A2) (Fig. 5.49). This pattern is repeated in the 1.4m – 1.6m time slice and the 1.9m – 2.1m time slice (Figs. 5.50 and 5.51). The 2.4m – 2.6m and 2.9m – 3.1m time slices reveal less variation and generally show the higher reflecting gravels (Figs. 5.52 and 5.53). Penetration is not achieved below the 2.9m - 3.1m depth slice and the gravel/bedrock contact is not seen.

From the depth of 0.9m - 2.1m variation is seen in the structure of the gravels. The reason for the variation in the gravel structure is not clear but it potentially relates to the structure of the gravel affecting the moisture content. Alternatively, T2A1 could possibly be relating to a palaeochannel on terrace 2, although this is speculative. Such an example highlights the importance of using integrated remote and ground based sensing methods for investigation of sedimentary units.

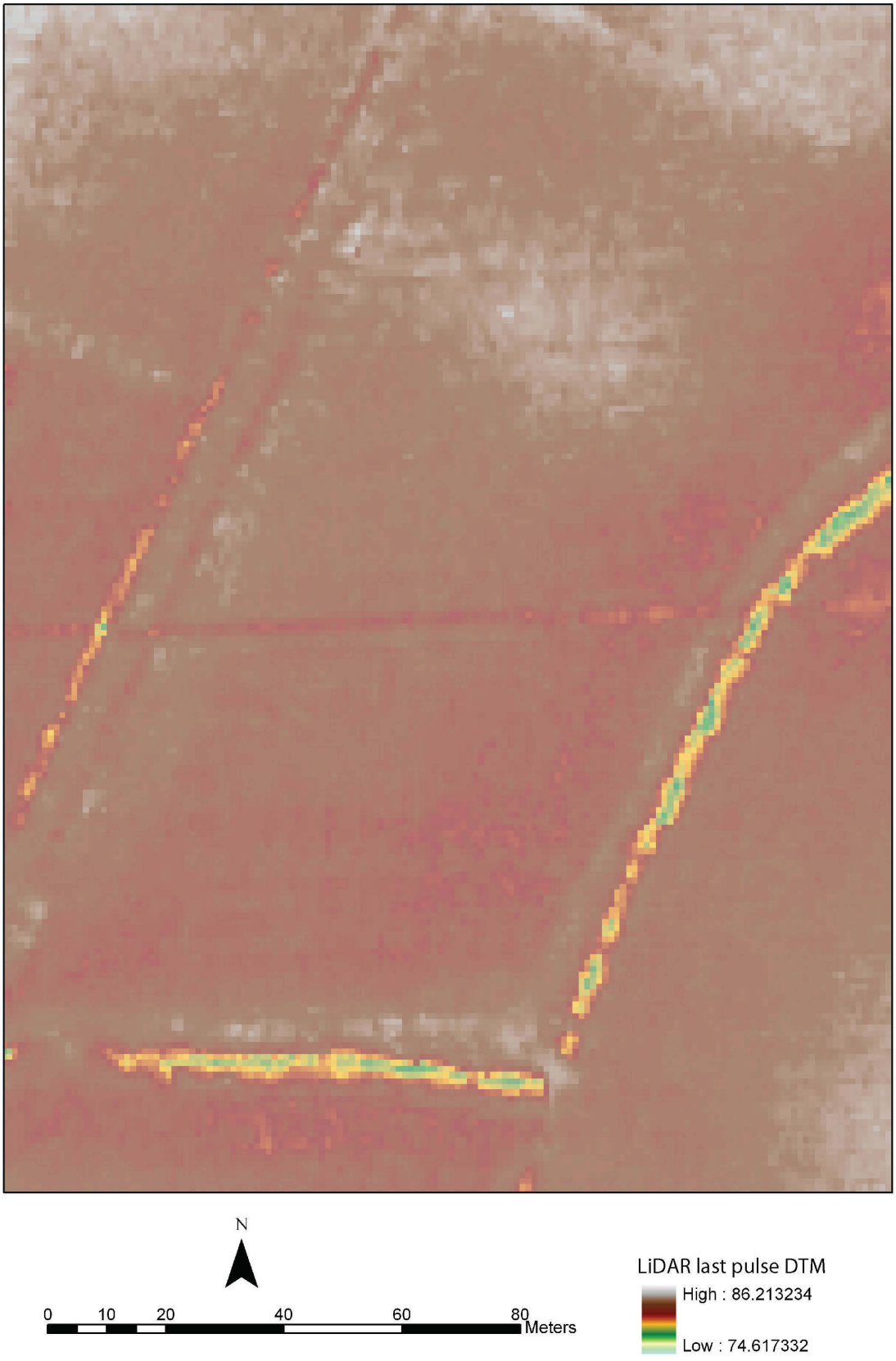

Fig 5.46: LiDAR last pulse DTM over the T2G1 survey area. No significant topographic variation is seen.

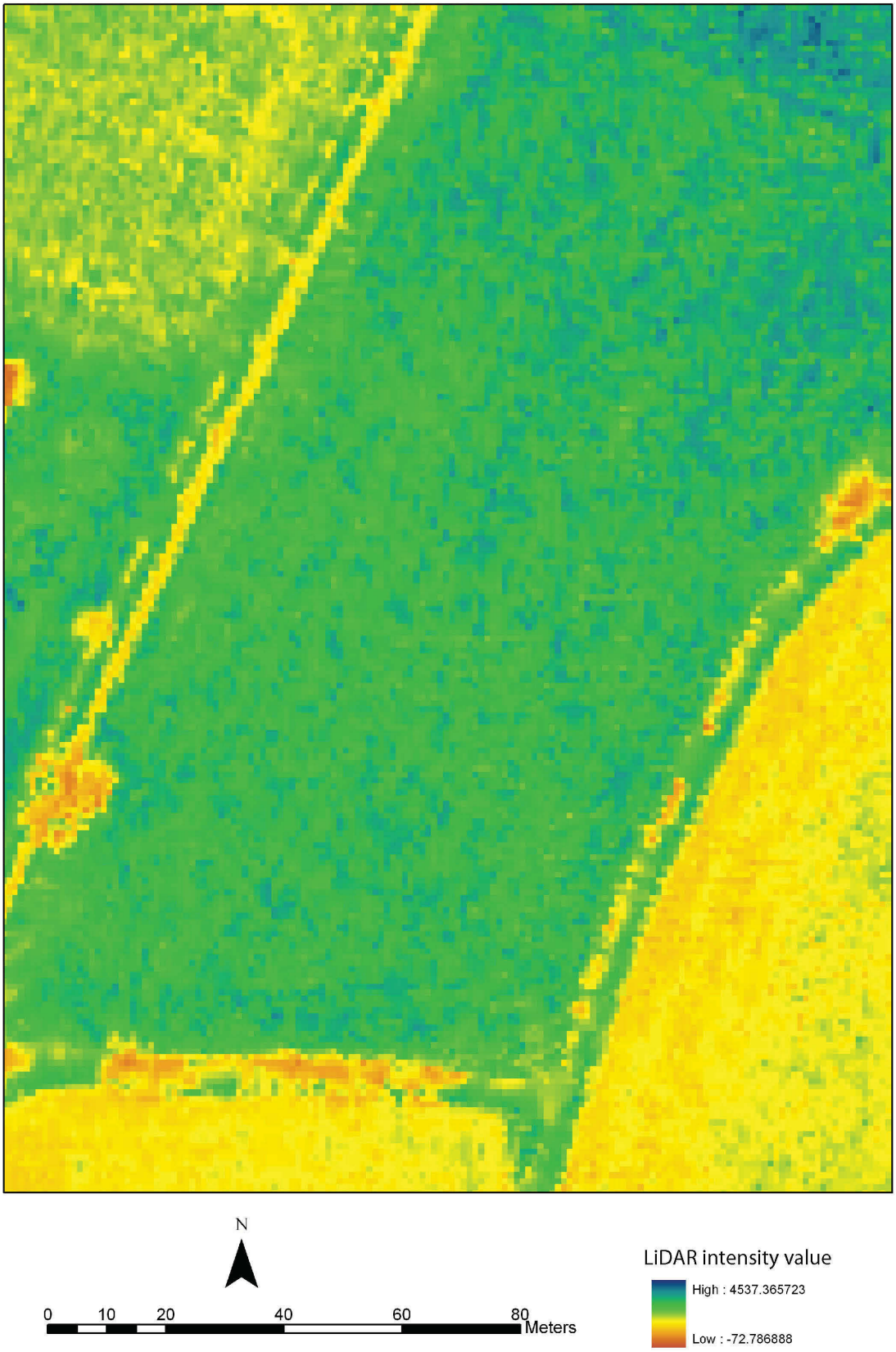

Fig 5.47: The LiDAR intensity values across the T2G1 survey area. Some subtle variation is discernable between the north and south of the survey area.

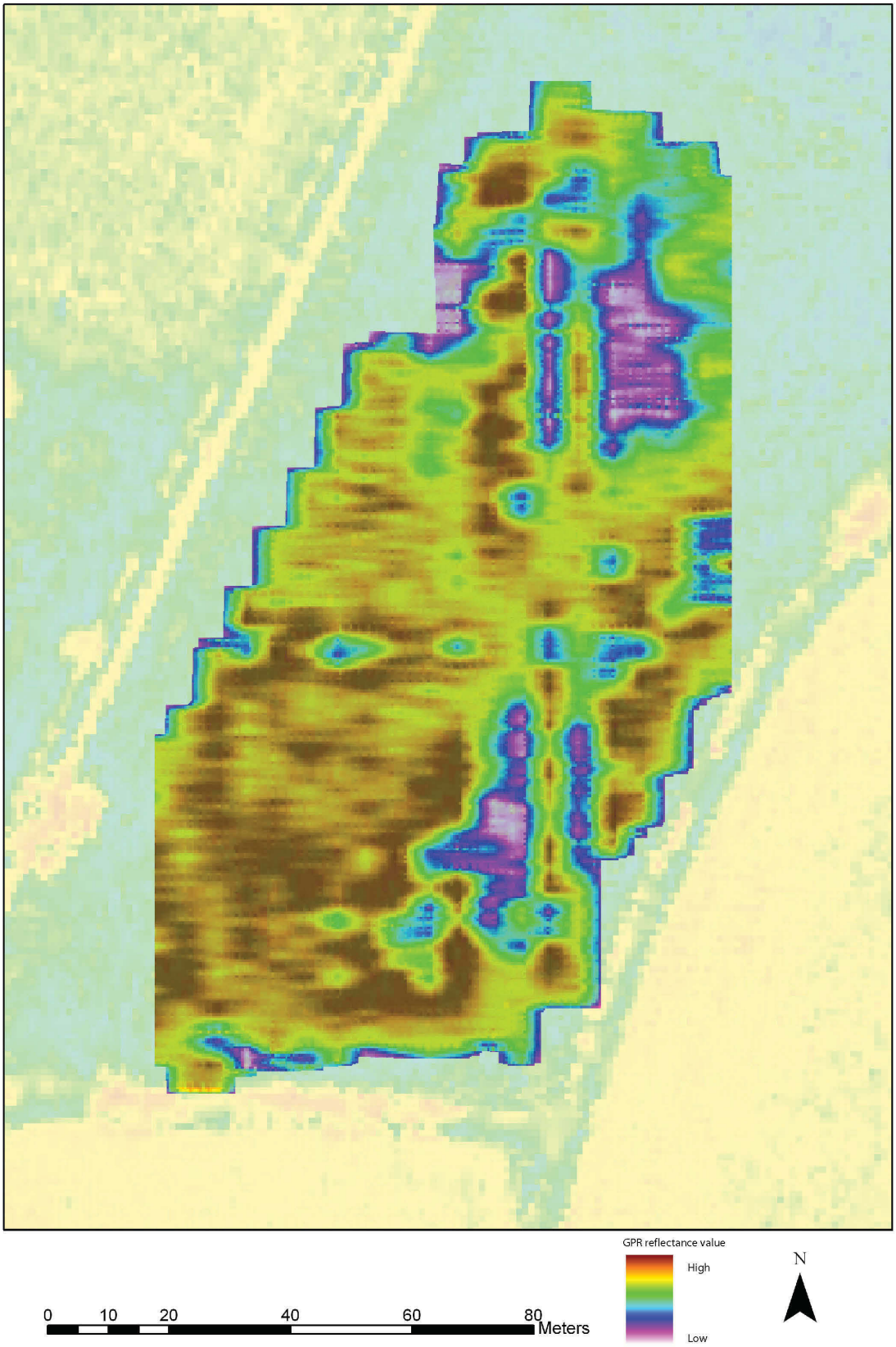

Fig 5.48: The T2G1 survey, 0.4m – 0.6m depth slice. A general area of high reflectance is seen across the survey area.

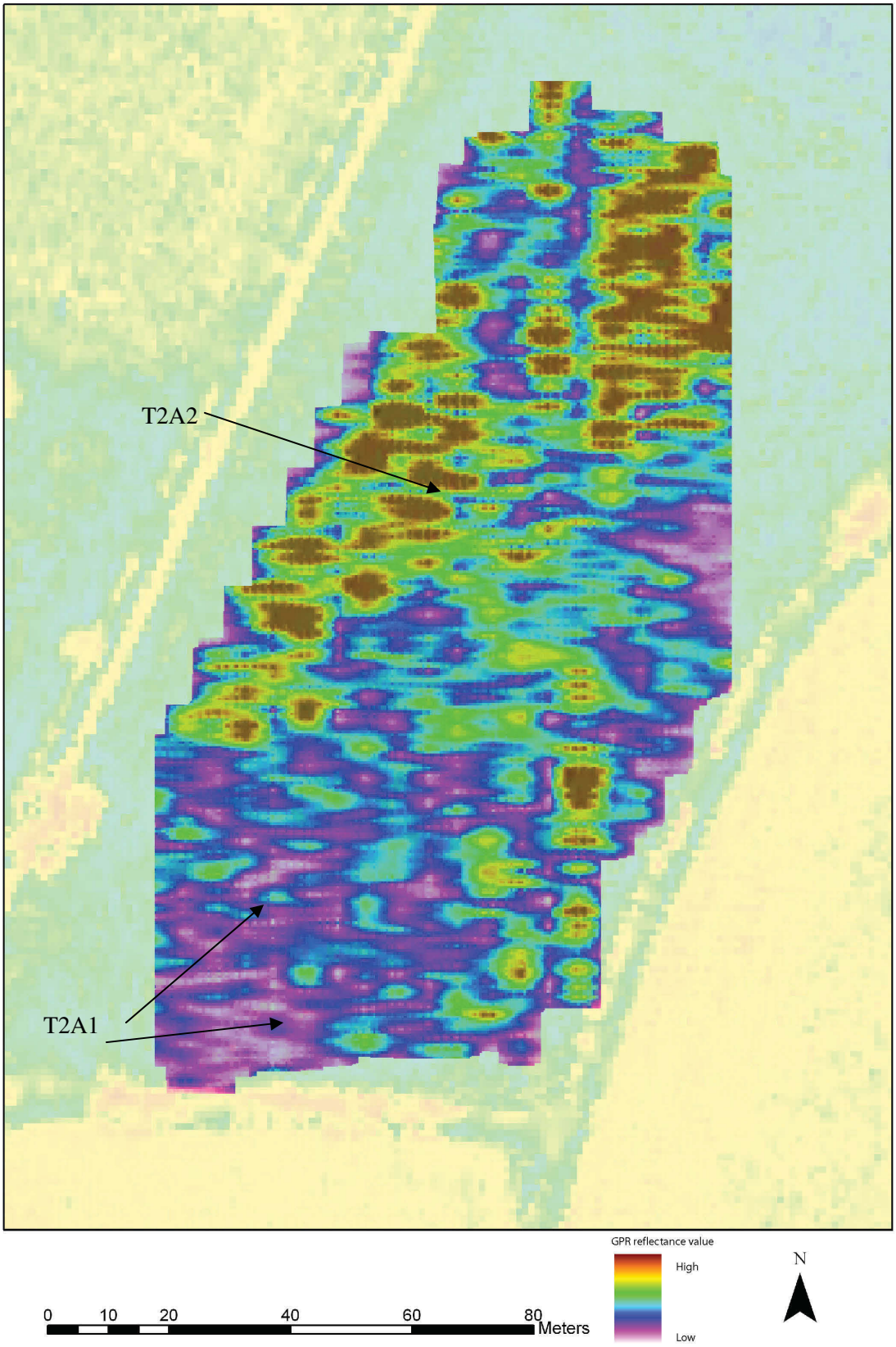

Fig 5.49: The T2G1 survey, 0.9m to 1.1m depth slice. Some variation is evident in the structure of the gravel deposits. Two distinct areas are visible, being T2A1 and T2A2.

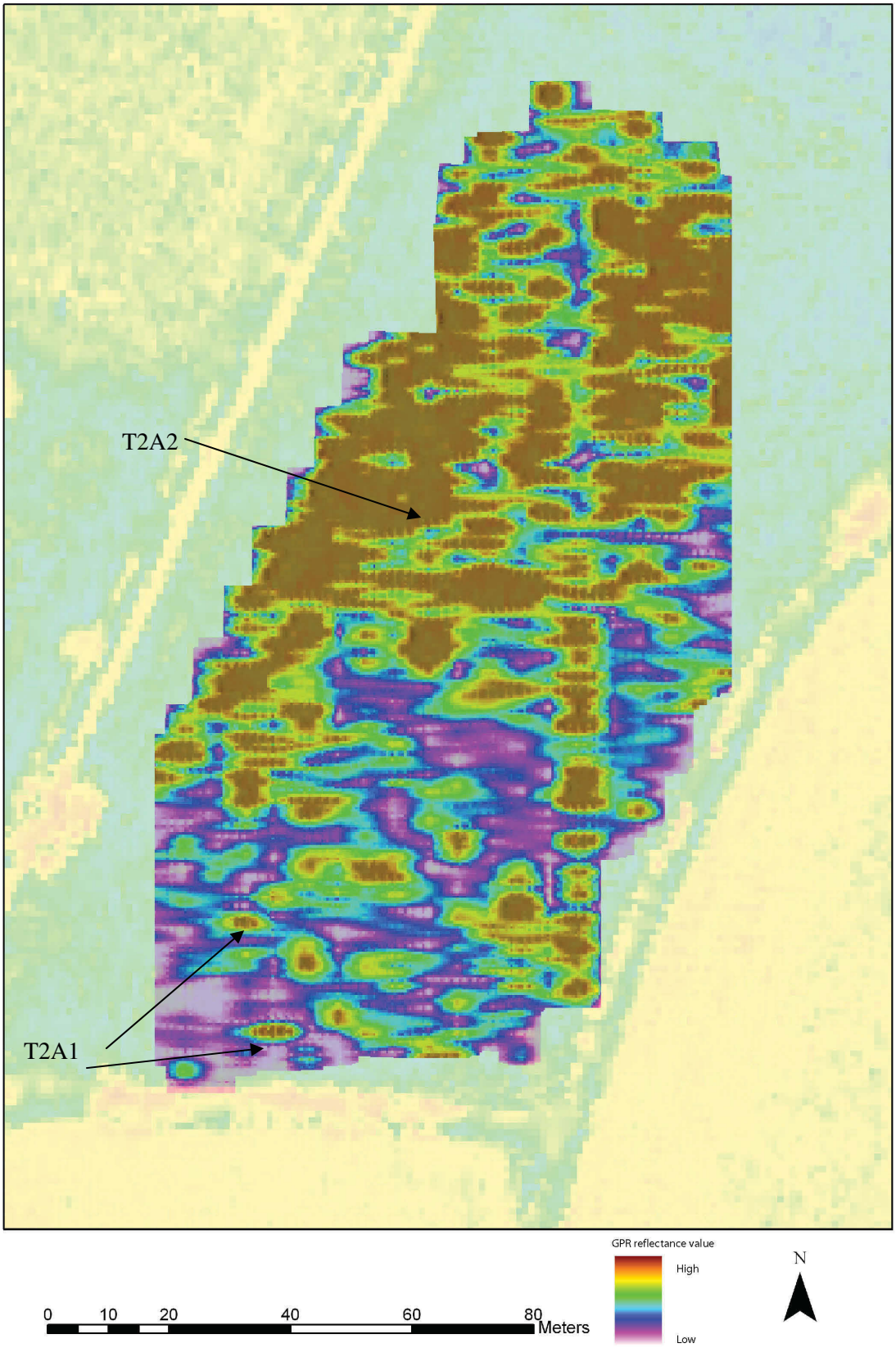

Fig 5.50: The T2G1 survey, 1.4m – 1.6m depth slice. Variation is still evident between T2A1 and T2A2.

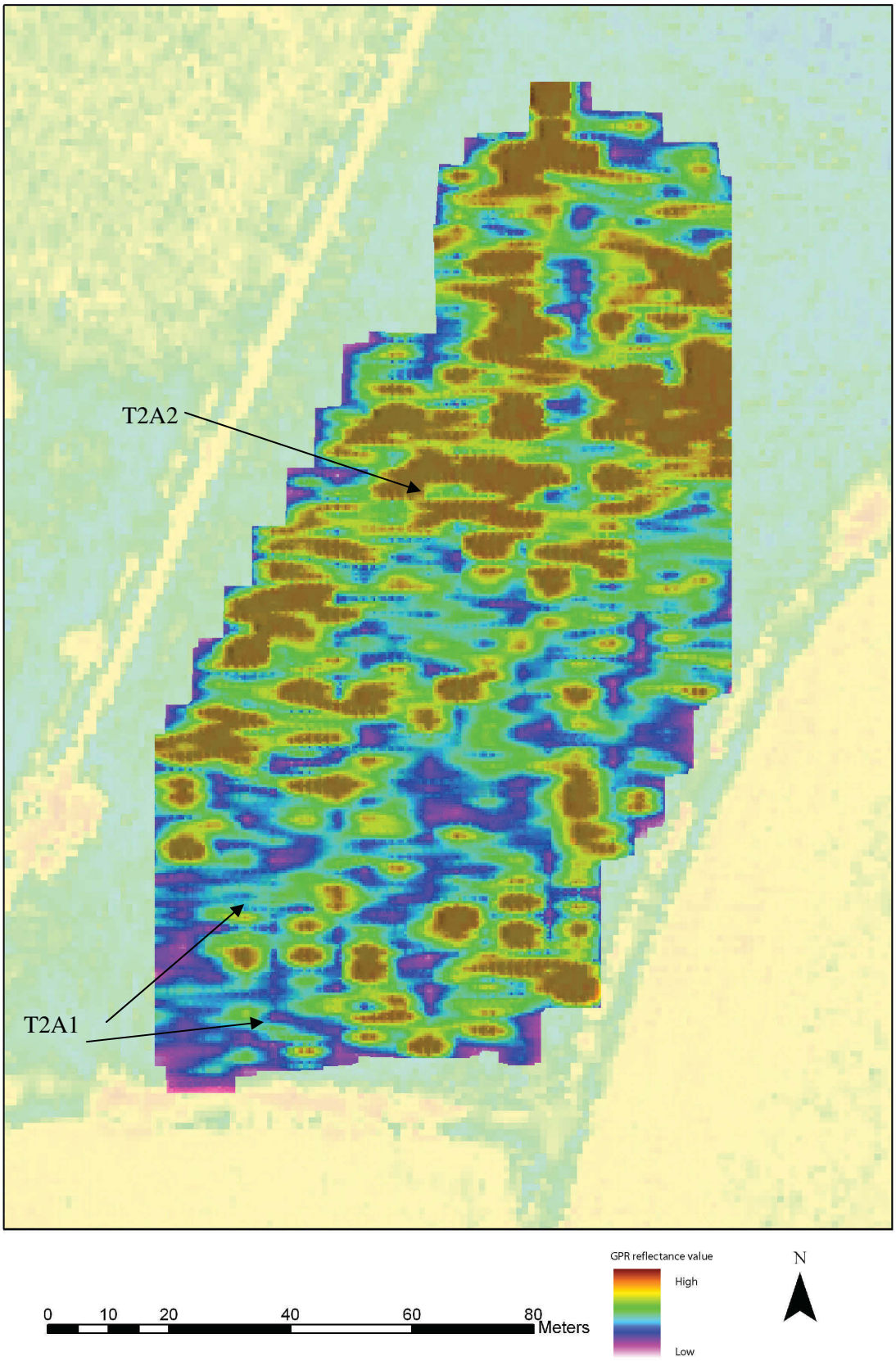

Fig 5.51: The T2G1 survey, 1.9m – 2.1m depth slice. There is still some variation in the gravel deposits, with T1A1 and T1A2 visible.

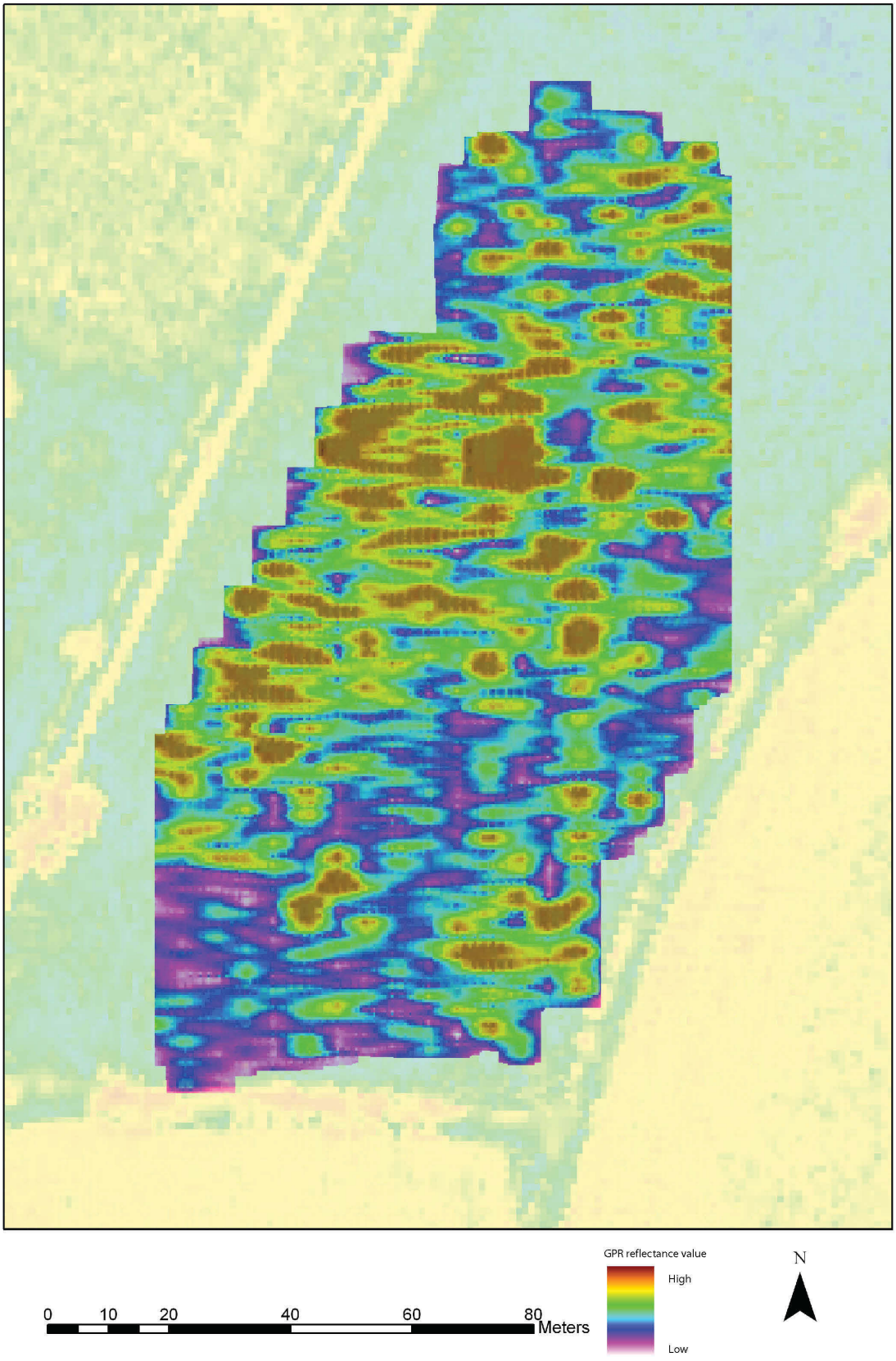

Fig 5.52: The T2G1 survey, 2.4m – 2.6m depth slice.

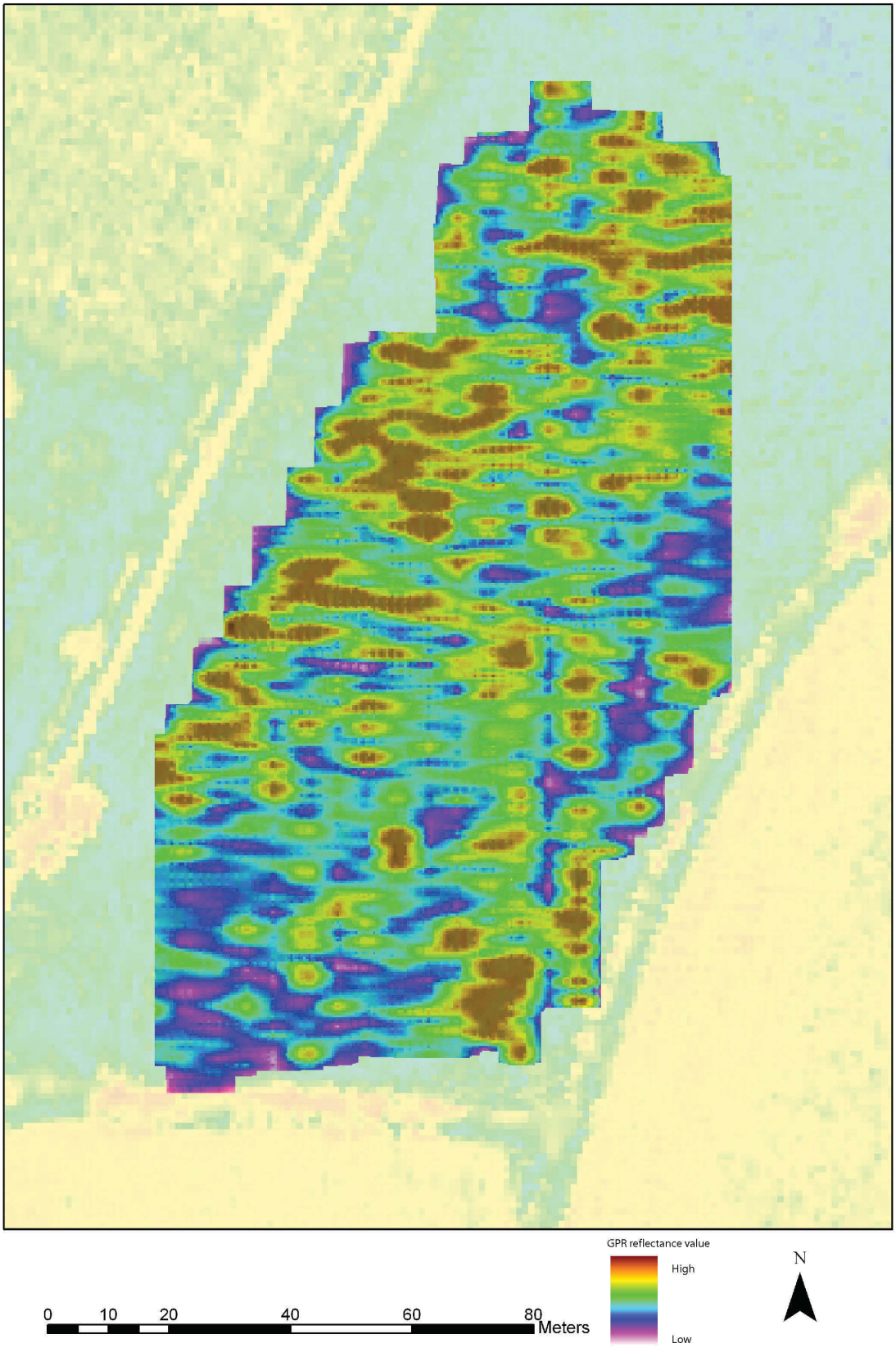

Fig 5.53: The T2G1 survey, 2.9m – 3.1m depth slice.

5.5.3 Summary of the GPR surveys on the upper unit

From the two GPR surveys undertaken on terrace 2 the main points can be summarised as:

- In the areas of the T2T1 and T2G1 surveys Terrace 2 had a thin layer of alluvium overlying substantial gravel deposits.
- The gravel deposits have a contact with bedrock at circa 4m thick.
- The relatively deep GPR penetration on terrace 2 is a product of a lower water table and lower overall substrate water content.
- Within the terrace 2 survey areas no well-preserved palaeochannels were identified.
- The palaeoenvironmental potential within the survey areas on terrace 2 is considered to be low.
- Variation was seen in the T2G1 grid gravels, which may possibly relate to a palaeochannel, although this is a speculative interpretation.

5.4 Comparison of the GPR surveys with bore hole data

Data was made available by Lafarge quarries on a series of boreholes recorded across the study area from water table monitoring. Five boreholes have spatial proximity to the GPR surveys (Fig. 5.54). Of these bore holes LKN90/78b is located on terrace 2, LKN89/20 and LKN90/57 are located in palaeochannels on terrace 1 and LKN90/61 and LKN90/16 and located on terrace 1. These bore holes provide complimentary data for comparison with the stratigraphy recorded from the GPR surveys (Fig. 5.55).

The GPR survey T2T1 is interpreted as reaching the gravel bedrock interface. The depth of gravels, although not constant, varies between 3m and 4.1m although it becomes shallower on the eastern edge of the transect. In comparison the core LKN90/78b produces a depth to bedrock of 4.4m. The borehole produces a depth to bedrock of circa 50cm below the level seen from the GPR interpretation. The borehole LKN90/78b is not adjacent to T2T1 and therefore variations in terrace 2 may account for some of the difference. It is also possible that the GPR profile is slightly too shallow, calibrated through the alluvial depth, which has had the effect of compressing the gravel depth.

The LKN89/20 and LKN90/57 bore holes both sample palaeochannels associated with terrace 1. In LKN89/20 the depth to pebbly sand is 4.0m and to bedrock 4.7m. In LKN90/57 the depth to a silt below the sand and gravel is 3.5m, with a pebbly sand to 3.9m, with bedrock being encountered at 5.8m. Located on the gravels of terrace 1 LKN90/61 reveals a depth to bedrock of 6.0m, whilst LKN90/16 reveals a depth to bedrock of 5.3m. The GPR surveys on terrace 1 struggled to penetrate to the depth of the interpreted bedrock/gravel interface. On the T1T1 survey high gains were used that attempted to penetrate to this depth. A major junction is seen at circa 3.5m across the transect. The borehole data strongly suggests this is not the gravel/bedrock interface. There are two possibilities: either a pebbly/sand layer below the gravel has been reached (analogous to LKN89/20) or a silt layer below gravel, (analogous to LKN90/57). In either situation the GPR has not penetrated through this layer and the contact with bedrock is not seen.

The borehole data also produces data on the level of alluvium on terraces 1 and 2 and the nature of the palaeochannel fills. LKN90/78b shows this area of terrace 2 to have 1.4m of combined topsoil and red brown silty clay. This compares with the 0.4m covering seen in T2T1. This bore has importance in

showing that some areas of terrace 2 have substantial coverings of alluvium over the terrace gravels. It also highlights that substantial differences exist in the floodplain stratigraphy between the bore LKN90/78b and survey T2T1.

The two boreholes on terrace 1 have alluvial depths of 1.8m (LKN90/61) and 1.1m (LKN 90/16). Both of these figures are in good agreement with some of the surveys conducted on terrace 1, such as T1G1 and T1QT, which both showed circa 1.4m of alluvium overlying terrace gravels. Notably, LKN90/16 I located within part of the potential palaeochannel identified in T1G3 and this may explain the depth of 1.1m of alluvium at this point.

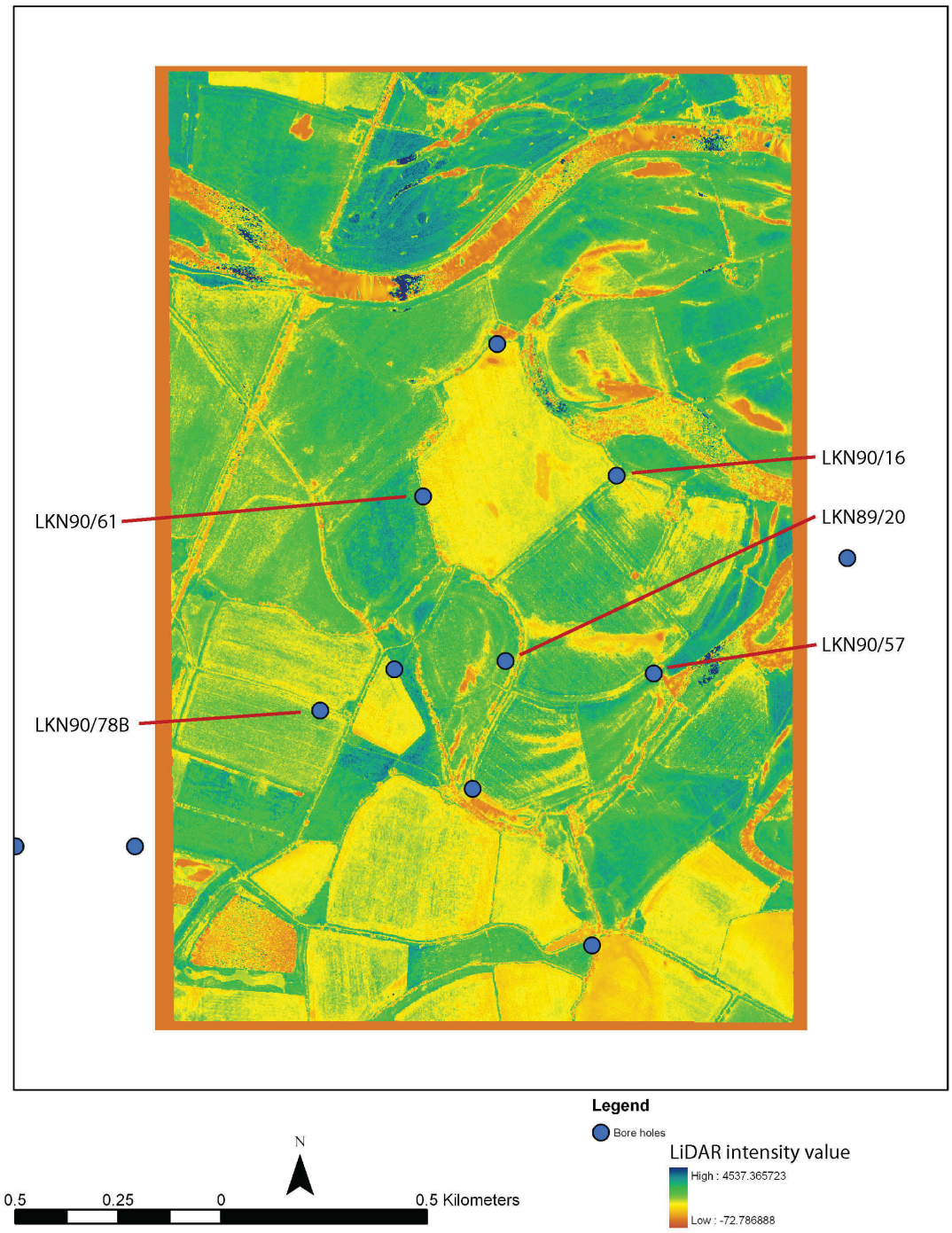

Fig 5.54: The location of five bore holes within the survey area.

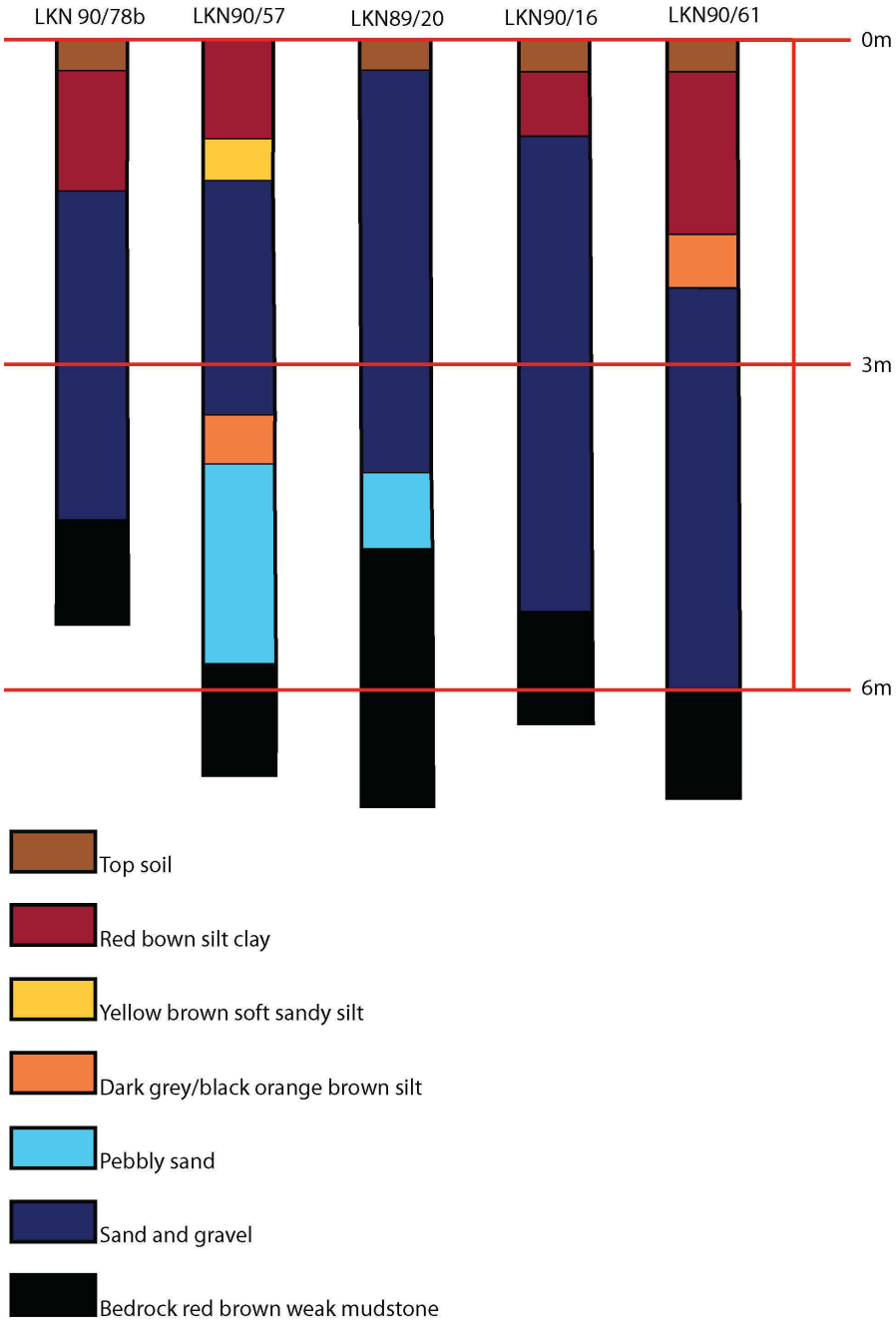

Fig 5.55: The stratigraphy of the boreholes.

5.5 A summary of ground penetrating radar survey within alluvial environments

The application of Ground Penetrating Radar to map the subsurface stratigraphy of an alluvial environment has produced mixed results. Primarily, the GPR has been effective in mapping the depth of alluvium above the gravels, the composition of the upper gravel deposits and identifying boundaries and variation between gravels and palaeochannels on the modern floodplain, terrace 1 and terrace 2. Conversely, the GPR penetration into the palaeochannels was generally poor. Where the channels had high water/clay contents, GPR penetration was particularly weak. Therefore, GPR cannot be used to investigate the structure of high water/clay content palaeochannel fills, which are the palaeochannels that have high palaeoenvironmental potential. However, by using this criteria, palaeochannels that cause rapid attenuation of the radar signal should be earmarked for palaeoenvironmental sampling, due to the nature of the fill causing the loss of signal. It was possible to see the cross section of some palaeochannels and variation in their fill. Such palaeochannels are suggested to have a low palaeoenvironmental potential, due to the lack of highly conductive material within their fill such as clay, which would cause rapid attenuation of the GPR signal. Through looking at the patterns of deposition within the GPR transect it is possible to build simple chronological models of deposition of the sedimentary units.

The two and three dimensional GPR surveys recognised distinct sedimentary structures in the heterogeneous alluvium deposits. Sedimentary units were interpreted according to their reflection pattern and interpreted shape. The reflection amplitudes that were recorded related to differences in the sedimentary architecture of different geomorphological units. However, it was not possible to unambiguously predict the physical properties of a geomorphological unit from GPR reflection data. In general it was possible to differentiate between alluvium, palaeochannels, gravel and variations within the gravel, through changes in their relative RDP and hence reflectance pattern. However, in some cases different sedimentary units gave similar patterns of reflectance, e.g. gravels were generally seen as units of high reflectance but some clay layers (e.g. QT5 on the T1QT survey) produced a very similar reflectance pattern.

The integration with the remote sensed LiDAR data has been excellent. It has allowed an assessment to be made of the ability of LiDAR to map surface sediment deposits. The LiDAR intensity values in particular seemed to reflect changes in subsurface sediments. Through using the 200MHz antenna the contact between the gravels and the bedrock was not seen, except for on the T2T1 survey. The 200MHz antenna was effective in mapping the stratigraphy and composition of the upper gravel deposits. These are shown to be heterogeneous in their structure. The correlation between the LiDAR results and the GPR surveys highly ghts the potential for integration between remote sensing and ground based prospection.

In methodological terms of the GPR data quality and penetration the results were best on terrace 2, and worst on the modern floodplain, with terrace 1 intermediate between them. This difference in data quality is interpreted as a function of the water content, with the modern floodplain having the highest water content of sediments. The presence of the high water table within surveys was a key factor in reducing penetration of the GPR signal. The use of a 5m transect interval is suggested as a maximum for all grid surveys, collecting a minimum of twenty transects of data per grid. In the future, it is suggested that GPR surveys on alluvial environments used to assess geoarchaeological potential should follow the sequence:

1. Consult remote sensed data (e.g. IFSAR, LiDAR, aerial photography) for areas in which to undertake GPR surveys, targeting different areas of the modern floodplain and terrace sequence.
2. Undertake a series of single evaluative GPR transects, combined with topographic modelling and gouge core survey.

3. Evaluate results from 2.
4. Undertake grid plan GPR surveys on areas identified through 3.
5. Integrate remote sensed and ground based prospection data.

CHAPTER 6: DATA INTEGRATION OF REMOTE SENSED AND GROUND PENETRATING RADAR SURVEY DATA

The data from the LiDAR surveys has been combined with the GPR data in two ways. Firstly, the LiDAR data has been used for the presentation and analysis of the GPR results (chapter 5) and was layered with the GPR data in ArcGIS. In addition specific GPR surveys have been integrated with the LiDAR data and layered in a quasi 3D environment using ArcScene.

Combining these two data sources has importance for several reasons. Both methods provide a means of cross validating the results obtained through the other, and in nearly all cases the correlation between the LiDAR and the GPR data has been good. The combination of the two techniques also allows a 2D plot produced by LiDAR to have the third stratigraphic element added through GPR. Lastly, it is important to develop methods of integrating remote sensed and ground prospection based methods, as both are set to play an increasing role in geoarchaeological investigations.

6.1 Integration in ArcScene

Four GPR surveys were combined with LiDAR data, being surveys MFG1, T1G1, T1G3 and T2G1. For each survey it was not possible to show all the depth slice data, so specific depth slices have been selected.

6.1.1 Integration of MFG1 and LiDAR data

The integration of MFG1 with the LiDAR data used the LiDAR last pulse DTM, combined with the depth slices of 1.4m – 1.6m and 2.4m - 2.6m (Fig. 6.1). From this image the correlation between the LiDAR DTM and the GPR depth slice stratigraphy is particularly powerful. The palaeochannels MFC1, MFC2 and MFC3 are visible in the LiDAR and in the GPR depth slices as are the gravel deposits MF3 and MF4. This image demonstrates how sub surface stratigraphy can be imaged in the surface topography.

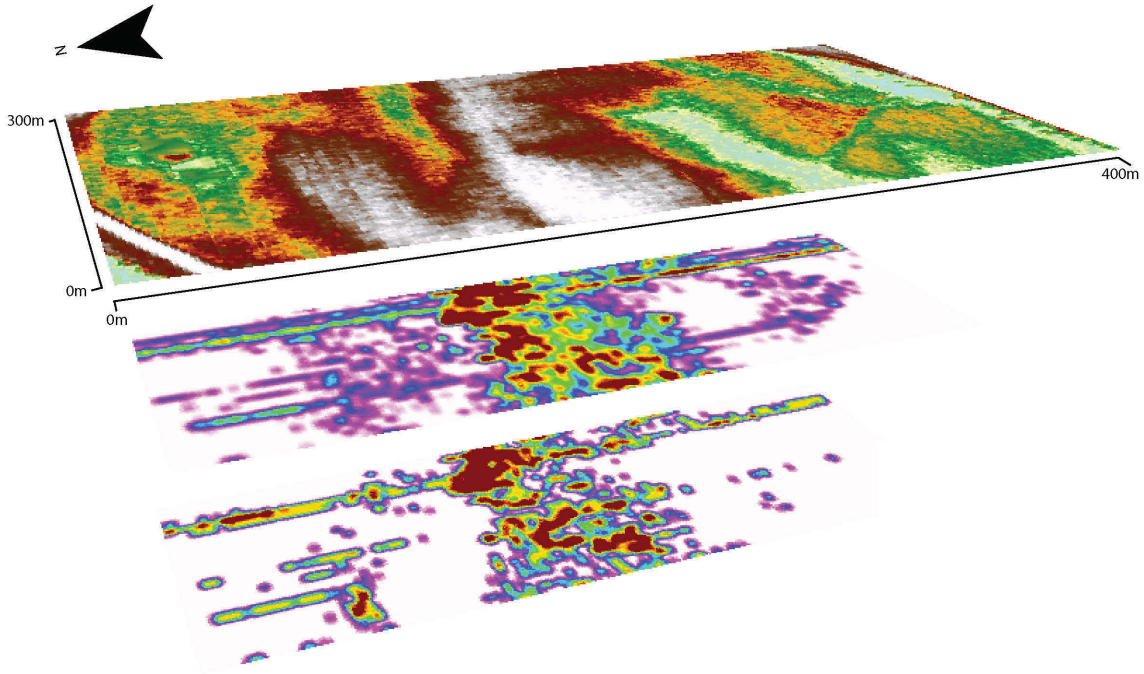

Fig 6.1: The LiDAR last pulse DTM combined with the 1.4m – 1.6m and 2.4m – 2.6m depth slices on the MFG1 survey.

6.1.2 Integration of T1G1 and LiDAR

The integration of the T1G1 survey used the LiDAR intensity plot combined with the GPR depth slices of 0.4m – 0.6m, 0.9m - 1.1m, 1.9m – 2.1m and 2.4m – 2.6m (Fig. 6.2). The correlation between the LiDAR intensity and the GPR depth slices is excellent. Terrace 1 is visible in the LiDAR intensity and also in the GPR depth slices, as is the palaeochannel T1C6. With movement down through the GPR depth slices the same features are evident but the reflectance values change. For example at 0.4m – 0.6m terrace 1 is a higher reflecting unit than the palaeochannel, although this is depth slicing in alluvium on top of the terrace gravels. Below this at 0.9m – 1.1m the palaeochannel T1C6 is shown as a higher reflecting unit than terrace1, although at this depth the terrace 1 gravel are still buried under alluvium. At the 1.9m – 2.1m this reflectance has changed again, with the terrace 1 gravels being clearly evident, as at 2.4m – 2.6m. The difference in the GPR reflectance between the terrace 1 and the palaeochannel is a product of different sediment types. It would appear that the LiDAR intensity values map these different sediments through changes in the sediment water content. As suggested in chapter 4, LiDAR intensity appears to have the ability to map changes in sediment structure through soil moisture content. These changes are confirmed through the GPR depth slices.

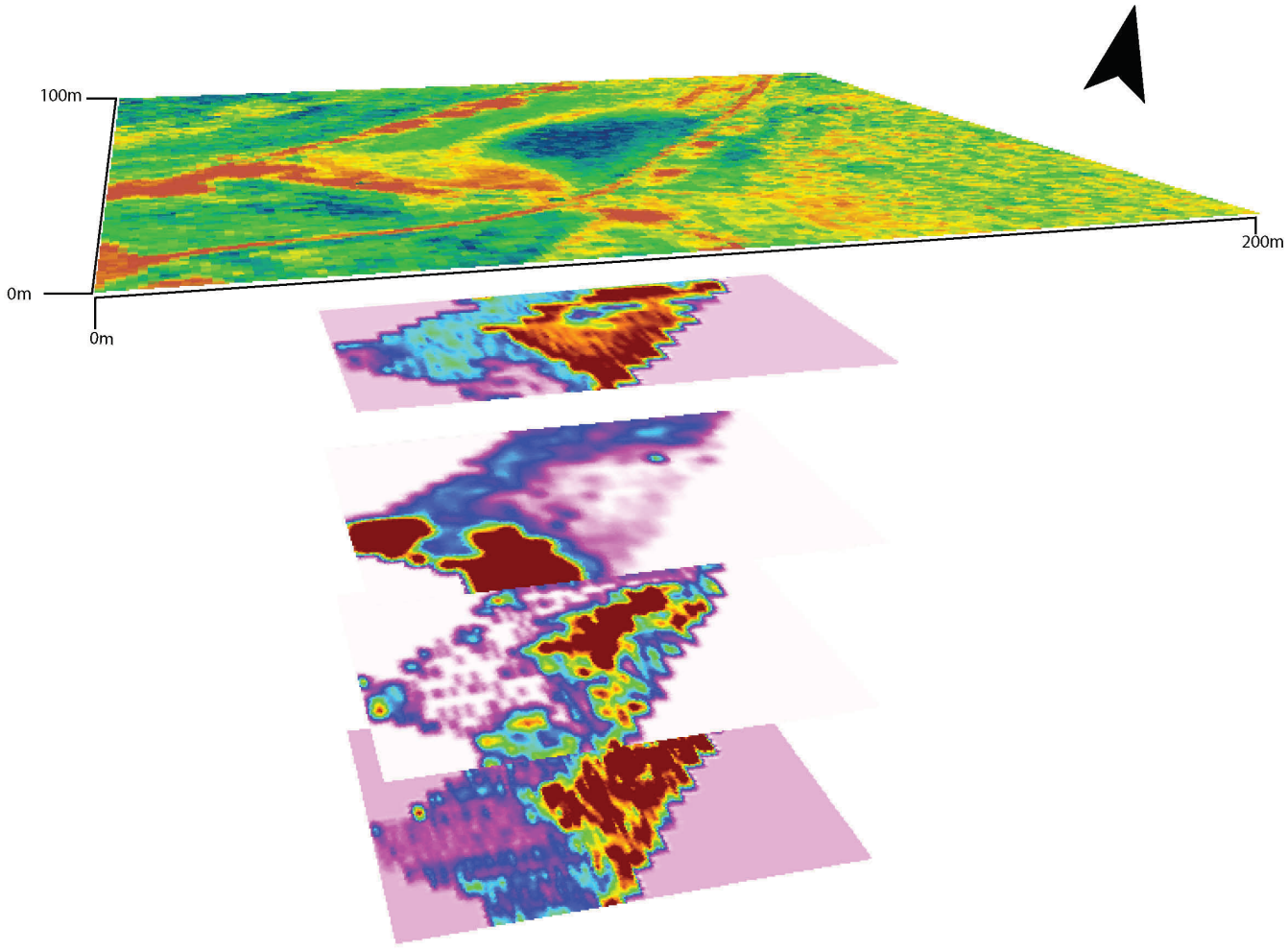

Fig 6.2: The T1G1 survey combing the GPR depth slices of 0.4m – 0.6m, 0.9m - 1.1m, 1.9m – 2.1m and 2.4m – 2.6m with the LiDAR intensity.

6.1.3 Integration of T1G3 and LiDAR

The T1G3 also investigated an area of terrace 1 with associated palaeochannel. The integration used the LiDAR last pulse DTM combined with the GPR 0.4m – 0.6m, 1.4m – 1.6m and 2.4m – 2.6m depth slices (Fig. 6.3). The relationship between the topography identified by the LiDAR and the GPR depth slices is excellent. The palaeochannel T1C8 is clearly visible in the LiDAR DTM and in the 0.4m – 0.6m and 1.4m –1.6m depth slices. Again with movement down through the depth slices the reflectance values change, for example at 0.4m – 0.6m terrace 1 is shown as a high reflecting unit. At 1.4m – 1.6m the palaeochannel T1C8 is the highest reflecting unit. By the 2.4m – 2.6m the limit of effective penetration has been reached, although some higher reflecting gravels are visible on terrace 1.

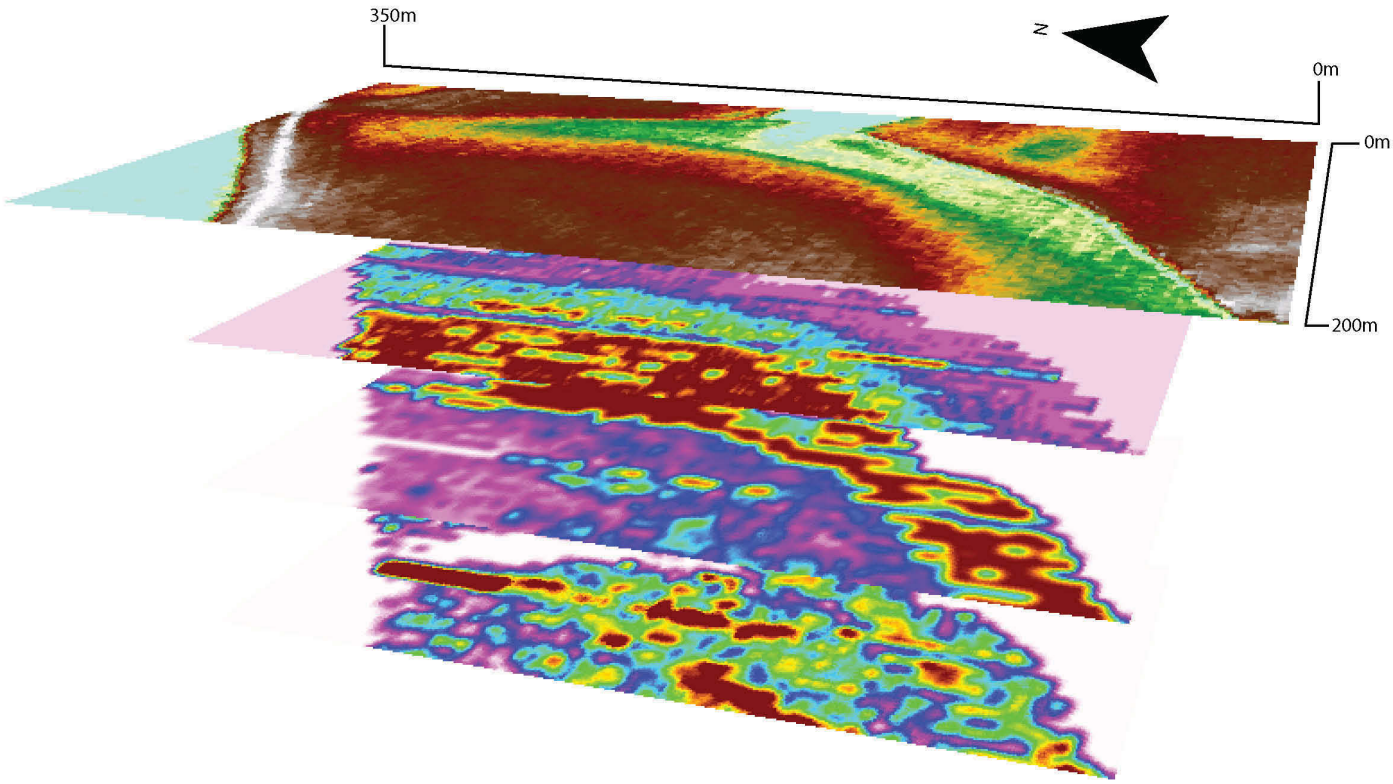

Fig 6.3: The T1G3 survey combining the GPR depth slices of 0.4m – 0.6m, 1.4m – 1.6m and 2.4m – 2.6m with the LiDAR last pulse DTM.

6.1.4 Integration of T2G1 and LiDAR

The T2G1 survey integrated the GPR depth slices of 0.4m – 0.6m, 1.4m – 1.6m and 2.4m – 2.6m with the LiDAR intensity image. The correlation between the LiDAR intensity values and the GPR depth slices is excellent. A change in LiDAR intensity is seen moving across the T2G1 survey area from North (higher intensity) to the south (lower intensity). This difference is mirrored in the underlying sediments, with the 1.4m – 1.6m and 2.1m – 2.6m showing the difference between T2A1 (lower reflecting area) and T2A2 (higher reflecting area). Again the reflectance properties of the GPR depth slices change through the profile, with the depth slice of 0.4m – 0.6m showing a general area of high reflection, not displaying the same variation as the two deeper depth slices. It is again interpreted that the changes in the LiDAR intensity and the GPR reflectance values is caused by a change in the soil moisture content, itself a product of the sedimentary architecture. This again the highlights the potential of using LiDAR intensity values as a means of identifying variation in sediment structure.

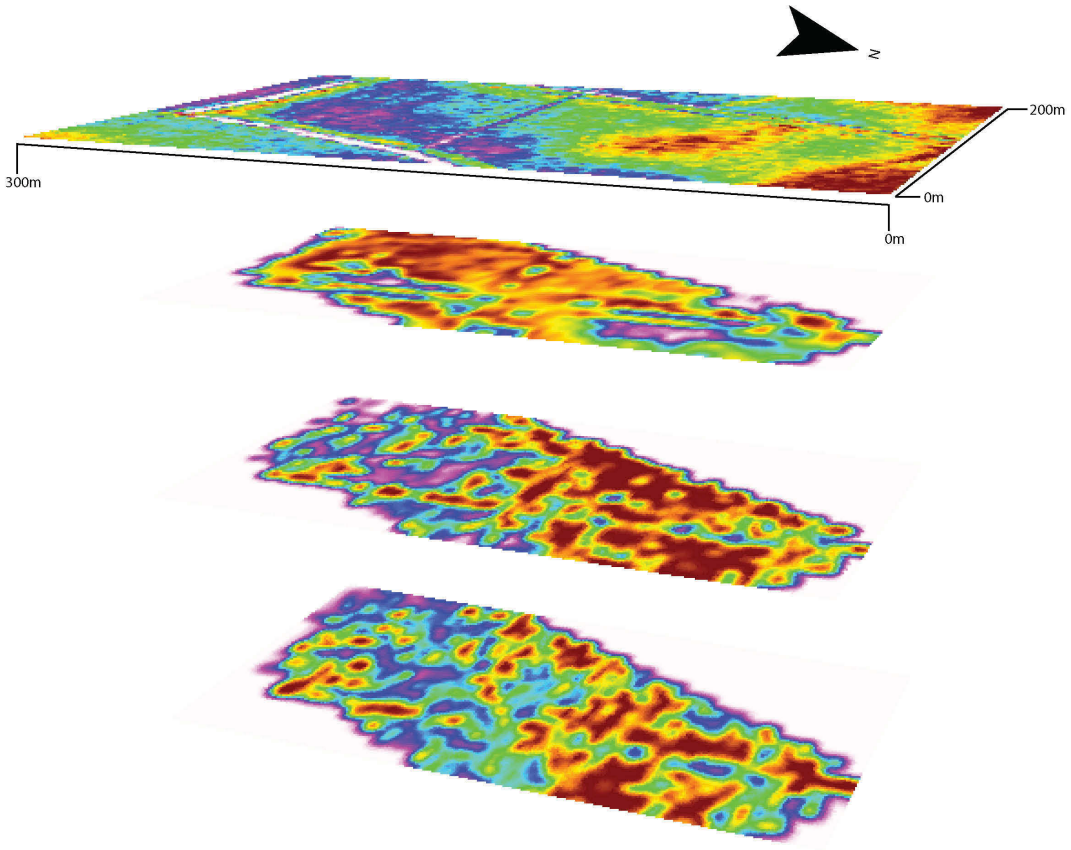

Fig 6.4: The T2G1 survey combining the GPR depth slices of 0.4m – 0.6m, 1.4m – 1.6m and 2.4m – 2.6m with the LiDAR intensity.

CHAPTER 7: GEOLOGY AND GEOMORPHOLOGICAL MAPPING

7.1 Geology

The area was mapped at 1:50,000 scale by BGS (sheet 141, 1974). This data has been extracted and is shown in Figure 7.1, with the study area highlighted.

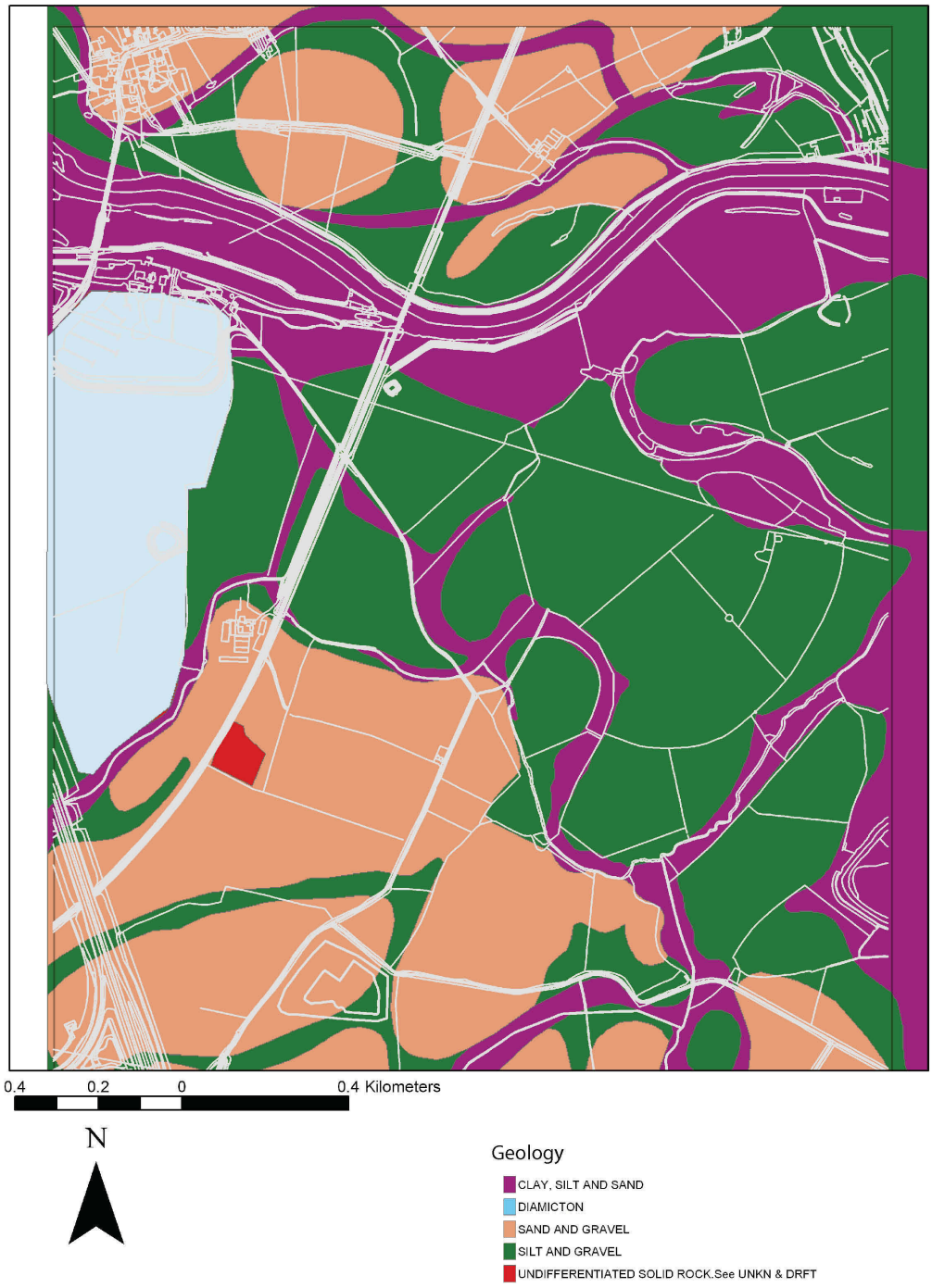

Fig 7.1: The abstracted lithology map of the study area. Data from BGS sheet 141.

Within the study area there are four lithologies:

1. Sand and Gravel: this forms the terraces to the south west and north west of the study area. Although not differentiated at this scale the 1:50,000 map identifies it as Holme Pierrepoint Sand and Gravel (Fig. 7.2). This maybe correlated with the basal Devensian gravels at Hemington which contain numerous cryoturbation features (Brown and Salisbury in press) and was formed by a braided river with a snowmelt dominated regime.

2. Silt and gravel: this covers the middle part of the study area and is generally intermediate in height between the sand and gravel and clays and silt of the channel margins. These are mapped by the BGS as the Hemington Terrace; however, as noted above this terrace is bi-partite with the lower member being of Devensian age (Brown and Salisbury in press). Aerial photographs of the flood shows much of this area is inundated at floods of only 1-2 years return period (see below). These gravels were probably deposited by channel migration and by braiding or incipient braiding. There age is not known directly, however, they are likely to be early to mid Holocene in age.

3. Clay, silt and sand: this covers the area adjacent to the modern channels and along the larger and lower palaeochannels and is a combination of lateral deposits and overbank deposits. It is mapped by the BGS as alluvium.

4. Diamicton: on the western edge of the study there is some poorly consolidated material, classified as diamicton.

The BGS also map a small area of sand and gravel in the southeastern corner of the study area as Syston Sand and Gravel as it is a low terrace of the River Soar. On Redhill there is also mapped glaciofluvial deposits (undifferentiated) which given the height above the floodplain (3.7m) are likely to be of considerable antiquity.

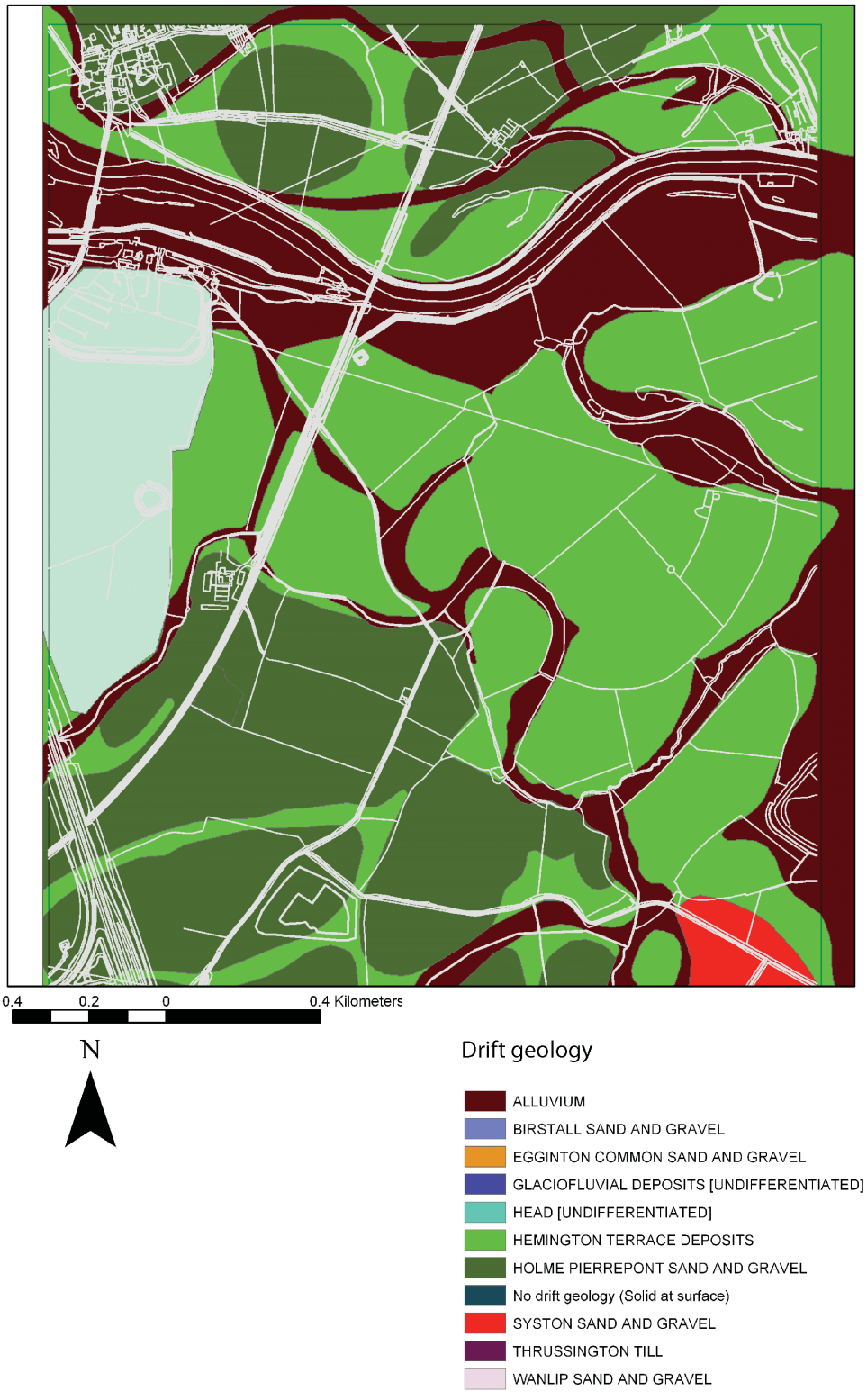

Fig 7.2: The drift geology of the study area.

A map of the geological stages of the deposits has also been produced with includes only the Holocene (MIO 1) and Devensian (MIO 2-4).

Fig 7.3: The geological stage map of the study reach.

7.2 Geomorphological Mapping

This was conducted entirely by one of the authors (Brown) on a field by field basis using a 1:2,500 base map. Standard geomorphological procedures were followed. The result is the map shown in Figure 7.4.

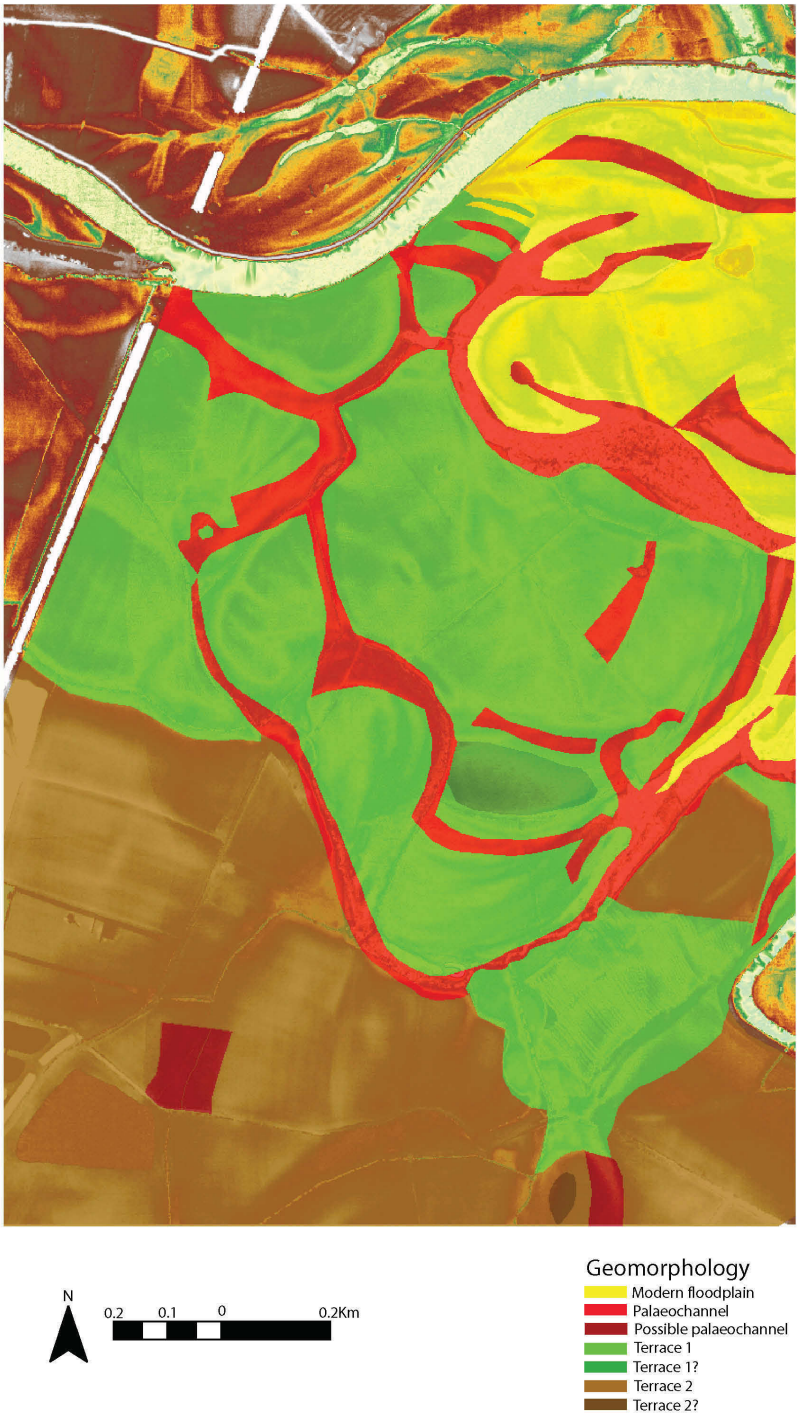

Fig 7.4: Geomorphological map of the study reach.

The geomorphological map differentiates the valley floor area into two terrace levels, palaeochannels and the modern floodplain. However, as mentioned before the term floodplain as used here is the lower area of valley floor that surrounds the modern channel system. This mapping was then compared with three topographic transects/profiles derived from the LiDAR data.

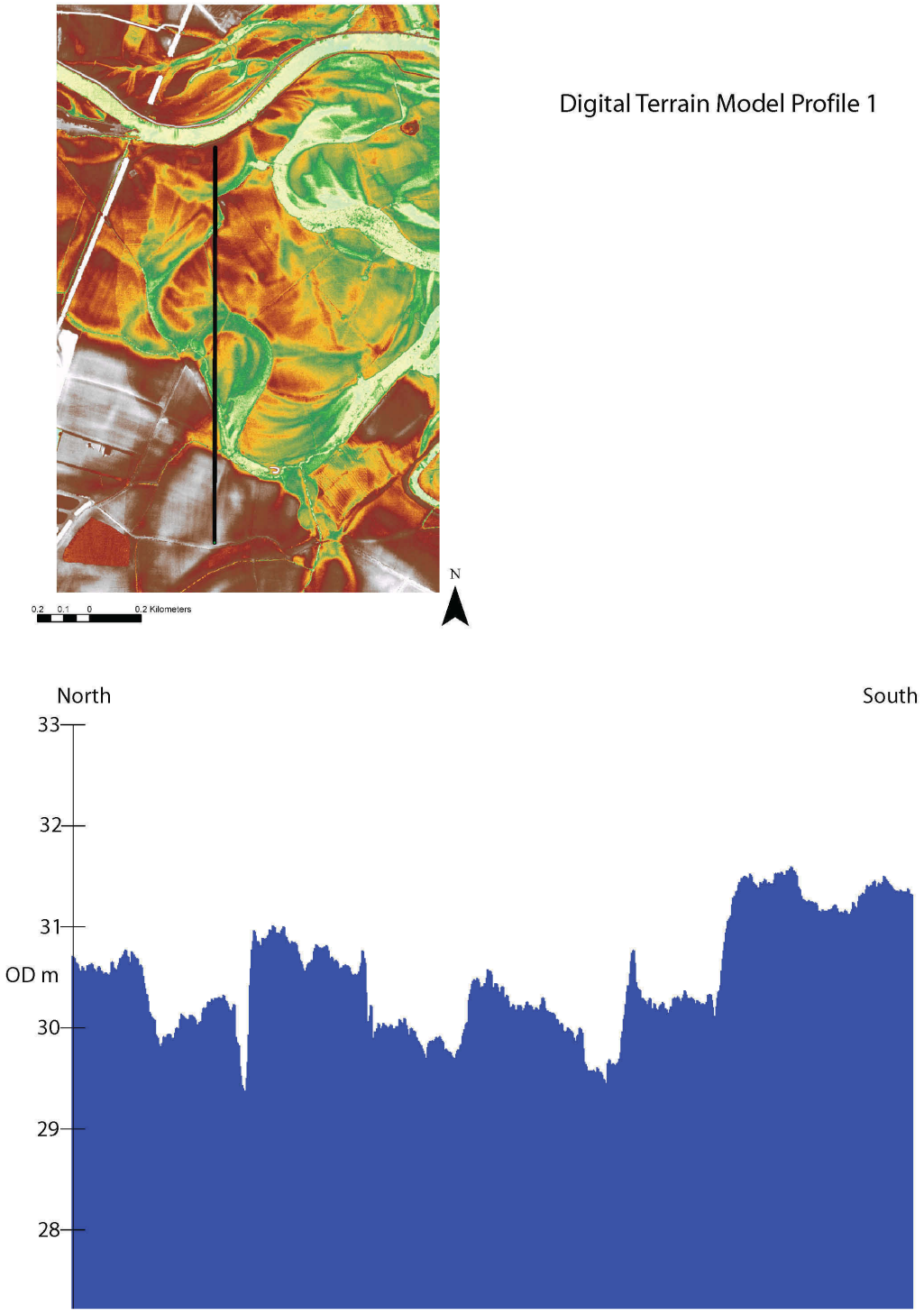

Fig 7.5: Profile 1 generated from the LiDAR DTM.

The profile is approximately normal to the modern channel and valley of the Trent being from north to south. The topographic profile is highly irregular although it does show an overall trend of decreasing altitude south to north. This profile cuts the palaeochannels at oblique angles and this partially explains the widths of the low areas between the high surfaces. However, even the surfaces are uneven with a tendency to a regular low-amplitude undulation and/or a slope either to or away from the present river.

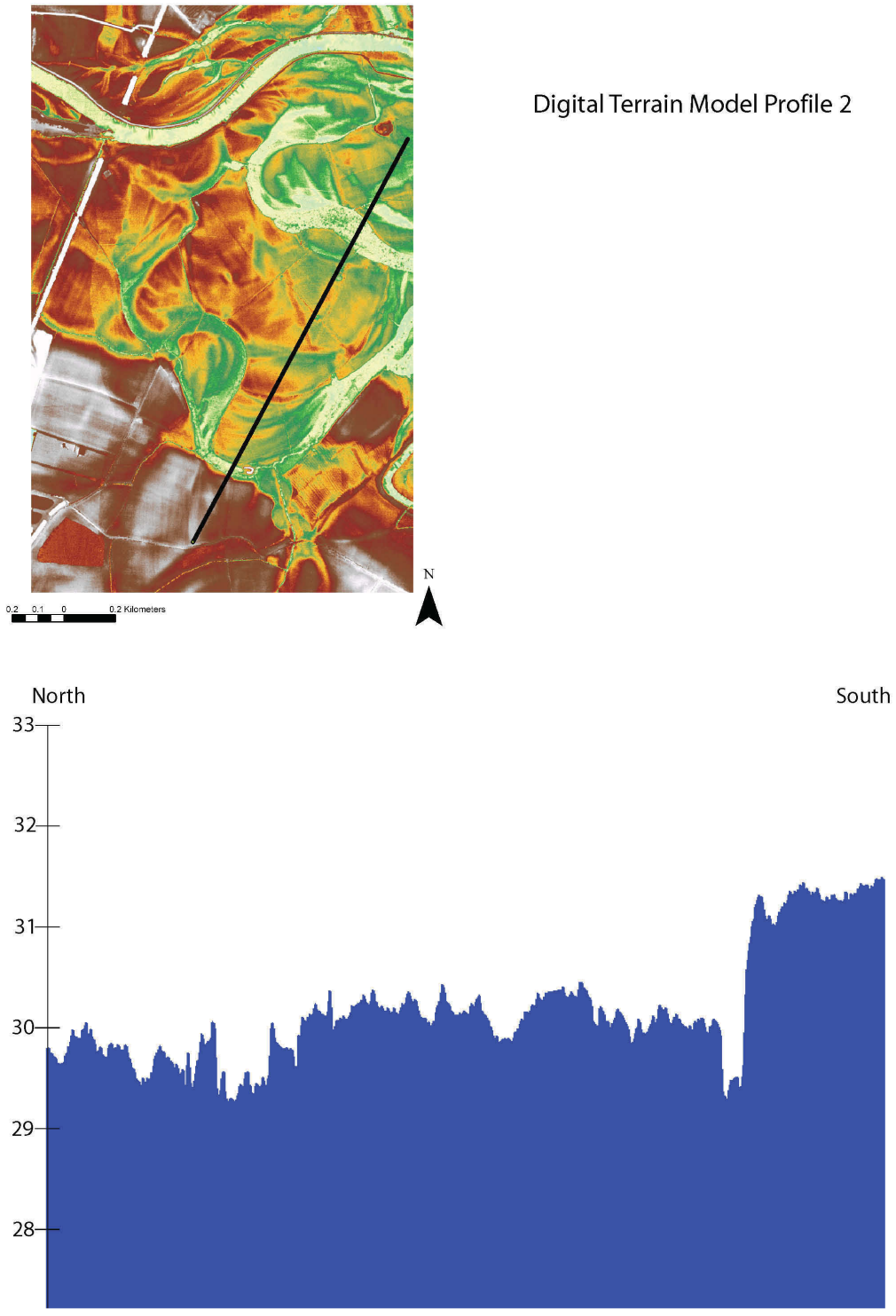

Fig 7.6: Profile 2 generated from the LiDAR DTM.

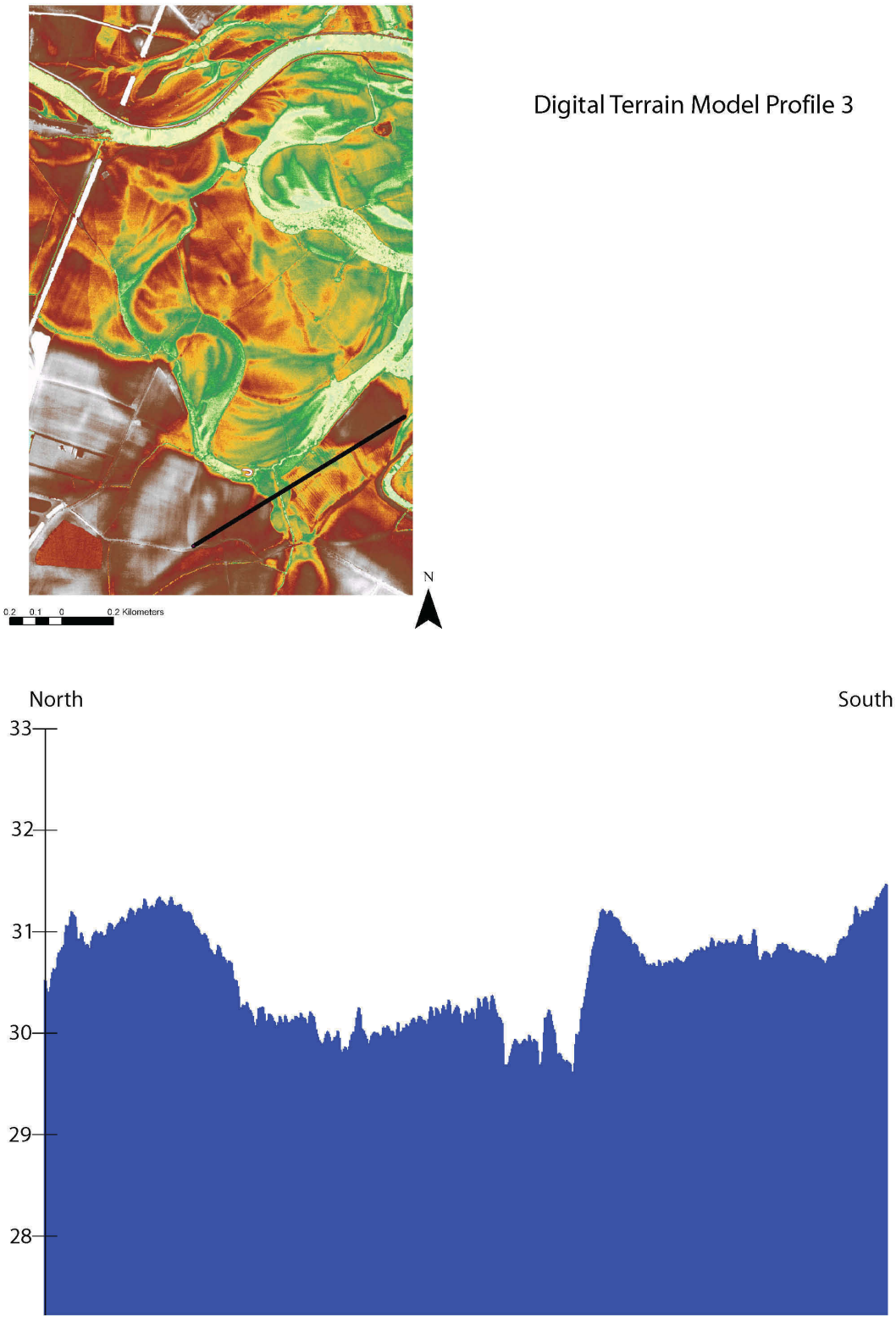

Fig 7.7: Profile 3 generated from the LiDAR DTM.

Profile two shows similar features although it is far less irregular and this is partly due to the diagonal trend southwest to northeast, which crosses the main palaeochannels approximately normally. Here a tri-partite topographic division is supported with a significantly higher southwesterly terrace, a middle level and then lower level close to the river. However, the profile also clearly shows that the middle level is divided into two sections by a palaeochannel. It is also evident that each surface is truncated by a palaeochannel and this is likely to have genetic meaning.

The third profile (Fig. 7.7) is also approximately southwest to northeast but upstream of the modern junction and across the River Soar. It is also less irregular than profile 1 but has an obvious mound adjacent to the modern channel of the Soar. This is unlike the other terrace remnants reaching an average height higher that the terrace in the southwest end of the transect. This agrees well with the identification of this terrace as a remnant of the Syston Terrace of the Soar valley. It suggests that it could pre-date the Holme Pierrepoint terraces as it had been higher but has been degraded over time.

These profiles show far greater irregularity of the terrace and floodplain surfaces than is generally assumed. There are several reasons for this irregularities some of which are listed below.

- There has been erosion by channels of formerly flat floodplain surfaces. This also helps explain the occurrence of palaeochannels across the highest terrace surfaces in the study area. It does, however, require a river level some 2-3 m higher than at present.
- The topography represents the natural topographic variation of a former floodplain dominated by scroll-bars and braid-plain topography. This has been noted on many terraces and represents former generally higher energy conditions and abundant coarse sediment supply.
- The modern river has deposited overbank deposits in spatially discrete units (such as levees) on the terrace and floodplain levels. However, there is no sedimentary data supporting this for the upper levels.
- Other geomorphic processes such as sand dune movement have created ridges on the terrace surfaces. Whilst this is known from Europe there is no sedimentary data supporting this for the upper levels.

The first two explanations are the most likely and are not mutually exclusive.

Overall the geomorphological mapping facilitates a higher level of valley floor differentiation, which agrees well with the LiDAR generated DTM. This data is invaluable for the creation of a chronostratigraphic model (see chapter 9).

CHAPTER 8 ARCHAEOLOGICAL ASSESSMENT OF THE STUDY AREA AND ITS ENVIRONS

And of the British floods, though but the third I be,
Yet Thames and Severne both in this come short of me,
For that I am the mere of England, that divides
The north part from the south, on my so either sides, that reckoning how these tracts in compasse be extent,
Men bound them on the north, or on the south of Trent

Michael Drayton, *Poly-Olbion*, The Sixe and Twentieth Song, 1622

The environs for the study area is taken as a transect along the Trent floodplain from Swarkestone to the west of the study area, and Attenborough to the east. The wider environs allows consideration of the Trent's confluence zone with the Derwent and Soar, an area where significant archaeological discoveries spanning the Lower Palaeolithic to the Post-Medieval period have occurred. It is suggested below that the rich archaeological resource of this area is partly due to the confluence zone being an important communications node.

The information included in the report is derived from an SMR search for the eight square kilometre study area (Leicestershire and Derbyshire), a review of published and unpublished reports from the study area and a general search of published data for the environs. The regional and national significance of the sites and monuments in the study area is gauged against the recent regional research frameworks initiative (N.J. Cooper in prep).

The recognition of the archaeological resource in the Trent-Soar-Derwent confluence zone was initially linked with aggregates extraction. Palaeolithic handaxes were recovered from quarries in the Beeston area in the 1920s while occasional finds of Bronze and Iron Age metalwork from the Trent produced the first glimpses of the later prehistoric period (Scurfield 1997; Watkin *et al.* 1996). Aerial photography from the 1940s first began to reveal the hidden past landscapes represented by cropmark evidence on the gravel terraces. The first of the Lockington barrows was located by St Joseph in 1947 and subject to survey and trial excavation in 1954 (Posnansky 1955). Aerial reconnaissance within the study area from the 1960s led to the discovery of further barrows (Pickering and Hartley 1985) and the Lockington Iron Age and Romano-British settlement and villa (St Joseph 1961 and 1968, Frere and St Joseph 1983, Pickering and Hartley 1985), both now Scheduled Ancient Monuments. Follow-up fieldwalking survey of the two cropmarks produced both Iron Age and Romano-British pottery (Clay 1985).

Since the early 1990s the study area and immediate environs has seen much archaeological activity in relation to aggregates extraction, road schemes and proposed developments, all under the remit of PPG16. An area of the barrow cemetery was subject to evaluative and mitigative excavation in advance of the Derby Southern Bypass scheme and associated works (Hughes 2000). Noteworthy was the near-complete excavation of Barrow VI which revealed a multi-phased monument and a spectacular pit deposit of metalwork and ceramics. Two possible ring ditches seen as very faint cropmarks were confirmed by trial trenching in the same field. More recently desk-based survey, geophysical survey, field survey and evaluation have increased the size of the Lockington barrow cemetery area and the Iron Age/Romano-British settlement and associated field systems (Clark 1995; Ripper and Butler 1999).

Perhaps one of the most significant developments in recent years has been the discovery of waterlogged archaeological remains in the palaeochannels in the Derwent-Soar-Trent confluence zone. Hemington Quarry immediately west of the study area has revealed palaeochannels going back as far as the Late Glacial period. These have produced highly significant palaeoenvironmental data while the medieval channels of 9th-14th century date have preserved unique structural evidence for fisheries, bridges and river management.

8.1 Lower-Middle Palaeolithic

Although no finds of this date have been reported from the study area several artefacts have been recovered from the environs, all from gravel pits at Beeston and Stapleford parish. Wymer (1999) records 20 handaxes from the Beeston Sand and Gravel (OIS 4), one from Hemington Terrace Deposits (OIS 1-2) and one from alluvium. Some 16 handaxes and several flakes were recovered from the Tottle Brook pit (Smith 1928; Posnansky 1963). It remains uncertain whether the finds from the Beeston terrace are Devensian or earlier in date (Wymer 1999, 115). Posnansky (ibid) noted the fresh condition of some of the material from Tottle Brook pit, which might suggest that some is of Devensian age, while other pieces were rolled and would seem to be secondary deposits. The mapped Soar-Trent terraces across the study area are probably of OIS 1-2 date and have some potential for derived Lower-Middle Palaeolithic artefacts.

River confluences were favoured places for Lower and Middle Palaeolithic hunter-gatherers (Wymer 1999) and, given the finds from the Beeston terrace, it is suggested that the study area has some potential for the preservation of artefactual and ecofactual evidence for this period. The finds from the environs are among some of the more northerly European Lower Palaeolithic finds and may help to address questions of colonisation and population dynamics (Graf 2002).

8.2 Upper Palaeolithic

Early Upper Palaeolithic evidence is absent from the Trent valley, but this is not surprising as such sites are rare at the national level. While this partly reflects low population densities there is also a problem in recognising sites of this period. Early Upper Palaeolithic sites are identified on the basis of limited lithic typology, in the finding and recognition of leaf points, Font Robert points or Aurignacian type fossils (Jacobi 1980; Barton 1997). An Early Upper Palaeolithic presence in the region is well attested at Creswell Crags (Jacobi 1980), while the recently investigated site at Glaston, Leics. demonstrates the considerable potential for open-air sites in the East Midlands (Thomas and Jacobi 2001; Cooper 2001). While open sites are likely to have been detrimentally affected by periglacial conditions, these can also present some chance for preservation. Ice wedges, which were frequently seen at Hemington Quarry and on aerial photographs of the local terraces, can be repositories for early sites as demonstrated locally on the Wing to Whatborough pipeline (Graf 2002; Cooper 2002b). While only a single flake was recovered from the latter site, remarkable lithics and faunal assemblages have been reported from similar contexts e.g. Wilczyce, Poland (Fiedoeczuk and Schild 2002).

The onset of the Dimlington Stadial led to the abandonment of Britain for some 10,000 years. After the climatic amelioration of the Lake Windermere Interstadial Britain was re-colonised, but this was probably not a continuous process being affected by rapid fluctuations in climate and environment. Radiocarbon dating and distinct typological and technological differences in material culture (lithics and organic tools) suggests that the process was punctuated between 13,000 and 10,000 BP. Conventionally the material culture of this period is divided into the Late and Final Upper Palaeolithic (Barton 1997). The evidence for occupation of the Trent valley during this period is more compelling with a number of

reported later Upper Palaeolithic findspots and sites. Indeed the cluster of findspots within the East Midlands is one of the densest across the country (Jacobi 2004).

The earliest re-colonisation of Britain is associated with the Creswellian culture, dating to *c.* 12,900-12,000 BP (Barton et al. 2003), named after the cave sites at Creswell Crags on the Nottinghamshire/Derbyshire border; Mother Grundy's Parlour cave being the type site (Garrod 1926). The type fossil for this period is now seen as the Cheddar point, a trapezoidal backed blade (Jacobi 1991). A Cheddar point and possibly contemporary blades were recovered by fieldwalking from a field immediately west of the study area at SK 4662 2832, Lockington-Hemington (Cooper and Jacobi 2001). The findspot adds to the growing number of Creswellian sites in the Trent valley located by fieldwalking (Jacobi et al. 2001) including the nationally significant open-air site at Farndon (Garton 1993).

The pollen record of Northern Europe shows a change to a more wooded environment around 12,000 BP, the beginning of the *Allerod* chronozone. The distinctive lithics associated with this phase are the *federmesser* (convex backed blades) including a variant, the penknife point (shouldered, convex backed blade). *Federmesser* technologies appear across much of northern Europe and are probably linked to Azilian industries from southern Europe (Schwabedissen 1954). A *federmesser* from Castle Donington, Leics. (Cooper and Jacobi 2001) is the only certain Final Upper Palaeolithic finds from the study area environs, although other findspots are known within the Trent Basin (Jacobi *et al.* 2001).

The study area has great potential for Late Devensian palaeochannels. At Hemington Quarry eastern extension a truncated channel base produced radiocarbon dates of 11,735 ± 75, 10,960 ± 110, 11,725 ± 80 and 11,775 ± 80 BP (Cooper and Ripper 2001; Greenwood et al. 2003, 648). Another Late-glacial channel at Hemington Quarry (western extension) has produced similar dates (Cooper and Ripper 2001, 141; M. Greenwood, pers. comm.). The latter channel was of note in having a surface expression. The silted palaeochannels contained well-preserved organic remains including cold-climate caddis fly larvae and Greenwood *et al.* (2003) have demonstrated their usefulness as proxy climatic indicators in local and regional palaeo-environmental reconstructions. While there is an absence of Upper Palaeolithic finds from the study area there is considerable potential for their survival on the terrace deposits. Should any such sites have been preserved by alluvium they would be regarded as nationally significant.

8.3 Mesolithic

Mesolithic material is reported from several flint scatters within the study area (LE 4714, 7095, 7096, 7097, 7120), though none of the scatters have been as large as those seen at local upland sites. However, it should be noted that the identifications are based upon technological criteria; there are no typological identifications. Furthermore, the Leicestershire SMR has a tendency to record blade-like flakes as of a general Late Mesolithic – Early Neolithic date e.g. LE 7120. Repeat fieldwalking of the area has further sampled the scatters and the author has reported on this material. There are some Mesolithic debitage pieces in the collections, i.e. showing bladelet technology, but the evidence is slight. However, the fieldwalking within the study area was undertaken at 20m intervals a method not conducive to the location of small scatters.

A remarkable find of a Late Mesolithic antler harpoon from just north of the study area at Long Eaton, Derbs. or Thrumpton, Notts. (Knight and Howard 2004, 38) hints at the likely lost valley bottom sites. Systematic fieldwalking elsewhere in the Trent Valley has shown a widespread occurrence of sparse Late Mesolithic material, but Early Mesolithic material was apparently absent. However, an Early Mesolithic assemblage was reported from excavations at Swarkestone Lowes and, when considered within the Trent Valley context, was described as a rare resource (Jacobi and Garton 1999).

Palaeochannels of early Holocene date within the environs have been sampled. The potential for channels being archaeological repositories is highlighted by the recovery of a Late Mesolithic human femur from Staythorpe, Notts., a find that has allowed some real consideration of Mesolithic economy in the Midlands; stable isotope analysis showed that the female had subsisted on a diet rich in animal protein but lacking evidence for consumption of fish and marine food (Cooper, 2004).

8.4 Neolithic – Mid Bronze Age

The Middle Trent has a remarkable Neolithic ceremonial landscape within the confluence zone between the Dove and the Erewash[1]. Early Neolithic monuments are generally sparse but possibly occur in the environs of the study area at Barton in Fabis where an interrupted ditch system, a likely causewayed enclosure, is juxtaposed with a possible henge site (Harding with Lee 1987, 221; Deegan 1999). Another cropmark site is the probable henge at Round Hill, Twyford and Stenson (Harding with Lee 1987, 116).

Middle Neolithic monuments closer to the study area include the cursus monument at Aston, Derbs., first identified by aerial photography in 1966 (St Joseph 1966). The monument incorporated an earlier ring ditch (round barrow) along its western side while other associated ring ditches might be later additions (Gibson and Loveday 1979). The excavations of Aston I confirmed this to be an Early Bronze Age monument though earlier Neolithic features and artefacts were revealed beneath the mound (Reaney 1968). The NE-SW alignment of the monument is a common trait with cursus and similar monuments such as long mortuary enclosures. Such alignment has been claimed to represent positioning with respect to the solar calendar (Field 1999), although reference to other elements of the natural environment may have also occurred (Brophy 1999; McOmish 2003).

Some 70m west of the study area there is an enigmatic cropmark at the Lockington barrow cemetery (Rookery Lane) that plausibly could be a cursus terminal, or part of a long mortuary enclosure. This was first reported by Pickering and Hartley (1985, 37, fig 2), although the feature was not assigned to a particular monument class[2]. The faint cropmark comprised two parallel ditches some aligned NE-SW with a rounded terminus at its southern end. There is another possible cropmark that deserves mention; just to the west of the study area, near to the barrow excavated by Posnansky (1953), is a possible concentric pit circle (though slightly oval in plan). Pit circles have been recorded at Rearsby and Oakham, the latter excavated by Clay (1998) revealing a multi-phased monument of Late Neolithic and Early Bronze Age date. Both of these features are potentially significant additions to the ceremonial landscape at Lockington-Hemington and both urgently require further work to clarify their character and date.

The Lockington barrow cemetery just extends into the western edge of the study area. Posnanky (1953) partially excavated the first known barrow showing that it had a remnant mound. A central cremation burial had grave goods that included a bronze knife, bronze awl, a barbed and tanged arrowhead and three plano-convex knives (ibid). It is of some interest that the flintwork was all heat damaged.

Subsequent aerial survey recorded further ring ditches; Pickering and Hartley (1985) recorded seven examples including one enclosing a pit circle, and a concentric monument. Barrow VI was subject to an evaluation ahead of works associated with the Derby Southern Bypass and eventually full excavation

[1] A wider environs is considered necessary here to provide the landscape context of the study area.
[2] The feature could not be seen on the aerial photographs searched by the author. The feature is plotted in slightly different locations by Pickering and Hartley (1985) and Meek (2003).

(Hughes 2000). This revealed a remarkably complex monument: initially the site was demarcated with a palisade. An adjacent pit contained a remarkable group of deposits including substantial parts of two beaker vessels, a large copper dagger and two gold bracelets (ibid). Organic residues on the dagger produced radiocarbon dates of 2580-2200 and 2190-1880 cal BC, the latter date best fitting the typology of the dagger. Pre-mound activity has been interpreted as a pyre site but there was no evidence for burials associated with the pit deposits or the mound. The site identified as Barrow V by Pickering and Hartley (1985) was also subject to full excavation, revealing a pit group rather than a ring ditch (J. Meek in Hughes 2000).

The extent of this Late Neolithic - Bronze Age ceremonial landscape has greatly increased in recent years following more intensive assessment of aerial photographs, geophysical survey and fieldwork. Meek (2003) identified 27 possible Neolithic-Bronze Age monuments[3] while the present study adds a further four ring ditches and the afore-mentioned possible concentric pit circle. The 23 known or probable ring ditches are widely distributed, three km east-west by two kilometeres north-south, and might be classified as an 'area cemetery'. However, there is distinct clustering of Lockington sites 1-10, with a sub-group of seven aligned WSW-ENE[4]. The more northerly barrows also appear to be a distinct cluster and might better be termed the Hemington barrow cemetery. However, as much of the area between the two groups has been quarried this might be more apparent than real. A more systematic search of the older air photographs might be useful to assess the areas lost to gravel extraction and the construction of the M1.

Perhaps the most significant result of the recent fieldwork has been to demonstrate the survival of some barrows and associated features beneath alluvial cover (Ripper and Butler 1999). In contrast to the examples revealed by aerial survey, where long term ploughing has levelled and truncated monuments, the sub-alluvial barrows have excellent preservation potential. Deeper cut features such as graves, pits, shafts and enclosing ditches may well preserve organic remains. The location of the sub-alluvial monuments in and adjacent to the study area should be a priority for future research. The excavations at West Cotton, Raunds highlights how nationally significant monument complexes can be masked by alluvium (Windell 1989).

While the conspicuous Neolithic and Early Bronze Age monuments have gradually been revealed in recent years, there has been little evidence of Mid-Late Bronze Age cemeteries. It would be surprising if these did not exist. While many secondary cremation burials in barrows may have perished with the plough, some flat cemeteries can be anticipated. At Eye Kettleby, on the river Wreake, almost 100 cremations were recovered in a flat cemetery (N. Finn pers. comm.). There are numerous small cropmark features in the field containing the barrow excavated by Posnansky (1953) and it is quite plausible that these might be later cremation burials. The 1756 Gentleman's Magazine reported the discovery in Kegworth of ten earthen pots containing bones which fell to pieces when touched (Meek 1999).

As well as the fine metalwork deposited in and around barrows there is an increase in deposition in watery places in the study area environs (Scurfield 1997), mirroring a national picture of depositional translocation during the Bronze Age. The Middle Trent has provided several loci for Bronze Age metalwork clusters recovered from old channels or dredging of the modern Trent (Scurfield 1997). The study area lies between two such clusters at Attenborough (ibid) and Aston on Trent (Salisbury 2004). The Attenborough finds include Early and Late Bronze Age bronze artefacts, but the majority are Mid Bronze Age in date. A sword of this date was recovered from the Trent at Ratcliffe on Soar immediately east of the study area (Scurfield 1997, 54)

[3] 'Ring ditch' sites 26 and 27 are now known to have been infilled ponds while the 'henge' site 25 appears to be a palaeochannel.
[4] Four ring ditches exactly aligned, the remaining three very closely.

The Aston on Trent site has been very prolific producing 12 bronze artefacts from probable lake deposits including rapiers and axes dating from the Mid to Late Bronze Age (Salisbury 2004). A stone and timber structure, possibly a causeway, has also been dated to the Middle Bronze Age. The structure was at least 12 x 50m and comprised irregular rows of oak piles (250-300 in total) stabilised by brushwood and quarried Mercia mudstone blocks, probably from outcrops at Weston Cliff or Kings Mill, some 2km upstream. The structure might be compared with similar structures at Flag Fen, Peterborough and in the Witham Valley (Salisbury 2004). Two Middle Bronze Age logboats have also been recovered from the Aston Lakes, one of which contained a cargo of quarried stone blocks. Another metalwork cluster recovered from the Trent at Clifton in the 1930s included 22 bronze artefacts. The site also produced many wooden piles, boats and human skulls, all undated but quite feasibly associated (Scurfield 1997).

While the monumental archaeology is rich in the study area and environs, any evidence for contemporary settlement is sparse, mirroring the national picture. Several flint scatters from the study area and environs have produced diagnostic Late Neolithic - Early Bronze Age artefacts (LE 4657, 4714, 4724, 7625, 8053 & 9715). Of these the larger scatters with wider ranges of tool forms might be the best indicators for settlement. A large pit containing Peterborough Ware was located during an evaluation at Warren Farm (Ripper and Butler 1999) while other Late Neolithic features have been recorded in the environs at Castle Donington .

Late Neolithic palaeochannels at Hemington Quarry (eastern extension) provided palaeoenvironmental indicators of a cleared floodplain with evidence for use as pasture (Beamish *et al.* 2002). Nearby woodland was mixed oak and hazel, while lime and elm probably occurred on the higher ground. Rising up the profile were indications of further clearance and increasing cereal cultivation. A slightly later palaeochannel produced further evidence for an open environment of grassland. A section of wattle panel, interpreted as a fishweir fragment, produced a date of c. 3600-3300 Cal BC, making it the earliest known in Britain[5] (Clay and Salisbury 1990).

Many Neolithic channels in the Middle Trent have produced so-called 'bog oaks', often providing the dating and locational evidence for the channels (Salisbury *et al*. 1984). These have been seen as indicative of clearance of the wildwood from the valley, that is the result of soil erosion (Knight and Howard 2004, 51). An example was observed in the Warren Farm pit during the fieldwork stage of this project.

8.5 Late Bronze Age – Iron Age

The later prehistoric period sees a rise in the archaeology of settlement across the Middle Trent area, with a trajectory away from the previous ceremonial landscape and 'towards an enclosed landscape' (Knight and Howard 2004). The large corpus of archaeological data from this period in the study area environs allows some generalisation for this landscape development (ibid; Clay 2002; Willis forthcoming). At the start of this period open settlements, often just single buildings, occur in a landscape that has started to be 'marked out' by pit alignments. The earlier ceremonial monuments are often referenced by the pit alignments showing that they still played an important role defining the physical landscape. From the Middle Iron Age settlements start to be bounded by small enclosures while by the beginning of the first millennium AD the landscape has been fully enclosed (Willis forthcoming).

[5] However, there may have been problems with the radiocarbon date nb the Current Arch article on the 'Bronze Age' date for the Hemigton mill dam site, later re-dated to the medieval period.

Late Bronze Age – Early Iron Age structures have been recorded from the environs at Swarkestone Lowes (Guilbert and Elliott 1999), Willows Farm, Castle Donington and Hemington Quarry, Castle Donington (Cooper and Ripper forthcoming). Each site has produced only single buildings, each of distinctive post-ring construction. Postholes and gullies of probable Early Iron Age date were recorded at Red Hill, Ratcliffe-on-Soar immediately east of the study area (Elsdon 1983). Later prehistoric lithic scatters have been found at Willow Farm (pers. obs.), comprising small scatters demonstrating squat flake technology and a high tool index dominated by piercers and scrapers, often with linear retouch.

Pit alignments occur across much of the environs and within the study area itself. These are dated conventionally to the later prehistoric period although a longer currency into the Roman period may occur (Deegan 1999). Knight and Howard (2004, 104-5) suggest that the dating evidence for such monuments in the Trent Valley indicates a relatively late development, concomitant with the development of an enclosed landscape. An alignment at Willows Farm, Castle Donington was undated but LBA and Iron Age pottery was recovered from features adjacent to a gap in the alignment. None of the monuments within the study area has produced dating evidence.

There is a large settlement complex within the study area that is conventionally interpreted as an Iron Age nucleated settlement (Clay 1985; Clay 2004; Liddle 1982) although essentially the complex remains undated and, arguably, much of its more regular layout may be of Romano-British date (see below). Certain earlier elements are apparent such as some of the pit alignments and the smaller enclosures that lie uncomfortably with the later settlement. The current study has allowed a re-interpretation of the latest 'phase', that is an extensive co-axial settlement flanking a major Roman road (see below).

To the north of the large settlement there are indications of Iron Age and early Romano-British settlement from a small field scatter (LE 4721). The scatter straddles the Roman road but may also be related to a faint cropmark in the field immediately to the east, which appears to represent a D-shaped enclosure with a roundhouse towards the centre. The sites provide proxy-dating evidence for the underlying channel(s).

There is some continuation of metalwork being placed in watery places into the Late Bronze Age e.g. a sword was recovered from gravel working at Church Wilne, just north-west of the study area (Hughes 1998, fig 18). These depositional practices appear to end in the Early Iron Age but there is some resumption of ritual deposition in watery contexts in the later Iron Age. The Ratcliffe-on-Soar shield was found *c.* 500m east of the study area and is thought to date to *c.* 300 BC (Watkin et al. 1996). The quality of the metalwork led to it being described as standing 'at the head of a series of British masterpieces unsurpassed in Europe' (ibid. 27). The deposition of metalwork in this area might be related to the proximity of the suspected Iron Age religious site at Red Hill, immediately east of the study area (Elsdon 1983). Of course, it may also indicate the former presence of a ford at this location (Palfreyman and Evans 2003). The Red Hill cliffs at Ratcliffe-on-Soar with their colourful striped appearance (red clay and gypsum) are a dramatic sight rising from the wide Trent floodplain and it is not too difficult to imagine how it may have been deemed a special place. There is good evidence for a Romano-British temple site at Red Hill and it has been suggested that this developed from a late Iron Age shrine site (Elsdon 1983; Palfreyman and Evans 2003).

8.6 Romano-British

There are significant Romano-British sites both within the study area and its immediate environs, that is respectively, the villa complex at Lockington and the 'small town' at Redhill, Ratcliffe-on-Soar, both having clear origins as significant Iron Age sites (Liddle 1982; Elsdon 1982). The current study has

presented fresh evidence for a Roman road passing through the study area and it would appear that the co-axial elements of the so-called Iron Age settlement are actually Romano-British.

A Roman road (Margary 182) from Little Chester (Derventio) to Sawley passes into the study area north of the modern Trent (Margary 1967, Dool 1985). The line of the road in Sawley is that of Draycott Road with a continuation beyond the modern junction with the B6540, Tamworth Road. The line would appear to turn slightly following the property boundary to Grounds Farm and the river (a slight earthwork is shown on the OS map for part of this stretch). This takes one to the Billystones ford, a known crossing point until the 18th century. While Margary (1955) believed the Derby-Sawley road terminated at the river, implying a port in the area, a crossing point and a southern continuation has been postulated (Liddle 1982; Lycett 1999; Palfreyman and Ebbins 2003).

Liddle (1982) speculated that a route existed between Redhill and Leicester and Lycett (1999) has presented a convincing case for its course, from Leicester passing through the Charnwood uplands via Anstey, Shepshed and Long Whatton into the Soar/Trent floodplain through Kegworth into the study area, i.e. Long Lane, Lockington. The Leics. SMR suggests that the route continues beyond the modern T- junction, progressing to the Soar. Immediately north of this speculative crossing point there is a report of a layer of cobbles halfway up the riverbank, feasibly the remains of a road. However, the straight route of Long Lane is that of the turnpike road; Hartley (1984) plotted the lane overlying and cutting across the grain of ridge and furrow along its course. However, it is tempting to suggest a crossing to Red Hill in this vicinity; the historical crossing of the Soar is located in this area.

A more speculative proposal for a southern route has been made by Simon Marchini (http://www.btinternet.com/~simonmarchini/History/History_Measham.htm) suggesting that the Roman road linking Tamworth and Measham might extend to Sawley. He points to the straight parish boundaries, nearly 5km long, between the villages of Diseworth, Castle Donington and Lockington-Hemington and a land parcel in Lockington called King Street plantation; such names often indicating Roman roads (Margary 1967). The parish boundary of Castle Donington and Lockington-Hemington eventually kinks to the northeast and then follows the line of the Tipnall Bank. One might speculate that this could this have been the remains of a Roman road extending to the aforementioned crossing point in the study area.

The present study has presented strong evidence for a major Roman road heading north to the crossing point of the Derventio road. The afore-mentioned King Street Plantation actually lies on the parish boundary of Lockington-Hemington and Kegworth, *between* the two postulated routes mentioned above. Meek (1999) noted that 19th century documents refer to four adjacent closes called First King Street, Far King Street, King Street and King Street. The appellation can be given to Roman roads. The parish boundary here has a relative straightness. Indeed the straight line can be traced southwards to the northern parish boundary of Belton, with one slight kink. Projected northwards the line continues into the study area and is fossilised as Warren Lane. This continues to the north as a trackway to Cliff Farm. The most convincing evidence for the route is the co-axial arrangement of the large cropmark site flanking the postulated route. The terminus is remarkably close to the aforementioned Billystones ford site, the likely crossing point of the Derventio road, and passes through the Iron Age and Romano-British scatter of LE 4721.

The cropmark (Pickering and Hartley; Clay 1985) and geophysical survey (Ripper and Butler 1999, 102) show an extensive site flanking the postulated road, comprising co-axial trackways and field boundaries. To the east there is a parallel track some 100m from the road line, partly defined by double pit alignments and/or ditches. There are *c.* 20 roundhouses in this area, but it uncertain if they are contemporary or represent earlier settlement. The western side of the roadside settlement, recently revealed by geophysical survey, has many small enclosures that may represent paddocks. The dating evidence for the scheduled site is limited to Iron Age and Romano-British pottery recovered from the

surface. However, to the west and south, evaluation trenches have provided Roman dates for associated features. The site would appear to extend further south beyond Ratcliffe Lane but the cropmark evidence is poor, possibly due to alluvial cover. Further geophysical survey of this area could prove fruitful.

Lockington villa (SAM 140), just east of the afore-mentioned settlement, comprises the well-defined cropmark site of a corridor villa within a trapezoidal enclosure with associated buildings and structures including two large barns (Frere and St. Joseph 1983; Clay 1985; Pickering and Hartley 1985). Fieldwalking survey across the villa complex produced pottery of 2nd-4th century date, while limited excavations by Deaney produced pottery of a similar date (Clay 1985). The cropmark indicates that the walls of the complex have been robbed of masonry.

A rectangular earthwork at Sawley (SAM 228) just to the east of the Derby-Sawley road 'terminus' has been claimed as a small fort (Todd 1968). The earthwork was investigated by the Derbyshire Archaeological Society revealing a near square enclosure of 0.61 ha with a possible western entrance, but secure dating evidence was not found (Deegan 1999). The SMR records that medieval pottery was recovered from a section, but there are no details. There are two other earthworks also in the study area, the Bull Ring (LE 4719), a small rectangular raised platform with a surrounding ditch and the raised platform of Cliff Farm. These are both interpreted as later features.

8.7 Anglo-Saxon

On place name evidence it is assumed that both Hemington and Lockington were established in the late Anglo-Saxon period. Early Anglo-Saxon settlement evidence is recorded from the environs at Willows Farm and Hemington Quarry, both in Castle Donington parish. Two post-built halls and a sunken featured building were excavated at Willows Farm (Coward and Ripper 1999) while at Hemington Quarry two small, post-built structures of sub-square plan were excavated (pers. obs.). An Early Anglo-Saxon pottery vessel from an associated pit provided the only dating evidence for the latter site. Small buildings of similar form were recorded at the large Anglo-Saxon site of Eye Kettleby, Leics. where the excavator interpreted them as bothies; they occured away from the settlement areas, as defined by numerous post-built halls, within a craft-working area. It might be speculated that the Hemington Quarry structures were used for temporary occupations such as task-specific seasonal waterside activities such as fishing or withy harvesting.

Within the study area the evidence for Early Anglo-Saxon settlement is limited to a small number of sherds recovered by fieldwalking (LE4713). A small number of Early Anglo-Saxon sherds were reported from Red Hill (Palfreyman and Ebbins 2003) and a larger assemblage has also been recovered (N. Cooper, pers. comm.).

Anglo-Saxon exploitation of the river is well documented in the Middle Trent with fishweirs recorded at Colwick, Notts. and Hemington Quarry. At the latter some 46 fishweirs have been reported, although many of the observations were limited to fragments showing in the quarry faces. However, four recent examples were subject to more controlled excavation and have provided unique evidence for fishing methods and technologies in inland Britain (Cooper 2003). Radiocarbon dating of the fishweirs shows a chronological range from the 8th-12th century (Brown and Salisbury forthcoming; Cooper 2003).

It is quite likely that there would have been a crossing point of the Trent in the vicinity of the study area. Doomsday mentions a ferry at the Weston estate, one of only two along the Trent. Several Saxon cross fragments have been located in the northern part of the original Hemington Quarry and it might be speculated that these were once way-place markers for a crossing point.

8.8 Medieval

The study area lies within the prime champion landscape of the Trent Valley. Much of the area to the south of the Trent comprises part of the open field system of Lockington, the settlement focus being off the floodplain to the south of the study area. Hartley (1984, map 2) has partly mapped the field system from cropmarks and earthworks of the ridge and furrow. To the north of the Trent is the parish of Sawley and the medieval core of the settlement lies within the study area but this is mainly covered by modern development.

The SMR has few records for the study area but there is great potential for archaeological remains in medieval palaeochannels of the Trent and Soar. The Lockington estate map of 1849 (LRO Ti/202/1) shows that the northeastern extent of the modern parish was originally part of Sawley, reflected in the name of Sawley Cliff Farm. The palaeochannel in this vicinity would appear to be an oxbow of the old Soar. The calendar of Patent Rolls for 1402 mentions an avulsion episode for the Trent between Sawley and Lockington (Clay and Salisbury 1990), but this probably relates to the Sawley loop.

Archaeological work at Hemington quarry has demonstrated the incredible potential for preserved riverine structures from this period and some discussion of this evidence aptly demonstrates such potential. An important bridge crossing along this stretch of the Trent was located at Hemington *c.* 1km to the west of the study area (Cooper *et al*. 1994; Cooper 2003). The crossing linked Derby and the north with Leicester and the site, effectively the major route now known as the A6. Three successive bridges were excavated at Hemington Quarry between 1993-8. The earliest was a timber bridge constructed in 1097 and partly rebuilt *c.* 1111, evidently due to severe flood damage. The bridge was superseded by another timber structure in the later 12th century that in turn was replaced by a large masonry bridge in 1240/1. Each was built slightly upstream of its predecessor, demonstrating the importance of the crossing location. Documentary and proxy archaeological evidence suggest that the bridge crossing was redundant by *c.* 1311/12 when the Wilne Ferry was established, near the site of the modern crossing at Cavendish Bridge (Courtney forthcoming; Cooper 2003). The Sawley Ferry was established in 1321, possibly also reflecting the loss of the Hemington bridge crossing (Cooper and Ripper forthcoming). This was probably located at the site of the modern crossing of Harrison Bridge, in the northwestern corner of the study area.

Another class of monument recorded at the quarry was the 'shoot'. Salisbury (1985) described surviving 18th century 'shoots' (from the waterman vernacular) along the Trent, these being bankside works of stone and timber designed to protect the banks from erosion (their name derived from the local waterman vernacular). Up to six examples of 'shoot' structures have been recorded from the right (Leicestershire) bank of the medieval channel (Cooper & Ripper 2000; 2001) several dated to the 1320s (R. Howard, pers. comm.). It is suggested that the shoots were near-contemporary measures to protect the eroding right bank of the medieval river. The associated channel was traced for almost 500m, showing evidence for dynamic bank erosion (clasts of anaerobic clay from silted palaeochannels) and deep scouring, cutting through Devensian gravels, occasionally into the Mercian mudstone below. The evident dynamism of the channel would seem to reflect the national picture of climatic downturn seen in the period 1310-30 when severe winters caused damage to bridges almost every year (Brown *et al*. 2001) and, as suggested above, probably destroyed Hemington Bridge III and led to channel avulsion.

Hemington Quarry has also revealed rare structural and artefactual evidence for inland fishing in the form of 46 fishweir structures, numerous anchor stones and several fish traps (Salisbury 1991; Cooper 2003). A large weir structure (HL12), possibly a 'fixed engine' fishery was associated with fish baskets up to 2m long (Cooper 2003). However, the structure bears some resemblance to the 12th century mill dam excavated in 1985 (Clay and Salisbury 1990). The apparent demise of fishweirs from the 12th century may reflect the changing use of the river with water mills exacting greater control over the river.

8.9 Post-medieval

The Lockington estate has been described as old enclosure by Nichols and the open field system was likely to have been enclosed between 1601 and 1607 (Beresford 1948, 109). Warren Farm probably dates to this period (Smith and Ripper 2000) but its early status is uncertain. The early 18th century saw major investment in the road networks and much of the medieval landscape of the study area was lost to the new turnpike routes and enclosure. The study area was traversed by several major routes at this time, the Derby-Leicester road (modern A6) and the Tamworth-Sawley road (B6540). By the 18th century the respective crossings for these routes were bridges, Cavendish Bridge (1758) and Harrington Bridge (1788) across the Trent, each being the site of earlier ford and ferry crossings. The river crossing at Ratcliffe on Soar remained a ford until the construction of the Kegworth to Nottingham road (A453).

The 18th century also saw the rapid development of water transport with works to make the Trent navigable in the early 18th century, followed by the Soar Navigation and the Erewash Canal later in the century. There was a customs house at Cavendish Bridge and, in the study area, associated wharf development at Sawley. By the 19th century the area had several farms including Lockington Grounds Farm, Warren Farm and Long Lane Farm and, in Sawley, Grounds Farm. Warren Farm was a fine example of a model farm and was fully recorded prior to demolition (Smith and Ripper 2000). This agricultural landscape remains but has been further impinged upon by modern transport (M1 motorway, A453, A50), development (Sawley Marina) and mineral extraction.

8.10 Geomorphology and the archaeological resource

The archaeological resource within the study area has been identified though consulting the SMR databases at Leicestershire and Nottingham County Councils. This SMR search creates a 'known' archaeological resource, containing data on the location, morphology and in some cases dating evidence, of the archaeology. Conversely, the study area also has an 'unknown' archaeological resource, which is comprises of the undiscovered archaeological artefacts and sites. The known archaeological resource has been identified due to the 'visibility' of the sites and artefacts to conventional methods of archaeological detection. Such site detection methods are principally air photography and fieldwalking.

The BGS drift geology map provides the basis for describing the relationship of the archaeology to the geomorphology, labelling one area of older Devensian terrace (terrace 2), with younger Holocene drift geology making up terrace 1 and the modern floodplain (Fig. 8.1). The archaeological resource can be plotted against the LiDAR last pulse DTM to investigate patterns of the archaeological resource related to the terrace sequence (Fig. 8.2). The archaeological resource is plotted by method of investigation and two clear trends come out from the data. The 'known' archaeological resource effectively clusters on terrace 2. On terrace 1 and the modern floodplain there are six SMR entries, compared to nineteen entries on the much smaller area of terrace 2.

The method of identification highlights a second key trend. The greater number of SMR entries located on terrace 2 have been identified through three methods. Ten sites have been identified through cropmarks, seven sites from surface finds and two sites through excavation. This can be compared to the known archaeological resource within the Holocene deposits, which have identified two sites through earthworks, three sites from surface finds and only one from cropmarks.

The geomorphology of the terrace 2 deposits provides the explanation for the distribution of the known archaeological resource. The GPR investigations on terrace 2 have shown the terrace has a thin layer of alluvium overlying deep gravels deposits. The shallow alluvium (circa 40cm and often less) has meant the archaeological resource contained within it is visible. Much of the alluvium covering the terrace 2 gravels is within the plough zone. Therefore, archaeological structures can affect plant growth, identifying archaeology as cropmarks. The ploughing action has also disturbed artefacts allowing identification through surface survey/field walking.

The known archaeological resource in the Holocene deposits consists of one human skull as a surface deposit (SMR number 4683, terrace 1) but it is thought to be a disturbed deposit from stream dredging. The one cropmark (SMR 22595) was identified though a spectral air borne scanner. The two earthworks include a possible Roman Fort on terrace 1, although the site is more probably a post medieval enclosure (SMR 4719) and also a post medieval farmstead (SMR 4716). Of potential significance is a pottery spread of Iron Age/Romano-British (SMR 4721) located on terrace 1.

The known archaeological resource can also be plotted by the period of each site (Fig. 8.3). The Devensian terrace has a diversity of prehistoric sites and find locations, such as the Lockington Villa complex (Fig. 8.4). Whilst the terrace 1 deposits do not have such a visible archaeological record there are reasons to expect that terrace 1 has a significant archaeological resource. Terrace 1 has an Iron Age/Roman pottery scatter located on it. A second site not listed on the SMR database is visible as a cropmark (Fig. 8.5). Although there has been no dating evidence on this site its morphology (a D shaped enclosure) does suggest a Late Iron Age/Roman date. These two sites are strong evidence for later prehistoric/Roman activity and possible settlement on Terrace 1.

The reasons for the apparent invisibility of the archaeological resource on terrace 1 relates to riverine erosion and alluvial deposition on the terrace. Major channels have eroded away substantial areas of terrace 1. In this process, areas of the archaeological resource will have been destroyed. Secondly, as shown through Fig. 8.4, some archaeology has been buried by alluvial deposition. For example the GPR transect T1T1 showed the alluvial deposition from T1C5 that has partially buried the D shaped enclosure T1C5.

This process of alluvial deposition on terrace 1 was also discovered through the T1G1 survey, on a fragment of terrace 1 adjacent to a palaeochannel. In this instance over 1.4m of alluvial deposition was discovered before the terrace 1 gravels were discovered. The quarry transect (T1QT) also demonstrated that areas of terrace 1 will have substantial levels of alluvial deposition on top of the terrace gravels. Therefore, it is suggested that specific areas of terrace 1 will have a high archaeological potential dating back at least to the later prehistoric period, due burial and preservation under more recent alluvial deposition.

The archaeological potential on the modern floodplain is likely to be lower than terrace 1. Although the date range of the modern floodplain is not known, the level of alluvial deposition onto gravels was shown to be generally shallow (survey MFG1). Considering this factor plus the younger age of the modern floodplain compared to terrace 1 (although neither are dated) the archaeological potential is considered to be lower. However, this does not preclude the possibility of significant archaeological remains on the modern floodplain, giving that the age of the modern floodplain has not yet been absolutely dated (see chronostratigraphy Chapter 9).

Fig 8.1: The study area mapped by geological stage.

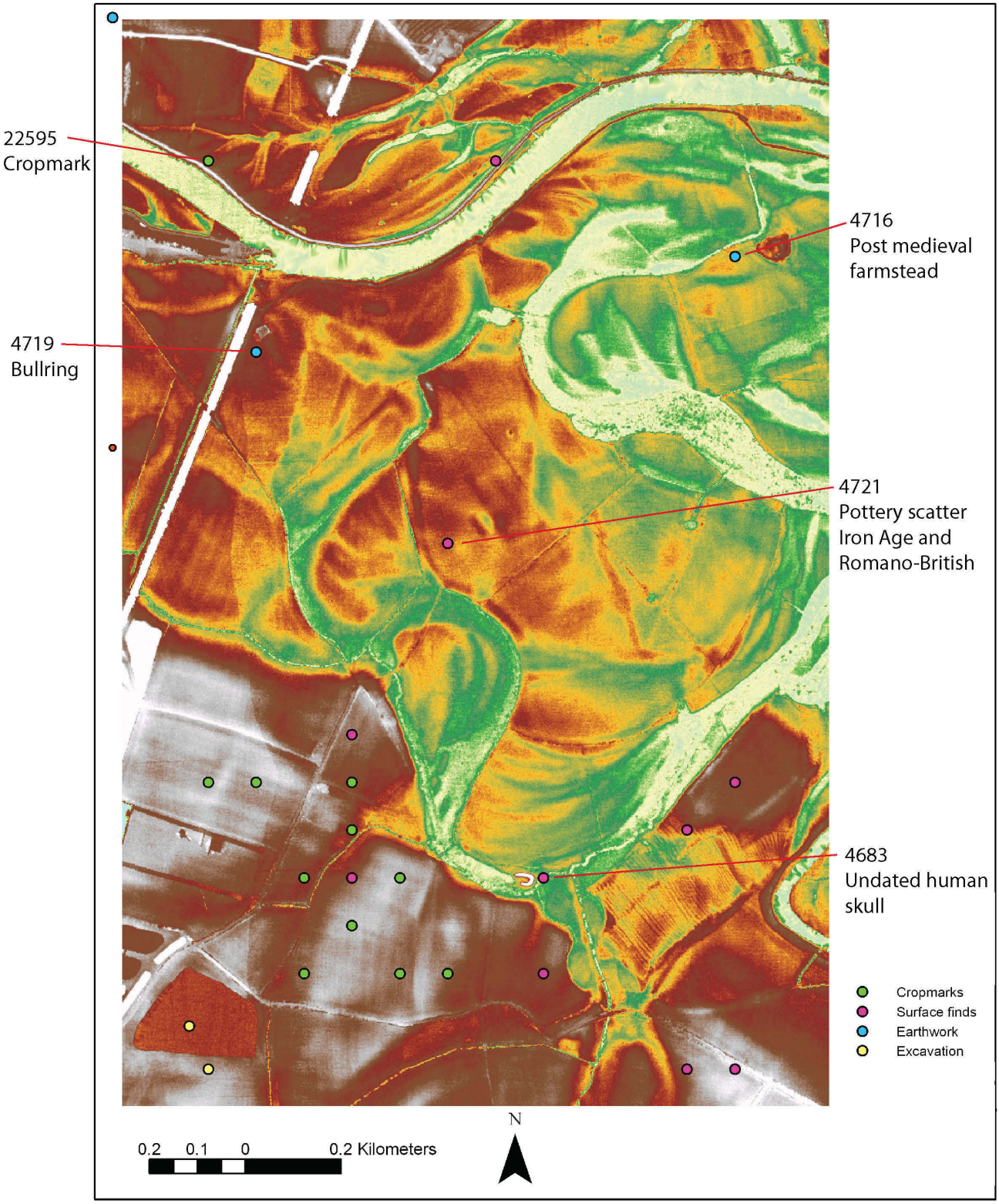

Fig 8.2: The archaeological resource plotted by its method of investigation, against the LiDAR last pulse DTM.

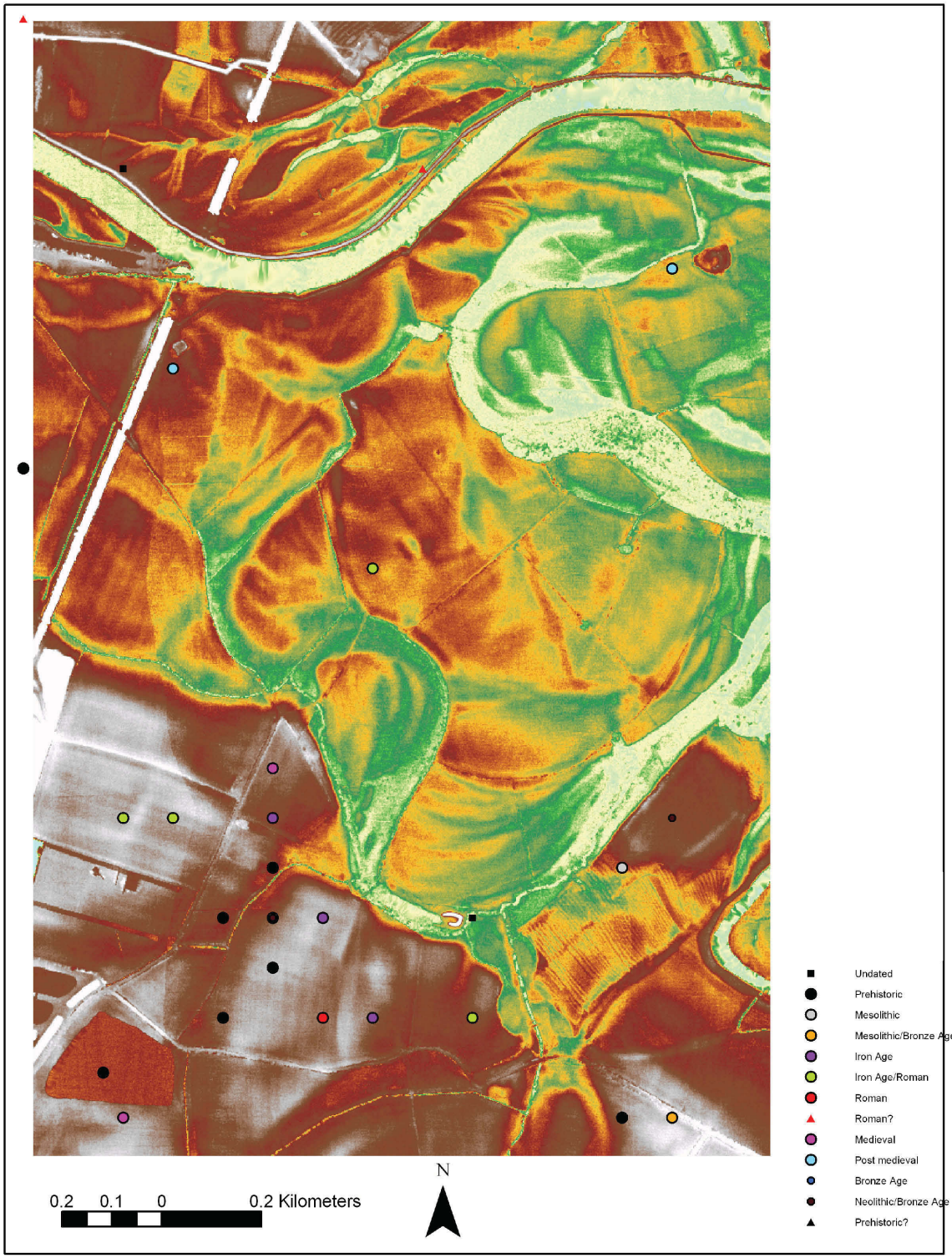

Fig 8.3: The archaeological resource plotted by period.

Fig 8.4: The 'Lockington Villa' complex within the study area. The complex contains a wealth of archaeological features, which are interpreted as dating from a range of periods, from the later prehistoric through to the Romano-British and possibly, post Romano-British periods. The complex is located on the Devensian terrace 2.

Fig 8.5: The cropmark enclosure on terrace 1. Although the enclosure is undated its morphology suggests a later prehistoric/early historic date.

8.11 Conclusions

The Trent-Derwent-Soar confluence zone, is an area with demonstrable, abundant archaeological remains from the Palaeolithic to the present while the study area encompasses significant known archaeological remains from the Mesolithic to present and great potential for remains as yet undiscovered. The cropmark evidence from the study area environs is very prolific on the terraces and new and old aerial photographs are a great resource. Indeed the present study has highlighted a number of new monuments in the study area and immediate environs including a possible pit circle, five ring ditches, a D-shaped enclosure, two pit alignments and other pre-medieval field boundaries. Further desk-based assessment has also proved fruitful in highlighting evidence for suspected Roman crossings of the Soar and Trent.

Previous geoarchaeological work in the environs has demonstrated the great mobility of the rivers in this confluence zone. This dynamism has undoubtedly truncated much archaeological evidence but has also been an agent of preservation, sealing sites under or within alluvium, such as the barrows mentioned above, and burying riverine sites within sand and gravel bars, most ably demonstrated by the discoveries at Hemington Quarry. The proximity of the latter site would suggest considerable potential for the study area.

One of the dominant themes to emerge from recent studies of the Trent Valley is the river as a physical and cultural boundary. While the river does, in a broad sense, delimit north and south, upland and lowland, possibly even different ethnic groups (Vince forthcoming), it also acts as a natural communications node along the waterways and through the valleys. The present study has presented some evidence for the importance of the study area as a central node in the regional communications network.

For the hunter-gatherers the zone would have been a crossing point for migrating animals and it is likely that the social and economic territories of the humans extended between upland and lowland. It is quite feasible that later prehistoric groups continued such movements in a transhumant economy. An appreciation of past communications and transport can be gained by examining the distribution of products and raw materials in the region. Loveday (2004) draws attention to the cluster of Charnwood Group XX axes around the Arbor Low henge environs. He has pointed to the 'exceptional potential' of the Middle Trent in understanding wider cultural and material connections in the Neolithic and Bronze Age. The ceremonial landscape of the study area and environs, in particular the cursus monuments, are seen to mediate these relations. Charnwood grano-diorite tempered pottery of Iron Age date has been widely recognised north of the Trent (Knight *et al.* 2003). In the Roman period Palfreyman and Ebbins (2003) have examined the role of the Red Hill site in the distribution of commodities and raw materials including iron, lead, coal, pottery, gypsum and salt. Similar distribution networks can be envisaged for the medieval period where there is a proliferation of markets around the Middle Trent. Courtney (forthcoming) has shown that the Trent was a very permeable barrier and that in the medieval and post-medieval period one would rarely have to travel over 2km to a crossing point. The major crossings such as Hemington, just outside the study area, formed part of the national infrastructure of roads while the Sawley crossing would have served these local markets and link to the larger network.

CHAPTER 9: CRONOSTRATIGRAPHIC MODELLING

9.1 Methodology

This model (Fig. 9.1) has been constructed using a correlation of the target area data listed below and a number of studies within this reach of the Trent largely from the Hemington area.

Target Area Data Sources	Data Sources Outside the Target Area
LiDAR – GPS altitude map	Hemington Bridges pit Report and maps
LiDAR intensity palaeochannel map	Hemington Western Extension chronostratigraphic model (Brown, in press)
Geomorphological map	Hemington Eastern Extension chronostratigraphic model (Brown, in press)
Geological map (BGS)	Dating of other palaeochannels (e.g. A6, Sawley)
GPR transects	Geological mapping (BGS)
Coring transects	MFT1, T1T1, T1T2, T2T1

Tab 9.1: Data sources used in the chronostratigraphic modelling

The palaeochannels segment the area into a series of levels:

High 38.7m OD
Middle 34.0m OD
Low 28.2m OD

It is apparent from flood photography that high magnitude floods within the contemporary flood frequency-magnitude distribution can inundate both the lower and middle levels but not the high surfaces of the Devensian terrace 2. The high level is also seen to correlate to the south and southwest with the large area of Beeston terrace as mapped by the BGS. However, both the LiDAR and GPR show broad shallow channels excavated into the surface of the terraces and by analogy elsewhere (Fyfe *et al*. 2004) these are most likely channels formed during the final stages of gravel deposition during the Lateglacial. There are, however, in this reach some deeper narrower channels that bisect the terraces and have been shown to be of early to mid Holocene age (Brown and Salisbury in press). The middle level is characterised by gravel overlain by a variable thickness of overbank sandy silts and clays. It correlates with similar floodplain parcels to the east including meander cores at Hemington. It also has later Prehistoric and Roman archaeology on its surface. It is bisected and eroded into by the southerly of the two major palaeo-Trent meander loops traversing the target area. The complex form of this palaeochannel, its significant depth of sediment and its truncation of later Roman channels all suggest a late prehistoric age. The series of scroll bars on its inner (northerly) floodplain suggest that over time it moved in a southwesterly direction and on this basis the meander core is also ascribed to the late Prehistoric period. This palaeochannel and floodplain is truncated by the large partially water-filled Trent palaeochannel. There are many similarities in altitude, form and location between this channel and the medieval channels associated with the Old Trent at Hemington. The width of the meander belt and its sinuosity are similar to the Sawley palaeochannel that is of Roman-6th Century age but a correlation cannot be proven. Closer to the channel there are a number of old channels sub-parallel to the modern Trent. In some cases the connections are only severed by an artificial levee. This zone also contains engineered river sections and channels such as the Sawley Cut and straightened sections of the Soar.

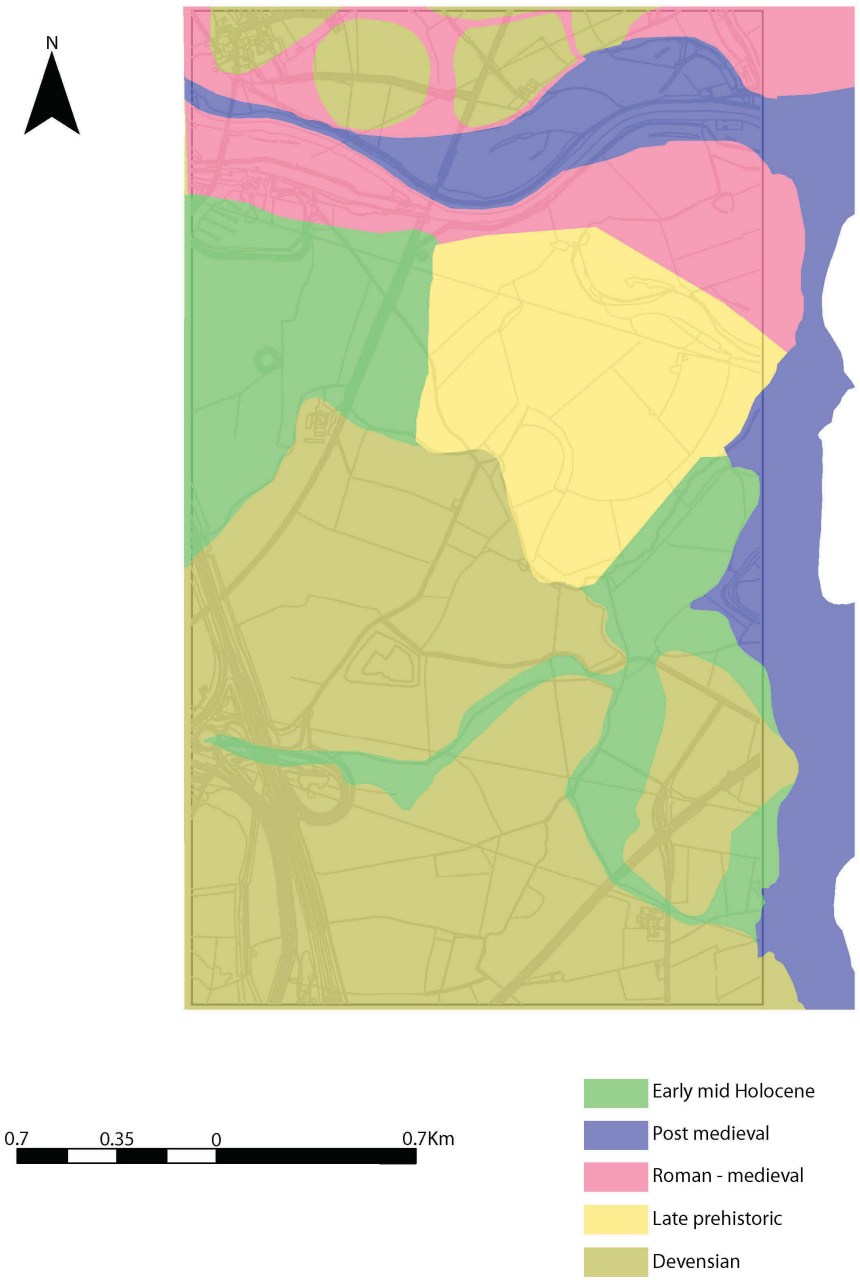

Fig 9.1: Chronostratigraphic model map of the Trent-Soar Junction.

9.2 The Chronostratigraphic Cross-section

This hypothesized cross-section (Fig. 9.2) has been based on the topography and estimated dating provided by the surface model. Sub-surface is generalized following stratigraphic and sedimentological observations at Hemington (including both the east and western extensions), the current Lafarge quarry at Sawley, faces exposed at Aston and earlier quarries as well as borehole records.

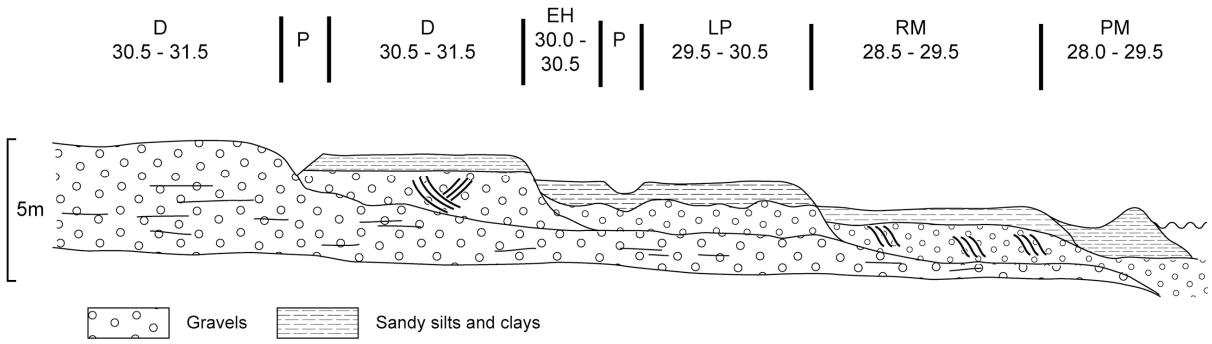

Fig 9.2: Hypothesised cross section across the study area.

The key question of archaeological significance is the depth of the Holocene sand and gravel and whether it overlies Devensian gravels. The fundamental problem is that the Devensian and Holocene gravels are very similar in grain size, clast lithology, shape and even fabric due to the derivation of the later from the former. This means that it is rarely possible to differentiate them from borehole records. It is possible from quarry faces due to the presence of archaeology, a different colour (due to Fe staining) and sometimes a different sedimentary structure. From the observations at Hemington it is hypothesized that the Devensian gravels underlie all the later phases of floodplain sedimentation with the exceptions of areas of scour near the present channel.

The testing of these models and their refinement forms a principal component of Phase II of this project.

CHAPTER 10: CONCLUSIONS AND FUTURE DIRECTIONS

10.1 Conclusions

The conclusions of the project are listed below in summarized form. More discussion of each can be found at the end of each of the relevant chapters.

- GPR technical questions relating to transect location, spacing, frequency choice, signal amplification and calibration are considered in the report and shown to require both some compromise and specification on different surfaces of the valley floor depending upon the sediment stratigraphy and height relative to the groundwater table.

- Radar penetration was greater over gravel-dominated bodies (up to 4+m) than over lower saturate palaeochannels where it could be less than 1m.

- In general penetration increased with height above the river level and local water table although this is complicated by the accompanied systematic changes in sediment type.

- The edge of terrace features and palaeochannels were well represented in the GPR transects and 3D models.

- On all surface levels there was good agreement between the GPR survey and gouge auger transects down to the buried surface of the gravels with the exception of the deepest parts of the lowest palaeochannels.

- In several locations GPR transects suggested sand and gravel bars associated with palaeochannels and these could have high potential for the burial of archaeology (as at Hemington).

- LiDAR intensity values appear to reflect changes in subsurface stratigraphy and sediment types.

- The LiDAR intensity values could not identify individual cropmarks but could identify areas in which cropmarks were likely to form.

- The LiDAR last pulse DTM produced an excellent topographic model of the study area and differentiated between the main geomorphological units.

- The LiDAR last pulse DTM reflected mircrotopographic variation within the geomorphological units and could identify natural features, e.g. ridge and swale and cultural features, e.g. ridge and furrow.

- On the LiDAR last pulse DTM the 1m resolution produced the best results, with a 2m resolution producing acceptable results but the 5m and 10m resolutions producing an appreciable loss in data quality.

- The combination of LiDAR with GPR depth slices has high potential for the 3D modelling of sediment stratigraphy even in such complex alluvial contexts.

- The known archaeological resource in the study area clusters on terrace 2 (upper surface) but not exclusively.

- The patterns of the archaeological resource are a result of differential taphonomy, visibility, and intensity of archaeological survey.

- The archaeological resource on terrace 1 (middle two LiDAR surfaces) has been affected by channel erosion recorded by palaeochannels and deposition by both lateral and overbank sediments.

- Only a small area of the study area, that on the lowest surface (modern floodplain), can be considered archaeological sterile and even this area contains post-medieval archaeology which may or may not be significant depending upon its character.

- The chronostratigraphic model suggests discrete zones of archaeological potential:

    - Palaeolithic to post-medieval (upper surface, terrace 2)
    - Late Devensian to mid Holocene (mid surface and palaeochannels, terrace 1)
    - Late Prehistoric (mid surface and palaeochannels, terrace 1)
    - Roman-Medieval (mid surface and palaeochannels, terrace 1)
    - Post-Medieval (lowest surface, modern floodplain)

- Although difficult to discontinue the use of the term modern floodplain for the lowest surface of the valley floor alone is, at least in this location, misleading on both hydrological and archaeological grounds.

- Using a combination of geomorphological mapping, dGPS, IFSAR, LiDAR and GPR a predictive chronostratigraphic model of the confluence zone was produced. This model will be tested in phase II by coring, sediment characterization and a dating programme.

11.0 Future directions

A full expansion of the Phase 2 project is provided in the Phase 2 UPD drafted by Brown et al. However, in summary, the aims of Phase 2 are to:

- Refine the detailed surface and subsurface landscape models of the study area developed during Phase 1, placing them within a secure, high resolution chronostratigraphic and palaeoenvironmental framework.
- Use this information to study the impact of confluence evolution on the archaeological environment over a time-scale of millennia and at spatial scales appropriate for archaeological management.

- Consider how data capture, archaeological preservation and the development of landscape evolution models and robust chronological frameworks within alluvial environments are affected by physical and chemical factors (i.e. taphonomic processes), especially dating evidence derived from organic-filled palaeochannels and other geomorphological contexts.
- Apply additional geophysical techniques to transect survey lines already surveyed using GPR to compare the effectiveness of different techniques within the alluvial zone.
- Continue to present the results of this work to a range of end-user communities.

These aims will be achieved through:

- coring across of a number of palaeochannel segments of demonstrably different ages to recover sediments for: (1) radiometric dating (^{14}C and OSL); (2) palaeobiological analysis using pollen and insect remains; and (3) measurement of physical and chemical properties.
- Radiometric (OSL) dating of sandy sediments recovered from bar-top and in-channel contexts.
- Refinement of stratigraphic models through the analysis of borehole data supplied for the confluence area by La Farge Aggregates Ltd.
- Characterisation of the hydrological environment using a combination of data provided by La Farge Aggregates Ltd (from borehole well logs) and soil moisture data collected by the research team.
- Additional geophysical survey of established transect lines using Electrical Resistivity Ground Imaging (ERGI), especially being used to investigate palaeochannel deposits.
- Presentation of the results at workshops, conferences, and through written reports/papers aimed at a number of different audiences (e.g. curators, field archaeologists and academics).

BIBLIOGRAPHY

Baker, S. 2003. *The Trent Valley: Palaeochannel Mapping from Aerial Photographs.* Trent Valley Geoarchaeology Research Report. Nottingham, Trent & Peak Archaeological Unit.

Barnes, I. 2003. Aerial remote-sensing techniques used in the management of archaeological monuments on the British army's Salisbury Plain training area, Wiltshire, UK'. *Archaeological Prospection,* **10**, pp. 83-90.

Barton, R.N.E. 1992. *Hengistbury Head: The Late Upper Palaeolithic and Early Mesolithic sites*. Monograph Series. Oxford University Committee for Archaeology.

Barton, R.N.E. 1997. *Stone Age Britain.* Swindon: English Heritage.

Barton, R.N.E. Jacobi, R.M. Stapert, D. and Street M.J., 2003. The Late-glacial reoccupation of the British Isles and the Creswellian. *Journal of Quaternary Science,* **18(7)**, pp. 631-643.

Beamish, M., Monckto, A., Brown, A.G., Greenwood, M.T. and Smith, D.N. 2002. *Late Glacial, Neolithic, Bronze Age and medieval environments from Hemington Quarry (Eastern Extension), Castle Donington, Leicestershire.* ULAS report 2002/166. Unpublished, deposited with Leics. SMR.

Bewley, Robert H. 2003. Aerial survey for archaeology. *The Photogrammetric Record,* **18 (104)**, pp. 273-292.

Bishop, M. (2003). Issues and agenda in archaeological research and management: a case study from the Trent Valley, UK. In Howard, A.J., Macklin, M.G. and Passmore, D.G. (eds) *Alluvial Archaeology in Europe.* Lisse: Balkema: pp. 123-131.

Bridge, J., Collier, R. and Alexander, J. 1998. Large-scale structure of structure of Calamas River deposits (Nebraska, USA)revealed using ground penetrating radar. *Sedimentology*, **45**, 977 – 986.

Bristow, C. S., Lancaster, N. and Duller, G. A. T. 2005. Combining ground penetrating radar surveys and optical dating to determine dune migration in Namibia. *Journal of the Geological Society*, **162**, pp. 315 – 321. London.

Brophy, K. 1999. Seeing the cursus as a symbolic river, *British Archaeology,* **44**.

Brown, A. G. and Salisbury, C. R. in press. Geomorphology. In L. Cooper and S. Ripper (Eds.) *The Hemington Bridges Project*. English Heritage/ULAS, Leicester.

Campbell, J.B. 1977. *The Upper Palaeolithic of Britain: a Study of Man and Nature in the Late Ice Age*. 2 vols. Oxford. Clarendon Press.

Challis, K. 1995. *A564 Derby Southern Bypass Contract B. Rookery Lane: Archaeological assessment and evaluation.* Unpublished report, Nottingham University Consultants.

Clay 1985 A survey of two cropmark sites at Lockington-Hemington, Leicestershire, *Transactions of the Leicestershire Archaeological and Historical Society*, **59**, pp. 17-26.

Clay, P. 1998. Neolithic/Early Bronze Age Pit Circles and their Environs at Burley Road, Oakham, Rutland. Proceedings of the Prehistoric Society, **64**, pp. 293-330.

Clay, P. 2002. *The Prehistory of the East Midlands Claylands,* Leicester Archaeology Monographs No. 9. School of Archaeology and Ancient History, University of Leicester.

Clay, P. and Salisbury, C.R. 1990. A Norman mill dam and other sites at Hemington fields, Castle Donington, Leicestershire', *The Archaeological Journal*, **147**, pp. 276-307.

Cooper, L., 2001 The Glaston glutton and other strange beasts, *Rescue News*, **83**, pp. 1-3

Cooper, L. 2002a. 'A Creswellian campsite, Newtown Linford', *Transactions of the Leicestershire Archaeological and Historical Society*, **76**, pp.

Cooper, L. 2002b. *The lithics in M. Beamish, Archaeology of the Wing to Whatborough Hill Trunk Main,* ULAS report 2002/099.

Cooper, L.P. 2003. Hemington Quarry, Castle Donington, Leicestershire, UK: a decade beneath the alluvium in the confluence zone, in A.J. Howard, M.G. Macklin and D.G. Passmore (eds), *Alluvial Archaeology in Europe*, *A.A. Balkema*, pp. 27-42.

Cooper, L. and Jacobi, R. 2001. Two Late Glacial finds from north-west Leicestershire, *Transactions of the Leicestershire Archaeological and Historical Society*, **75**, pp. 118-121.

Cooper, L., Ripper, S., & Clay, P. 1994. The Hemington bridges, Current Archaeology, **140**, pp. 316-21.

Cooper, L. and Thomas, J. 2001. Glaston, Grange Farm, *Transactions of the Leicestershire Archaeological and Historical Society*, **75**, pp. 158-9.

Cooper L. & Ripper, S. 2000. Castle Donington, Hemington Quarry (SK 455 299), Transactions of the Leicestershire Archaeological and Historical Society, **74**, pp. 233-5.

Cooper L. & Ripper, S. 2001. Castle Donington, Hemington Quarry (SK 455 299), *Transactions of the Leicestershire Archaeological and Historical Society,* **75**, pp. 137-42.

Cooper, L. and Ripper, S. forthcoming a. *The Hemington Bridges.*

Cooper, L. and Ripper, S. forthcoming b. *Excavations at Hemington Quarry Western Extension.*

Cooper, N.J. (ed), in prep. *An Archaeological Resource Assessment and Research Agenda for the East Midlands*. http://www.le.ac.uk/ar/east_midlands_research_framework.htm

Courtney, P. forthcoming. Hemington Bridge in its historical context, in L. Cooper & S. Ripper (eds) *The Hemington Bridges*.

Coward, J. and Ripper, S. 1999. *Castle Donington*. Willow Farm.

Davis, R., 1999 Bronze Age Metalwork from the Trent Valley, Newark, Notts, to Gainsborough, Lincs. *Transactions of the Thoroton Society,* **103**, pp. 25-48.

Deegan, A., 1999. *The Nottinghamshire Mapping Project*, unpublished RCHME report.

Dool, J. 1985. 'Derby Racecourse; Excavations on the Roman industrial settlement, 1974', *Derbyshire Archaeological Journal*, **105**, pp. 155-221.

Ekes, C. and Friele, P. 2003. Sedimentary architecture and post-glacial evolution of Cheekye Fan, southwestern British Columbia, Canada, in, C. S. Bristow and H. M. Jol, *Ground Penetrating Radar in Sediments*, Geological Society Special Publications, pp. 87 - 98. London.

Elliott, L., and Knight, D. 1999. 'An Early Mesolithic and first millennium BC settlement and pit alignments at Swarkestone Lowes, Derbyshire', *Derbyshire Archaeological Journal*, **119**, pp. 79-153.

Elsdon, S.M. 1983. Iron Age and Roman sites at Red Hill, Ratcliffe on Soar, Nottinghamshire: excavations of E. Greenfield, 1963 and previous finds, *Transactions of the Thoroton Society*, 86, pp. 14-48.

Fiedorczuk, J. and Schild, R. 2002. Wilczyce – a new late Magdalenian site in Poland in B.V. Eriksen and B. Bratlund (eds), *Recent Studies in the Final Palaeolithic of the European plain, Jutland Archaeological Society*, 91-100.

Field, D. 1999. *Bury the dead in a sacred landscape*. British Archaeology 43

Frere, S.S. and St. Joseph, J.K. 1983. *Roman Britain from the air.* Cambridge University Press.

Fyfe, R. M., Brown, A. G. and Coles, B. J. 2004 Vegetational change and human activity in the Exe Valley, Devon, UK. *Proceedings of the Prehistoric Society* 69, 161-182.

Garrod, D.A.E. 1926. *The Upper Palaeolithic Age in Britain.* Oxford. Clarendon Press.

Garton, D., 1993. 'A Late Upper Palaeolithic site near Newark, Nottinghamshire', *Transactions of the Thoroton Society*, **98**, pp. 126-9.

Graf, A. 2002. Lower and Middle Palaeolithic Leicestershire and Rutland: progress and potential, *Transactions of the Leicestershire Archaeological and Historical Society*, **76**, pp. 1-46.

Greenwood, M. T. Agnew, M. D. and Wood P. J. 2003. The use of caddisfly fauna (Insecta: Trichoptera) to characterise the Late-glacial River Trent, England. *Journal of Quaternary Science*, **18(7)**, pp. 645-661.

GSSI. 2004. *Radan 6.0 Users Manual*. New Hampshire, USA.

Heinz, J. and Aigner, T. 2003. Three dimensional GPR analysis of various Quaternary gravel-bed braided river deposits (southwestern Germany), , in, C. S. Bristow and H. M. Jol, *Ground Penetrating Radar in Sediments*, Geological Society Special Publications, pp. 99 - 110. London.

Hughes, G. 2000. *The Lockington Gold hoard. An Earlier Bronze Age barrow cemetery at Lockington, Leicestershire.* Oxford: Oxbow Books.

Hughes, G. and Roseff, R., 1995. Excavations at Croft Quarry (SP 517 968), Transactions of the Leicestershire Archaeological and Historical Society, **69**, pp. 100-108.

Hughes, R.G. 1999. Some unrecorded prehistoric tools from Derbyshire, Derbyshire Archaeological Journal, **119**, pp. 5-11.

Intermap. 2003. *Intermap Product Handbook*. Intermap Technologies.

Jacobi, R.M., 1980 'The Upper Palaeolithic in Britain, with special reference to Wales', in J.A. Taylor (ed), *Culture and Environment in Prehistoric Wales*, BAR British Series 76, Oxford, pp. 15-99.

Jacobi, R.M. 1982. Later hunters in Kent: Tasmania and the earliest Neolithic, in P.E. Leach (ed), *Archaeology in Kent to AD 1500*. CBA Research Report No **48**.

Jacobi, R., 1990 Leaf-points and the British Early Upper Palaeolithic in J.K. Kozlowski (ed) *Feuilles de Pierre: Les Industries à Pointes Foliacées du Paléolithique Supérieur Européen*. Études et Recherches Archéologiques de l'Université de Liège, **42**, pp. 271-89.

Jacobi, R., 1991. The Creswellian, Creswell and Cheddar, in N. Barton, A.J. Roberts and D.A. Roe (eds), *The Late Glacial in north-west Europe*: *Human adaptation and environmental change at the end of the Pleistocene*. CBA Research Report **77**.

Jacobi, R., 1997 'The 'Creswellian' in Britain', in J.-P. Fagnart and A. Thévenin (eds), Le *Tardiglaciaire en Europe du Nord-Ouest.* Paris. Éditions du Comité des travaux historiques et scientifiques, pp. 497-505.

Jacobi, R.M. 1978a. Population and landscape in Mesolithic lowland Britain, in S. Limbrey and J.G. Evans (eds), *The Effect of Man on the Landscape*, CBA Research Report **21**, pp. 77-85.

Jacobi, R.M. in press. The Late Upper Palaeolithic Lithic Collection from Gough's Cave, Cheddar, Somerset and Human Use of the Cave, *Proceedings of the Prehistoric Society*, **70**, 1-92.

Jacobi, R., Garton, D. and Brown, J. 2001. Field-walking and the Late Upper Palaeolithic in Nottinghamshire, *Transactions of the Thoroton Society*, **105**, pp. 17-22.

Knight, D. and Howard, A.J. 1994. 'The Trent Valley Survey', *Transactions of the Thoroton Society,* **99**, pp. 126-9.

Knight, D. and Malone, S. 1997. Evaluation of a Late Iron Age and Romano-British Settlement and Palaeochannels of the Trent at Chapel Farm, Shardlow and Great Wilne, Derbyshire, *unpublished Trent and Peak Archaeological Trust Report* (Derbyshire SMR).

Knight, D. and Malone, S. 1998. Further evaluations of an Iron Age and Romano-British Settlement and Fluvial features at Chapel Farm, Shardlow and Great Wilne, Derbyshire, *unpublished Trent and Peak Archaeological Unit Report* (Derbyshire SMR).

Knight, D., Malone, S., Howard, A.J. and Appleton, E. 1999. Chapel Farm, Shardlow, *Derbyshire, Archaeological Journal*, **119**, pp. 286.

Knight, D., Marsden, P. and Carney, J. 2003. 'Local or non-local? Prehistoric granodirorite-tempered pottery in the East Midlands' in A. Gibson (ed) *Prehistoric Pottery. People, Pattern and Purpose*. Oxford: British Archaeological Reports International Series, **1156**, pp. 111-125.

Knox, R. 2005. An archaeological resource assessment of the Mesolithic in Leicestershire and Rutland, East Midlands Archaeological Research Framework, online paper. http://www.le.ac.uk/archaeology/pdf_files/08leicmeso.pdf

Jol, H. M. and Bristow, C. S. 2003. GPR in sediments: a guide to good practice, in, C. S. Bristow and H. M. Jol, *Ground Penetrating Radar in Sediments*, Geological Society Special Publications, pp. 9 - 27. London.

Loveday, R. 2004. Contextualising monuments: the exceptional potential of the Middle Trent Valley, *Derbyshire Archaeological Journal,* **124**, pp. 1-12.

Mangerud, J., Andersen, S.T., Berglund, B.E. and Dönner, J.J. 1974. Quaternary stratigraphy of Norden, a proposal for terminology and classification, Boreas, **3**, pp.109-127.

Margary, I., 1967. *Roman Roads in Britain*. London.

McNabb, J. forthcoming. 'An Archaeological Resource Assessment and Research Agenda for the Palaeolithic in the East Midlands (part of Western Doggerland)' in N. Cooper (ed.) forthcoming, *An Archaeological Resource Assessment and Research Agenda for the East Midlands.* http://www.le.ac.uk/archaeology/pdf_files/emidpal.pdf

McOmish, D. 2003. Cursus: solving a 6,000-year-old puzzle, *British Archaeology*, **69**.

Meek, J. 1999. *Desk-based assessment of the proposed 'Fulcrum' site, Kegworth, Leicestershire*. Unpublished ULAS report 99/120.

Meek, J. 2000. *Archaeological desk-based assessment of Lockington barrow cemetery, Leicestershire*, Unpublished ULAS report 2000/162.

Myers, A.M. Forthcoming. An archaeological resource assessment and research agenda for the Mesolithic in the East Midlands, in N.J. Cooper (ed) forthcoming, *An Archaeological Resource Assessment and Research Agenda for the East* Midlands.http://www.le.ac.uk/archaeology/pdf_files/emidmeso.pdf

Optech. 2003. *ALTM 2033 Airborne Laser Terrain Mapper.* Optech, Toronto.

Palfreyman, A. and Ebbins, S. 2003. Redhill Iron Age and Romano-British site, Nottinghamshire: A new assessment, *Transactions of the Thoroton Society,* **107**, pp. 17-40.

Pickering, J. and Hartley R.F. 1985. *Past Worlds in a Landscape, Leicestershire Museums, Art Galleries and Records Service Archaeological Reports Series 11.*

Posnansky, M. 1963. The Lower and Middle Palaeolithic industries of the English East Midlands, Proceedings Prehistoric Society, **29**, pp. 357-94.

Prehistoric Society. 1999. *Research Frameworks for the Palaeolithic and Mesolithic of Britain and Ireland: A Report by the Working Party for the Palaeolithic and Mesolithic Day Meeting and the Council of the Prehistoric Society*. Prehistoric Society, Salisbury.

Riley, D.N. 1987. *Air Photography and Archaeology*. London: Duckworth.

Ripper, S. 1997. *An archaeological evaluation of land west of Warren Farm, Lockington, Leicestershire (NGR SK477 296 and SK466 293).* University of Leicester Archaeological Services.

Ripper, S., and Butler, A. 1999. Warren Farm, Lockington (SK 477 296 and SK 466 293), *Transactions of the Leicestershire Archaeological and Historical Society*, **73**, pp. 101-4.

Salisbury, C.R. 1985. Taming the Trent. *East Midlands Archaeology*, **1**, pp. 5-12.

Salisbury, C.R. 1991. Primitive British fish weirs. In G.L. Good, R.H. Jones, & M.W. Ponsford, (eds), Waterfront Archaeology, Proceedings of the Third International Conference 1988. CBA Research Report, **74**, pp. 76-87. London: Council for British Archaeology.

Salisbury, C.R. 2004. *Bronze Age Lakes at Aston on Trent, Derbyshire*, page on Trent Valley GeoArchaeology web-sitehttp://www.nottingham.ac.uk/~aczkdc/TVG/aston_crs.html

Salisbury, C.R., Whitley, P.J., Litton, C.D. and Fox, J.L. 1984. Flandrian courses of the river Trent at Colwick, Nottinghamshire, Mercian Geologist, **9**, pp. 189-207.

Schwabedissen, S.H., 1954 Die Federmesser-Gruppen des nordwesteuropäisschen Flachlandes. *Zur Ausbreitung des Spät-Magdelénien.* Neumünster. Karl Wachholtz.

Scurfield, C.J. 1997. Bronze Age Metalwork from the River Trent in Nottinghamshire, Transactions of the Thoroton Society, **101**, pp. 29-58.

Smith, D. and Ripper, S. 2000. *Building survey of Warren Farm farmhouse and farm buildings.* Unpublished ULAS report 2000/92.

St Joseph, J.K., 1961. *Journal of Roman Studies*, **XLI**, pp. 133-4.

St Joseph, J.K., 1968. *Journal of Roman Studies*, **XLVIII**, pp. 128.

Stringer, C., and Gamble, C. 1993. *In search of the Neanderthals.* Thames & Hudson.

Stringer, C. 2002. The Ancient Human Occupation of Britain (AHOB) project. *Before Farming: the archaeology of Old World hunter-gatherers 2002/1*. Western Academic and Specialist Press. Online publication:http://www.waspjournals.com/journal/news/occupation.php

Taylor, J. 1997. Space and place: some thoughts on Iron Age and Romano-British landscapes, in A. Gwilt and C.C. Haselgrove (eds), *Reconstructing Iron Age Societies. New Approaches to the British Iron Age*, Oxbow Monograph 71, Oxbow: Oxford, pp.192-204.

Thomas, J. and Jacobi, R. 2001. Glaston, *Current Archaeology,* **173**, pp.180-4.

Van Dam, R. L., Van Den Berg, E. H., Schaap, M. G., Broekema, L. H. and Schlager, W. 2003. Radar reflections from sedimentary structures in the vadose zone, in, C. S. Bristow and H. M. Jol, *Ground Penetrating Radar in Sediments*, Geological Society Special Publications, pp. 257 – 273. London.

Vince, A. forthcoming. An Archaeological Resource Assessment and Research Agenda for the Early and Middle Anglo-Saxon Period (c. 400-850) in the East Midlands, in N. Cooper, forthcoming

Watkin, J., Stead, I.M. and Palmer, S. 1996. A decorated shield-boss from the River Trent, near Ratcliffeon-Soar, *The Antiquaries Journal*, **76**, pp. 17-30.

Windell, D. 1989. A Later Neolithic 'Ritual Focus' at West Cotton, Northamptonshire, in A. Gibson (ed), Midlands Prehistory, BAR (British Series), **204**, pp. 85-94

Wymer, J. 1999. *The Lower Palaeolithic Occupation of Britain, Vols 1 and 2.* Salisbury: Wessex Archaeology and English Heritage.

Wehr, A. and Lohr, U. 1999. Airborne laser scanning – an introduction and overview. *ISPRS Journal of Photogrammetry & Remote Sensing,* **54**, 68-82.

Wilson, D.R. (1982). *Air Photo Interpretation for Archaeologists.* London: Macmillan.

Young, R. 1988. Mixed lithic scatters and the Mesolithic-Neolithic transition in the north-east of England: a speculation, in I. Brooks and P. Philips (eds), *Breaking the Stony Silence: Papers from the Sheffield Lithics Conference*. Oxford: BAR (British Series), **213**, pp. 161-86.